Investigating the Role of Parp1 in Xrcc1-linked Neuropathology

A thesis submitted to the University of Sussex for the degree of Doctor of Philosophy, Neuroscience

Jack Badman

January 2022

Declaration

I hereby declare that this thesis has not been, and will not be, submitted in whole or in part to another University for the award of any other degree.

Jack Badman

Acknowledgements

I would like to express my sincere gratitude to my supervisors, Keith Caldecott and Kevin Staras for their knowledge and guidance. I would also like to thank all members of the Caldecott and Staras labs past and present. In particular, I would like to thank Emilia Komulainen, without whom this work would not have come to fruition, kiitos kärsivällisyydestäsi. Thank you to Kate Fennell for her invaluable expertise and uncanny knowledge of optical reporters. Special thanks to Limei Ju, who made possible all work involving our animal subjects – to whom I am also grateful. Thanks to Alex, Greig, David, Rob, Jo and Sophie for the support, beer, and unsolicited opinions.

It is here that I would also like to express my thanks to my friends and family but, frankly, their contributions to molecular neuroscience have been limited at best. Regardless, to Dad, Joe, Alice, Roz and Annie – it wouldn't have been possible without you either.

To my mother; thank you.

Summary

The DNA repair scaffold protein XRCC1 orchestrates the activity of the DNA single-strand break repair (SSBR) machinery. DNA single-strand breaks (SSBs) are primarily detected by poly(ADP-ribose) Polymerase 1 (PARP1), which synthesises poly(ADP-ribose) at sites of damage, promoting XRCC1 recruitment. Mutations in *XRCC1* have recently been identified in several human patients, resulting in ataxia with ocular motor apraxia (AOA). In cells lacking XRCC1, SSBR is reduced, leading to the retention of PARP1 at sites of damage and the continuous synthesis of poly(ADP-ribose). In conditional knockout *Xrcc1*$^{Nes\text{-}Cre}$ mice, poly(ADP-ribose) accumulates in the brain, resulting in progressive ataxia and fatal seizures. Here, I aimed to establish a cell autonomous model of endogenous SSB induction and Parp1 activation in neuronal cells.

To do so, I developed primary cultures of hippocampal neurons from *Xrcc1*$^{Nes\text{-}Cre}$ mouse pups. I show that *Xrcc1*$^{Nes\text{-}Cre}$ hippocampal neurons exhibit elevated Parp1/NAD+ dependent poly(ADP-ribose) accumulation, recapitulating what has been observed *in vivo* in mouse brain. I also show that this elevated activity underlies the spontaneous death of *Xrcc1*$^{Nes\text{-}Cre}$ hippocampal neurons *in vitro*. Both the accumulation of poly(ADP-ribose) and spontaneous cell death can be rescued via the additional deletion of one or both alleles of *Parp1*, as well as with treatment by commercially available PARP inhibitors, highlighting the potential therapeutic application of PARP inhibition in the treatment of *XRCC1*-mediated neurodegeneration. In investigating the source of the endogenous DNA SSBs characterising Xrcc1-deficient cells, I highlight the nitric oxide (•NO) dependent production of reactive nitrogen species (RNS) as a likely source of damage.

I further demonstrate Parp1 dependent deregulation of presynaptic calcium signalling in *Xrcc1*$^{Nes\text{-}Cre}$ neurons, providing a compelling potential explanation for the seizures observed in the mouse brain. This synaptic phenotype can be rescued by chronic PARP inhibition, further indicating the therapeutic potential of PARP inhibition.

Finally, I aimed to investigate whether Parp1 dependent alterations to transcription could be identified in the *Xrcc1*$^{Nes\text{-}Cre}$ mouse brain. To do so, RNA sequencing was performed, highlighting a number of differentially expressed genes. This phenotype was, however, comparatively mild, and targets were not effectively validated in our small sample size.

In summary, I present a cell autonomous model of endogenous DNA SSBs, and demonstrate elevated poly(ADP-ribose) accumulation in *Xrcc1*$^{Nes\text{-}Cre}$ hippocampal neurons, resulting in aberrant presynaptic calcium signalling and a mild deregulation of

transcription. These data improve our knowledge of the pathological contribution of PARP1 to Xrcc1-defective phenotypes, and the therapeutic potential of PARP in treating XRCC1-linked disease.

Table of Contents

List of Abbreviations

5-cC – 5’-carboxylcytosine

5fC – 5’formylcytosine

5-hC – 5’-hydroxycytosine

5-hmC – 5’-hydroxymethylcytosine

5-mC – 5’-methylcytosine

8-oxoG – 8-oxo7,8-dihydroguanine

AAV – Adeno-associated Virus

AD – Alzheimer’s Disease

AIF – Apoptosis Inducing Factor

ALC1 – SNF2 Family ATPase Amplified in Liver Cancer 1

ALS – Amyotrophic Lateral Sclerosis

AMP – Adenosine Monophosphate

AMPAR – α-amino-3-hydroxy-5-methyl-4-isoxazolepropionic acid receptor

AOA – Ataxia with Ocular Motor Apraxia

AP – Abasic/Apurinic/Apyrimidinic

APE1 – Apurinic/Apyrimidinic Endonuclease 1

APLF – Aprataxin and PNKP Like Factor

APs – Action Potentials

APTX – Aprataxin

APV – (*2R*)-amino-5-phosphonovaleric acid

AraC – Cytosine Arabinoside

ARCA – Autosomal Recessive Cerebellar Ataxia

ARH3 – (ADPribosyl)hydrolase 3

ASD – Autism Spectrum Disease

AT – Ataxia Telangiectasia

ATM – Ataxia Telangiectasia Serine/Threonine Kinase

ATP – Adenosine Triphosphate

ATXN1 – Ataxin 1

AUC – Area under the curve

BARH1 – BarH Like Homeobox

BER – Base Excision Repair

BK – Large Conductance Calcium Activated Potassium Channel (Big Potassium)

BRCA – Breast Cancer Associated 1

BRCT – BRCAC-Terminal

BSA – Bovine Serum Albumin

Ca^{2+} - Calcium

CA8 – Carbonic Anhydrase 8

CaCl – Calcium Chloride

cADPr – Cyclic ADP-ribose

$Ca_{v2}2.1$ – P/Q type Ca^{2+} Channel

CBLN – Cerebellin 1 Precursor

CD38 – Cluster of Differentiation 38

CDH1 – Cadherin 1

CDHR1 – Cadherin Related Family Member 1

CGC – Cerebellar Granule Cell

CICR – Calcium Induced Calcium Release

CNQX – Cyanquixaline

CO_2 – Carbon Dioxide

CPT – Camptothecin

DAGLα – Diacylglycerol Lipase α

DAPI – 4’6-diamidino-2-phenylindole

ddH_2O – Double Distilled Water

DDR – DNA Damage Repair

DEG – Differentially Expressed Gene

DIV – Days in Vitro

DNA – Deoxyribonucleic Acid

DNMT – DNA Methyltransferase

DSB – Double-Strand Break

DSBR – Double-Strand Break Repair

E/I – Excitatory/Inhibitory

EA2 – Episodic Ataxia 2

EBS – Extracellular Bath Solution

EDTA – Ethylenediaminetetraacetic Acid

EGFP – Enhanced Green Fluorescent Protein

EPHB1 – Ephrin Receptor B1

EPSC – Excitatory Postsynaptic Current

ER – Endoplasmic Reticulum

FCS – Foetal Calf Serum

FEN1 – Flap Endonuclease 1

FHA – Forkhead Associated

FoxO1 – Forkhead Box O1

GABA – Gamma aminobutyric Acid

GADD45 – Growth Arrest and DNA Damage-inducible 45

GRID2 – Glutamate Receptor Ionotropic Delta

GRID2IP – Glutamate Receptor Ionotropic Delta 2 Interacting Protein

H_2O_2 – Hydrogen Peroxide

HBSS – Hank's Buffered Saline Solution

HD – Huntington's Disease

HEPES – 4-(2-hydroxyethyl)-1-piperazineethanesulfonic acid

HK1 – Hexokinase 1

HR – Homologous Recombination

HRP – Horseradish Peroxidase

IGE – Idiopathic Generalised Epilepsy

IL-1β – Interleukin 1 Beta

INPP5a – Inositol Polyphosphate-5-Phosphatase A

IP3 – Inositol 1,4,5-triphosphate

IP3R – Inositol 1,4,5-triphosphate Receptor

IR – Ionising Radiation

ITPR2 – Inositol 1,4,5-trisphosphate Receptor 2

K^+ - Potassium

KCl – Potassium Chloride

KCNJ10 – Potassium Inwardly Rectifying Channel Subfamily J, Member 10

KCNMA1 – Potassium Calcium-Activated Channel Subfamily M Alpha 1

LIG3 – Ligase IIIα

Log2FC – Log Fold Change

L-NAME - N_{ω}-Nitro-L-arginine methyl ester hydrochloride

MAP2 – Microtubule Associated Protein 2

MAR – mono(ADP-ribose)

MCSZ – Microcephaly with Early Onset Seizures

MEM – Minimal Essential Medium

MgCl – Magnesium Chloride

MIF – Macrophage Migratory Inhibitory Factor

MMS – Methyl Methanesulfonate

MOI – Multiplicity of Infection

MPTP – Mitochondrial Permeability Transition Pore

Na^+ - Sodium

NAADP – Nicotinic Acid Adenine Dinucleotide Phosphate

NaCl – Sodium Chloride

NAD – Nicotinamide Adenine Dinucleotide

NAM – Nicotinamide

NAMPT – Nicotinamide Phosphoribosyltransferase

NaOH – Sodium Hydroxide

NB – Neurobasal

NCX – Na^+/Ca^{2+} exchanger

NELF – Negative Elongation Factor

NER – Nucleotide Excision Repair

NeuN – Neuronal Nucleus

NF-KB –

NHEJ – Non-Homologous End Joining

NLS – Nuclear Localisation Sequence

NMDAr – N-Methyl D-Aspartate Receptor

NMN – Nicotinamide Mononucleotide

nNOS – Neuronal Nitric Oxide Synthase

NO – Nitric Oxide

NOS – Nitric Oxide Synthase

NR – Nicotinamide Riboside

NRF1 – Nuclear Respiratory Factor 1

NRF2 – Nuclear Respiratory Factor 2

NuRD – Nucleosome Remodelling and Deacetylase

O_2 - Oxygen

$O_2^{\bullet-}$ - Superoxide

oAADPR – O-acetyl-ADP-ribose

OGG1 – 8-oxoguanine DNA Glycosylase 1

OH – Hydroxyl Radical

$ONOO^-$ - Peroxynitrite

p53 – Tumour Protein p53

PAR – poly(ADP-ribose)

PARG – poly(ADP-ribose) Glycohydrolase

PARP1 – poly(ADP-ribose) Polymerase 1

PARP2 – poly(ADP-ribose) Polymerase 2

PBS – Phosphate Buffered Saline

PBST – Phosphate Buffered Saline with Tween

PC – Purkinje Cell

PCR – Polymerase Chain Reaction

PD – Parkinson's Disease

PFA – Paraformaldehyde

PLCL1 – Phospholipase C Like 1 (inactive)

PNKP – Polynucleotide Kinase 3'-phosphatase

POLβ – DNA Polymerase β

PSD95 – Postsynaptic Density Protein 95

RNA – Ribonucleic Acid

RNAP – RNA Polymerase

RNS – Reactive Nitrogen Species

ROI – Region of Interest

ROS – Reactive Oxygen Species

RRP – Readily Releasable Pool

RyR – Ryanodine Receptor

SARseq – Synthesis Associated with Repair Sequencing

SCA – Spinocerebellar Ataxia

SCAN – Spinocerebellar Ataxia with Axonal Neuropathy

SDS-PAGE – Sodium Dodecyl Sulfate Polyacrylamide Gel Electrophoresis

Sema – Semaphorin

SERCA – Sarcoplasmic/Endoplasmic Reticulum Ca^{2+}-ATPase

SEZ6 – Seizure Related 6

SIRT1 – Sirtuin 1

SMAD3/4 – SMAD Family Member 3/4

SNARE - soluble *N*-ethylmaleimide-sensitive factor attachment protein receptor

SOD – Superoxide Dismutase

SSB – Single-Strand Break

SSBR – Single-Strand Break Repair

SUDEP – Sudden Unexpected Death During Epilepsy

SV2C – Synaptic Vesicle Glycoprotein 2C

SYN3 – Synapsin 3

TBST – Tris Buffered Saline with Tween

TDG – Thymine DNA-Glycosylase

TDP1 – Tyrosyl-DNA Phosphatase 1

TDP2 – Tyrosyl-DNA Phosphatase 2

TET – Ten-Eleven Translocation

TGF-β – Transforming Growth Factor Beta

Top1 – Topoisomerase 1

Top1cc – Topoisomerase 1 Cleavage Complex

TOP2 – Topoisomerase 2

Tris-HCl – Tris(hydroxymethyl)aminomethane Hydrochloride

TUNEL – Terminal Deoxynucleotidyl Transferase dUTP Nick End Labeling

USP3 – Ubiquitin Specific Protease 3

UV – Ultraviolet

VDAC – Voltage-dependent Anion Channels

VGCC – Voltage Gate Ca^{2+} Channel

VGKC – Voltage-Gated Potassium Channels

VGSC – Voltage-Gated Sodium Channels

X1BRCTa – XRCC1 BRCT Domain

XL2 – XRCC1 Linker Segment 2

XP – Xeroderma Pigmentosum

XRCC1 – X-Ray Repair Cross-Complementing Protein 1

List of Figures

List of Tables

Chapter One – Introduction

1.1 – DNA Damage

Cells are constantly exposed to endogenous and exogenous sources of genotoxic stress, and consequently the induction of DNA damage, the repair of which is critical for the maintenance of genomic integrity (Caldecott, 2008). DNA lesions are highly diverse, with their incidence being estimated at 70,000 per cell per day (Lindahl and Barnes, 2000). The array of lesions capable of compromising genomic integrity include DNA single-strand breaks (SSBs), DNA double-strand breaks (DSBs), DNA base modifications, and DNA base mismatches (Chatterjee and Walker, 2017). SSBs and DSBs represent discontinuities in one or both strands of the DNA double helix, respectively. SSBs are the most commonly arising lesion in the cell, occurring more than 10,000 times per cell, per day (Lindahl, 1993, Tubbs and Nussenzweig, 2017). The repair of SSBs occurs following their detection by poly(ADP-ribose) polymerase (PARP) enzymes, and the recruitment of scaffold proteins and end processing factors to restore conventional 3' hydroxyl and 5' phosphate termini, prior to DNA gap filling and DNA ligation (described in detail in section 1.3) (Caldecott, 2008). DSBs are less common than SSBs but are more cytotoxic (Cannan and Pedersen, 2016). If unrepaired, DSBs result in cell death, and if incorrectly repaired can result in chromosomal deletions, duplications, and translocations, which can underpin carcinogenesis (Iarovaia, *et al*., 2014, Cannan and Pedersen, 2016). SSBs can be converted to DSBs if they are in close proximity on opposite strands (Vilenchik and Knudson, 2003, Mehta and Haber, 2014). Similarly, DNA polymerases encountering SSBs can lead to DNA replication fork stalling, leading to fork collapse and the formation of DSBs (Roth and Wilson, 1988, Pfeiffer, *et al*., 2000). The repair of DSBs can occur through non-homologous end joining (NHEJ), the direct resealing of broken DNA, which occurs independently of sequence homology, potentially resulting in the loss of genetic information (Davis and Chen, 2013). Homologous recombination (HR) is a more accurate pathway, utilising a homologous DNA template and extensive end processing to faithfully repair DSBs during the S and G2 phase of the cell cycle (Wright, *et al*., 2018).

DNA possesses an inherent degree of instability and is prone to modification through various processes, such as through oxidation by endogenously produced reactive oxygen species (ROS) (Lindahl, 1993). The modification of DNA nucleobases represents a threat to genome stability, due to their potential mutagenicity, and must be repaired (Moriya, 1993, Kamiya, 2003). To do so, the base excision repair (BER) pathway facilitates the removal of these lesions and their replacement (Caldecott, 2020).

Errors in DNA metabolism, or aberrant DNA processing during DNA repair, recombination, and replication, represent a further mechanism by which the integrity of DNA can be compromised by endogenous sources (Li, 2008). Typically, replicative DNA polymerase are characterised by high replication fidelity, whereas translesion DNA polymerases, which act to bypass DNA lesions, exhibit much lower fidelity (Plosky and Woodgate, 2004, McCulloch and Kunkel, 2008). The consequence of this decreased replication fidelity is nucleotide misincorporation, resulting in base mismatches that must be repaired in order to safeguard genomic integrity (Li, 2008, Vaisman and Woodgate, 2017). The repair of base mismatches occurs through mismatch repair (MMR), involving the excision of misincorporated nucleotides, with gap filling performed by DNA polymerases δ and ε, and ligation by LIG1 (Pećina-Šlaus, *et al*., 2020).

Genomic integrity is also threatened by exogenous sources of DNA damage, including ionising radiation (IR), ultraviolet (UV) radiation, and numerous chemical agents (Hakem, 2008). Ionising radiation (X-ray and gamma (γ) waves, alpha (α) and beta (β) particles, and neutrons) has sufficient energy to release electrons from atoms and molecules, resulting in the breakage of covalent bonds, affecting the structure of DNA by directly inducing DNA breaks (Reisz, *et al*., 2014, Santivasi and Xia, 2014). Further, IR results in the formation of ROS, resulting in indirect damage through the generation of abasic sites, SSBs, and sugar modifications (Datta, *et al*., 2012, Yamamori, *et al*., 2012, Borrego-Soto, *et al*., 2015). Highly proliferative cells are particularly sensitive to IR, and as such radiotherapy (exposure to IR) is widely used in cancer therapy (Borrego-Soto, *et al*., 2015).

A separate and ubiquitous source of exogenous DNA damage is UV irradiation from sunlight (Hakem, 2008). UV radiation is classified by wavelength, UVA (315-400nm), UVB (290-315nm) and UVC (100-290nm), the latter of which is mostly absorbed by the ozone layer (Yu and Lee, 2017). Both UV irradiation is a causative agent in skin cancer, due to a capacity to induce DNA damage (Watson, *et al*., 2016, Yu and Lee, 2017). Two major UV induced DNA lesions are 6-4 photoproducts and cyclobutane pyrimidine dimers, caused by the covalent modification of neighbouring pyrimidine nucleobases (Mouret, *et al*., 2006, Yokoyama and Mizutani, 2014). The repair of UV induced DNA damage occurs through nucleotide excision repair (NER), which facilitates the removal of bulky, helix distorting lesions (Spivak, 2015). Mutations in several genes encoding proteins involved in NER underpin various forms of Xeroderma Pigmentosum, disorders characterised by an elevated incidence of skin cancer and, in some cases, neurological involvement (Cleaver and Bootsma, 1975, Anttinen, *et al*.,

2008, Koch, *et al*., 2016). Indirectly, UV irradiation can induce DNA damage through the production of ROS, a source of SSBs (De Lager, *et al*., 2017).

1.1.1 DNA Single-Strand Breaks

DNA single-strand breaks are the most prominent lesions in the cell, arising either directly via the oxidation of the deoxyribose-phosphate backbone, indirectly through DNA BER, or through abortive topoisomerase activity (Pogozelski & Tullius, 1998, Caldecott, 2008, Andersen, *et al*., 2015, Li & Liu, 2016). The diversity of DNA lesions arising in the cell is reflected by the variety of processes evolved to facilitate their repair. The DNA sugar moiety is prone to direct breakage and modification by ROS, a by-product of cellular respiration (Balasubramanian, *et al*., 1998, Dizdaroglu and Jaruga, 2012). Transcriptional demand, and the subsequent relaxation of torsional stress by Topoisomerases represent a further means by which SSBs may arise endogenously, as the formation of Top1-linked cleavage complexes can lead to Top1 associated SSBs (Li and Liu, 2015, Huang and Pommier, 2019). These endogenously arising lesions reflect a means by which critical cellular functions are coupled to the production of DNA breaks, which must be repaired in order to preserve genome stability (Chakarov, *et al*., 2014). The physiological relevance of unresolved SSBs is perhaps best highlighted by neurodegenerative conditions linked to hereditary defects in DNA single-strand break repair (SSBR), which underlie the cerebellar ataxias (Yoon and Caldecott, 2018, Beaudin, *et al*., 2019).

Mutations in SSBR proteins are typically associated with cerebellar degeneration, ataxia, and ocular motor apraxia (Takashima, *et al*., 2002, Le Ber, *et al*., 2003, Shen, *et al*., 2010, Hoch, *et al*., 2017, Yoon and Caldecott, 2018). These mutations are not typically associated with an increased risk of cancer, and present primarily with neurological involvement (Yoon and Caldecott, 2018). In proliferating cells, one consequence of unresolved DNA damage is the stalling and collapse of DNA replication forks, and the formation of DNA double-strand breaks (DSBs), which can be repaired through DSBR pathways, such as homologous recombination (HR) and non-homologous end joining (NHEJ) (Cox, *et al*., 2000, Alexander and Orr-Weaver, 2016). Mature neurons are post-mitotic and may continue to accumulate unresolved DNA damage throughout their lifespan (Kruman, *et al.,* 2004, Bianco and Lyubchenko, 2017). The absence of replication-dependent mechanisms of SSB conversion into DSBs, and subsequent DSBR to restore an intact genome may explain the importance of functional SSBR in neurons (Welty, *et al*., 2018). Similarly, the comparatively high rate of oxygen consumption by the nervous system, and relatively low antioxidant capacity, might

underpin the neurological phenotype associated with hereditary defects in SSBR (McKinnon, 2017). Unresolved SSBs may present a blockade for RNA polymerase progression, interfering with gene expression; the relevance of which may only become clear in post-mitotic neurons, due to their longevity, absence of replication-dependent repair mechanisms, and functional reliance of activity-dependent transcription (Kathe, *et al*., 2004, Abbotts and Wilson, 2017, Herbst, *et al*., 2021). A further mechanism by which nervous tissue might be particularly prone to defects in SSBR is through epigenetic reprogramming, which involves BER-mediated removal of 5'-methylcytosine and 5'-hydroxymethylcytosine (the latter of which is highly enriched in the brain) through a SSB intermediate (Kress, *et al*., 2006, Kriaucionis and Heintz, 2009, Guo, *et al*., 2011).

In this chapter, I will provide an overview of the means by which endogenously occurring SSBs arise, as well as the processes by which they are detected and repaired. I will primarily focus on the roles of the SSB detector protein, poly(ADP-ribose) Polymerase 1 (PARP1), and its binding partner; the SSBR scaffold protein X-Ray Repair Cross- Complementing Protein 1 (XRCC1). I will highlight the effects of mutations in these, and other proteins involved in SSBR, on the maintenance of neuronal homeostasis and neurodegeneration.

1.2 – The Source of SSBs

1.2.1 – Oxidative DNA Damage

Reactive Oxygen Species (ROS) represent a threat to genomic integrity through the induction of oxidative DNA damage (Cooke, *et al*., 2003). ROS may be generated by both endogenous and exogenous sources; endogenously through chemical processes undertaken during cellular metabolism, or exogenously through inflammatory processes and environmental toxins (Mena, *et al*., 2009, Paiva and Bozza, 2014, Markkanen, 2017). ROS mediated oxidative DNA damage typically accompanies development and is among the most common sources of germline mutagenesis (Crow, 2000, Martincorena and Campbell, 2015). Further, oxidative damage is heavily linked to the aging process, and is understood to underpin several factors in the aetiology of age-related conditions and neurodegeneration (Finkel, *et al*., 2007, Lodato, *et al*., 2018).

The endogenous production of ROS is primarily associated with oxidative metabolism; wherein the reduction of oxygen during aerobic respiration results in the formation of the superoxide anion ($O_2^{\bullet-}$) (Hayyan, *et al*., 2016). Superoxide undergoes enzymatic dismutation via Superoxide Dismutase (SOD) to form molecular oxygen (O_2) and hydrogen peroxide (H_2O_2) (Juarez, *et al*., 2008). H_2O_2 is relatively inert, with a low potential for reactivity. However, it is endogenously converted into a toxic, highly reactive

hydroxyl radical (˙OH) through fenton-like reactions (Thomas, *et al*., 2008). ˙OH radicals are capable of causing many oxidative lesions through base modification, such as 5'-hydroxycytosine (Plongthongkun, *et al*., 2014). These degradation products may require removal through BER, though ˙OH may also result in the cleavage of glycosidic linkages and the direct formation of an abasic site (Lenz, *et al*., 2015, Caldecott, 2020). The production of the superoxide anion is further associated with the activity of Nitric Oxide Synthases (NOS), enzymes catalysing the formation of nitric oxide (˙NO), which is combined with $O_2^{\bullet-}$ to form peroxynitrite ($ONOO^-$), a reactive nitrogen species (RNS) (Radi, 2013, Radi, 2018). RNS are particularly relevant to the nervous system, due to the prevalence of neuronal nitric oxide synthase (nNOS) in the brain, and the usage of diffuse ˙NO in neuronal signalling (Bredt and Snyder, 1994, Chachlaki and Prevot, 2020).

ROS and RNS can result in SSB formation through direct oxidation of the DNA sugar moiety, as well as through the modification of nucleobases, such as guanine. Guanine is highly susceptible to modification by singlet oxygen ($^1O_2$), a biologically relevant ROS typically associated with the UVA component of solar radiation, resulting in the formation of 8-oxo7,8-dihydroguanine (8-oxoG) (Cooke, *et al*., 2003, Epe, 2012, Fleming and Burrows, 2013, Dumont and Monari, 2015). 8-oxoG may also form due to reactivity of ˙OH. This reaction is estimated to occur up to 500 times per day per cell (Lindahl, 1993, Poetsch, 2020). The accumulation of 8-oxoG can result in alterations to the binding of transcription factors, as well as the deregulation of replication and gene stability through the alteration of the secondary structure of DNA (the formation of G-Quadruplex folds) (Fleming and Burrows, 2013, Poetsch, 2020). Further, 8oxoG-Adenine mismatch pairings can result in transcriptional mutagenesis and translational error (Dai, *et al*., 2018). The removal of 8-oxoG occurs through BER, notably via the activity of the bifunctional glycosylase OGG1 (Allgayer, *et al*., 2013).

1.2.2 – DNA Base Excision Repair (BER)

Due to the inherent instability of DNA, damage to nucleobases occurs frequently, and a robust system by which to repair them is required. Further, the heterogeneity of DNA base damage requires an array of DNA N-glycosylases to detect and excise small, non-helix-distorting, base lesions (Lindahl, 1993, Jacobs and Schar, 2012, Caldecott, 2020). Glycosylases may be monofunctional or bifunctional; the former having exclusively DNA glycosylase activity, wherein the removal of a nitrogenous base leaves an intact apurinic/apyrimidinic site (AP Site), which undergoes further processing via an AP endonuclease (Mullins, *et al*., 2019, Caldecott, 2020) (Figure 1.1). Bifunctional

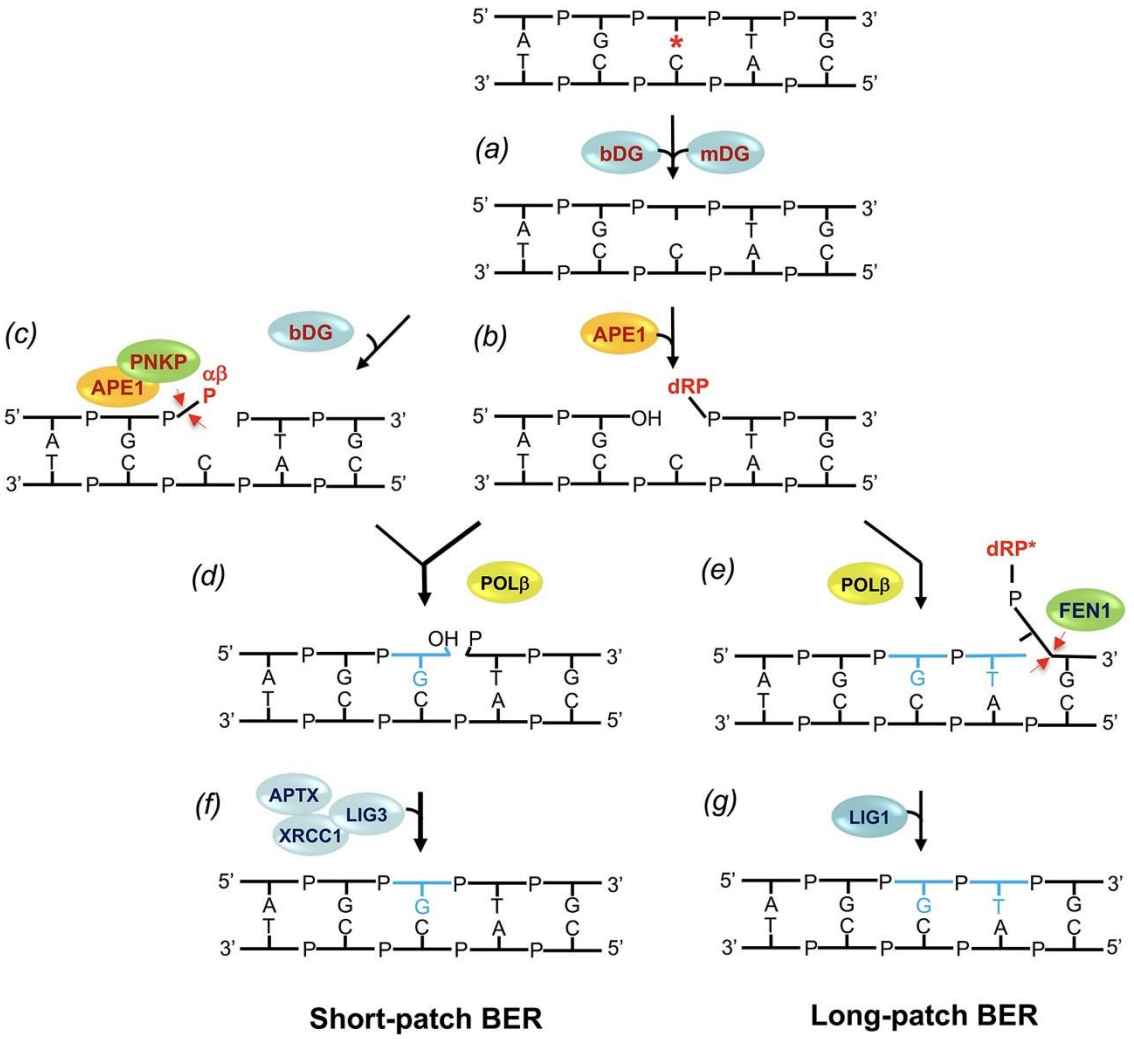

Figure 1.1. *A Model for Mammalian Base Excision Repair*. A) Modified bases are removed by either monofunctional (mDG) or bifunctional (bDG) DNA glycosylases, one of eleven enzymes that excise small, non-helix distorting lesions in DNA. B) Monofunctional glycosylases leave behind an intact abasic site, which is cleaved by APE1. C) Bifunctional glycosylases, such as OGG1, also cleave the 3' abasic site, leaving behind either a 3'-phosphate (P) or a 3'-αβ unsaturated aldehyde, which are removed by PNKP and APE1 respectively. D) Short patch gap filling, wherein POLβ replaces a single missing nucleotide. E) Long patch gap filling, wherein POLβ replaces several nucleotides, the consequence of which being the displacement of a 5' single strand, which is removed by FEN1. Long patch repair typically occurs in response to oxidised abasic sites, which cannot be removed by the lyase activity of POLβ. F) DNA ligation by XRCC1 and LIG3 completes short patch BER. G) Ligation by LIG1 is the terminal step in long patch BER. Figure taken from Caldecott, 2020.

glycosylases, such as OGG1, possess additional lyase activity and further cleave the AP site on the 3' of the baseless sugar moiety; leaving a single-strand break (Ba and Boldogh, 2018, Wang, *et al*., 2018, Mullins, *et al*., 2019, Caldecott, 2020) (Figure 1.1). APE1 is an AP endonuclease that functions following the activity of a monofunctional glycosylase, wherein it cleaves the 5' of the abasic site, creating a single-strand break intermediate (Demple, *et al*., 1991, Caldecott, 2020) (Figure 1.1). APE1 is retained at the break, possibly inhibiting the inappropriate repair of the SSB-intermediate while promoting the activity of POLβ. POLβ enables gap-filling, replacing nucleotides and removing the 5' sugar phosphate, displacing bound APE1 (Beard, *et al*., 2019, Caldecott, 2020). This small-scale gap-filling constitutes short-patch repair. However, in the case of oxidised abasic sites, during which the lyase activity of Polβ cannot remove the residual 5'-deoxyribose following APE1 activity, long-patch repair occurs. Long-patch repair is sub-pathway involving the insertion of multiple nucleotides, resulting in the 5' single-strand being displaced and requiring the activity of flap endonuclease-1 (FEN1) (Klungland and Lindahl, 1997, Robertson, *et al*., 2009, Wallace, 2014, Beard, *et al*., 2019) (Figure 1.1). DNA ligation is the final step of the BER process, facilitated by the XRCC1 binding partners LIG3 and APTX during short-patch repair, and LIG1 during long-patch BER (Cappelli, *et al*., 1997, Levin, *et al*., 2000, Ahel, *et al*., 2006).

1.2.3 – TOP1 Associated SSBs

Topoisomerases are enzymes that relax torsional stress in DNA, by creating a transient nick in the DNA, to which the topoisomerase is covalently bound (McKie, *et al*., 2021). DNA torsional stress is a consequence of several process. For example, the unwinding of DNA strands during replication results in DNA supercoiling and torsional stress which topoisomerase activity is required to relieve (Pommier, *et al.,* 2006, Buzun, *et al*, 2020). Similarly, and perhaps more appropriately for post-mitotic neurons, RNA polymerase II creates both positive (ahead of the polymerase) and negative supercoiling (behind the polymerase) during transcription (Ma and Wang, 2016, Baranello, *et al*, 2016). TOP1 and TOP2 are required for the transcription of long genes linked to autism spectrum disorders (ASD) (King, *et al*., 2013). Similarly, numerous neurodegenerative conditions, as well as intellectual impairment syndromes are linked to aberrant topoisomerase activity (Stoll, *et al*., 2013, Xu, *et al*., 2013).

Topoisomerase 1 facilitates the relaxation of torsional stress by covalently attaching itself the DNA; whereupon the active site tyrosine of the enzyme induces scission of the DNA phosphodiester bond (McKinnon, 2016, McKie, *et al*., 2021) . The result of this TOP1 mediated nucleophilic attack is the genesis of a transient and

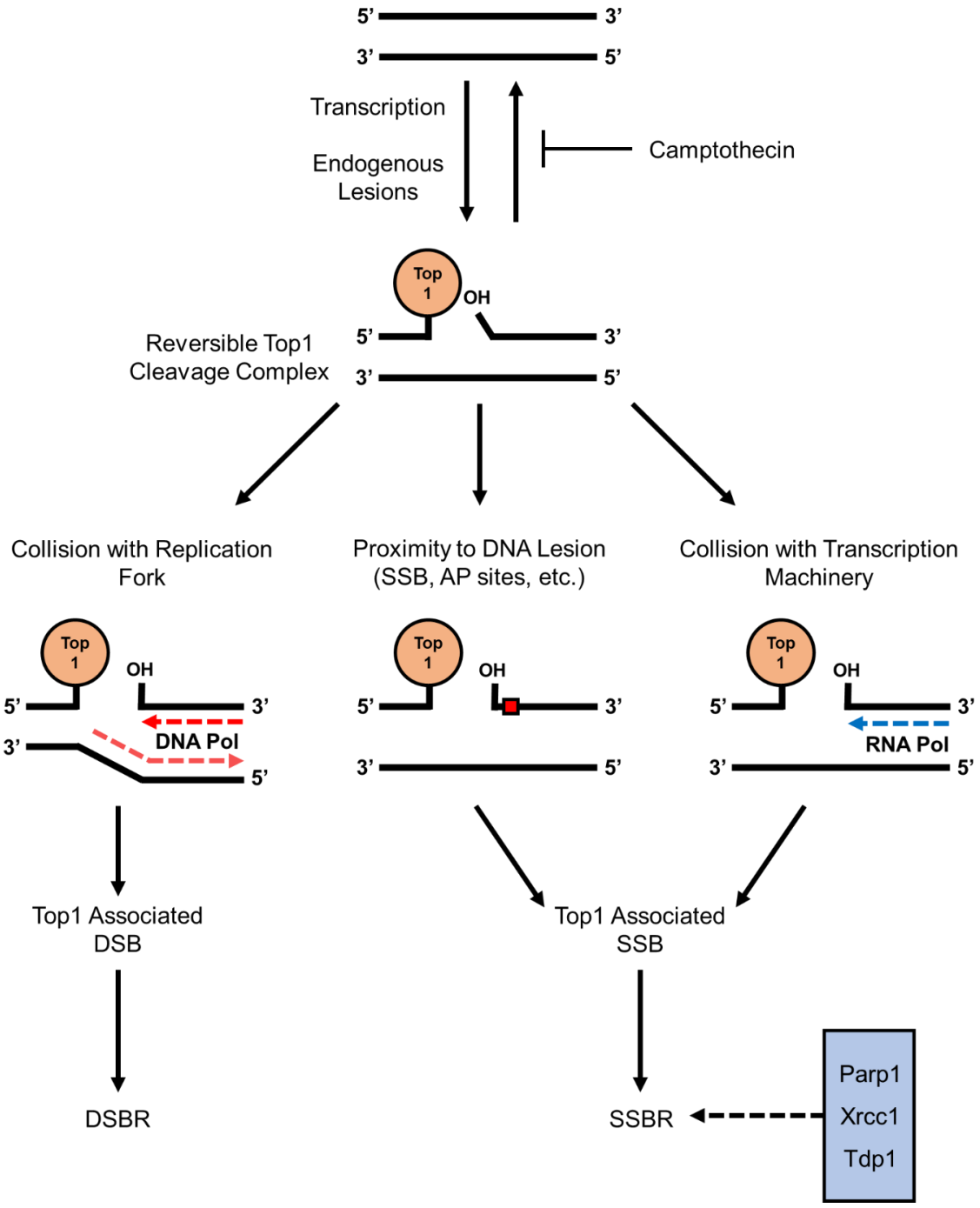

Figure 1.2. *The Formation of Top1 Associated SSBs*. Topoisomerase 1 acts to transiently nick DNA in order to relax torsional stress, through the covalent attachment of Top1 to the 3' end, forming the cleavage complex (Top1cc). The anticancer drug camptothecin is a Top1 poison that stabilises the cleavage complex by inhibiting the ligation step of Top1. In mitotic cells, the Top1cc can be converted to a DSB through collision with the replication fork. The Top1cc can be converted into a SSB either through proximity to an existing lesion, such as an abasic site, or through collision with the transcription machinery, resulting in the recruitment and activity of the SSBR machinery. Figure created with information from El Khamisy and Caldecott, 2006.

reversible DNA nick to which TOP1 is covalently attached at the 3' end; an intermediate denoted the TOP1 cleavage complex (TOP1cc) (Figure 1.2) (Stewart, *et al*., 1998, Pommier, *et al*., 2006). Abortive TOP1 activity, caused by the collision of an RNA polymerase with the TOP1cc, or TOP1 cleavage at sites of pre-existing lesions which trap the topoisomerase, results in the formation of a TOP1-associated SSB (Pourquier, *et al*., 1997a, Pourquier, *et al*., 1997b, El-Khamisy and Caldecott, 2006) (Figure 1.2). In order to repair the cleavage complex, trapped TOP1 is proteasomally degraded, leaving a TOP1 peptide-DNA linkage, a substrate for tyrosyl-DNA-phosphatase 1 (TDP1) (Figure 1.2) (Yang, *et al*., 1996, Pommier, *et al*., 2015, Kawale and Povirk, 2018).

Similarly, TOP2 acts to cleave DNA, however this process results in the formation of both SSBs and DSBs and is dependent on the hydrolysis of ATP (whereas TOP1 cleavage is an energy-independent process) (Atkin, *et al*., 2019). Should TOP2 be retained at the site of DNA damage, TDP2 facilitates the hydrolysis of the phosphodiester linkage with the TOP2 adduct (Ledesma, *et al*., 2009). Given that neuronal function is coupled to activity-driven changes in gene expression, it is unsurprising that the faithful repair of DNA damage resulting from abortive topoisomerase activity is critical for cell fate (West and Greenberg, 2011, Yan, *et al*., 2015, Herbst, *et al*., 2021). The importance of this repair is best highlighted by the consequence of mutation in TDP1 and TDP2, both of which are linked to hereditary, neurodegenerative disorders (Takashima, *et al*., 2002, Gomez-Herreros, *et al*., 2014, Zagnoli-Vieira, *et al*., 2018, Ericchiello, *et al*., 2020).

1.2.4 – The Consequences of Unresolved SSBs

Unrepaired SSBs have the capacity to threaten genomic integrity. In proliferating cells, the presence of unresolved SSBs may lead to the collapse of the DNA replication fork, resulting in the formation of DSBs (Kuzminov, 2001, Nickoloff, *et al*., 2021). Unresolved SSBs may pose a threat to the progression of RNA polymerases during transcription, as they have been shown to result in RNA polymerase stalling *in vitro* where damaged termini are present (Kathe, *et al*., 2004). Similarly, SSBs at abasic sites, and bulky lesions such as UV-induced cyclobutane pyrimidine dimers result in the stalling of RNA polymerase, representing a threat to faithful transcription (Zhou and Doetsch, 1993, Donahue, *et al*., 1994). As such, the accumulation of unresolved DNA damage in neuronal cells which, in humans, may survive >80 years, could result in defective transcription. A further consequence of the presence of unresolved SSBs is due to the activity of the chromosomal SSB sensor protein poly(ADP-ribose) polymerase 1 (PARP1), which I will further explore in sections 1.3. In brief, when PARP1 detects a

SSB it catalyses the NAD+ dependent synthesis of poly(ADP-ribose), which facilitates the recruitment of the SSBR machinery (Hassa, *et al*., 2006, Azarm, *et al*., 2020). One consequence of the hyperactivation of PARP1 is cell death through an apoptosis-independent pathway known as parthanatos (Fatokun, *et al*., 2014, Zhou, *et al*., 2021).

1.3 – The Detection and Repair of SSBs

Poly(ADP-ribose) polymerases (PARPs) constitute a family of 17 proteins that regulate several cellular processes such as DNA repair, chromatin remodelling and transcription, the stress response, and cell death (Krishnakumar and Kraus, 2010, Morales, *et al*., 2014). SSB detection occurs primarily through the activity PARP1, with additional detection by PARP2 and PARP3 (Chambon, *et al*., 1963, Amé, *et al*., 1999, Hassa, *et al*., 2006, Boehler, *et al*., 2011, Grundy, *et al*., 2016). These enzymes bind to DNA strand breaks and catalyse the NAD+ dependent synthesis and poly(ADP-ribose) (Chambon, *et al*., 1963, Caldecott, 2008). Poly(ADP-ribosylation) by PARP-family enzymes constitutes the synthesis of anionic poly(ADP-ribose) polymer, and modification of target proteins such as histones and transcription factors (D'amours, *et al*., 1999, Eustermann, *et al*., 2015). Through the steric hindrance of intramolecular reactions by the PAR polymer, poly(ADP-ribosylation) facilitates the activation or inhibition of protein function, the relocalisation of target proteins, or the disruption of protein-protein interactions (Hottiger, *et al*., 2010). Autoribosylation, wherein PARP1 modifies itself with poly(ADP-ribose) residues, facilitates the recruitment of XRCC1 and subsequently the SSBR machinery, a collection of proteins which process and repair damaged DNA termini (Ueda, *et al*., 1982, Masson, *et al*., 1998, Breslin, *et al*., 2015, Azarm, *et al*., 2020) (Figure 1.3). PARP1 activation is increased up to 500-fold in the presence of SSBs and leads to the poly(ADP-ribosylation) of itself (autoribosylation) and various acceptor proteins (transribosylation), such as transcription factors, histones, and helicases (Messner, *et al*., 2010, Berti, *et al*., 2013, Palazzo, *et al*., 2018). The autoribosylation of PARP1 facilitates dissociation from the detected break via electrostatic destabilisation (Mortusewicz, *et al*., 2007).

1.3.1 – DNA Break Detection by PARP1

DNA-damage induced PARP1 activation is one of the earliest responses to genotoxic stress (Polo and Jackson, 2011). Following the induction of SSBs, PARP1 responds rapidly, and is recruited to the site of damage within seconds, whereupon it catalyses the synthesis of poly(ADP-ribose) (Kreimeyer, *et al*., 1984, Eustermann, *et al*., 2015, Krüger, *et al*., 2020). Mammalian PARP1 is comprised of three domains; the N-terminal

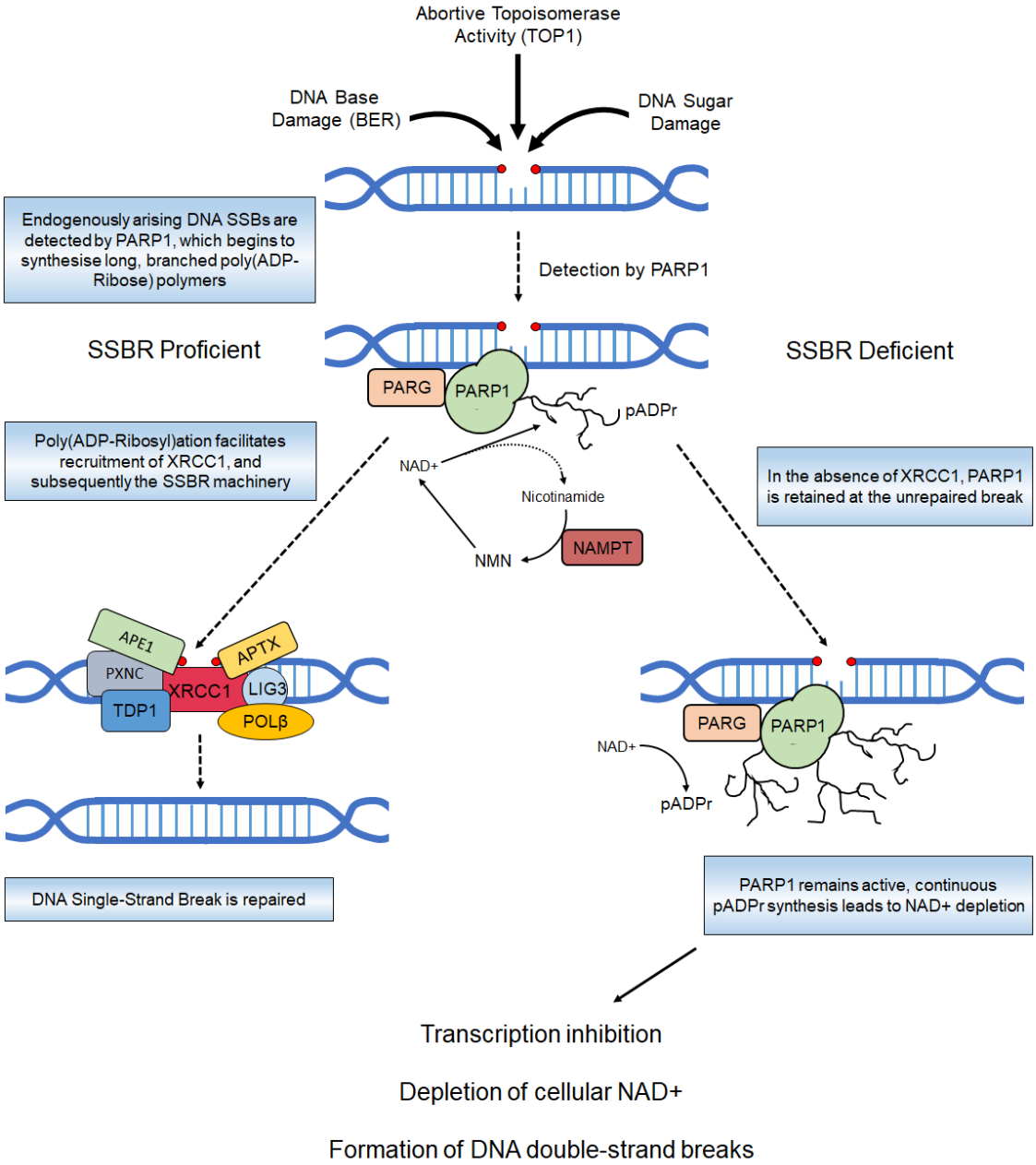

Figure 1.3. *A Simplified Model for the Repair of Endogenous SSBs*. Endogenously arising SSBs are detected by PARP1, which catalyses the NAD+ dependent synthesis of poly(ADP-ribose) (pADPr), which it attaches to itself and acceptor proteins. The autoribosylation of PARP1 facilitates the recruitment of XRCC1, a DNA repair scaffold protein which orchestrates the activity of SSBR enzymes, such as APTX, PNKP, and TDP1, mutations in which are associated with neurodegeneration. In SSBR deficient cells, such as those lacking XRCC1, PARP1 is retained at the break, constitutively synthesising poly(ADP-ribose). The consequences of unresolved SSBs are the inhibition of transcription, the depletion of cellular NAD+ by PARP1 and, in mitotic cells, the replication dependent formation of DSBs.

DNA binding domain consists of a nuclear localisation signal and three zinc finger motifs (Spiegel, *et al*., 2021). Two homologous zinc finger motifs, Zn1 and Zn2, recognise DNA lesions and are required for DNA binding (Ikejima, *et al*., 1990, Langelier, *et al*., 2011). A third zinc finger, Zn3, is unrelated to F1 and F2 but functions in the allosteric activation of PARP1 (Langelier, *et al*., 2011, Langelier, *et al*., 2012). Within the central PARP1 automodification domain are many of the best-characterised autoribosylation sites, and the BRCT subdomain which, while dispensable for catalytic activity and DNA binding, interacts with proteins such as XRCC1 (Masson, *et al*., 1998, Beernink, *et al*., 2005, Chapman, *et al*., 2013). The C-terminal domain contains the tryptophan, glycine, arginine (WGR) motif, which also binds DNA, and the catalytic subdomain responsible for the poly(ADP-ribosylation) reaction (Langelier, *et al*., 2012, Alemasova and Lavrik, 2019). Within the automodification domain is the BRCA C-terminal (BRCT domain), which facilitates interactions with the protein and is critical in the recruitment of SSBR enzymes (Loeffler, *et al*., 2011, Alemasova and Lavrik, 2019). The catalytic domain is required for the binding of PARP1 to its substrate; NAD+, which it hydrolyses to catalyse transfer of an ADP-ribose moiety to an amino acid target or to a progressively extending poly(ADP-ribose) polymer (Langelier, *et al*., 2018). The catalytic domain consists of two subdomains, the helical domain (HD), which undergoes local unfolding following activation of PARP1 in order to bind NAD+, and ADP-ribosyltransferase (ART) domain, which catalyses the transfer of ADP-ribose (Dawicki-McKenna, *et al*., 2015, Alemasova and Lavrik, 2019). Poly(ADP-ribosylation) is further regulated by the activity of HPF1, which remodels the catalytic domain of PARP1, restricting automodification and promoting histone modification (Gibbs-Seymour, *et al*., 2016, Sun, *et al*., 2021). Further, remodelling of the PARP1 active site by HPF1 alters the amino acid specificity of ADP-ribosylation from glutamate/aspartate to serine, the major target of PARP1 during the DDR (Sun, *et al*., 2021).

1.3.1.1 – PARP1 Inhibition

PARP inhibitors are a novel class of anti-cancer drug, typically acting to compete with NAD+ for the catalytic site of PARP enzymes (Rose, *et al*., 2020). Given that PARP1 is the main PARP to be active following DNA damage, it is the predominant target for PARP inhibition; however, due to structural similarities in the NAD+ binding domain, there is often a lack of specificity in targeting PARP1 over other family members, such as PARP2 (Murai, *et al*., 2012). PARP inhibitors have proven to be effective in the treatment of homologous repair (HR)-deficient tumours, such as those with *BRCA1/2* mutation (Bryant, *et al*., 2005, Famer, *et al*., 2005).

The inhibition of PARP1 results in the accumulation of unresolved SSBs, which can be converted to DSBs following collision of replicative polymerases with the lesion (Liao, *et al*., 2018). Further, the activity of PARP1 is required to facilitate the MRE-11 mediated restart of stalled replication forks (Bryant, *et al*., 2009). In cells that are not HR-proficient, these collapsed replication forks cannot be repaired, resulting in the specific killing of HR deficient cells via PARP inhibition (Bryant, *et al*., 2005, Liao, *et al*., 2018). The trapping mechanism of PARP inhibitors is likely linked to their efficacy, as the inhibition of PARP1 is significantly more cytotoxic than genetic deletion or depletion (Ström, *et al*., 2011, Murai, *et al*., 2012). PARP inhibitors compete with NAD+ for the catalytically active site, leaving PARP1 unable to autoribosylate and dissociate from the break (Mortusewicz, *et al*., 2007, Langelier, *et al*., 2018). The trapping of PARP1 at the SSB leaves a lesion that most likely cannot be bypassed by the replication fork, resulting in stalled forks and inhibiting their reversal, leading to fork collapse and DSB formation (Chaudhuri, *et al*., 2012, Murai, *et al*., 2012, Rose, *et al*., 2020). In HR deficient cells, these DSBs can only be repaired through NHEJ, a potentially error prone system that can result in genomic instability and cell death (Patel, *et al*., 2012, Davis and Chen, 2013). PARP inhibition also results in the phosphorylation of DNA-dependent protein kinase substrates, selectively stimulating error prone NHEJ at replication and transcription associated DSBs in HR deficient cells, resulting in genomic instability and/or cell death (Patel, *et al*., 2012, Min, *et al*., 2013).

Initial observations of PARP1 inhibition were made via treatment with nicotinamide and thymidine. Later studies highlighted NAD+ competition by benzamides as capable of inhibiting PARP1 activity, however the clinical viability of such treatments is limited by low specificity and potency (Purnell and Whish, 1980, Skalitzky, *et al*., 2003). Several PARP inhibitors are currently approved for the treatment of BRCA1/2 mutated (HR-deficient) breast, ovarian, prostate, and pancreatic tumours, including Olaparib, Rucaparib, Niraparib, and Talazoparib (Rose, *et al*., 2020). Veliparib and Fluzoparib are two further examples of PARP inhibitors but are not yet approved for the treatment of human disease (Rose, *et al*., 2020). Pharmacodynamically, the above PARP inhibitors are all similar in their ability to interact with the NAD+ binding site of PARP1 through a benzamide core pharmacophore (Valabrega, *et al*., 2021). However, differences in size and flexibility of the molecules result in differential trapping capacities, impact on DNA SSBR capabilities, as well as differences in apoptosis induction and protein phosphorylation (Valabrega, *et al*., 2021). Talazoparib is the most potent PARP1 inhibitor, with a trapping efficiency 100-fold higher than Niraparib, the second most efficient trapper (Murai, *et al*., 2014, Boussios, *et al*., 2020, Valabrega, *et al*., 2021).

Trapping efficiency is seemingly linked to the physical properties of the inhibitor in question, given their mechanism of action involves interaction with the NAD+ binding domain, leading to alterations in the critical allosteric regulatory domain of PARP1 (the helical domain, HD, which is adjacent to the NAD+ binding domain) (Murai, *et al*., 2012, Zandarashvili, *et al*., 2020). Different PARP1 inhibitors have different effects on HD stability, with some interactions leading to destabilisation of the HD, increasing the affinity of PARP1 for DNA, leading to its retention (Zandarashvili, *et al*., 2020). Different alterations to HD stability may explain the differential trapping capacities of clinically available PARP inhibitors, however the exact allosteric alterations caused by each of these molecules is, as yet, unknown.

Niraparib is a highly selective inhibitor of PARP1, unlike Talazoparib, Olaparib and Rucaparib, which are potent inhibitors of both PARP1 and PARP2 (the lack of specificity for either protein being due to similarities in the NAD+ binding domain) (Valabrega, *et al*., 2021). Other differences between clinically available PARP inhibitors include off-target kinase activity, with both Niraparib and Rucaparib administration resulting in the inhibition of CDK16, DYRK1s, and PIM3, important kinases (Antolin, *et al*., 2020). Another difference between these inhibitors is their ability to cross the blood-brain barrier (BBB). Niraparib is capable of permeating the BBB, sustaining PARP inhibition and limiting intracranial tumour growth, as opposed to Olaparib, which does not efficiently cross the BBB nor successfully maintain inhibition (Sun, *et al*., 2018). Similarly, both Rucaparib and Talazoparib exhibit inefficient penetration of the BBB (Parrish, *et al*., 2016, Kizilbash, *et al*., 2017).

A major obstacle in the clinical use of PARP inhibitors is the high degree of pre-existing and acquired resistance (Noordermeer and van Attikum, 2019). Mutations in *PARP1* can result in a reduced degree of trapping on DNA, resulting in PARP inhibitor resistance (Pettitt, *et al*., 2018). Similarly, the loss of poly(ADP-ribose) glycohydrolase (PARG) contributes to PARP inhibitor resistance, as this results in a partial restoration of poly(ADP-ribosylation), diminishing trapping (Gogola, *et al*., 2018). The loss of factors facilitating NHEJ, such as 53BP1 and its downstream factors, RIF1 and REV7, result in a loss of resection inhibition which promotes the BRCA1-independent reinitiation of HR, and PARP inhibitor resistance (Bouwman, *et al*., 2010, Feng, *et al*., 2013, Xu, *et al*., 2015). A further mechanism by which PARP inhibitor resistance may arise is through the stabilisation of replication forks, for example by loss of PTIP (Noordermeer and van Attikum, 2019). PTIP facilitates the recruitment of MRE11, a nuclease which degrades nascent DNA strands at stalled forks, leading to fork collapse and chromosomal aberration (Chaudhuri, *et al*., 2016). The loss of PTIP (among several proteins involved

in replication stress) also induces PARP inhibitor resistance in both BRCA1 and BRCA2 cells (Chaudhuri, *et al*., 2016, Noordermeer and van Attikum, 2019).

1.3.1.2 – Poly(ADP-ribose) Glycohydrolase (PARG)

The catabolism of poly(ADP-ribose) is primarily mediated by poly(ADP-ribose) glycohydrolase (PARG), which hydrolyses PAR and has been shown to protect against PARP1 induced cell death (Koh, *et al*., 2004, Isabelle, *et al*., 2010, Feng, *et al*., 2013). Despite the abundance of PARP1 activity following the induction of damage, the degradation of poly(ADP-ribose) occurs rapidly (Feng and Koh, 2013). Several alternatively spliced isoforms of PARG exist, with variable patterns of expression, but full length (110kDa) PARG is located in the nucleus (Haince, *et al*., 2006, Meyer, *et al*., 2007). Drosophila PARG knockout is viable but shows marked neurodegeneration and the accumulation of poly(ADP-ribose) in nervous tissue, and the overexpression of PARG has been highlighted as neuroprotective following excitotoxicity and stroke (Hanai, *et al*., 2004, Cozzi, *et al*., 2006, Park, *et al*., 2020).

While PARG can efficiently cleave ribose-ribose bonds in the poly(ADP-ribose) polymer, it is unable to remove the protein proximal, terminal ADP-ribose moiety (Slade, *et al*., 2011). As such, ADP-Ribosyl Hydrolase 3 (ARH3) and terminal ADP-ribose glycohydrolase (TARG) are required to remove the terminal ADP-ribose monomer from the ribosylated serine and aspartate/glutamate residues of modified proteins, respectively (Kasamatsu, *et al*., 2011, Sharifi, *et al*., 2013, Hanzlikova, *et al*., 2020). Mutations in *ADPRHL2*, which encodes ARH3, were recently identified in patients presenting with progressive neurodegeneration, episodic ataxia, and seizures (Danhauser, *et al*., 2018, Ghosh, *et al*., 2018). Fibroblasts from patients with pathogenic mutations in *ADPRHL2* exhibit increased cell death following H_2O_2 treatment (Mashimo, *et al*., 2019). Further, Hanzlikova, *et al*. identified the accumulation of mono-ADP-ribose ‘scars’ in *ARH3/ADPRHL2* patient fibroblasts following the induction of DNA damage, the result of an inability to remove terminal ADP-ribose moieties following PARG cleavage.

Much like PARP1, inhibitors of PARG have investigate for their potential as novel cancer therapeutics (Harrision, *et al*., 2020). PARG inhibitors compete with poly(ADP-ribose) for the PARG binding site, resulting in the persistence of the PAR polymer (James, *et al*., 2016). PARG inhibition leads to the increased incidence of reversed forks following replication stress, likely due to the poly(ADP-ribosylation) of RECQ1 by PARP1, which must be removed in order to promote branch migration and replication restart (Berti, *et al*., 2013, Margalef, *et al*., 2018). Synthetic lethality has been observed

following the treatment of BRCA2 deficient cells with PARG inhibitor (as well as in other HR deficient cells), owing to elevated replication associated DNA damage and replication fork collapse, leading to an increased reliance on the HR pathway (Fathers, *et al*., 2012, Gravells, *et al*., 2017).

1.3.2 – XRCC1 and the Single-Strand Break Repair Machinery

The SSBR scaffold protein XRCC1, while lacking inherent enzymatic activity, coordinates the association and activity of multiple DNA repair proteins, and is important for the restoration of damaged termini; interacting directly during DNA end processing with APTX, Pol β, and PNKP (Caldecott, *et al*., 1996, Whitehouse, *et al*., 2001, Clements, *et al*., 2004, Mok, *et al*., 2019) (Figure 1.3). XRCC1, as a DNA repair scaffold, is responsible for the assembly of the SSBR machinery, multiple constituents of which are mutated in various forms of cerebellar ataxia (Moreira, *et al*., 2001, El-Khamisy, *et al*., 2005, Shen, *et al*., 2010, Bras, *et al*., 2015, Leal, *et al*., 2018). XRCC1 recruitment is facilitated by PARP1 activation due to its preferential binding to autoribosylated PARP1, subsequently allowing SSBR proteins to accumulate at sites of DNA damage (Masson, *et al*., 1998, Dantzer, *et al*., 1999).

1.3.2.1 – XRCC1

As a consequence of the heterogeneity of lesions arising in DNA, their repair may require several enzymatic processes (Abbotts and Wilson, 2017). Scaffold proteins are integral to the co-ordination of these processes, ensuring that the complete repair process can take place without the chance of releasing potentially toxic, labile repair intermediates (Krokan and Bjørås, 2013). Scaffold proteins, such as XRCC1, form heterogeneous complexes that enable the complete repair of various DNA lesions (Andres, *et al*., 2015). XRCC1 was first identified as protective against ionizing radiation (IR), and later UV induced damage and alkylation (Thompson, *et al*., 1990, Caldecott, *et al*., 1992, Zdzienicka, *et al*., 1992).

The function of XRCC1 is facilitated by its three globular domains (London, 2015). The central BRCT domain contains a poly(ADP-ribose) binding motif and mediates the poly(ADP-ribose) dependent recruitment of XRCC1 to autoribosylated PARP1, and also DNA binding activity critical for retention at sites of damage (Masson, *et al*., 1998, Taylor, *et al*., 2002, Breslin, *et al*., 2015, Mok, *et al*., 2019). The N-terminal domain of XRCC1 facilitates binding to DNA Polymerase β, an interaction required for efficient BER (Kubota, *et al*., 1996, Dianova, *et al*., 2004, Cuneo and London, 2010). The C-terminal domain interacts with another binding partner of XRCC1, DNA ligase IIIα, forming a stable complex to facilitate the ligation of the DNA phosphodiester backbone (Caldecott,

et al., 1994, Caldecott, *et al*., 1995, Parsons, *et al*., 2010). The interaction of XRCC1 with other enzymes involved in SSBR is facilitated by a linker segment between the central and C-terminal BRCT domain, which binds the forkhead-associated (FHA) domains of APTX, APLF, and PNKP (Date, *et al*., 2004, Ali, *et al*., 2009, Lu, *et al*., 2010, Kim, *et al*., 2017).

1.3.3 – Hereditary Defects in SSBR

Autosomal recessive cerebellar ataxias (ARCA) represent a large group of neurological diseases, with a phenotypic heterogeneity that reflects the numerous ways in which cerebellar dysfunction may result in movement disorders (Beaudin, *et al*., 2019). While ataxia is a characteristic symptom of cerebellar degeneration, it is also a presenting feature of a number of encephalopathies, or inborn errors of metabolism (Chambliss, *et al*., 1998, Leegwater, *et al*., 2001, Rossi, *et al*., 2018). Mutations in proteins responsible for both SSBR and DSBR are associated with cerebellar ataxia; notably APTX (Ataxia with Ocular Motor Apraxia Type 1 (AOA1)), PNKP (Microcephaly with Seizures (MCSZ), Ataxia with Ocular Motor Apraxia Type 4 (AOA4), and Charcot-Marie-Tooth disease (CMT2B2)), and TDP1 (Spinocerebellar Ataxia with Axonal Neuropathy Type 1 (SCAN1)) (Moreira, *et al*., 2001, Takashima, *et al*., 2002, Leal, *et al*., 2018, Yoon and Caldecott, 2018, Kalasova, *et al*., 2019) (Figure 1.4). While these disorders are heterogeneous in their presentation, they are typically associated with cerebellar atrophy and progressive ataxia (Caldecott, 2008, Beaudin, *et al*., 2019) (Figure 1.4). The heterogeneity of these disorders may reflect the different subsets of damaged termini repaired by the mutated protein in question.

TOP1 acts to incise DNA, doing so by forming a covalent bond between itself and the cleaved 3’-phosphate terminus (Li and Liu, 2015). TDP1 is responsible for the hydrolysis of this linkage between TOP1 and DNA at sites of Topoisomerase 1 cleavage leaving 3’-phosphate and 5’-hydroxyl termini for which PNKP is necessary to repair (Yang, *et al*., 1996, Plo, *et al*., 2003, Interthal and Champoux, 2011, Pommier, *et al*., 2015, Kawale and Povirk, 2018). There are several endogenous sources of lesions which may prevent religation following Top1 incision, including abasic sites or oxidative base lesions such as 5’-hydroxycytosine (Interthal, *et al*., 2005a, Zhou, *et al*., 2009, Flett, *et al*., 2018). Further, TDP1 may act outside of the resolution of Top1-linked cleavage complexes, as it possesses the capacity to repair sugar fragments such as 3’-phosphoglycolates resulting from ROS induction or UV irradiation, and has been shown to have AP endonuclease activity, perhaps indicating it may operate as a redundancy

for APE1 function (Interthal, *et al*., 2005a, Zhou, *et al*., 2005, Lebedeva, *et al*., 2013, Flett, *et al*., 2018).

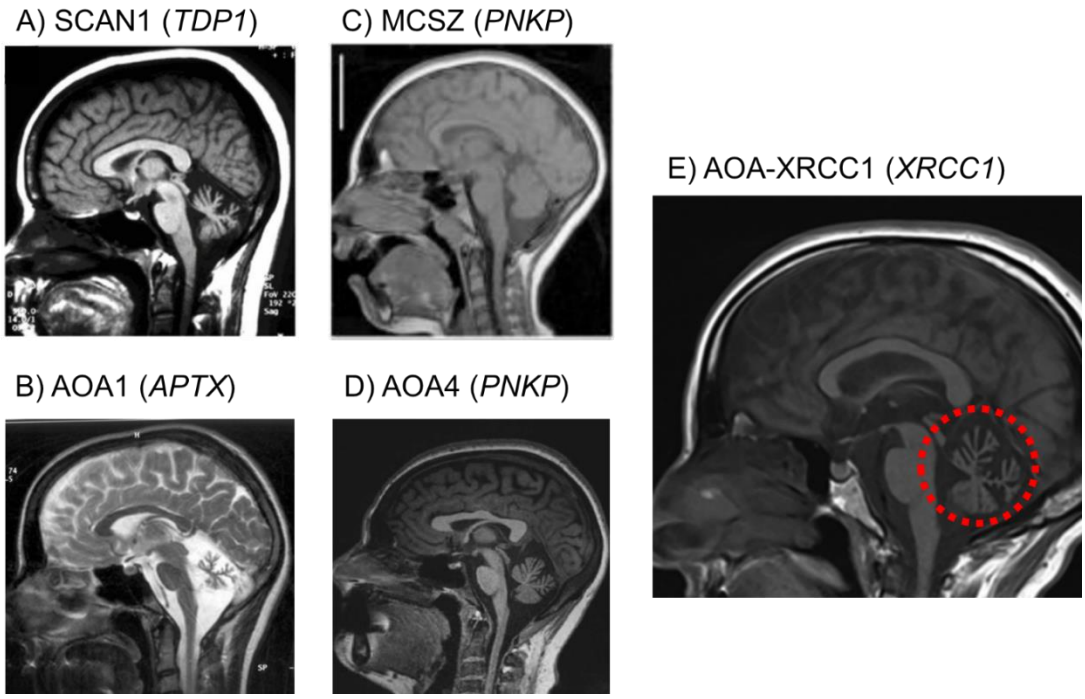

Figure 1.4. *Clinical Features of the Cerebellar Ataxias*. MRI images showing cerebellar degeneration and atypical brain morphology associated with hereditary defects in SSBR enzymes. A) Sagittal section of a 36-year-old with SCAN1, caused by a mutation in *TDP1*, B) a 21-year-old with AOA1, caused by mutation in *APTX*, C) a 7-year-old with MCSZ, and D), a 28-year-old with AOA4, both caused by mutations in *PNKP*. E) Sagittal MRI of a 47-year-old female with AOA-XRCC1, caused by mutation in *XRCC1*, highlighting atrophy of the cerebellum. Figure created with images from Takashima, *et al*., 2002, Le Ber, *et al*., 2003, Shen, *et al*., 2010, Paucar, *et al*., 2016, and Hoch, *et al*., 2017.

A mutation resulting in the inability of TDP1 to catalyse its self-hydrolysis from DNA results in the neurological disorder SCAN1 (Takashima, *et al*., 2002, Pommier, *et al*., 2014). Mutations in *TDP1* result in an inability to repair the Top1 associated SSBs (Interthal, *et al*., 2005b, El-Khamisy, *et al*., 2005, Pommier, *et al*., Huang and Pommier, 2019). It has been proposed that the pathology of SCAN1 is a result of the increased transcriptional demand in neuronal cells; as this would result in the further accumulation of TDP1-linked DNA complexes, and unrepaired SSBs (Sordet, *et al*., 2010, Yap and Greenberg, 2018). Further, transcription arrest at irresolvable complexes is likely linked to ATM activation, double strand break formation, and subsequent cell death (Sordet, *et al*., 2010, Blackford and Jackson, 2017). There is further evidence to suggest that mitochondrial ROS production, and mitochondrial DNA damage (as the mitochondrial form of TDP1 is identical to its nuclear form) may result in cell death (Sykora, *et al*., 2012). This may explain the pronounced cerebellar involvement associated with SCAN1, given the high metabolic demand of the cerebellum (Bolanos, 2016) (Figure 1.4).

APTX is involved in the repair of adenosine monophosphate (AMP)-linked 5' termini, resulting from incomplete/abortive activity of DNA ligases (Ahel, *et al*., 2006). During BER, the collision of DNA ligases with modified termini, such as oxidate strand breaks and incised 5' abasic sites, resulting in the covalent attachment of AMP to the 5' phosphate terminus of the ligation substrate and the formation of blocked BER intermediates (Caglayan, *et al*., 2014, Carroll, *et al*., 2015, Schellenberg, *et al*., 2015). APTX is responsible for the removal of the 5'-AMP moiety from these intermediates, allowing repair to continue (Ahel, *et al*., 2006). Presumably, AOA1 (caused by mutations in *APTX*) is a result of the accumulation of these 5' adenylated breaks, although auxiliary repair may exist via the lyase activity of DNA polymerase β, which can remove 5' adenylated deoxyribose phosphate residues, and/or by FEN1 mediated long-patch repair (Ahel, *et al*., 2006, Reynolds, *et al*., 2009, Caglayan, *et al*., 2014, Caglayan, *et al*., 2015, Howard, *et al*., 2017). Further, the accumulation of mitochondrial DNA damage following mutation of the mitochondrial *APTX* has been shown to result in decreased APE1 expression – resulting in the downregulation of NRF1 and NRF2, and subsequently the reduced expression of proteins involved in mitochondrial electron transport – which may account for some aspects of the AOA1 phenotype, as mitochondrial dysfunction is also linked to cerebellar ataxia (Castellotti, *et al*., 2011, Bargiela, *et al*., 2015, Garcia-Diaz, *et al*., 2015).

PNKP encodes DNA Polynucleotide Kinase/Phosphatase; mutations in which are associated with MCSZ, AOA4, and CMT2B2 (Shen, *et al*., 2010, Nakashima, *et al*., 2014, Leal, *et al*., 2018, Kalasova, *et al*., 2019). PNKP is an enzyme required for SSBR,

as well as both NHEJ and alternative-NHEJ, catalysing both the dephosphorylation of 3' phosphate termini and phosphorylation of 5' hydroxyl termini (Dumitrache and McKinnon, 2016). PNKP further functions following the proteolytic degradation of Top1 cleavage-complexes and the subsequent activity of TDP1 (Jilani, *et al*., 1999, Plo, *et al.*, 2003, Shimada, *et al*., 2015). Mutations in *PNKP* result in MCSZ, a disorder characterised by microcephaly, early-onset seizures, and neurodevelopmental delay, and AOA4, associated with mutations in the kinase domain and characterised by cerebellar atrophy, ataxia with ocular motor apraxia, and peripheral neuropathy (Reynolds, *et al*., 2012, Bras, *et al*., 2015, Shimada, *et al*., 2015) (Figure 1.4). MCSZ is a clinically heterogeneous disorder, with certain mutations having been found to result in both cerebellar atrophy and early onset seizures and microcephaly (Poulton, *et al*., 2013). MCSZ patient-derived fibroblasts are characterised by impaired SSBR and hyperactivity of the SSB sensor PARP1, and this neurodevelopmental disease is most likely the result of reduced DNA 3' phosphatase activity (Kalasova, *et al*., 2020). By contrast, neurodegeneration associated with AOA4 and CMT2B2 is most likely a result of the loss of *PNKP* DNA 5'-kinase activity (Kalasova, *et al*., 2020). The degree of 5'-kinase impairment is consistent with disease severity and onset of neurodegeneration, as this reduction was found to be greater in AOA4 patient fibroblasts than in CMT2B2 (Kalasova, *et al*., 2020). Knockout of *Pnkp* is embryonic lethal in mice, due to extensive DNA damage and subsequent p53 dependent apoptosis in the developing brain, however Nes-Cre driven knockout produces mice viable until p5 (Shimada, *et al*., 2015). That *Pnkp* knockout is far more detrimental than either *Tdp1* or *Aptx* may reflect the multifaceted roles of PNKP in the DDR, being both critical for SSBR and NHEJ, or perhaps the breadth of SSB termini that it processes (Dumitrache and McKinnon, 2016).

1.3.3.1 – Biallelic *XRCC1* Mutation in a Human Patient

Recently, it was shown that biallelic mutations in *XRCC1* result in a novel Ataxia with Oculomotor Apraxia (AOA-XRCC1) (Hoch, *et al*., 2017, O'Connor, *et al*., 2018). The disorder presents primarily with progressive cerebellar atrophy, ocular motor apraxia, and peripheral neuropathy (Hoch, *et al*., 2017) (Figure 1.4). Patient fibroblasts exhibited drastic reductions in XRCC1 levels (roughly 5% of the protein remaining) and, subsequently, a reduction in LIG3 – consistent with observations regarding the stability of LIG3 in the absence of its partner protein (Caldecott, *et al*., 1995, Hoch, *et al*., 2017). Patient fibroblasts demonstrated defective recruitment of XRCC1 to chromatin following the induction of SSBs, and subsequently delayed repair kinetics indicative of the central role of XRCC1 in the orchestration of SSBR (Caldecott, 2008, Hoch, *et al*., 2017). In the absence of XRCC1, SSBR occurs more slowly, resulting in prolonged activation of the

SSB sensor PARP1, and elevated levels of poly(ADP-ribose) synthesis (Hoch, *et al*., 2017).

1.3.3.2 – The Conditional Knockout Mouse: *Xrcc1*$^{Nes\text{-}Cre}$

Mutations in *XRCC1* result in cerebellar ataxia and ocular motor apraxia (Hoch, *et al*., 2017). While germ line deletion of *Xrcc1* is embryonic lethal, *Xrcc1*$^{Nes\text{-}Cre}$ mice are viable (Tebbs, *et al*., 1999, Lee, *et al*., 2009). In *Xrcc1*$^{Nes\text{-}Cre}$ mice, the deletion of *Xrcc1* occurs at E15.5, through nestin driven cre recombination and, as such, *Xrcc1*$^{Nes\text{-}Cre}$ mice lack the protein only in nervous tissue (Lee, *et al*., 2009) *Xrcc1*$^{Nes\text{-}Cre}$ mice exhibit elevated poly(ADP-ribose) levels in the brain, greatly reduced levels of cerebellar interneurons, cerebellar ataxia, and juvenile mortality (ordinarily between p15 and p21) (Lee, *et al*., 2009, Hoch, *et al*., 2017, Komulainen, *et al*., 2021). Cerebellar interneuron death in *Xrcc1*$^{Nes\text{-}Cre}$ mice can be rescued by the additional deletion of p53, a cell cycle checkpoint and regulator of cell death; indicating that interneuron death occurs during neurogenesis, during which time cerebellar neurons are still mitotic (Lee, *et al*., 2009). *Xrcc1*$^{Nes\text{-}Cre}$ mice exhibit seizures which, ultimately, result in their shortened lifespan (Komulainen, *et al*., 2021). The additional deletion of *Parp1* prevents loss of interneurons, and reduces the extent of cerebellar ataxia (Lee, *et al*., 2009, Hoch, *et al*., 2017*). Parp1* deletion also dramatically increases lifespan in *Xrcc1*$^{Nes\text{-}Cre}$ mice, resulting in an ~8-fold increase in the longevity of *Parp1*$^{-/-}$/*Xrcc1*$^{Nes\text{-}Cre}$ mice, likely due to the absence of terminal seizures (Komulainen, *et al*., 2021). Heterozygous deletion of *Parp1* results in a greater extension of lifespan than homozygous knockout (25-fold), potentially indicating an additional role for Parp1 in the SSBR defective brain, though whether these mice ultimately exhibit terminal seizures is still unclear (Komulainen, *et al*., 2021).

1.4 – Cerebellar Function and Ataxia

Ataxia is defined as the impaired co-ordination of voluntary muscle movement, classically associated with cerebellar dysfunction (Ashizawa and Xia, 2016). The cerebellum is a region of the brain responsible for motor function, and its degeneration is linked to several hereditary ataxia disorders (Beaudin, *et al*., 2019). The sole output of the cerebellum occurs through the firing of Purkinje cells (PC), some of the largest neurons in the brain (Hoxha, *et al*., 2016). PCs exhibit highly a highly arborised dendritic structure, which is required for the complex co-ordination of inputs and outputs to produce the wide range of spike patterns that form the basis of motor control (Hoxha, *et al*., 2016, Attwell and Mehta, 2021). Far smaller but in much greater number are the cerebellar granule cells (CGC), which make up roughly three quarters of the neurons in an adult human brain (Badura and De Zeeuw, 2017). The function of CGCs is to relay

the input of mossy fibres (the main cerebellar input, originating primarily in the cerebral cortex) to PC dendrites via parallel fibres, the axons of the CGC (Schonewille, *et al*., 2021). The degeneration of PCs is the most common clinical finding in cerebellar ataxia models (Huang and Verbeek, 2019). Similarly, mutations resulting in alterations to the intrinsic properties of the PC membrane can result in ataxia due to alterations in the rate or pattern of PC firing (Hoxha, *et al*., 2018).

There are many different forms of cerebellar ataxia (Beaudin, *et al*., 2019). Spinocerebellar ataxia 1 (SCA1) occurs as a result of mutations in *ATXN1*, which encodes Ataxin 1, a DNA binding protein involved in the regulation of gene expression and nuclear transport (Zhang, *et al*., 2020). In SCA1 patients, the expansion of a CAG repeat in *ATXN1* results in an expanded polyglutamine tract in the protein, leading to the dysfunction and degeneration of cells in the cerebellum, primarily PCs (Menon, *et al*., 2013). Spinocerebellar Ataxia with Axonal Neuropathy (SCAN1) is another form of cerebellar ataxia, caused by mutations in *TDP1* (Takashima, *et al*., 2002). SCAN1 is characterised by cerebellar degeneration, however it is as yet unclear why the cerebellum in particular is affected. One possibility is that TDP1 is highly expressed in the cerebellum, particularly in PCs, which are prone to degeneration in the *Tdp1*$^{-/-}$ mouse (Hirano, *et al*., 2007). Alongside *TDP1*, mutations in several genes encoding elements of the SSBR machinery, such as *PNKP* and *XRCC1,* result in cerebellar degeneration and ataxia, though the mechanisms underlying this are unclear (Hoch, *et al*., 2017).

Recent evidence has suggested that the deregulation of calcium signalling in PCs may underlie cerebellar ataxia (Kasumu and Bezprozvanny, 2012). Voltage-gated calcium channels regulate the entry of calcium into the cell following depolarisation and are highly enriched in the dendritic arbor of PCs. $Ca_{v2}2.1$, or P/Q type calcium channels, make up roughly 90% of the calcium channels in PC dendrites (Gruol, *et al*., 2012, Hoxha, *et al*., 2018). Mutations in the alpha subunit of P/Q type calcium channels are associated with episodic ataxia type 2 (EA2) and spinocerebellar ataxia type 6 (SCA6) (Giunti, *et al*., 2015, Sintas, *et al*., 2017, Indelicato and Boesch, 2021). Mice with a mutated form of the P/Q type calcium channel exhibit reduced firing frequency of PCs, impaired pacemaking activity and, subsequently, ataxia (Todorov, *et al*., 2012). Ataxia is associated with decreased excitation of PCs, and it has been proposed that the decreased entry of Ca^{2+} into the cell inhibits the opening of Ca^{2+} dependent K^{+} channels, leading to the perpetuation of a depolarised membrane (Bushart, *et al*., 2018, Hoxha, *et al*., 2018). Interestingly, missense mutations in inositol 1,4,5-triphosphate receptor type 1 (IP3R1) were found to result in spinocerebellar ataxia type 29 (SCA29), as well as SCA15 (Marelli, *et al*., 2011, Zambonin, *et al*., 2017). IP3R1 is a membrane bound

tetrameric Ca^{2+} found at intracellular Ca^{2+} stores such as the endoplasmic reticulum, and highly expressed in PCs, and regulates Ca^{2+} release following the binding of its ligand, IP3 (Lanner, *et al*., 2010, Karagas and Vankatachalam, 2019). The absence of IP3R1 results in morphological defects of PCs, profound ataxia, and seizures (Matsumoto, *et al*., 1996). Analysis of many ataxia disease genes have found distinct convergence around both calcium and IP3 signalling (Schorge, *et al*., 2010). Interestingly, genes involved in the regulation of calcium and inositol triphosphate signalling were found to be deregulated in a Parp1/NAD+ dependent manner in the SCA7 mouse (Stoyas, *et al*., 2020).

1.5 – Synaptic Transmission and Calcium Signalling

Neuronal communication occurs through two primary mechanisms; the rapid transfer of information facilitated by synaptic transmission, and the comparatively slow signalling mediated by messengers such neuropeptides, monoamines, and endocannabinoids (Südhof and Malenka, 2008). Chemical synapses are heterogeneous junctions at which neuronal communication occurs, specialised for the conversion of electrical signals into neurotransmitter release (Südhof, 2012). Once an action potential (a transient change in neuronal membrane polarity) invades the presynaptic terminal, the depolarisation of the membrane drives the opening of voltage gated Ca^{2+} channels (VGCCs), and the influx of extracellular Ca^{2+} into the presynaptic terminal down its electrochemical gradient (Südhof, 2012) (Figure 1.5). This highly localised increase in presynaptic calcium results in the rapid fusion of vesicles with the presynaptic membrane due to the binding of Ca^{2+} with synaptotagmin, facilitating interactions with the core release machinery (Sabatini and Regehr, 1996, Kiessling, *et al*., 2018, Dolphin and Lee, 2020). Ca^{2+} signalling is such an intrinsic element of the propagation of neuronal signalling that it has long been utilised as a reliable experimental proxy for neuronal activity (Ali and Kwan, 2019). Synaptotagmins do not directly enable the exocytosis of synaptic vesicles with the presynaptic membrane, but rather couple the influx of Ca^{2+} to soluble *N*-ethylmaleimide-sensitive factor attachment protein receptor (SNARE) proteins, which provide the driving force behind membrane fusion (Jackson, 2010, Kiessling, *et al*., 2018). Following exocytosis, synaptic transmission occurs through the release of neurotransmitter across the synaptic cleft, where it is subsequently detected by postsynaptic receptors, completing the conversion of an electric impulse to chemical transmission (Dolphin and Lee, 2020). Transmitter release is, however, probabilistic; meaning that the presence of an action potential does not guarantee synaptic vesicle fusion (Branco and Staras, 2009). In particular, the relationship between presynaptic $[Ca^{2+}]$ and release probability is highly non-linear, with

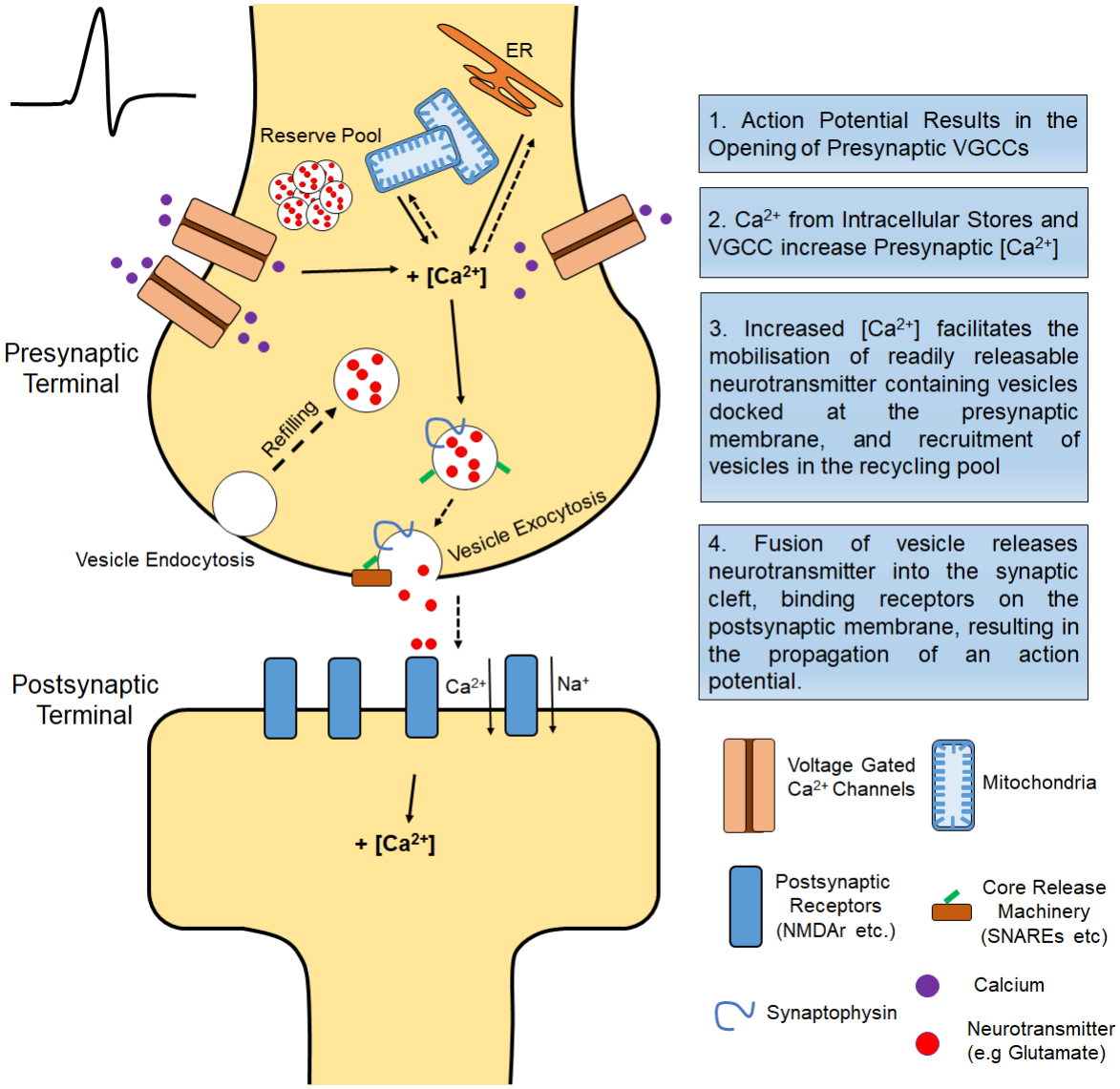

Figure 1.5. *Calcium Control of Neurotransmitter Release*. The influx of Ca^{2+} into the presynaptic terminal is a pivotal step in the fusion of neurotransmitter-containing vesicles. The invasion of the nerve terminal by an action potential precedes the opening of Voltage Gated Ca^{2+} Channels (VGCCs), through which extracellular Ca^{2+} enters the presynaptic terminal. Similarly, Ca^{2+} is released from intracellular organelles, such as the mitochondria and the endoplasmic reticulum, which also serve to buffer cytosolic calcium to dynamically modulate presynaptic Ca^{2+} signalling. The binding of Ca^{2+} to synaptotagmins facilitates the release and fusion of neurotransmitter containing vesicles. Vesicle fusion enables the release of neurotransmitters, such as glutamate, across the presynaptic cleft.

relatively small increases in concentration being linked to significant alterations in the likelihood of vesicle fusion (Heidelberger, *et al*., 1994, Sakaba and Neher, 2001).

The influx of ionic Ca^{2+} does not occur entirely through VGCCs. Organelles, such as the endoplasmic reticulum (ER) provide intracellular Ca^{2+} stores that also serve to regulate neurotransmitter release probability (Padamsey, *et al*., 2018) (Figure 1.5). The release of Ca^{2+} from the ER is facilitated in part by ryanodine receptors (RyR), a family of Ca^{2+} release channels on the ER membrane (Arias-Cavieres, *et al*., 2018). RyRs are activated by cADPr, a calcium mobilising second messenger synthesised by CD38 from NAD+ (Arias-Cavieres, *et al*., 2018, Hogan, *et al*., 2019). Calcium release from the ER also occurs via IP3Rs, Ca^{2+} release channels activated in the presence of inositol triphosphate and Ca^{2+}, through a phenomenon known as calcium induced calcium release (CICR) (Lanner, *et al*., 2010, Karagas and Vankatachalam, 2019). The inhibition of CICR has been shown to affect the dynamics of depolarisation induced Ca^{2+} responses, highlighting the additional level of regulation afforded by release mechanisms from intracellular stores (Friel and Tsien, 1994).

Presynaptic terminals are rich in mitochondria, which generate the high levels of ATP required for the above processes to occur. However, mitochondria also serve to sequester cytosolic [Ca^{2+}] to regulate the spatial and temporal dynamics of neurotransmitter release (Padamsey, *et al*., 2018). The hyperpolarised resting membrane potential of the mitochondria allows the sequestration of Ca^{2+} along the electrochemical gradient, regulating release probability and recovery from synaptic depression following activity (Contreras, *et al*., 2010, Zorova, *et al*., 2011). Similarly, the activity of sarcoplasmic/endoplasmic reticulum Ca^{2+}-ATPases (SERCA) act to regulate calcium homeostasis, maintaining the concentration of Ca^{2+} in the ER lumen at a level three orders of magnitude greater than cytosolic [Ca^{2+}] (Meldolesi and Pozzan, 1998, Shen, *et al*., 2011).

The importance of calcium homeostasis is best exemplified by the multitude of disorders in which it is deregulated, such as SCA, AD, PD, and epilepsy (Schapira, 2013, Rajajulendran and Hanna, 2016, Popugaeva, *et al*., 2017, Hisatsune, *et al*., 2018). Many variants of SCA are characterised by calcium dyshomeostasis resulting from inappropriate Ca^{2+} release by IP3Rs, which are highly expressed in cerebellar PCs (Kasumu and Bezprozvanny, 2012, Hisatsune, *et al*., 2018). Mutations in *CACNA1A*, which encodes the α subunit of $Ca_v2.1$, the P/Q type voltage gated calcium channel (high voltage activated, expressed highly in the PCs of the cerebellum), are associated with episodic ataxia, and cerebellar ataxia with absence seizures (Giunti, *et al*., 2015,

Sintas, *et al*., 2017, Indelicato and Boesch, 2021). Mutations in both *CACNA1H* and *CACNA1G*, which encode T type calcium (low voltage activated calcium channels) have been found in cases of idiopathic generalised epilepsy (IGE) (Singh, *et al*., 2007, Eckle, *et al*., 2014). Seizures can be considered a result of a distortion in the balance of excitation and inhibition in the brain (E/I balance) (Fritschy, 2008). In the mouse hippocampus, the maintenance of the E/I balance is coupled to the regulation of $Ca_v2.1$ by calcium sensing proteins (Nanou, *et al*., 2018). Perhaps the clearest evidence of the involvement of Ca^{2+} in underpinning seizure mechanics comes from the observation of sustained, elevated intracellular [Ca^{2+}] in hippocampal neurons during status epilepticus *in vitro* (Pal, *et al*., 1999).

The hippocampus is a region of the brain embedded in the temporal lobe, which predominantly functions in cognition, learning and memory (Rubin, *et al*., 2014, Anand and Dhikav, 2015). The most common neurons in the hippocampus are pyramidal cells, alongside GABAergic interneurons, and the granule cells of the dentate gyrus (Keller, *et al*., 2018). The hippocampus is highly plastic (owing to large quantities of NMDA receptors), and is particularly susceptible to injury, particularly as a result of glutamate excitotoxicity (explained in 1.6) (Anand and Dhikav, 2015, Choi, 2020). Alongside the cerebellum, elevated levels of poly(ADP-ribose) are seen in the *Xrcc1*$^{Nes\text{-}Cre}$ hippocampus, which may be of particular relevance given the frequent involvement of the hippocampus in seizures and epilepsy (Wiebe, 2000, Komulainen, *et al*., 2021).

1.6 DNA Damage in the Nervous System

The nervous system constitutes an array of tissue and cell types, and represents the most complex, and poorly understood area of human physiology. There are purportedly up to 100 billion neurons in the human brain, and many more glial cells – with each functional unit displaying a vast array of connections that underpin cognition, consciousness, and autonomic function (Lent, *et al*., 2012). While cell proliferation occurs during neurogenesis, occurring mostly during development, mature neuronal cells are post-mitotic, requiring the strict maintenance of genomic integrity throughout the lifespan of an organism (McKinnon, 2017, Frade and Ovejero-Benito, 2015). Due to the specialised physiology of neuronal cells, they are frequently exposed to nervous system specific, endogenous sources of DNA damage (McKinnon, 2017).

Nitric Oxide (NO) is a gaseous molecule, produced by nitric oxide synthases (NOS), capable of easily diffusing across biological membranes (Garthwaite, *et al*., 1988). In neurons, neuronal nitric oxide synthase (nNOS) is responsible for the Ca^{2+} dependent production of NO by catalysing the oxidation of L-arginine (Schmidt, *et al*.,

1992, Stuehr, 2004). Neuronal NO predominantly acts as a retrograde neurotransmitter, where its synthesis is stimulated by the influx of Ca^{2+} through glutamate bound NMDA receptors, which binds CaM to activate nNOS (Schmidt, *et al*., 1992, Picón-Pagés, *et al*., 2019). Retrograde signalling refers to the diffusion of postsynaptic NO across to the presynaptic terminal, where it stimulates Ca^{2+}-independent vesicle exocytosis, resulting in an activation loop that promotes long term potentiation (LTP, the persistent strengthening of synaptic connections due to a repeated pattern of activity) (Meffert, *et al*., 1994, Arancio, *et al*., 1996, Bliss and Cooke, 2011). NO is particularly important for hippocampal function, being critical in the maintenance of signalling pathways involved in learning and memory, as well as dendritic spine growth (Dinerman, *et al*., 1994, Paul and Ekambaram, 2011, McLeod, *et al*., 2020). This form of signalling is not, however, without negative consequences, as NO reacts with $O_2^{\bullet-}$ to form $ONOO^-$. $ONOO^-$ avoids SOD activity, as the affinity of $O_2^{\bullet-}$ for NO is ten times that of SOD (Beckman, *et al*., 1990, Huie and Padmaja, 1993). The protonated form of $ONOO^-$, ONOOH, produces both nitrogen dioxide ($\bullet NO_2$) and $OH\bullet$, capable of nitrating and oxidating nucleobases, respectively (Coddington, *et al*., 1999, Niles, *et al*., 2006). Further, the nitration of other proteins such as peroxiredoxin 6, can further limit the antioxidant capacity of the neuron (Coma, *et al*., 2005). The elevated concentration of $ONOO^-$ results in cell death, and is associated with neurodegenerative diseases, such as AD (Smith, *et al*., 1997, Tajes, *et al*., 2013).

Glutamate is the predominant excitatory neurotransmitter in the brain (Zhou and Danbolt, 2014). Despite the prevalence of glutamate transmission in the brain, excessive activation of glutamate receptors results in the accumulation of DNA damage, PARP activation, and cell death, through a process known as glutamate excitotoxicity (Andrabi, *et al*., 2011, Lewerenz and Maher, 2015). Glutamate excitotoxicity is associated with the pathology of numerous neurodegenerative disorders but is perhaps best understood in response to cerebral ischemia (Lewerenz and Maher, 2015, Sun, *et al*., 2019). In response to the disruption of cerebral blood flow, there is disruption of oxidative phosphorylation and, subsequently, ATP depletion and ionic imbalance that precede the depolarisation of the neuronal membrane, and Ca^{2+} uptake via the plasma membrane Na^+/Ca^{2+} exchanger (NCX) (Lee and Kim, 2015, Rueda, *et al*., 2016). The influx of ionic calcium regulates the inappropriate and excessive release of glutamate at the presynaptic terminal (Zhou and Danbolt, 2014) (Figure 1.6). The subsequent activation of NMDA receptors triggers the downstream deregulation of Ca^{2+} dependent processes, •NO synthesis, and the production of peroxynitrite, as well as stimulating the production of mitochondrial ROS (Lewerenz and Mager, 2015, Wang and Swanson, 2020) (Figure

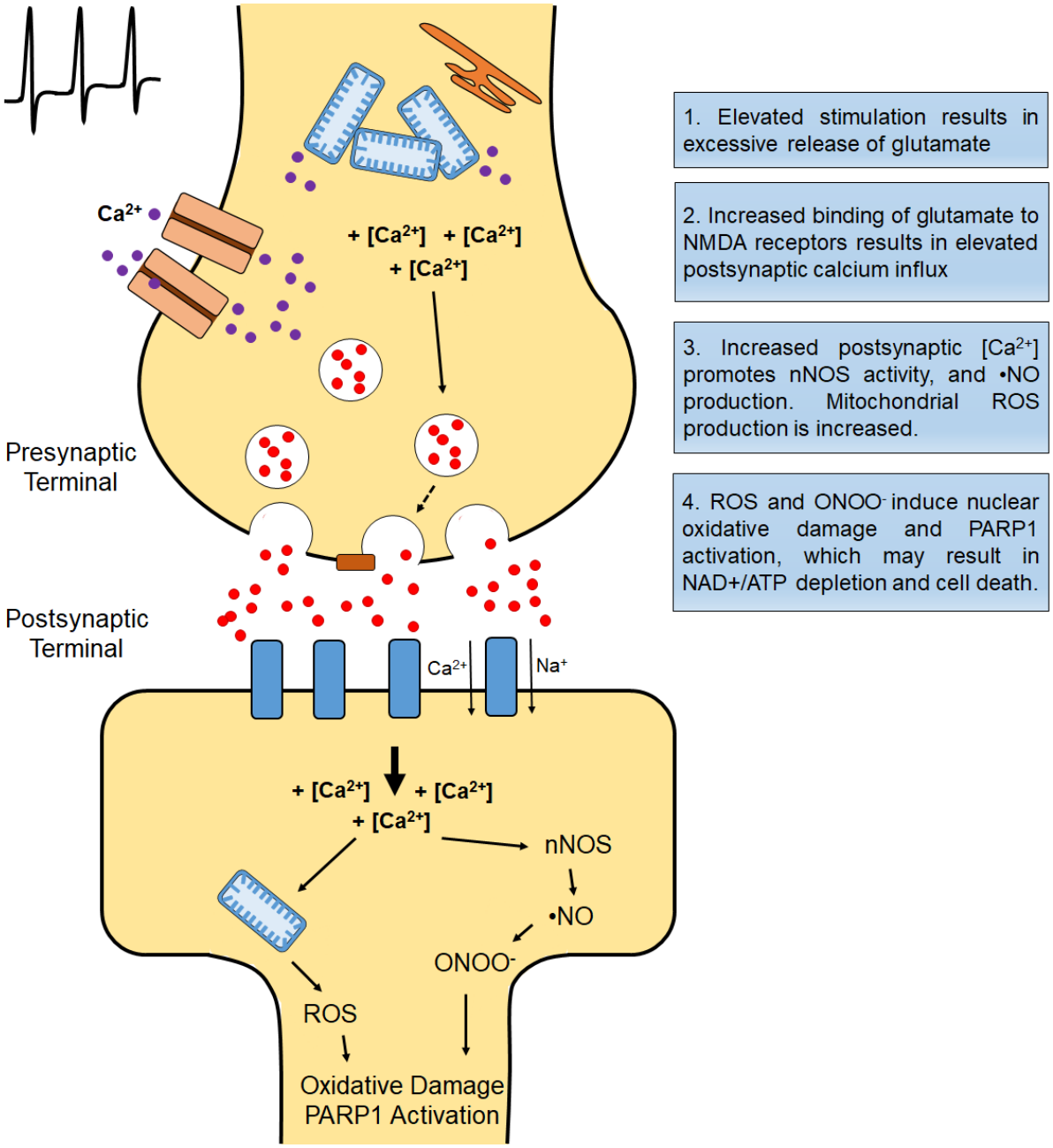

Figure 1.6. *Glutamate Excitotoxity and Nitric Oxide Induced DNA Damage.* Excessive neuronal activity results in the influx of large quantities of Ca^{2+} into the presynaptic terminal. This causes the fusion of neurotransmitter containing vesicles, and the excessive release of glutamate. Glutamate persistently binds NMDA receptors, resulting in the elevated influx of Ca^{2+} into the postsynaptic terminal. Elevated postsynaptic Ca^{2+} results in the stimulation of nNOS, which synthesises nitric oxide. Similarly, excessive postsynaptic Ca^{2+} results in the elevated production of mitochondrial ROS. Nitric oxide, in conjunction with ROS, can form peroxynitrite ($ONOO^-$), an RNS. These reactive species are capable of inducing DNA damage, resulting in PARP1 activation, NAD+/ATP depletion, and cell death.

1.6). Peroxynitrite induced damage results in the activation of PARP1 and cytotoxicity, linking glutamate excitotoxicity with parthanatotic cell death (Pacher and Szabo, 2008, Mazzone and Nistri, 2011).

In recent years, increasing evidence has highlighted the importance of various forms of epigenetic modification in the regulation of plasticity (Karpova, *et al*., 2017). One such mechanism, DNA methylation and demethylation, represents an activity-dependent, highly dynamic epigenetic modification in neuronal cells that, in order to modulate stimulus-driven transcriptional cues, exposes the brain to the induction of SSBs (Gavin, *et al*., 2013, Bayraktar and Kreutz, 2018). The methylation and demethylation of DNA at both intergenic and regulatory regions results in alterations to gene expression (Bayraktar and Kreutz, 2017). In cycling cells, DNA can be demethylated passively, by diluting methylated nucleobases across replication cycles in the absence of DNMT (DNA Methyltransferase) activity (Inoue and Zhang, 2011). Neuronal cells are, however, postmitotic, and cannot demethylate DNA in this way, relying on a separate, biochemical demethylation process (Bayraktar and Kreutz, 2018). The methylated form of cytosine, 5mC (5-methylcytosine) is demethylated by Ten-eleven translocation (TET) enzymes, three proteins which regulate the successive oxidation of 5mC to 5hmC (5-hydroxymethyl cytosine), followed by its conversion to 5fC (5-formylcytosine), and finally 5cC (5-carboxylcytosine) (Ito, *et al*., 2011, Rasmussen and Helin, 2016). Thymine DNA Glycosylase (TDG) can excise both 5fC and 5cC through physical interaction with TET2 and GADD45B, which is expressed following LTP induction, generating an AP site which is processed through BER (Zhu, 2009, He, *et al*., 2011, Maiti and Drohat, 2011, Li, *et al*., 2015). Recent studies have found that active demethylation of CpG sites at neuronal enhancers results in site-specific SSB formation, a result of the BER process (Wu, *et al*., 2021). Active demethylation is a process ten times more frequent in postmitotic neurons than in replicative cells, exposing nervous tissue to elevated levels of endogenously occurring SSBs, that must be repaired in order to maintain genomic integrity (Kraucionis and Heintz, 2009).

1.6.1 – Neurological Disorders Associated with DNA Damage Repair

DNA damage first came to be associated with neurodegeneration following the discovery of neurological dysfunction in patients with Xeroderma Pigmentosum (XP), a disorder characterised by the defective repair of UV induced damage (Cleaver, 1968, Shabbir, 2015). XP is a result of one of several mutations in proteins regulating Nucleotide Excision Repair (NER), and its most prominent manifestation is in the development of skin cancer (Koch, *et al*., 2016). However, neurological disorders

frequently manifest in patients, a result of apoptotic neuronal death, gliosis, and cortical atrophy – owing to the accumulation of unresolved UV induced DNA-damage (Shabbir, 2015, Koch, *et al*., 2016).

Ataxia Telangiectasia (AT) is a disorder characterised by cerebellar ataxia, telangiectasia, immunodeficiency, and an increased incidence of cancer, caused by mutations in the *ATM* gene (Rothblum-Oviatt, *et al*., 2016). ATM is a member of the phosphoinositide 3-kinase-related kinases (PIKK) family, which is activated by DSBs, phosphorylating many proteins involved in the regulation of DNA repair, cell cycle progression, and apoptosis (Lavin, 2009, Lovejoy and Cortez, 2009, Paull, 2015). The mechanism underlying neurodegeneration in AT is unclear, but recent evidence has implicated ROS/PARP1 dependent toxic protein aggregation (Lee, *et al*., 2018). The location of protein aggregates in the AT brain are consistent with disease pathology, with elevated aggregation in the cerebellum likely underlying AT-linked cerebellar ataxia (Lee and Paull, 2021). Recently, the decreased expression of IP3R1, alongside CA8, INPP5A, and CBLN1; proteins important for inositol triphosphate regulated calcium signalling, was identified in the AT cerebellum (Türkmen, *et al*., 2009, Yang, *et al*., 2015, Lee, *et al*., 2021). There are several further neurodegenerative disorders associated with defective DNA repair, such as Cockayne Syndrome (the result of impaired transcription coupled repair), Nijmegen Breakage Syndrome (the result of defective DSBR), and Seckel syndrome, among others (Tauchi, *et al*., 2002, Alderton, *et al*., 2004, Kitsera, *et al*., 2014).

1.6.2 – The Role of PARP1 in Neurodegeneration

Some of the earliest investigations of PARP1 mediated neuropathology were in models of cerebral ischemia and reperfusion injury. During and after ischemia, the uncoupling of the mitochondrial electron transport chain results in the elevated production of $O_2^{\bullet-}$, which is furthered exacerbated by the reoxygenation following reperfusion (Narasimhan, *et al*., 2003, Dawson and Dawson, 2017). Further, the neuronal depolarisation associated with ATP depletion following ischemia results in the release of synaptic glutamate, activating NMDA receptors, resulting in excitotoxicity and the stimulation of $^{\bullet}$NO synthase. $^{\bullet}$NO, in the presence of $O_2^{\bullet-}$ forms $ONOO^-$, which is further capable of activating PARP1 (Eliasson, *et al*., 1999). The genetic deletion or inhibition of Parp1 significantly attenuates injury following cerebral ischemia (Eliasson, *et al*., 1997, Chen, *et al*., 2020).

Neurodegenerative disorders are often characterised by cognitive dysfunction and motor defects, and in recent years have come to be associated with age-related

DNA damage and PARP1 activity (Love, *et al*., 1999, Pazzaglia and Pioli, 2020). PARP1 activity is linked to the regulation of autophagy, the process by which old, damaged organelles may be disposed of in the cell (Jiang, *et al*., 2018). Poly(ADP-ribsylation) of autophagy regulating proteins has been shown to inhibit degradation of α-synuclein in a model of Parkinson's Disease (PD) (Mao, *et al*., 2020). This inhibition of autophagy represents a significant threat to cellular homeostasis, increasing the susceptibility of neuronal cells to the aggregation of pathogenic proteins, and oxidative stress (Fujikake, *et al*., 2018, Park, *et al*., 2020). Alongside the role of PARP1 as neuroprotective in response to oxidative DNA damage, its activation is associated with the expression of inflammatory cytokines, such as Interleukin 1 Beta (IL-1β) (Choudhury and Gard, 2020). The activation of PARP1 in microglia is associated with neuronal injury and impaired glutamate uptake, resulting in neuroinflammation characteristic of neurodegenerative disorders (Suh, *et al*., 2007).

Recently, Kam *et al*., highlighted the role of PARP1 in the pathogenesis of PD, demonstrating that the accumulation of α-synuclein in neurons results in the activation of PARP1, and further, PARP1-dependent fibrilliation. In addition, inhibition of PARP1 results in decreased aggregation of α-synuclein in the brain. Similarly, the activation of PARP1 results in elevated Amyloid-β plaque deposition and Tau fibrillation in AD (Martire, *et al*., 2015). The aggravation of AD pathology by PARP1 is thought to be related to chronic neuroinflammation, notably through the transribosylation of NF-κB, a protein complex that regulates cytokine production, cell survival, and transcription (Bohio, *et al*., 2019). The binding of NF-κB to microglial DNA is regulated by PARP1 activation in AD pathology, and inhibition of PARP1 has been shown to inhibit microglial activation and delay AD progression (Stoica, *et al*., 2014). Similarly, microglial activation is mitigated in *Parp1*$^{-/-}$ mice (Kauppinen, *et al*., 2011). A further factor is the neuroprotective role of Sirtuin 1 (SIRT1) in AD, PD, and ALS. SIRT1 is an NAD+ dependent histone deacetylase, responsible for regulating the activity of numerous transcription factors responsible for expression of proteins linked to metabolism, the response to oxidative stress, and longevity (Elibol and Kilic, 2018, Herskovitzs, *et al*., 2018). The decreased availability of NAD+ by PARP1 overactivation results in the inhibition of SIRT1 activity, and the overexpression of SIRT1, supplementation of bioavailable NAD+, or SIRT1 promotion via the inhibition of PARP1 have been shown to be neuroprotective in AD models (Lalla and Donmez, 2013, Hou, *et al.,* 2018, Wencel, *et al*., 2018).

1.6.3 – The Role of PARP1 in the Regulation of Transcription

Alongside the canonical role of PARP1 in the recognition of DNA SSBs, and the subsequent recruitment of the SSBR machinery, PARP1 has been identified as a direct regulator of transcription (Kraus, 2008, Matveeva, *et al*., 2019). The loading of PARP1 onto chromatin, following the recognition of damage, results in the modification of nucleosome spacing (Sultanov, *et al*., 2017, Thomas, *et al*., 2019). This, alongside the direct posttranslational modification of core and linker histones through transribosylation can regulate the accessibility of RNA polymerase to histones (Kraus and Hottiger, 2013, Verdone, *et al*., 2015, Ciccarone, *et al*., 2017). The activation of PARP1 at sites of DNA damage is a further regulator of transcription, as the binding of PARP1 to the nucleosome is inhibited by heavy autoribosylation, and as such it will not bind following high levels of activation (Beneke, 2012, Muthurajan, *et al*., 2014). By contrast, more moderately ribosylated PARP1 displays an affinity for the nucleosome, facilitating the regulation of DNA-damage related alterations to transcription (Muthurajan, *et al*., 2014). PARP1 acts to regulate transcription silencing during DNA damage. PARP1 facilitates the recruitment of polycomb repressive complex 1 and 2, as well as the NuRD complex, to modulate chromatin structure and induce transcriptional arrest at sites of DNA damage (Chou, *et al*., 2010).

Further targets for transribosylation by PARP1 are sequence-specific DNA binding factors. Smad3 and Smad4 are known to be poly(ADP-Ribosyl)ated by PARP1, upon which they dissociate from DNA and attenuate Smad-specific gene expression (Lönn, *et al*., 2010). Poly(ADP-ribosylation) of NELF (negative elongation factor) promotes the release of NELF from stalled RNA Polymerase II, enabling the production and elongation of RNA. PARP1 further regulates transcription by direct binding, such as to the FoxO1 (Forkhead box O1) promoter, which regulates the transcription of several processes involved in cell maintenance, such as apoptosis, doing so in a polymerase independent manner (Tikhanovich, *et al*., 2013, Gibson, *et al*., 2016, Tian, *et al*., 2020). Recently, alterations to transcription have been reported in a SCA7 mouse model, which were linked to Parp1 activation (Stoyas, *et al.,* 2020). In the SCA7 mouse, it was proposed that Parp1 activation resulted in the depletion of NAD+ in the cerebellum and consequently the decreased activity of Sirt1, an NAD+ dependent deacetylase that regulates chromatin structure and transcription of genes involved in longevity and cell survival (Elibol and Kilic, 2018, Herskovitzs, *et al*., 2018, Stoyas, *et al*., 2020). Interestingly, many aspects of the SCA7 mouse phenotype were rescued by either NAD+ replacement therapy or Sirt1 overexpression (Stoyas, *et al*., 2020). Recently, a role for XRCC1 has been identified in the protection of the transcriptome. Adamowicz,

et al., found that in the absence of XRCC1, there is a PARP1-dependent inhibition of transcription upon induction of DNA damage, the result of decreased USP3 ubiquitylation.

In the mouse brain, Parp1 has been identified as a regulator of activity-dependent transcription. Following neuronal stimulation, Parp1 activity results in the increased expression of *Fos* and *Arc*, key transcription factors in the expression of immediate early genes (Visochek, *et al*., 2016). Interestingly, this increased expression could not be identified in *Parp1*-null mice, nor in the presence of PARP inhibitors (Visochek, *et al*., 2016). In neurons treated with H_2O_2, the activity-dependent expression of these transcription factors also disappeared, implying that the function of Parp1 in the regulation of activity-dependent transcription is independent from its regulation of SSBR, and may have implications in SSBR deficient models, such as the *Xrcc1*$^{Nes\text{-}Cre}$ mouse (Visochek, *et al*., 2016, Cohen-Armon, *et al*., 2019).

1.6.4 – The PARP1/NAD+/SIRT1 Axis

NAD+ is an essential redox molecule that primarily functions in electron transfer reactions during metabolism, though it also acts as a co-factor for several other enzymes (Pehar, *et al*., 2018). Three main classes of enzyme utilise NAD+ as a substrate. These are the PARP family, Sirtuins, and ADP-ribosyl cyclases (cADPR) (Pehar, *et al*., 2018). Redox function is reversible, and as such results in no net loss of NAD+ (Zu, *et al*., 2003). However, NAD+ use by the aforementioned proteins consumes the molecule (Pehar, *et al*., 2018). PARP1 hyperactivation has been previously shown to decrease cellular NAD+ levels and inhibit glycolysis, though it is unclear if this is a direct result of PARP1 activity and the modification of glycolytic proteins, or substrate competition (Fouquerel, *et al*., 2014). In the *Xrcc1*$^{Nes\text{-}Cre}$ brain, the consequence of Parp1 hyperactivation is depletion NAD+ in the brain (Komulainen, *et al*., 2021). The depletion of cellular NAD+ may impact the activity of other NAD+ consuming enzymes due to substrate availability, with SIRT1 activity being particularly dependent on NAD+ levels in the cell (Imai and Guarente, 2016). CD38 is an enzyme highly expressed in brain that hydrolyses NAD+ to form cyclic ADP-ribose (cADPr); a calcium mobilising agent (Pawlikowska, *et al*., 1996, Mayo, *et al*., 2008). The expression of CD38 matches closely with that of ryanodine receptors in the central nervous system, regulators of intracellular calcium storage, and the cADPr-dependent activation of these receptors may provide a link between declining NAD+ levels and alterations to signalling activity in the brain (Kip, *et* al, 2006, Ma, *et al*., 2018).

1.6.5 – PARP1-Mediated Cell Death

Parthanatos is a caspase independent form of cell death following the activation of PARP1 (Yu, *et al*., 2002, Wang, *et al*., 2021). It is characterised by large-scale fragmentation of DNA following the translocation of the protein Apoptosis Inducing Factor (AIF) from the mitochondrial membrane to the nucleus (Fatokun, *et al*., 2014). It is thought that the accumulation of poly(ADP-ribose) following the induction of damage precedes the release of branched polymers from the nucleus into the cytosol, whereupon it may bind AIF and induce its release (Fatokun, *et al*., 2014). AIF binds the DNA nuclease Macrophage Migratory Inhibitory Factor (MIF), and together translocate to the nucleus, resulting in DNA cleavage (Wang, *et al*., 2016) (Figure 1.7). Alongside the large-scale fragmentation of DNA, parthanatotic cell death is characterised by metabolic inhibition. The modification of hexokinase 1 (HK1) by PARP1 results in glycolytic inhibition (Andrabi, *et al*., 2014). The depletion of NAD+/ATP by PARP1 further acts to induce metabolic collapse, however it is unclear whether this depletion is required for cell death (Zhou, *et al*., 2011). While it is not known whether parthanatotic cell death occurs following Parp1 hyperactivation in the *Xrcc1*$^{\text{Nes-Cre}}$ mouse, a link between PARP1 and cell death is well established as having a role in the pathologies of Parkinson's disease, Alzheimer's disease, Amyotrophic Lateral Sclerosis and Huntington's disease (Hivert, *et al*., 1998, Love, *et al*., 1999, Vis, *et al*., 2005, Kam, *et al*., 2020). Further, depletion of the BER glycosylase OGG1 has been demonstrated to partially rescue the parthanatotic cell death of neurons exposed to oxidative DNA damage, likely by limiting the detection of SSBs by PARP1 (Wang, *et al*., 2018).

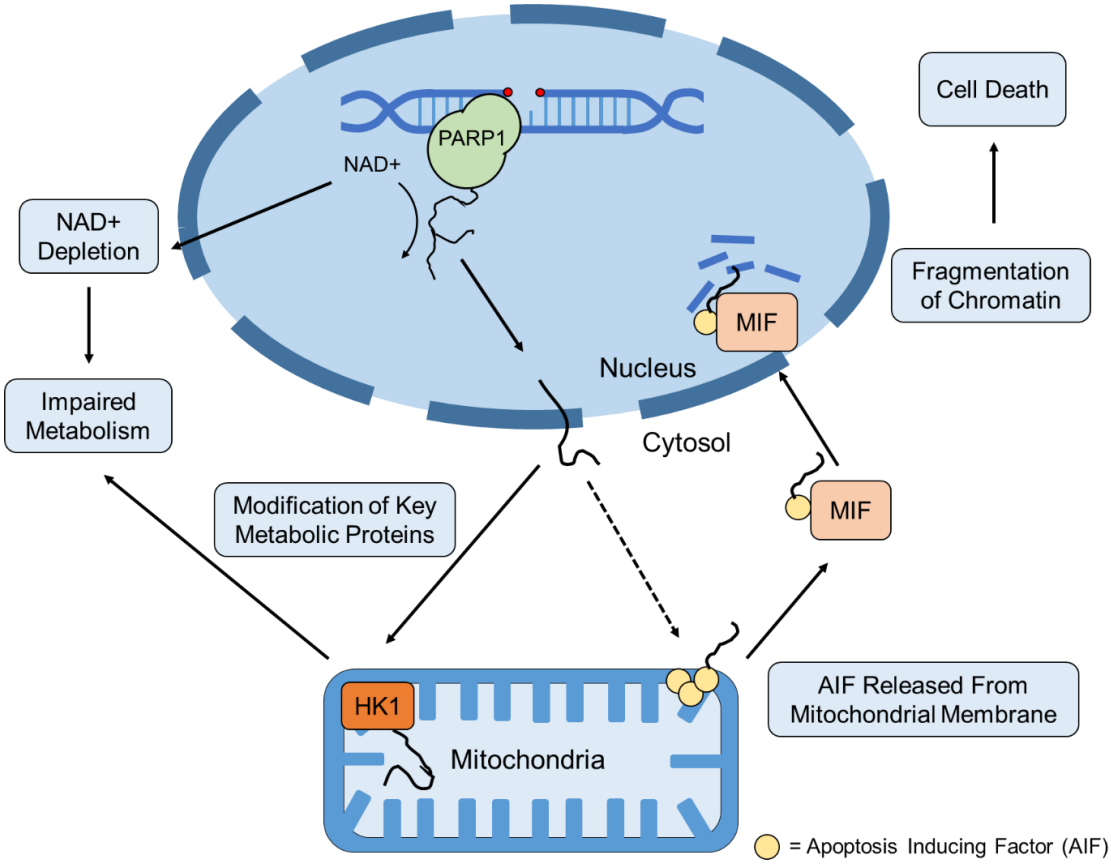

Figure 1.7. *Parthanatotic Cell Death.* The excessive activation of PARP1 at sites of DNA damage results in a PARP1-dependent cell death pathway known as parthanatos. Excessive poly(ADP-ribosyl)ation results in the nuclear translocation of AIF from the mitochondria. AIF translocation also results in the recruitment of MIF to the nucleus. MIF is a nuclease, which facilitates the large-scale fragmentation of chromatin, resulting in cell death. Parthanatotic cell death also involves the inhibition of cellular metabolism. Modification of mitochondrial proteins, such as hexokinase 1 (HK1) by PARP1, results in impaired glycolysis. This, in conjunction with the depletion of NAD+ by PARP1 leads to metabolic collapse. It is not clear whether parthanatotic cell death underlies cerebellar degeneration in the *Xrcc1*$^{Nes\text{-}Cre}$ mouse, however it has been implicated in the pathology of several neurodegenerative diseases, such as PD.

1.7 – Thesis Aims

The *Xrcc1*$^{Nes\text{-}Cre}$ mouse brain is characterised by elevated poly(ADP-ribose) levels, the result of Parp1 hyperactivity at endogenous SSBs. The aim of this thesis is to investigate the impact of these endogenous breaks *in vitro*, investigating whether the neurological presentation associated with hereditary defects in SSBR is the result of altered neuron functionality. Further I aim to characterise the impact of Parp1 hyperactivation on these endpoints in neurons, utilising synaptic connections in hippocampal circuits as a key, *in vitro* model. Finally, I will investigate the possible use of clinically available PARP inhibitors in the rescue of neuron functionality in *Xrcc1* defective neurons.

2. Chapter Two – Methods

2.1 Animal Welfare and Maintenance

Experiments took place in accordance the UK Animal (Scientific Procedures) Act 1986 and satisfied local institutional regulations at the University of Sussex. *Parp1*$^{-/-}$, *Xrcc1*$^{Nes\text{-}Cre}$, and *Ape1*$^{Nes\text{-}Cre}$ mice were generated previously. Intercrosses between *Parp1*$^{-/-}$ and *Xrcc1*$^{Nes\text{-}Cre}$, as well as *Ape1*$^{Nes\text{-}Cre}$ and *Xrcc1*$^{Nes\text{-}Cre}$ mice were maintained in a mixed background C57Bl/6 × S129 strain and housed on a 12 -h light/dark cycle with lights on at 07:00. Temperature and humidity were maintained at 21°C (± 2°C) and 50% (± 10%), respectively. All experiments were performed under the UK Animal (Experimental Procedures) Act, 1986. Mice were maintained under UK Home Office Project License PP5058749.

2.2 Mouse Genotyping

Tissue samples were taken either through ear notching, or by removing roughly 2mm of tissue from the end of the tail, depending on the expedience required in genotyping. Tissue was submerged in 75µl alkaline lysis buffer (25mM NaOH, 0.2mM EDTA), 5µl Proteinase K at room temperature for 10 minutes, prior to 5 minutes inactivation at 95˚C and subsequent addition of 75µl neutralisation buffer (40mM Tris-HCl) and storage at 4˚C until use. PCR reagents utilised were 7.5µl REDExtract-N-AMP PCR reaction mix (containing buffer, salts, dNTPs and REDTaq DNA Polymerase), 3.2µl double-distilled H_2O, 4µl tissue digests, and 0.1µl primers per reaction. Upon completion of PCR, 10µl of product was run at 40-50V for between 45-60 minutes on a 1.5% agarose, 0.2% Ethidium Bromide gel, before identifying products under UV light.

2.3 Primary Culture of Hippocampal Neurons

P1–2 mouse pups were decapitated, and brains were removed and placed in ice-cold Hank's buffered saline solution (HBSS), 0.1 M HEPES. Hippocampi were isolated and then washed three times in warmed 10% FCS, 20 mM glucose and 1% Pen/Strep Minimal Essential Media (MEM) (Gibco). Hippocampi were manually dissociated by trituration and diluted to a density of 50,000 cells/well and plated on poly-D-Lysine (20 µg/ml) coated 15-mm glass coverslips. 2 h after plating, the media was replaced with 2% B27, 1% glutamax and 1% Pen/Strep-supplemented neurobasal A medium (Gibco). Cells were maintained without cytosine arabinoside, typically used to manage glial cell count, to prevent induction of exogenous DNA damage (Zhuo *et al,* 2018). Cells were maintained in 5% CO_2 at 37°C and fed every 3 days through half-exchange of media. Hippocampal cells were taken for ICC experiments at DIV6 and live imaging at DIV15–

17. Due to limited survivability, hippocampal neurons cultured from *Ape1*$^{Nes\text{-}Cre}$/*Xrcc1*$^{Nes\text{-}Cre}$ mice were plated at a density of 100,000 cells/well, to increase the chance of identifying viable neurons.

2.4 Acquisition of Tissues from p15 Mice

P15 mice were culled by cervical dissociation, prior to exsanguination by decapitation. A cut was made down the midline of the skull, and across the bridge of the nose, allowing the brain to be removed. The cerebellum was detached from the base of the brain prior to separation of the hemispheres and extraction of the hippocampus from the surrounding cortical tissue. Cerebella, hippocampi, and cortices were snap frozen in liquid nitrogen prior to storage at -80°C.

2.5 Homogenisation of Animal Tissues for Western Blotting

Tissues were removed from -80°C and suspended in 10µL/mg ice cold lysis buffer containing 20mM HEPES pH 7.4, 2mM EGTA, 50mM β-glycerophosphate, 1% Triton-X, 10% Glycerol, 1mM Benzamide. Fresh DTT (1mM), Phosphatase and Protease inhibitors (1% and 2% v/v respectively) were added to buffer prior to homogenisation until smooth with pre-cooled glass homogenisers. Lysates were left for 15 minutes with occasional, gentle mixing. Lysates were then passed through a 27G needle 8 times. Samples were then sonicated for 30 seconds, prior to pre-clearing of unbroken cells by centrifugation at 4°C, 500 g, for 10 minutes. Supernatant was extracted, to which we added 5X laemmli buffer, containing Tris base, SDS, glycerol, 2-mercapto-ethanol and bromophenol blue dye. Protein content of lysates was quantified using the Pierce BCA Protein Assay Kit (Thermofisher).

2.6 SDS-Page and Western Blotting of Brain Lysates

Brain extracts were resolved using pre-cast 4-20% gradient polyacrylamide gels (Bio-Rad) by electrophoresis in 1X running buffer (25 mM Tris-HCl, 250 mM glycine, 0.01% SDS), run at 120 V. Proteins were transferred to nitrocellulose Hybond-C membrane (GE Healthcare) in 1X TOWBIN (25 mM Tris-HCl, 192 mM glycine, 10% methanol) for 90 minutes at 400 mA. Membranes were stained with Ponceau S stain to confirm equal loading between samples, prior to overnight blocking in 10% TBST (20 mM Tris-HCl, 150 mM NaCl, 0.1% Tween-20), 10% non-fat dried milk powder. Primary and secondary antibodies were applied in TBST/5% milk, followed by triplicate TBST washes (5 minutes each) post incubation. Incubation with the appropriate primary antibodies was done overnight, with secondary incubation for 1 hour. Following the removal of the secondary antibody by triplicate TBST washes, the membrane was

incubated in enhanced chemiluminescence detection reagent (ECL) (GE Healthcare), prior to detection with autoradiography film. Quantification of immunoblot intensity was done manually through ImageJ.

2.7 Indirect Immunofluorescence and Microscopy

For indirect immunofluorescence, RPE-1 cells were seeded at 50,000 cells per 12mm glass round coverslip 1 day prior to fixation. Cells were pre-treated for 4 hours with 10µM PARP inhibitor KU00058948 or NAMPT inhibitor FK866 where indicated. Primary hippocampal cultures were plated at a density of 50,000 cells per 12mm glass round coverslip, before being allowed to develop for 6 days (DIV6) in low serum, B27/N2 containing NB media, prior to treatment and fixation. Neuronal cultures were pre-treated for 4 hours with PARP and NAMPT inhibitors as above, as well as well as the nNOS inhibitor L-NAME (100µM) and the proteasome inhibitor MG132 (25µM) where indicated. In both RPE-1 and primary hippocampal cultures, cells were treated with 10µM PARG inhibitor PDD00017273 prior to fixation where indicated.

Cells were fixed in 4% paraformaldehyde and washed thoroughly with PBS before permeabilising in 0.2% Triton-X for 2 minutes. They were then blocked in 10% Goat Serum, 5% Bovine Serum Albumin (BSA), 0.3% Triton-X for 30 minutes and incubated at room temperature with relevant concentrations of primary antibodies for 1 hours. After washing with PBST in triplicate, 5 minutes, they were incubated with relevant secondary antibodies for a further hour. Following another triplicate wash in PBST, nuclei were counterstained with DAPI, dried thoroughly, and mounted with Vectashield. Images were acquired using either a Zeiss Widefield Apotome microscope at 40x/1.4, or a Zeiss LSM-880 Airyscan compatible microscope for super resolution acquisition. A motorised IX83 microscope with ScanR Image Acquisition and Analysis was used for automated imaging. For immunofluorescence of brain tissue, 10-micron sections were taken from perfused brains (E. Komulainen), which were washed in PBS before boiling in 10% antigen retrieval solution/ddH_2O (Nacalai Tesque, Histo VT One). After cooling for an hour, sections were stained as described above. Image analysis was conducted using the ZEN Blue (Zeiss) and ImageJ (Fiji) software. Images and figures were prepared in Inkscape.

2.8 Determination of Neuronal Survival

For longitudinal studies, primary hippocampal cultures were fixed in 4% paraformaldehyde at indicated times. Cultures were fixed at DIV6, which represented our T0 timepoint, DIV12, and DIV18. Viable neurons were identified based on the presence of the neuronal markers MAP2 and NeuN. Neuronal survival was calculated

based on the population of MAP2/NeuN positive cells across 30, separate, randomly chosen visual fields at 40x/1.4 magnification, relative to those present in their genotype matched T0 control. In determining neuronal sensitivity to PARG inhibitor, cells were treated at DIV6 with indicated concentrations of PDD00017273 for 3 days, prior to fixation at DIV9. Cell survival was again quantified following staining with MAP2/NeuN, with survival of treated cells being calculated relative to vehicle treated, genotype matched controls. For longitudinal studies, cultures were maintained without serum in order to prevent the overpopulation of co-cultured glia (Chou and Langan, 2003).

2.9 Clonogenic Survival Assay

Cells were trypsinised at roughly 70% confluence, and WT and *XRCC1*$^{-/-}$ RPE-1 cells were plated in 100mm plates at 33.3 cells/ml, to amounts of 300 cells per dish in 9ml of media. After adhering for 4 hours, the volume was made up to 10ml with the addition of media containing varying concentrations of the PARG inhibitor. Following a 14-day incubation period, cells were washed twice in PBS, before being fixed and stained in 0.05% Crystal Violet, 20% methanol in ddH_2O, and counted manually. Survival was calculated by dividing those colonies present in treated groups, by those in the untreated group of their respective genotype.

2.10 PAR Immunoblot of Cultured RPE-1 Cells

RPE-1 cells were lysed in Sodium Dodecyl Sulfate containing sample buffer, and lysates were subjected to SDS-PAGE before transfer to a nitrocellulose membrane as described above. Membranes were blocked in 10% milk in TBST overnight, before probing with anti-ADP-Ribose (PAN) reagent at (1:1000) for 1 hour, and incubation with HRP conjugated secondary antibodies in 10% milk/TBST (1:1000), 1 hour. Blots were developed in a dark-room developer. Quantification of immunoblot intensity was achieved through manual quantification of intensity in ImageJ.

2.11 SyGCaMP6f Imaging

Hippocampal neurons were infected with AAV6_SyGCaMP6f at DIV6/7 at a multiplicity of infection (MOI – the number of virions added per cell in culture) of 100. Images were acquired using a 60x/1.0 NA objective on an Olympus BX61WI microscope fitted with an electron multiplying charge coupled device Andor Ixon+ camera (40 ms exposure, 20 Hz acquisition frequency and 4x4 binning, EM gain 7) controlled by custom-written Micromanager routines. Coverslips were placed in a custom-built imaging chamber and a Grass SD9 Stimulator was used to apply field stimulation (voltage: 22.5V, 1 ms pulse width). All experiments were carried out in Extracellular Bath

Solution (EBS) containing (in mM), 136 NaCl, 10 HEPES, 10 D-Glucose, 2.5 KCl, 2 $CaCl_2$, 1.3 $MgCl_2$. EBS was supplemented with 50 µM APV and 20 µM CNQX to inhibit NMDA and AMPA receptors respectively, so as to prevent the propagation of spontaneous signals and recurrent stimulation. Experiments were performed in a darkened room with steps taken to minimise extraneous light, with room temperature maintained at 23°C.

Image stacks were analyzed using IGOR Pro 8. Stacks were imported via the SARFIA plugin and stored as single-precision floating-point arrays (termed 'waves') (Dorostkar, *et al*., 2010). Sequential videos (image stacks) were taken from the same regions were corrected for x-y drift using the built-in image registration function (Thévenaz, *et al*., 1998). Following correction of motion artifacts, regions of Interest (ROIs) were detected via image segmentation, using a threshold of (-3) X SD of all pixel values in the Laplace operator (a methodology frequently used for edge sharpening and detection of units of lower contrast) (Burger and Burge, 2008). ROIs, once detected, were numbered and collated in a matrix referred to as the ROI mask (possessing identical *x* and *y* values to the original image stack). Mean background intensity was subtracted to account for alterations to background fluorescence by selecting and averaging fluorescence values of a small, empty region of the image, allowing the average intensity of each ROI in the ROI mask matrix to be analysed at each time point (frame) of the captured video/image stack. In order to account for differences in initial baseline intensity of ROIs, ΔF/F (fluorescence change) values were calculated using the 10 frames prior to stimulation as a baseline. A custom script was used to determine whether ROIs had exceeded a threshold change in fluorescence intensity following stimulation and ROIs that failed to reach threshold intensity were removed from the mask, leaving individual ΔF/F values of each responsive ROI in an image stack, across all time points, ready for collation. A separate script was utilised to form average traces from bleach corrected ΔF/F values. Quantification of synaptic calcium flux was achieved through a custom script, where the area under the curve (AUC) of each generated trace, by synapse, was calculated as an arbitrary measure of Ca^{2+} signalling intensity.

2.12 Isolation of RNA from Frozen Brain Tissue

For qPCR samples, hippocampal tissues were acquired as described above, and stored at -80°C prior to RNA isolation. Isolation was done utilising the RNeasy Lipid Tissue Kit (Qiagen), following manufacturers guidelines. In brief, isolation was done in a fume hood, liberally cleaned with RNAzap and MilliQ water. Tissue samples (up to 100mg) were homogenised on ice in 1ml provided lysis reagent, prior to the addition of

200µM chloroform and 15 seconds of vigorous shaking, followed by 3 minutes resting at room temperature. Samples were then centrifuged at 12,000 g for 15 minutes at 4°C. The aqueous phase was transferred to a separate tube, which was centrifuged through a provided RNeasy spin column, supplemented with 70% ethanol, or provided buffers as instructed. 30µM RNAse free water was added to the prepared spin column membrane, with isolated RNA eluted following a final centrifugation for 1 minute at 8000 g, room temperature. Isolated RNA was quantified using a nanodrop, which also allowed for the assurance of RNA integrity and quality. Isolated RNA was stored at -80°C prior to use.

For RNA sequencing experiments, hippocampi were extracted from 3 wild type and 4 *Xrcc1*$^{Nes\text{-}Cre}$ mice, from 3 separate litters, ensuring each knockout mouse was harvested with a wild type littermate control. Extraction was done following cleaning of the dissection room, dissection area, and dissecting tools with RNAzap and MilliQ water Hippocampi were lysed in the phenol containing Trizol reagent in a glass homogeniser, on ice. Samples were stored at -80°C, before being sent for extraction at the institute of molecular genetics (IMG), Prague. Sequencing and analysis of isolated RNA also occurred at IMG.

2.13 cDNA Synthesis

Isolated RNA from mouse hippocampal tissue was used for cDNA synthesis using the RevertAid First Strand cDNA Synthesis Kit (Thermofisher), following manufacturers' instructions. cDNA was quantified using a nanodrop and stored at -80°C prior to use.

2.14 RT-qPCR

For validation of mRNA targets identified through RNA sequencing, we utilised RT-qPCR. To do so, we utilised the Luna Universal qPCR Master Mix, following manufacturers' instructions, using diluted cDNA created from isolated RNA from the mouse hippocampus. Housekeeping genes were selected based on their expression in the brain. The chosen housekeeping genes were NeuN, Gfap, and Gapdh. Primers used for housekeeping genes were as follows:

Oligo Name	Sequence
NeuN Forward	CTACACACCCGCACAGACTC
NeuN Reverse	GTCTGTGCTGCTTCATCTGC
Gfap Forward	CGCCACCTACAGGAAATTG
Gfap Reverse	CTGGAGGTTGGAGAAAGTCTGT
Gapdh Forward	AGAACATCATCCCTGCATCC

Gapdh Reverse	CACATTGGGGGTAGGAACAC

Primers used for target genes were as follows:

Oligo Name	**Sequence**
Sez6 Forward	GGTTCCAGAGGTCATGTCTAAG
Sez6 Reverse	AGTGGTAATGATGGTGGTAGTG
Sema5a Forward	CACTGGCACAACACAAACAC
Sema5a Reverse	GGAGGAAGTAGGGAGGGAAATA
Syn3 Forward	GAGTGTGGTGTGGGAAGTAAG
Syn3 Reverse	CAGGTCATTACCCAGGCATTAG
Plcl1 Forward	CGTTGCTCTGCCTTCCTCTTA
Plcl1 Reverse	GGGTTCTATGAGCGGATTCTAC
Tnr Forward	CTCCCTGTCCTCTCCTATCTTT
Tnr Reverse	GGTTAGATGGTGGCTGTTTCT
Dcx Forward	GACCACCTGGAGCAAGAATAG
Dcx Reverse	CCCTTGGTGTGATGGCTAAT
Draxin Forward	CCCAGCATCTGGCTTCTAAT
Draxin Reverse	GCATCTGTCCTCCATCTGTATC
Ephb1 Forward	AAGTCAACACGGAAGTCAGG
Ephb1 Reverse	CGGACAGAAAGGAGAGAGACATAC
Lrrc55 Forward	CACCTTGACCTTCTCCCATTAG
Lrrc55 Reverse	GGTGCTGAGGGTGATTACTT
Erbb4 Forward	GCCACCCTTGCCATCCAAAC
Erbb4 Reverse	TGGCCCGTCCATGGGTAGTA
Itpr2 Forward	GTACCTGACGGTGAACAAGAG
Itpr2 Reverse	CTTCCAGAACGGATGGATGTAG

Table 2.1 *Primer Sequences for RT-qPCR*.

RT-qPCR was done using an AriaMX Real Time PCR machine, using a fluorescence-based program design, with an initial denaturation at 95ºC for 60 seconds, followed by 45 cycles of 15 seconds denaturation at 95ºC and 30 seconds of extension at 60ºC, at which point a fluorescence readout was given. Program design was based on manufacturer guidelines, with the melt curve being calculated by the AriaMX

machine. Data was analysed using the Agilent Aria 1.8 program, based off Cq values and normalised to each reference gene. Samples were run in triplicate.

2.15 Antibodies and Reagents

Antibodies utilised for indirect immunofluorescence and western blotting during this study were anti-pan-ADP-ribose binding reagent Millipore (ICC & WB 1:500); MABE1016, Chicken anti-MAP2 (ab5392; Abcam) (ICC 1:500), anti-NeuN mouse monoclonal (Millipore MAB337) (ICC 1:500), mouse monoclonal, anti-phospho-Histone H2A.X (Ser139) (05-636; Millipore) (ICC 1:1500), mouse anti-Daglα (E6) sc-390409 (SCBT) (1:500), mouse anti-Grid2ip (A4) sc-390952 (SCBT) (WB 1:500), anti-P/Q-type Ca^{++} CP α1A (Cacna1a) Antibody (C-2) sc-390004 (SCBT) (WB 1:500), and Anti-IP3R-I/II/III Antibody (B-2) sc-377518 (SCBT) (WB 1:500). Secondary antibodies utilised for ICC experiments were goat anti-chicken Alexa 488 (Abcam; ab150173), goat anti-mouse 488 (abcam; ab150113), and goat anti-rabbit Alexa 555 (abcam; ab150078), all at 1:1000. Secondary antibodies used for WB were goat anti-rabbit conjug. HRP (Dako, P0448) and rabbit anti-mouse conjug. HRP (Dako, P0260), both at 1:5000. Beta-Nicotinamide Mononucleotide was purchased from Sigma (N3501). PARG inhibitor PDD 00017273 (Tocris), PARP inhibitor Ku-0058948. The NAMPT inhibitor FK866 was purchased from Sigma-aldrich, cat. F8557. The 26s proteasome inhibitor MG132 was purchased from Merck, cat. M7449. The nNOS inhibitor L-NAME was purchased from Merck, cat. N5751. The viral construct hSyn1:SyGCaMP6f was given by the University of Helsinki.

Data Analysis and Statistics

Tests performed are indicated in relevant figure legends, as are the number of repeats. Statistical significance was calculated through Graphpad Prism 8. Manual quantification of fluorescence intensity took place via measurement of selected ROIs in ImageJ. Statistical significance is denoted as *, where $p < 0.05$, ** $p < 0.01$, *** $p < 0.005$, and **** $p < 0.001$.

3. Chapter Three: Parp1 Hyperactivation at Sites of Endogenous SSBs in Xrcc1 Deficient Hippocampal Neurons

3.1 Introduction and Aims

The inherent instability of DNA has led to the evolution of highly conserved mechanisms by which to repair lesions (Lindahl, 1993, Caldecott, 2008). The most commonly occurring of these lesions is the DNA single-strand break, discontinuities in a single strand of the DNA double helix, frequently associated with damaged 5' and 3' termini (Caldecott, 2008). The repair of DNA single-strand breaks (SSBs) may occur through a variety of mechanisms, however repair in post-mitotic cells is dependent on XRCC1, PARP1, and a variety of other SSBR proteins; hereditary defects in which are associated with neurological disorders. These disorders commonly present with cerebellar degeneration and, in some cases, seizures (McKinnon, 2009, Dumitrache, *et al*., 2018).

SSBs can arise through several endogenous mechanisms; abortive TOP1 activity leaving a SSB intermediate, direct oxidation of the DNA sugar moiety, such as by reactive oxygen species (ROS) generated during cellular metabolism, or indirectly through base excision repair (Caldecott, 2008, Beard, *et al*., 2019). The induction of oxidative DNA damage poses a threat to genomic integrity and represents the most common source of germline mutation during development. Endogenously, ROS are generated during oxidative metabolism, where the reduction of oxygen during cellular respiration results in the formation of $O_2^{\bullet-}$. SOD catalyses the conversion of $O_2^{\bullet-}$ to O_2 and H_2O_2 which, while relatively inert, is endogenously converted to $^{\bullet}OH$, a radical capable of inducing oxidative base modification, which are repaired through BER (Poetsch, 2020). Further, ROS can modify the sugar phosphate backbone, leading to the direct disintegration of the oxidised sugar moiety (Poetsch, 2020). In neuronal cells, activity-dependent oxidative damage can occur in response to nitric oxide signalling, where $^{\bullet}NO$ is combined with the superoxide anion $O_2^{\bullet-}$ to form $ONOO^-$, which can result in both the direct oxidation of the DNA sugar, or base modification (Szabo and Ohshima, 1997, Neitz, *et al*., 2015). The increased production of $^{\bullet}NO$ also occurs during glutamate excitotoxicity. The excessive activation of NMDA receptors by the neurotransmitter glutamate results in elevated postsynaptic Ca^{2+} influx, the increased activation of nNOS, and the deregulated mitochondrial production of $O_2^{\bullet-}$, which forms $ONOO^-$ in conjunction with $^{\bullet}NO$ (Lau and Tymianski, 2010). Damage to nucleobases is repaired through the action of an array of glycosylase, which catalyse the removal of modified, nitrogenous bases, leaving behind an intact AP site (Brooks, *et al*., 2013). Monofunctional

glycosylases, such as TDG, possess only glycosylase activity, and the resultant AP site requires processing by an AP endonuclease (such as APE1), which cleave the 5' end of the baseless backbone, leaving behind a SSB (Moor and Lavrik, 2018). Bifunctional glycosylases, such as OGG1, possess additional lyase activity, cleaving the 3' end of the AP site, bypassing the need for an AP endonuclease, and generating a SSB (Roychoudhury, *et al*., 2020).

Topoisomerases, such as TOP1, act to relieve the torsional stress applied to DNA during transcription and replication (McKinnon, 2016). To do so, TOP1, transiently induce a nick to which it is covalently bound, creating a TOP1 cleavage complex (TOP1cc), downstream of which DNA can be rotated to relieve tension (Wang, *et al*., 1971, Ashour, *et al*., 2015, Baranello, *et al*., 2016, Pommier, *et al*., 2016). During replication, the collision of a Top1cc with a replicative polymerase will cause the formation of DSBs and, as such, must be removed to maintain strand continuity (Sordet, *et al*., 2010). To do so, the TOP1cc is degraded by the proteasome, leaving a SSB (Lin, *et al*., 2008). In neuronal cells, the transcriptional demand associated with development and activity-driven changes in protein expression result in the comparatively high expression of TOP1 in brain (Stott, *et al*., 2021).

Due to the heterogeneous nature of DNA SSBs, several enzymatic processes may be required for their repair, the coordination of which may be dependent on a scaffold protein to facilitate the complete process without the release of toxic intermediates (Krokan and Bjørås, 2013). XRCC1 is a DNA repair scaffold protein which lacks enzymatic activity but is required for the recruitment and coordination of the SSBR machinery, interacting directly with several components of the SSBR machinery and forming heterogeneous complexes to facilitate the repair of various types of SSB (Caldecott, *et al*., 1996, Whitehouse, *et al*., 2001, Clements, *et al*., 2004, Mok, *et al*., 2019). For XRCC1 to be recruited to the SSB, it must first be recognised by PARP enzymes, such as PARP1. PARP1 binds at the SSB, synthesising poly(ADP-ribose) using NAD+ as a cofactor, modifying itself (autoribosylation) and other proteins (transribosylation) such as core and linker histones (Polo and Jackson, 2011, Eustermann, *et al*., 2015). XRCC1 binds preferentially to autoribosylated PARP1, whereupon it facilitates the repair of the break through interactions with other SSBR proteins. In cells lacking XRCC1, PARP1 is retained at the break, continuously synthesising nuclear poly(ADP-ribose) at sites of unresolved damage (Hoch, *et al*., 2017). In dividing cells, such as mitotic glia, auxiliary repair may occur through homologous recombination (HR), or through their replication dependent conversion to DNA-DSBs and robust mechanism by which to resolve them, such as non-homologous

end joining (NHEJ), the primary pathway for DSB repair (Caldecott, 2008, Davis and Maizels, 2014, Vriend and Krawczyk, 2017). In mice lacking Xrcc1, Parp1 hyperactivation in the brain leads to elevated poly(ADP-ribose) in the cerebellum and hippocampus, resulting in cerebellar degeneration, ataxia, and seizures leading to juvenile mortality.

The hyperactivation of PARP1 has been reported in numerous disorders and neurological conditions, notably following ischemia-reperfusion injury, and in the pathology of AD and PD (Martire, *et al*., 2015, Hagam, *et al*., 2021). The accumulation of poly(ADP-ribose), and the subsequent depletion of the cellular NAD+/ATP pool is known to result in an apoptosis-independent cell death pathway; *parthanatos* (Fatokun, *et al*., 2014, Zhou, *et al*., 2021). In parthanatotic cell death, the excessive synthesis of poly(ADP-ribose) leads to the migration of the polymer from the nucleus of the cell to the mitochondria, resulting in glycolytic inhibition through the PARP1-dependent modification of enzymes involved in the regulation of glycolysis and the citric acid cycle (Fouquerel, *et al*., 2014). Alongside the deregulation of metabolism, poly(ADP-ribose) interacts with AIF, which resides in the intermembrane space of the mitochondria, resulting in its translocation to the nucleus (Daugas, *et al*., 2000, Wang, *et al*., 2016, Zhou, *et al*., 2021). The translocation of AIF facilitates the recruitment of macrophage migration inhibitory factor (MIF), a nuclease which cleaves DNA into large fragments (Wang, *et al*., 2016). It is unclear whether DNA fragmentation or glycolytic inhibition result in death, as both depletion of MIF and the supplementation of TCA substrates suppress parthanatos (Ying, *et al*., 2002, Wang, *et al*., 2016, Yang, *et al*., 2020). Alongside PARP1, a further mediator of parthanatotic cell death is PARG, an endogenous enzyme which regulates levels of poly(ADP-ribose) in the cell. PARG catalyses the hydrolysis of poly(ADP-ribose) to free ADP-ribose units (Feng, *et al*., 2013). The overexpression of PARG results in significant protection from cell death induced by exogenous DNA damaging agents (Mortusewicz, *et al*., 2011, Marques, *et al*., 2019). Similarly, PARG knockout is embryonic lethal, resulting in the accumulation of poly(ADP-ribose) in cells and, subsequently, cell death (Hanai, *et al*., 2004, Blenn, *et al*., 2006). Due to the toxicity associated with poly(ADP-ribose) accumulation, PARG inhibitors have been developed in the hopes of exploiting the genomic instability of cancer cells, stabilising. PARG inhibitors stabilise poly(ADP-ribose) by competing for the PARG active site, occupying the region that binds the adenine moiety of ADP-ribose.

PARP inhibitors are used clinically for the treatment of some cancers, such as those with BRCA mutation (Sachdev, *et al*., 2019, Rose, *et al*., 2020). The impairment of BER in cancer cells through PARP inhibition results in the continuous accumulation of DNA

SSBs; which go on to become DNA DSBs through replication fork collapse (Matsumoto, *et al*., 2019). In particular, cells with HR deficiency (such as those with *BRCA1/2* mutation) are sensitive to PARP inhibition, as they are limited in their capacity to repair these transformed lesions (Bryant, *et al*., 2005, Dziadkowiec, *et al*., 2016, Matsumoto, *et al*., 2019). Similarly, HR deficient cells are sensitive to PARG inhibitors, as the accumulation of poly(ADP-ribose) prevents repair, promoting replication fork collapse and DSB formation (Fathers, *et al*., 2012). While the use of PARP inhibitors has been approved for the treatment of some cancers, their efficacy in the treatment of SSBR-related neurodegeneration is unclear. Previous observations have indicated that PARP inhibition, unlike deletion, does not rescue the decreased lifespan of the *Xrcc1*$^{\text{Nes-Cre}}$ mouse (Komulainen, E. unpublished observations). There may be several reasons for this discrepancy, such as the maintenance of PARP inhibition in the brain. Further, the mechanism by which commercial PARP inhibitors function is through trapping PARP1 at the break, resulting in the retention of toxic PARP-DNA intermediates, and as such does not phenocopy Parp1 deletion (Murai, *et al*., 2012). Toxicity associated with PARP inhibitor treatment might also be linked to a lack of specificity for Parp1 over Parp2, which also responds to DNA damage, albeit to a lesser extent (Murai, *et al*., 2012). The retention of Parp2 function likely explains the very mild phenotype associated with *Parp1* deletion, however the deletion of both *Parp1* and *Parp2* is embryonic lethal (de Murcia, *et al*., 2003, Piskunova, *et al*., 2008).

The focus of this chapter will be on establishing a cell autonomous model of endogenous DNA damage, in both mitotic cells and post-mitotic, cultured neurons. I aim to investigate the role of Xrcc1 and Parp1 in the repair of DNA SSBs, and their contribution to the phenotype of *Xrcc1*$^{\text{Nes-Cre}}$ mouse neurons. Using a PARG inhibitor to stabilise poly(ADP-ribose) at sites of endogenous SSBs, I aim to investigate the activity of Parp1 in Xrcc1-deficient neurons, and the underlying source of the lesions to which Parp1 is recruited. I further aim to investigate the therapeutic potential of PARP inhibition in the treatment of XRCC1-linked disease.

3.2 Results

3.2.1 PARG Inhibition Uncovers Elevated Levels of poly(ADP-ribose) in SSB Repair-Defective *XRCC1*$^{-/-}$ RPE-1 Cells.

In this chapter, I aimed to establish a cell autonomous model by which endogenous SSBs and their consequences could be investigated. To do so, I reasoned that the inhibition of PARG (which prevents poly(ADP-ribose) degradation), would enable the detection of poly(ADP-ribose) at sites of PARP1 activation at endogenous SSBs (Feng, *et al*., 2013, Hanzlikova, *et al*., 2018). To confirm that this approach would work, I first utilised human *XRCC1*$^{-/-}$ RPE-1 cells. Cells were treated with PARG inhibitor prior to fixation and staining with PAN ADP-ribose Binding Reagent, a reagent which selectively binds both mono and poly(ADP-ribose). Acute treatment with 10μM PARG inhibitor for 1 hour resulted in the significant accumulation of nuclear poly(ADP-ribose) in *Xrcc1*$^{-/-}$ RPE-1 cells, which I reasoned to be the result of PARP1 activity at sites of endogenous SSBs (Figure 3.1 A). Pre-treatment for 4 hours with 5μM of the PARP inhibitor KU00058948 ablated this accumulation. In wild type controls, I observed poly(ADP-ribose) accumulation in some nuclei, consistent with previous findings by Hanzlikova *et al*., which demonstrated high levels of poly(ADP-ribose) in S phase cells, likely reflecting a role in the ligation of Okazaki Fragments during S-phase.

Next, I measured the steady-state level of poly(ADP-ribose) using western blotting. I incubated *XRCC1*$^{-/-}$ RPE-1 cells with 10 μM PARG inhibitor for 1 hour prior to lysis and blotting, in order to investigate the accumulation of the polymer. I identified a significant accumulation of poly(ADP-ribose) in *XRCC1*$^{-/-}$ RPE-1 cells following PARG inhibition. 4-hour pre-treatment with the NAMPT inhibitor FK866, which drastically limits the bioavailability of the PARP1 substrate; NAD+, was sufficient to significantly reduce the accumulation of poly(ADP-ribose) in cells (Figure 3.1 B). Similarly, pre-treatment with a PARP inhibitor eliminated poly(ADP-ribose) synthesis. Together, these data confirm that *XRCC1*$^{-/-}$ RPE-1 cells undergo continuously elevated synthesis of poly(ADP-ribose) at sites of unrepaired endogenous SSBs.

3.2.2 *XRCC1*$^{-/-}$ RPE-1 Cells Exhibit PARP1/NAD+-Dependent Sensitivity to PARG Inhibition.

In order to establish the effects of poly(ADP-ribose) accumulation in *XRCC1*$^{-/-}$ RPE-1 cells, I conducted clonogenic cell survival assays in which cells were chronically treated with various concentrations of the PARG inhibitor. Chronic treatment with 10μM PARG inhibitor was sufficient to induce hypersensitivity in *XRCC1*$^{-/-}$ human RPE-1 cells (Figure 3.2 A). Further, additional deletion of *PARP1* conferred resistance to PARG

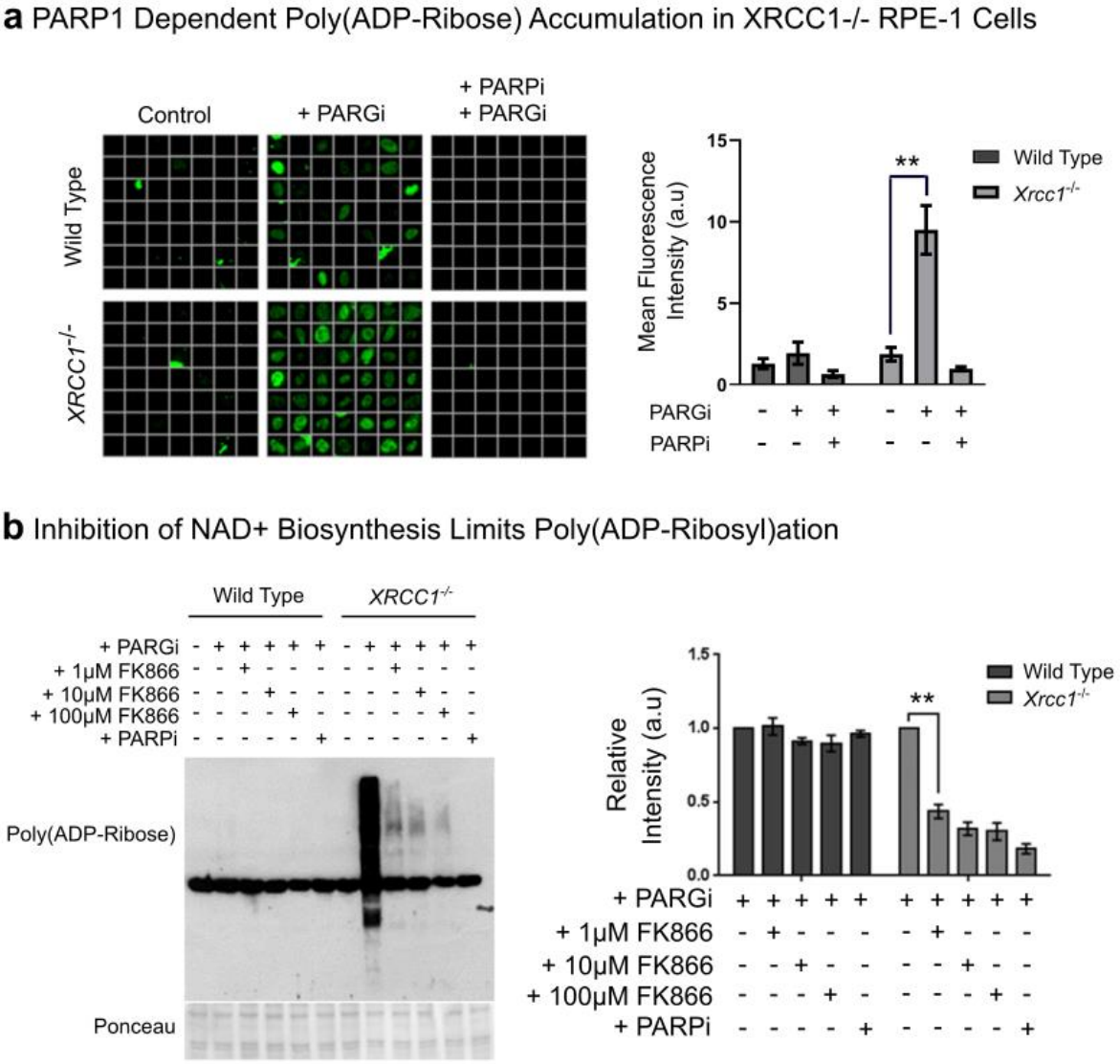

Figure 3.1 *Elevated poly(ADP-ribose) accumulation in human XRCC1$^{-/-}$ RPE-1 cells*. A) *Left,* representative SCANr galleries of poly(ADP-ribose) immunofluorescence in and *XRCC1$^{-/-}$* RPE-1 cells pre-treated for 4 hr with 5μM PARP inhibitor or DMSO vehicle prior to treatment with 10μM PARG inhibitor for 1hr prior to fixation. *Right,* quantification from three individual repeats where ** denotes statistical significance at p <0.01 by student's t-test. B) *Left,* Western blot showing the accumulation of poly(ADP-ribose) in wild type and *Xrcc1$^{-/-}$* RPE-1 cells following PARG inhibition and pre-treatment for 24 hr with indicated concentrations of FK866, a NAMPT inhibitor, an enzyme responsible for the bulk of cellular NAD+ production, or 5μM PARP inhibitor. Right, quantification from three independent experiments with statistical significance determined by student's t-test (**p < 0.01). Histograms show mean ± SEM.

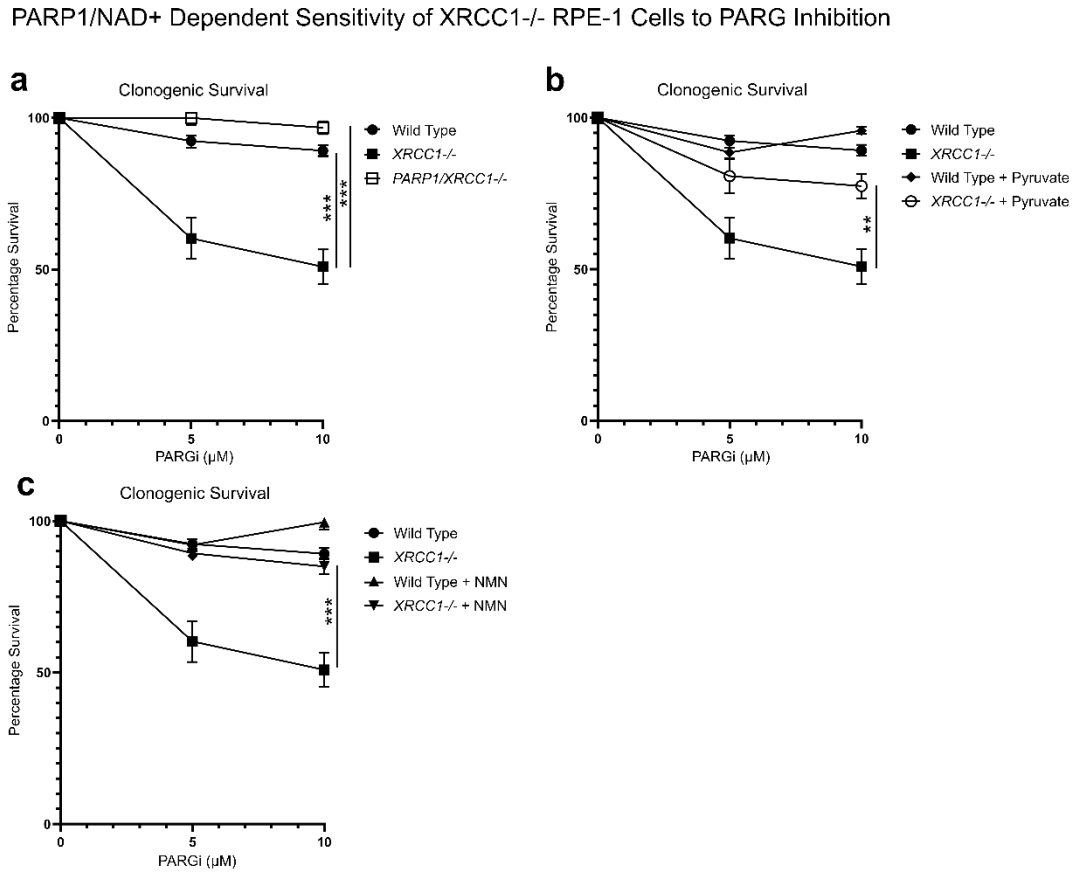

Figure 3.2 *PARP1/NAD+ Dependent Phenotype Sensitivity of Human XRCC1$^{-/-}$ RPE-1 Cells to PARG Inhibition*. A) Clonogenic survival curves demonstrating PARGi sensitivity of cells lacking XRCC1 in comparison to wild type cells, and the rescue afforded by the additional deletion of *PARP1*. B) and C) Survival curves demonstrating the rescue of XRCC1 dependent PARGi sensitivity by the TCA substrate sodium pyruvate, and the NAD+ precursor nicotinamide mononucleotide (NMN) respectively. All experiments performed in triplicate. Significance calculated via one-way ANOVA, $P < 0.0012$, with post-hoc Tukey-Kramer comparison of means identifying between group significance where ** denotes $p < 0.01$ and *** denotes $p < 0.005$). Data from three individual repeats.

inhibitor toxicity in *XRCC1*-deficient RPE-1 cells (Figure 3.2 A), confirming that PARP1 was the source of the PARG inhibitor sensitivity. Interestingly, the sensitivity of *XRCC1*$^{-/-}$ RPE-1 cells to PARG inhibitor was partially rescued by supplementation with the citric acid cycle substrate sodium pyruvate (Figure 3.2 B). Previous studies have demonstrated PARP1-dependent deregulation of metabolism through modification of HK1 (Hexokinase 1), a mitochondrial membrane protein required for glucose phosphorylation, and the subsequent suppression of parthanatotic cell death by supplementation with the citric acid cycle substrates sodium pyruvate and α-ketoglutarate (Ying, *et al*., 2002, David, *et al*., 2009, Andrabi, *et al*., 2014, Fouqerel, *et al*., 2014). Similarly, several studies have implicated the consumption and subsequent reduction of NAD+ bioavailability in parthanatotic cell death (David, *et al*., 2009, Huang, *et al*., 2014). That sodium pyruvate supplementation rescues the sensitivity of *XRCC1*$^{-/-}$ RPE-1 cells to PARG inhibition suggests a mechanism of toxicity related to metabolic collapse. To confirm this, I repeated the clonogenic assays, supplementing cells with the NAD+ precursor nicotinamide mononucleotide (NMN) and observe an even greater rescue of PARG inhibitor toxicity in *XRCC1*$^{-/-}$ RPE-1 cells, consistent with observations to NAD+ repletion also rescues parthanatotic cell death (Figure 3.2 C) (Ying, *et al*., 2003). These data suggest that, in the case of proliferating XRCC1-deficient RPE-1 cells, PARG inhibitor toxicity is a result of the excessive consumption of NAD+ by PARP1, resulting in PARP1/NAD+ dependent cell death following metabolic collapse.

3.2.3 Defective SSBR in Dissociated *Xrcc1*$^{Nes\text{-}Cre}$ Hippocampal Neurons

Typically, conditions associated with hereditary defects in SSBR, such as SCAN1, MCSZ, and AOA-XRCC1, present with neurological involvement, and have yet to be associated with an increased risk of cancer (Caldecott, 2008). Following the discovery that *XRCC1* deletion in mitotic cells results in poly(ADP-ribose) accumulation and PARG inhibitor sensitivity, we next sought to investigate the consequences of *Xrcc1* deletion in post-mitotic neurons. To do so, we created dissociated hippocampal cultures from p1-2 wild type and *Xrcc1*$^{Nes\text{-}Cre}$ mouse pups. Whole body knockout of *Xrcc1* is embryonic lethal (Tebbs, *et al*., 1999). However, by employing conditional expression of Cre recombinase by utilising the Nestin promoter, in which the targeted protein is conditionally deleted in nervous tissue from embryonic day (E)15.5, viable *Xrcc1*$^{Nes\text{-}Cre}$ pups are obtainable (Tebbs, *et al*., 1999, Dubois, *et al*., 2006, Lee, *et al*., 2009).

Given that *XRCC1* deletion in human cells results in elevated poly(ADP-ribose) accumulation and cell death following treatment SSB-inducing agents, I first aimed to confirm the presence of elevated SSB-induced PARP activity in *Xrcc1*$^{Nes\text{-}Cre}$

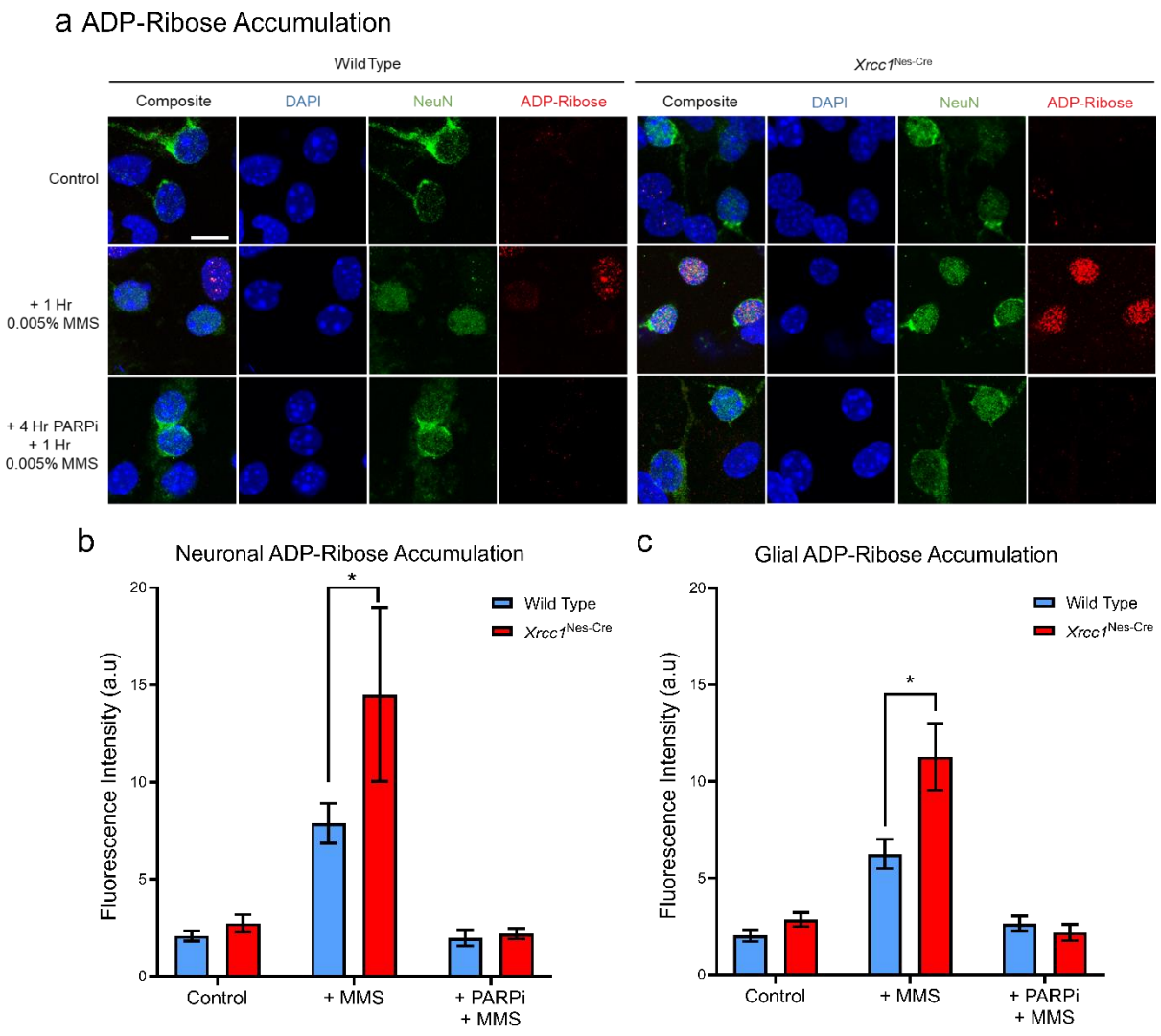

Figure 3.3 *Methyl Methanesulfonate (MMS) Treatment Highlights Defective SSBR in Xrcc1$^{Nes-Cre}$ Hippocampal Neurons*. Indirect immunofluorescence of DIV6 hippocampal neurons cultured from p1-2 Wild Type and *Xrcc1$^{Nes-Cre}$* mice. Cells were pre-treated with 5μM PARP inhibitor or vehicle for 4hrs prior to 1hr treatment with 0.005% MMS, and alkylating agent, stained for NeuN, a marker of the neuronal nucleus, and ADP-Ribose. Scale bars = 20μm. Quantified in NeuN positive (neuronal) cells in B), and in NeuN negative (glial) cells in C, significance is denoted by * where $p < 0.05$ by student's t.test, n = 3, cells were manually quantified in ImageJ, where at least 30 cells were measured for immunofluorescence per replicate (> 90 cells). Histograms show mean ± SEM.

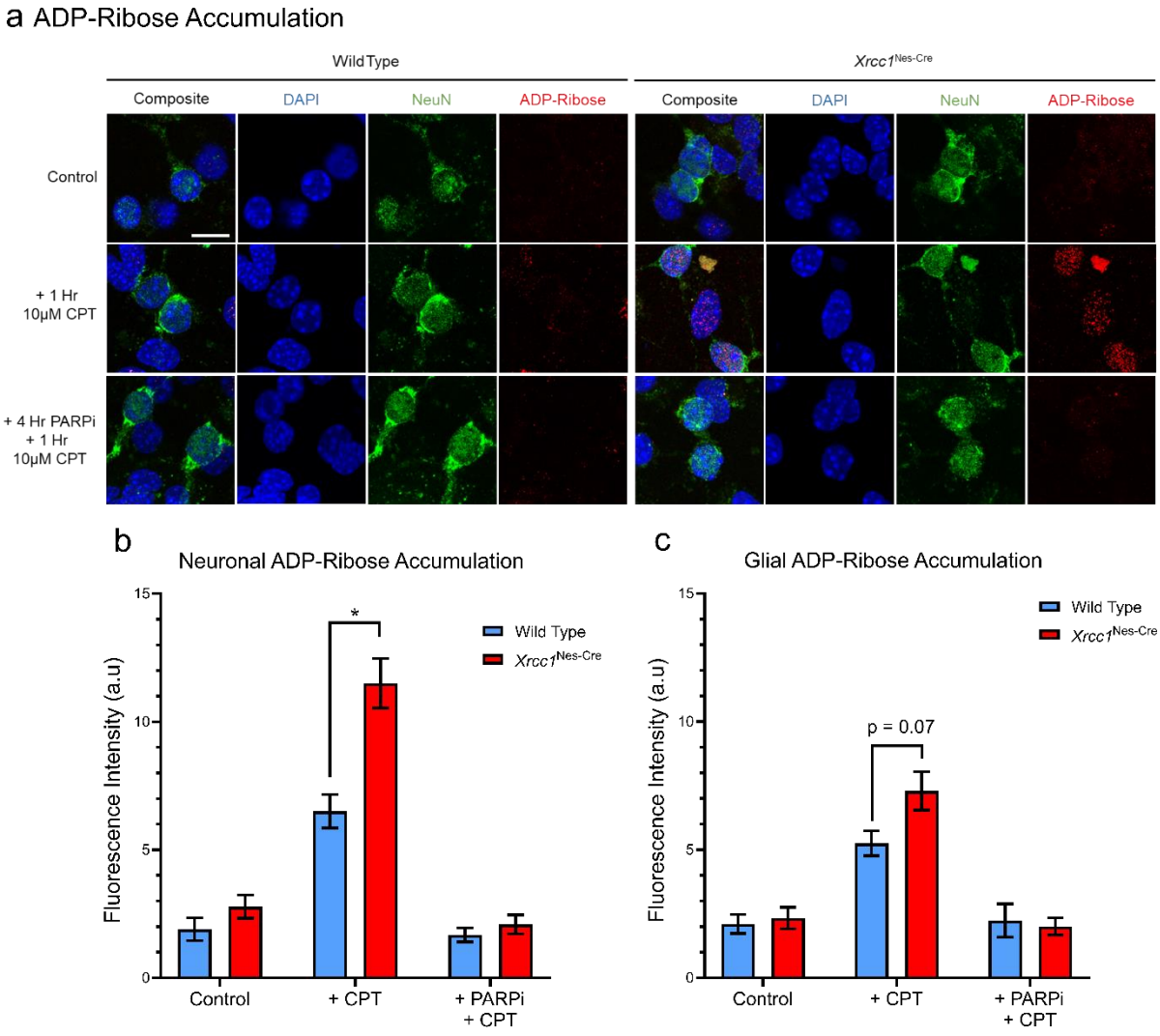

Figure 3.4 *Camptothecin (CPT) Treatment Further Highlights Defective SSBR in Xrcc1$^{Nes-Cre}$ Hippocampal Neurons*. Indirect immunofluorescence of DIV6 hippocampal neurons cultured from p1-2 Wild Type and *Xrcc1$^{Nes-Cre}$* mice. Cells were pre-treated with 5μM PARP inhibitor or vehicle for 4hrs prior to 1hr treatment with 10μM of the Top1 poison Camptothecin, stained for NeuN, a marker of the neuronal nucleus, and ADP-Ribose. Scale bars = 20μm. Quantified in NeuN positive (neuronal) cells in B), and in NeuN negative (glial) cells in C, significance is denoted by * where $p < 0.05$ by student's t.test, n = 3. Cells were manually quantified in ImageJ, where at least 30 cells were measured for immunofluorescence per replicate (> 90 cells). Histograms show mean ± SEM.

Hippocampal neurons (Hoch, *et al*., 2017). To do so, I pre-treated mixed cultures (cultures containing both primary neurons and glial cells) for 4 hrs with either PARP inhibitor or DMSO control, prior to a further 1 hr treatment in the presence of either 0.005% (45µM) methyl methanesulfonate (MMS), a DNA-SSB inducing alkylating agent, or 10µM Camptothecin (CPT), a Topoisomerase 1 poison. Following either treatment, *Xrcc1*$^{Nes\text{-}Cre}$ hippocampal neurons exhibit significantly elevated poly(ADP-ribose) accumulation when compared to wild type neurons (Figure 3.3 A & B, Figure 3.4 A & B), consistent with the decreased SSBR capacity associated with Xrcc1 deficiency^{e} neurons (Lee, *et al*., 2009). Given that these cultures of hippocampal neurons are mixed (containing both neuronal and glial cells), I employed the neuronal marker NeuN to discriminate between neurons and glia. In *Xrcc1*$^{Nes\text{-}Cre}$ mixed cultures, both NeuN-positive (neurons) and NeuN-negative (glia) cells exhibited greater levels of poly(ADP-ribose) from exogenous sources than in cell type matched wild type controls (Figure 3.3 C, Figure 3.4 C).

3.2.4 A Cell Autonomous Model of Endogenous Parp1 Activation in Neuronal Cultures

Previous observations have identified elevated poly(ADP-ribose) in the mature hippocampus of the *Xrcc1*$^{Nes\text{-}Cre}$ mouse (Figure 3.5) (Komulainen, *et al*., 2021). Given that poly(ADP-ribose) levels are elevated in the *Xrcc1*$^{Nes\text{-}Cre}$ mouse hippocampus *in vivo* in the absence of exogenous damaging agents (Figure 3.5 and Komulainen, *et al.,* 2021), I next aimed to determine whether dissociated *Xrcc1*$^{Nes\text{-}Cre}$ neurons could provide a cell autonomous model of endogenous damage and Parp1 activation. I therefore pre-treated the hippocampal cell cultures for 4 hours with either 5µM PARP inhibitor or vehicle control, prior to treatment with 10µM PARG inhibitor for 1 hour. I saw increased accumulation of poly(ADP-ribose) in *Xrcc1*$^{Nes\text{-}Cre}$ hippocampal neurons *in vitro* in the absence of exogenous DNA damaging agents (Figure 3.6 A & B). This accumulation of ADP-ribose suggests that *Xrcc1*$^{Nes\text{-}Cre}$ hippocampal neurons exhibit elevated steady-state levels of endogenous SSBs, with PARG inhibition stabilising the nascent poly(ADP-ribose) synthesised by Parp1; providing a cell autonomous model by which we can examine endogenous poly(ADP-ribose) synthesis in neuronal cells. When *Xrcc1*$^{Nes\text{-}cre}$ neurons were pre-incubated with a PARP1 inhibitor prior to PARG inhibition, this effect was suppressed entirely, confirming that the elevated ADP-ribosylation is a result of constitutive synthesis of nascent poly(ADP-ribose). I also noted elevated poly(ADP-ribose) accumulation in post-mitotic neurons compared to proliferative glial cells when quantified based on the presence of neuronal marker (Figure 3.6 B and C).

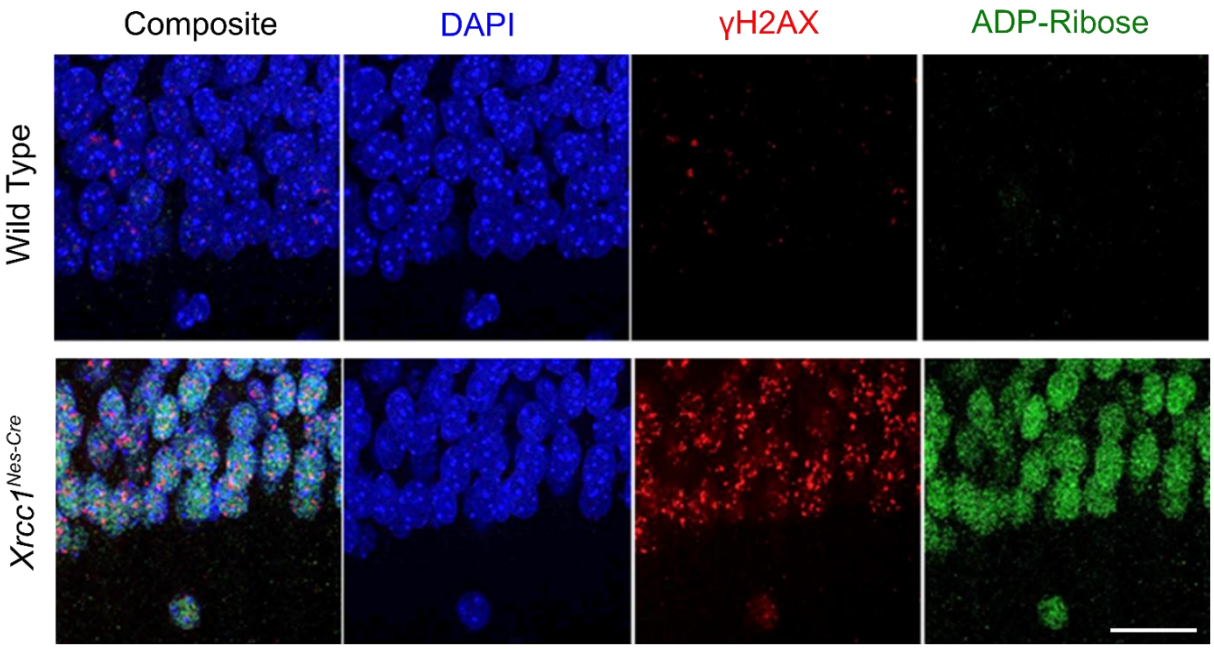

Figure 3.5 *Poly(ADP-ribose) Accumulation in the In Vivo Xrcc1*$^{Nes\text{-}Cre}$ *Mouse Hippocampus.* A] Indirect immunofluorescence of 10 micron CA1 hippocampal sections from p15 wild type and *Xrcc1*$^{Nes\text{-}Cre}$ mice, perfused transcardially with 4% PFA, stained for ADP-Ribose and γH2AX. Elevated ADP-Ribose and γH2AX are observed in the *Xrcc1*$^{Nes\text{-}Cre}$ hippocampus, as previously reported by E. Komulainen. Scale bar = 50μm.

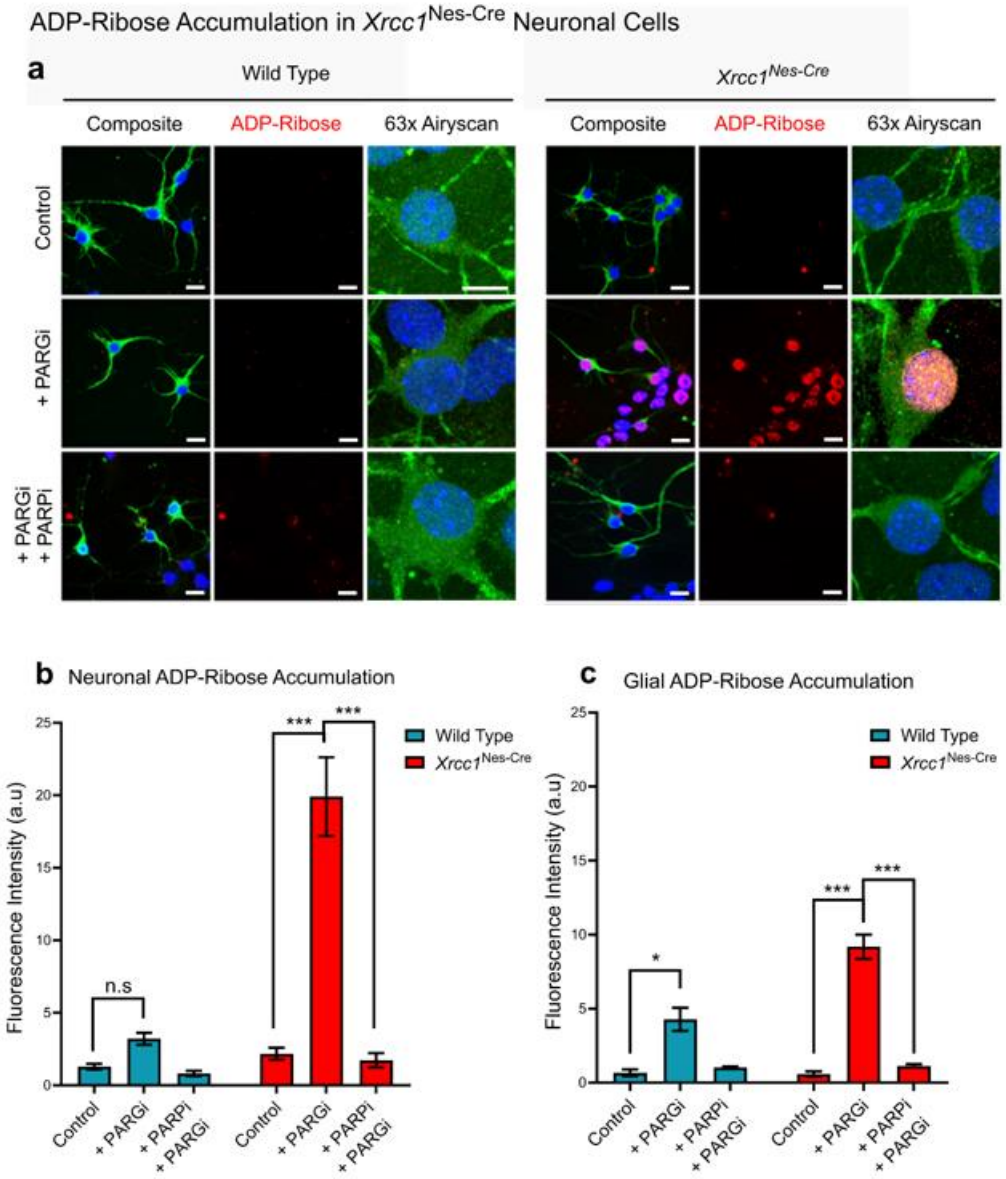

Figure 3.6 *Acute PARG Inhibition Reveals Endogenous Damage and Nascent ADP-Ribose Synthesis* A) Indirect immunofluorescence of DIV6 hippocampal neurons cultured from p1-2 Wild Type and *Xrcc1*$^{Nes\text{-}Cre}$ mice. Cells were pre-treated with 5μM PARP inhibitor or vehicle for 4hrs prior to 1hr treatment with 10μM PARG inhibitor, stained for MAP2 and ADP-Ribose. Scale bars = 20μm. B) Quantification of ADP-ribose intensity in MAP2+ve (neuronal) cells from Wild Type (n = 6, > 180 cells per condition), *Xrcc1*$^{Nes\text{-}Cre}$ (n = 6, > 180). Quantification of ADP-Ribose intensity in MAP2 negative (glial) cells in C) from three replicates, > 90 cells. Significance denoted by *** where P > 0.005 by student's t.test, indicating significantly elevated poly(ADP-ribose) accumulation in *Xrcc1*$^{Nes\text{-}Cre}$ Hippocampal neurons. Histograms show mean ± SEM.

Given that pre-treatment with a PARP inhibitor suppresses PARG inhibitor induced poly(ADP-ribose) accumulation, thereby indicating nascent synthesis, the elevated poly(ADP-ribose) in neuronal cells suggests that the elevated steady-state level of endogenous DNA SSBs is higher in, or is specific to, post-mitotic neurons, when compared to glia.

3.2.5 *Parp1* Deletion Supresses poly(ADP-ribose) Accumulation in *Xrcc1*$^{Nes\text{-}Cre}$ Hippocampal Neurons

Next, I investigated the effect of *Parp1* deletion on the cellular phenotype of elevated poly(ADP-ribose) accumulation. The deletion of either one or both alleles of *Parp1* is sufficient to suppress or eliminate the accumulation of poly(ADP-ribose) in the *Xrcc1*$^{Nes\text{-}Cre}$ mouse hippocampus (Komulainen, *et al*., 2021). Similarly, *Parp1* deletion drastically rescues the premature mortality that characterises the *Xrcc1*$^{Nes\text{-}Cre}$ mouse; the deletion of one or both alleles increasing lifespan by ~25 fold and ~8 fold respectively (Komulainen, *et al*., 2021). To investigate whether *Parp1* deletion suppresses the elevated PAR in dissociated Xrcc1$^{Nes\text{-}Cre}$ hippocampal cells, I prepared hippocampal neurons from *Parp1*$^{+/-}$/*Xrcc1*$^{Nes\text{-}Cre}$ and *Parp1*$^{-/-}$/*Xrcc1*$^{Nes\text{-}Cre}$ mouse pups, which were then treated as described in the previous section. I observed a partial reduction in poly(ADP-ribose) accumulation in *Parp1*$^{+/-}$/*Xrcc1*$^{Nes\text{-}Cre}$ neurons similar to that reported in hippocampus in brain slices from *Parp1*$^{+/-}$/*Xrcc1*$^{Nes\text{-}Cre}$ mice (Figure 3.7 A & B) (Komulainen, *et al*., 2021). Deletion of both *Parp1* alleles was sufficient to reduce poly(ADP-ribose) accumulation in *Xrcc1*$^{Nes\text{-}Cre}$ neurons to a level similar to or below that in wild type neurons, as observed in *Parp1*$^{-/-}$/*Xrcc1*$^{Nes\text{-}Cre}$ brain slices (Figure 3.7 A & B) (Komulainen, *et al*., 2021).

3.2.6 *Xrcc1*$^{Nes\text{-}Cre}$ Hippocampal Neurons Exhibit *Parp1*-Dependent Shortened lifespan *in vitro*

Previous studies have indicated that cerebellar dysfunction in the *Xrcc1*$^{Nes\text{-}Cre}$ mice may in part be related to death of the cerebellar interneurons, and TUNEL staining of the mature mouse brain has also suggested elevated cell death in the cerebellar granule layer in the pathology of this mouse (Lee, *et al*., 2009, Komulainen, E. unpublished observations). Interestingly, the death of cerebellar interneurons in *Xrcc1*$^{Nes\text{-}Cre}$ mice can be rescued by the additional deletion of p53, a tumour suppressor gene which induces cell cycle arrest and apoptosis in response to DNA damage, indicating that this death occurs during neurodevelopment, when neural progenitors are still undergoing cell division (Lee, *et al*., 2009). We have not, as yet, observed significant cell loss in *Xrcc1*$^{Nes\text{-}Cre}$ hippocampus *in vivo*. *In vitro*, however, *Xrcc1*$^{Nes\text{-}Cre}$ hippocampal

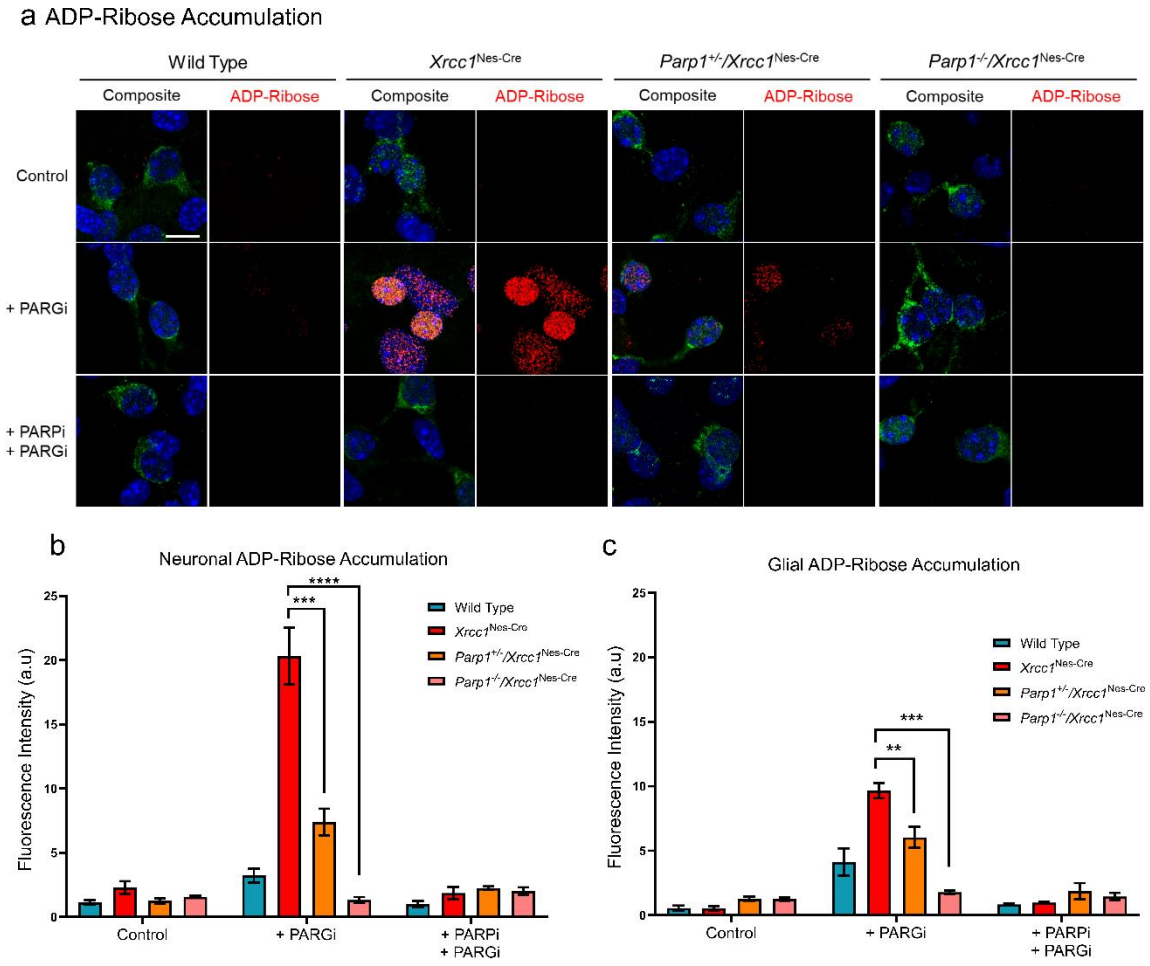

Figure 3.7 *The Additional Deletion of Either One or Both Alleles of Parp1 Rescues poly(ADP-ribose) Accumulation in Xrcc1*$^{Nes\text{-}Cre}$ *Hippocampal Neurons.* A) Indirect immunofluorescence of DIV6 hippocampal neurons cultured from p1-2 Wild Type, *Xrcc1*$^{Nes\text{-}Cre}$ mice, *Parp1*$^{+/-}$*/Xrcc1*$^{Nes\text{-}Cre}$ and *Parp1*$^{-/-}$*/Xrcc1*$^{Nes\text{-}Cre}$. Cells were pre-treated with 5μM PARP inhibitor or vehicle for 4hrs prior to 1hr treatment with 10μM PARG inhibitor, stained for NeuN and ADP-Ribose. Scale bars = 20μm. B) Quantification of ADP-ribose intensity in NeuN positive (neuronal) cells from Wild Type (n = 6, > 180 cells per condition), *Xrcc1*$^{Nes\text{-}Cre}$ (n = 6, > 180), *Parp1*$^{+/-}$*/Xrcc1*$^{Nes\text{-}Cre}$ (n = 3, > 90), and *Parp1*$^{-/-}$*/Xrcc1*$^{Nes\text{-}Cre}$ (n = 3, > 90) mice, indicating that the accumulation of ADP-Ribose in *Xrcc1*$^{Nes\text{-}Cre}$ hippocampal neurons following acute PARG inhibition is suppressed by *Parp1* deletion (one-way ANOVA, $p < 0.0001$, Tukey's post-hoc indicating significance where *** denotes $p < 0.005$). C) Quantification of ADP-Ribose intensity in MAP2-ve (glial) cells from Wild Type (n = 3, > 90), *Xrcc1*$^{Nes\text{-}Cre}$ (n = 3, > 90), *Parp1*$^{+/-}$*/Xrcc1*$^{Nes\text{-}Cre}$ (n = 3, > 90), and *Parp1*$^{-/-}$*/Xrcc1*$^{Nes\text{-}Cre}$ (n = 3, > 90) mice, again indicating significant accumulation of ADP-ribose in *Xrcc1*$^{Nes\text{-}Cre}$ hippocampal neurons (one-way ANOVA, $p < 0.0001$, Tukey's post-hoc indicating significance where * denotes $p < 0.05$, ** $p < 0.01$, and *** $p < 0.005$). Histograms show mean ± SEM

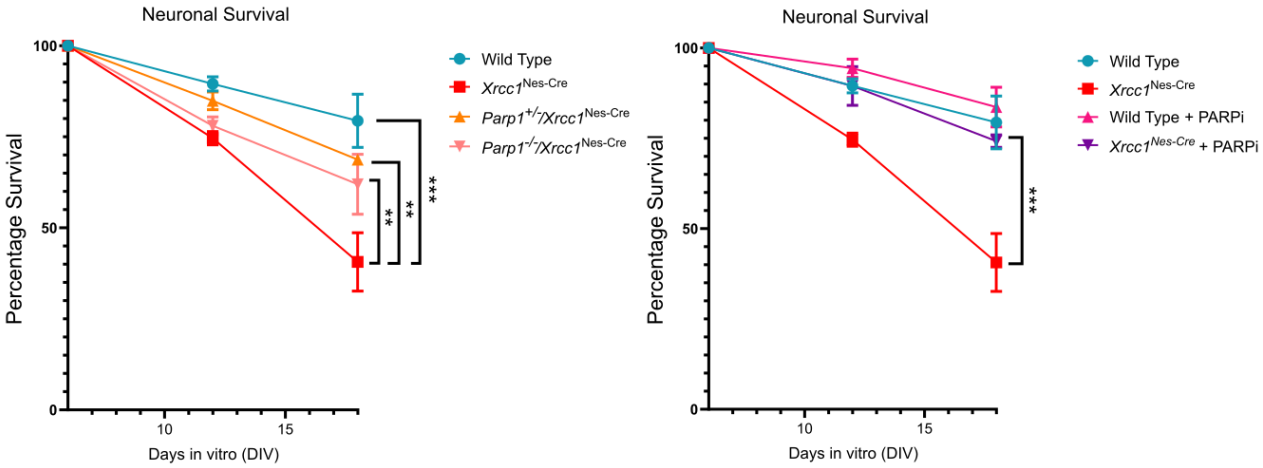

Figure 3.8 *Parp1-dependent death in Xrcc1$^{Nes-Cre}$ hippocampal neurons, in vitro.* Survival curves demonstrating time-dependent loss of *Xrcc1*$^{Nes-Cre}$ hippocampal neurons in culture. Neuronal survival was calculated following fixation of cells and staining with the neuronal marker, MAP2, at the indicated timepoints. MAP2-positive cells (neurons) were counted at the indicated time points using a fluorescent microscope and expressed graphically as a fraction of cells present relative to their T(0) DIV6 timepoint. Survival curves demonstrate the effects of additional *Parp1* deletion (left) and Parp1 inhibition (right) on neuronal survival. Statistical significance was determined using one-way ANOVA and Tukey's post-hoc multiple comparisons * $p < 0.05$, ** $p < 0.01$, and *** $p < 0.005$. Wild Type n = 6 cultures, *Xrcc1*$^{Nes-Cre}$ n = 4, *Parp1*$^{+/-}$*/Xrcc1*$^{Nes-Cre}$ n = 3, *Parp1*$^{-/-}$*/Xrcc1*$^{Nes-Cre}$ n = 3, Wild Type + PARP inhibitor, n = 4, *Xrcc1*$^{Nes-Cre}$ + PARP inhibitor, n = 4.

neurons exhibited shortened lifespan, as indicated by a time-dependent decrease in MAP2 positive cells, when compared to wild type neurons (Figure 3.8 A). Parp1 deletion resulted in significant rescue of hippocampal neuron lifespan, although deletion of either one or both parp1 alleles restored survival to wild type levels (Figure 3.8 A). In addition, chronic incubation of *Xrcc1*$^{Nes\text{-}Cre}$ hippocampal cells with a PARP inhibitor throughout the time course of the experiment was sufficient to rescue the survival of *Xrcc1*$^{Nes\text{-}Cre}$ hippocampal neurons (Figure 3.8 B). These data would suggest that Parp1 activity at sites of endogenous SSBs results in the decreased lifespan of *Xrcc1*$^{Nes\text{-}Cre}$ hippocampal neurons *in vitro*.

3.2.7 Parp-Dependent Sensitivity of *Xrcc1*$^{Nes\text{-}Cre}$ Hippocampal Neurons to PARG Inhibition

I next examined whether, similar to proliferating *XRCC1*$^{-/-}$ RPE-1 cells, *Xrcc1*$^{Nes\text{-}Cre}$ hippocampal neurons were sensitive to chronic PARG inhibition. Cells were treated at DIV6 for 3 days with various concentrations of the PARG inhibitor. I observed highly significant sensitivity to PARG inhibitor in *Xrcc1*$^{Nes\text{-}Cre}$ hippocampal neurons and glia when compared to wild type hippocampal neurons (Figure 3.9). This drastic sensitivity to PARG inhibition would indicate that poly(ADP-ribose) accumulation in neuronal cells is highly toxic, as wild type neurons did exhibit sensitivity at high doses of PARG inhibitor. Chronic treatment with a PARP inhibitor was sufficient to rescue the sensitivity of both *Xrcc1*$^{Nes\text{-}Cre}$ and wild type neurons to PARG inhibitor (Figure 3.9). Hippocampal neurons cultured from *Parp1*$^{-/-}$/*Xrcc1*$^{Nes\text{-}Cre}$ mice exhibited complete rescue of PARG inhibitor sensitivity, surpassing wild type neuronal survival. We observed partial rescue of sensitivity in neurons cultured from *Parp1*$^{+/-}$/*Xrcc1*$^{Nes\text{-}Cre}$ mice, with intermediate survival likely owing to their retention of one allele of *Parp1*, and their still-elevated poly(ADP-ribose) accumulation. We also investigated the sensitivity of co-cultured glia to PARG inhibition. *Xrcc1*$^{Nes\text{-}Cre}$ glia do exhibit sensitivity to PARG inhibition, with roughly 50% of cells surviving following 3-day incubation with 50μM PARG inhibitor (Figure 3.10). This sensitivity was also rescued by the additional deletion of *Parp1*. The increased sensitivity of *Xrcc1*$^{Nes\text{-}Cre}$ neurons compared to co-cultured glia might be related to the elevated poly(ADP-ribose) accumulation in neuronal cells. Interestingly, PARP inhibition rescued the sensitivity of *Xrcc1*$^{Nes\text{-}Cre}$ glial cells to PARG inhibitor, despite reports of PARP1 blockade being synthetically lethal in XRCC1 deficient proliferative cells due to replication fork collapse and DSB accumulation (Horton, *et al*., 2014, Ali, *et al*., 2020). In order to reduce proliferation during longevity experiments, cells were maintained in serum free medium, limiting cell cycle progression and thus bypassing PARP inhibitor induced replication fork collapse (Chou and Langan, 2003).

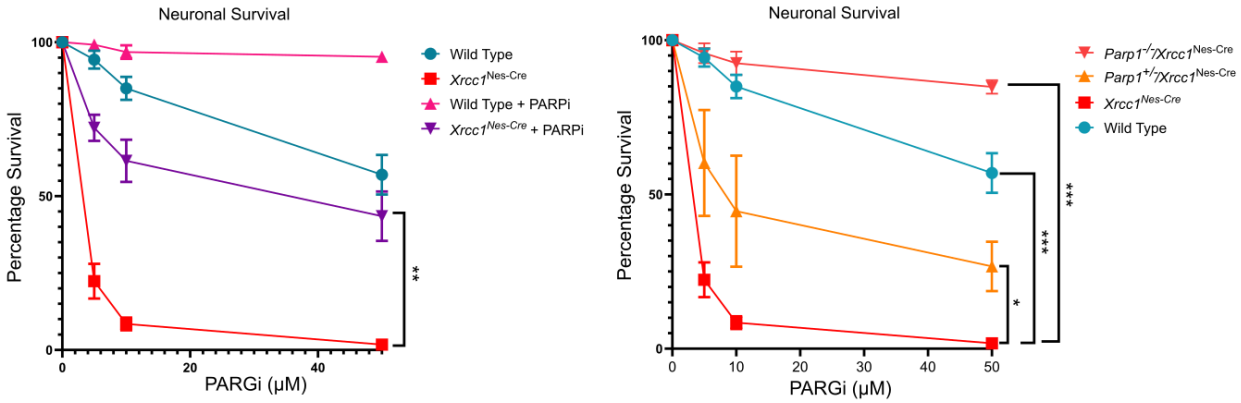

Figure 3.9 *Parp1 Dependent Phenotypic Sensitivity to PARG Inhibition in Xrcc1*$^{\text{Nes-Cre}}$ *Hippocampal Neurons.* Survival curve demonstrating sensitivity of *Xrcc1*$^{\text{Nes-Cre}}$ hippocampal neurons to PARG inhibition. Cells were treated at DIV6, with PARGi present for 72hrs prior to fixation, whereupon MAP2 positive cells were counted in relation to their respective genotype's DMSO control. Survival curves demonstrate the effect of Parp1 inhibition (right) and deletion (left). *Xrcc1*$^{\textit{Nes-Cre}}$ hippocampal neurons exhibit significant sensitivity to PARG inhibition, which is rescued by the additional deletion of *Parp1* (Wild Type n = 7 cultures, *Xrcc1*$^{\textit{Nes-Cre}}$ n = 5, *Parp1*$^{+/-}$*/Xrcc1*$^{\textit{Nes-Cre}}$ n = 3, *Parp1*$^{-/-}$*/Xrcc1*$^{\textit{Nes-Cre}}$ n =3, PARPi conditions n = 3, one-way ANOVA, $p < 0.0001$, Tukey's post-hoc indicating significance as * where $p < 0.05$, ** $p < 0.01$, and **** $p < 0.005$).

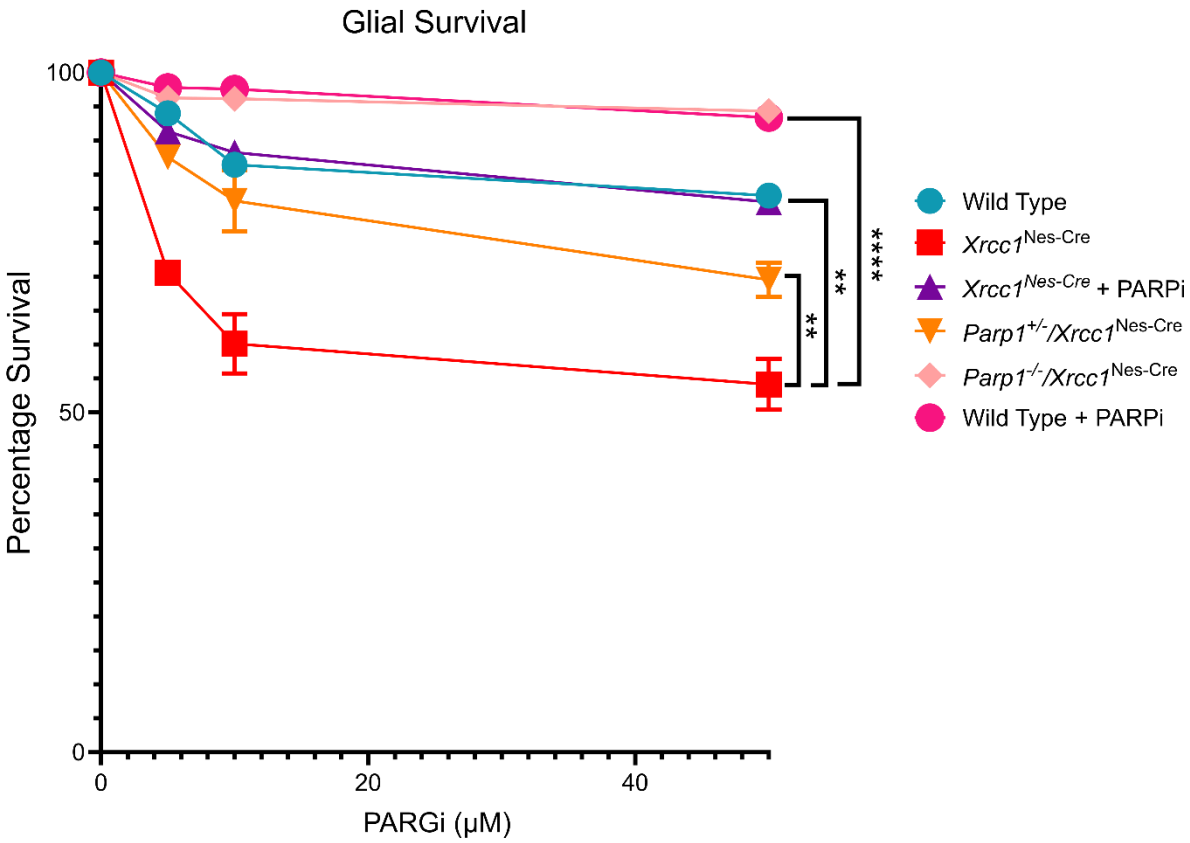

Figure 3.10 *Phenotypic Sensitivity to PARG Inhibition in Xrcc1$^{Nes\text{-}Cre}$ Glial Cells*. Survival curve demonstrating sensitivity of *Xrcc1*$^{Nes\text{-}Cre}$ glial cells to PARG inhibition. Cells were treated at DIV6, with PARG inhibitor present for 72hrs prior to fixation, whereupon MAP2 negative cells were counted in relation to their respective genotype's DMSO control. *Xrcc1*$^{Nes\text{-}Cre}$ glial cells exhibit significant sensitivity to PARG inhibition, which is rescued by the additional deletion of *Parp1,* or through PARP inhibition (Wild Type n = 5 cultures, *Xrcc1*$^{Nes\text{-}Cre}$ n = 5, *Parp1*$^{+/-}$*/Xrcc1*$^{Nes\text{-}Cre}$ n = 3, *Parp1*$^{-/-}$*/Xrcc1*$^{Nes\text{-}Cre}$ n =3, PARPi conditions n = 3, one-way ANOVA, $p < 0.005$, student's t-test indicating ** where $p < 0.01$, and **** $p < 0.005$).

3.2.8 NMN Supplementation Rescues PARGi Sensitivity, but is Insufficient to Rescue Spontaneous Cell Death in *Xrcc1*$^{Nes\text{-}Cre}$ Hippocampal Neurons

My previous experiments suggested that the increased sensitivity to PARG inhibition in *XRCC1*$^{-/-}$ RPE-1 cells is a result of chronic depletion of cellular NAD+, and that supplementation with the precursor NMN can rescue this (Figure 3.2 C). I next sought to investigate whether the spontaneous cell death observed in *Xrcc1*$^{Nes\text{-}Cre}$ hippocampal neurons might also be rescued by supplementation of the NAD+ precursor, NMN. *Xrcc1*$^{Nes\text{-}Cre}$ hippocampal neurons were examined at DIV6, DIV12, and DIV18 in the absence/presence of 500μM NMN, and surviving neurons counted and plotted as a fraction of those in the respective DIV6 controls. However, NMN treatment did not rescue the spontaneous death observed in *Xrcc1*$^{Nes\text{-}Cre}$ hippocampal neurons, suggesting that the cause of death is unlikely to be NAD+ depletion (Figure 3.12).

To confirm that NMN was functioning in my cell system, I examined its ability to restore Parp1 activity in Xrcc1 defective neurons that were first depleted of NAD+ by incubation with the NAMPT inhibitor FK866. This idea was based on my earlier experiments in which I showed that FK866 ablates poly(ADP-ribose) synthesis in *XRCC1*$^{-/-}$ RPE-1 cells (Figure 3.1). Indeed, 4hr pre-treatment with FK866 suppressed the elevated endogenous level of poly(ADP-ribose) in Xrcc1$^{Nes\text{-}Cre}$ neurons, and this was restored by additional supplementation with 500μM NMN (Figure 3.11 A, B & C). Moreover, NMN treatment partially rescued the sensitivity in *Xrcc1*$^{Nes\text{-}Cre}$ hippocampal neurons to PARG inhibitor, as it did in XRCC1$^{-/-}$ RPE1 cells (Figure 3.12), confirming the efficacy of NMN in my hippocampal neurons. Collectively, these data suggest that, in contrast to the impact of PARG inhibition on reduced survival of Xrcc1 defective neurons, the intrinsic/spontaneous decrease in lifespan of *Xrcc1*$^{Nes\text{-}Cre}$ hippocampal neurons is unlikely to be due to NAD+ depletion (Figure 3.12).

3.2.9 Abortive Top1 Activity is Unlikely to be the Source of Endogenous DNA SSBs in *Xrcc1*$^{Nes\text{-}Cre}$ Hippocampal Neurons

Next, I exploited the elevated endogenous Parp1 activity to address the source of the endogenous SSBs that trigger this activity. Neurons exhibit an elevated transcriptional demand, a consequence of their longevity, plasticity, and range of function (Stott, *et al*., 2021). Given that transcription is linked to the reorganisation of chromatin and the subsequent generation of topological stress, I reasoned that perhaps the elevated steady-state level of DNA SSBs observed in *Xrcc1*$^{Nes\text{-}Cre}$ hippocampal neurons is the result of abortive Top1 activity, as the neuronal expression of long genes is reliant on Top1 (King, *et al*., 2013, Baranello, *et al*., 2016, Pommier, *et al*., 2016).

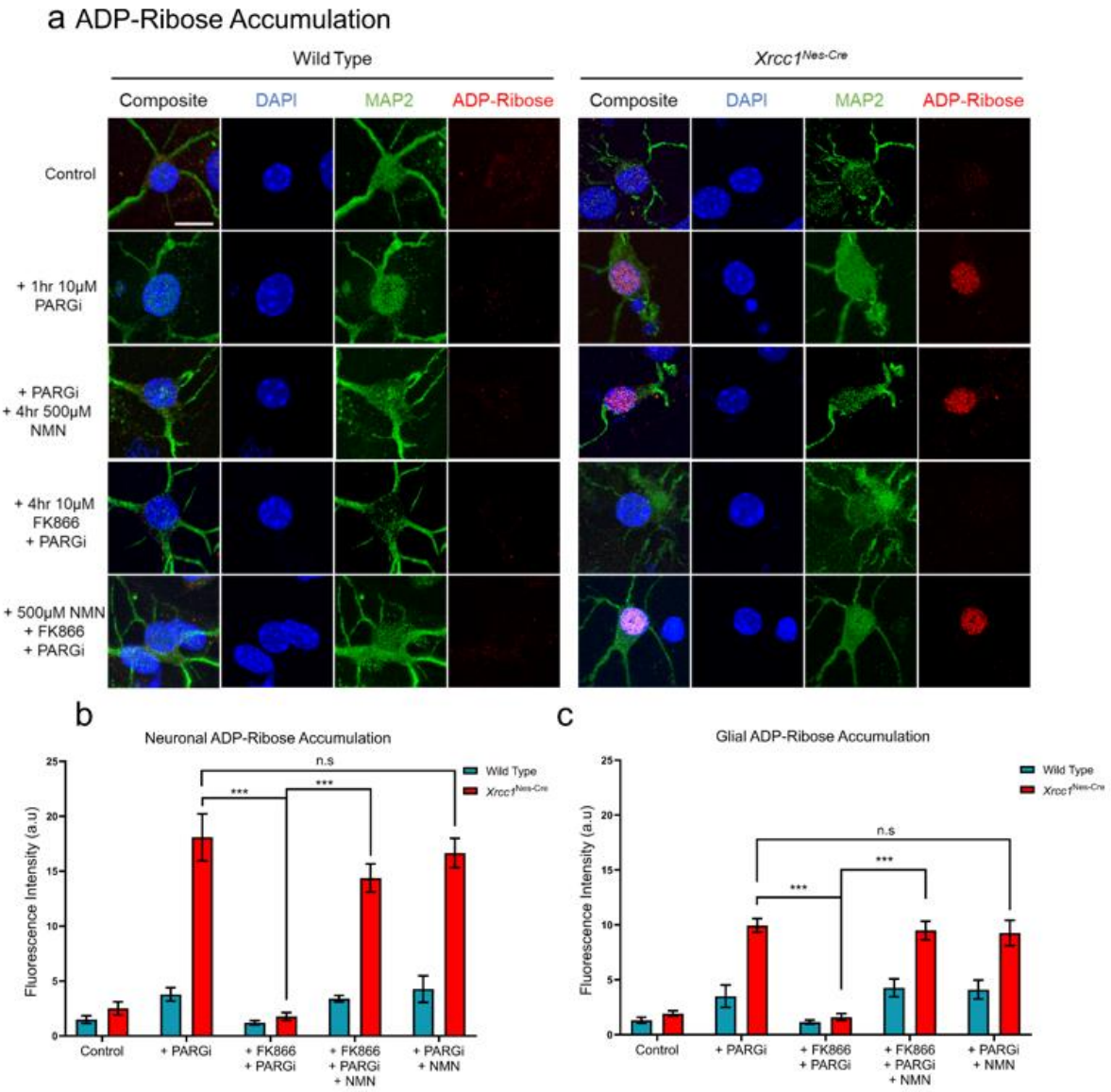

Figure 3.11 *NAD+ Dependent poly(ADP-ribosyl)ation in Xrcc1$^{Nes-Cre}$ Hippocampal Neurons*. Indirect immunofluorescence of DIV6 hippocampal neurons cultured from p1-2 Wild Type and *Xrcc1$^{Nes-Cre}$* mice. Cells were pre-treated for 4hrs with either the NAMPT inhibitor FK866, the NAD+ precursor NMN, both compounds, or vehicle controls prior to 1hr treatment with a PARG inhibitor. FK866 is shown to significantly impair poly(ADP-ribose) synthesis. NAD+ repletion with NMN following FK866 is sufficient to restore poly(ADP-ribose) accumulation, indicating it is being utilised by the cell. Scale Bar = 20μM. Quantification of poly(ADP-ribose) intensity in neuronal cells in B) where *** denotes significance, $p < 0.005$ by student's t.test. Quantification in glial cells in C), where *** denotes significance, $p < 0.005$ by student's t.test. Histograms show mean ± SEM. Data from three individual repeats, > 90 cells quantified in each group.

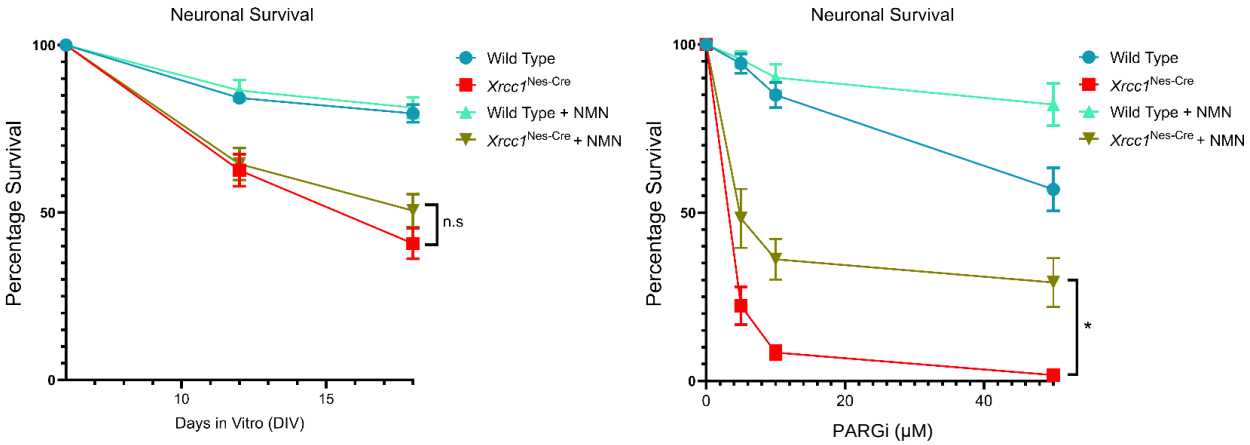

Figure 3.12 *NAD+ Repletion Rescues PARGi Sensitivity, but not Spontaneous Cell Death*. Survival curves of cultured hippocampal neurons, one being cells measured for spontaneous cell death from DIV6 to DIV18, the other having been calculated following 3 days treatment with PARG inhibitor. Cells were chronically treated with either 500μM NMN or PBS vehicle. Wild Type n = 3 cultures from separate mice, *Xrcc1*$^{Nes\text{-}Cre}$ n = 3, + PARPi n = 3. NMN repletion does not significantly rescue spontaneous cell death ($p = 0.18$). NMN treatment does, however, significantly rescue death attributed to PARG inhibitor sensitivity, where $p < 0.05$ by student's t.test

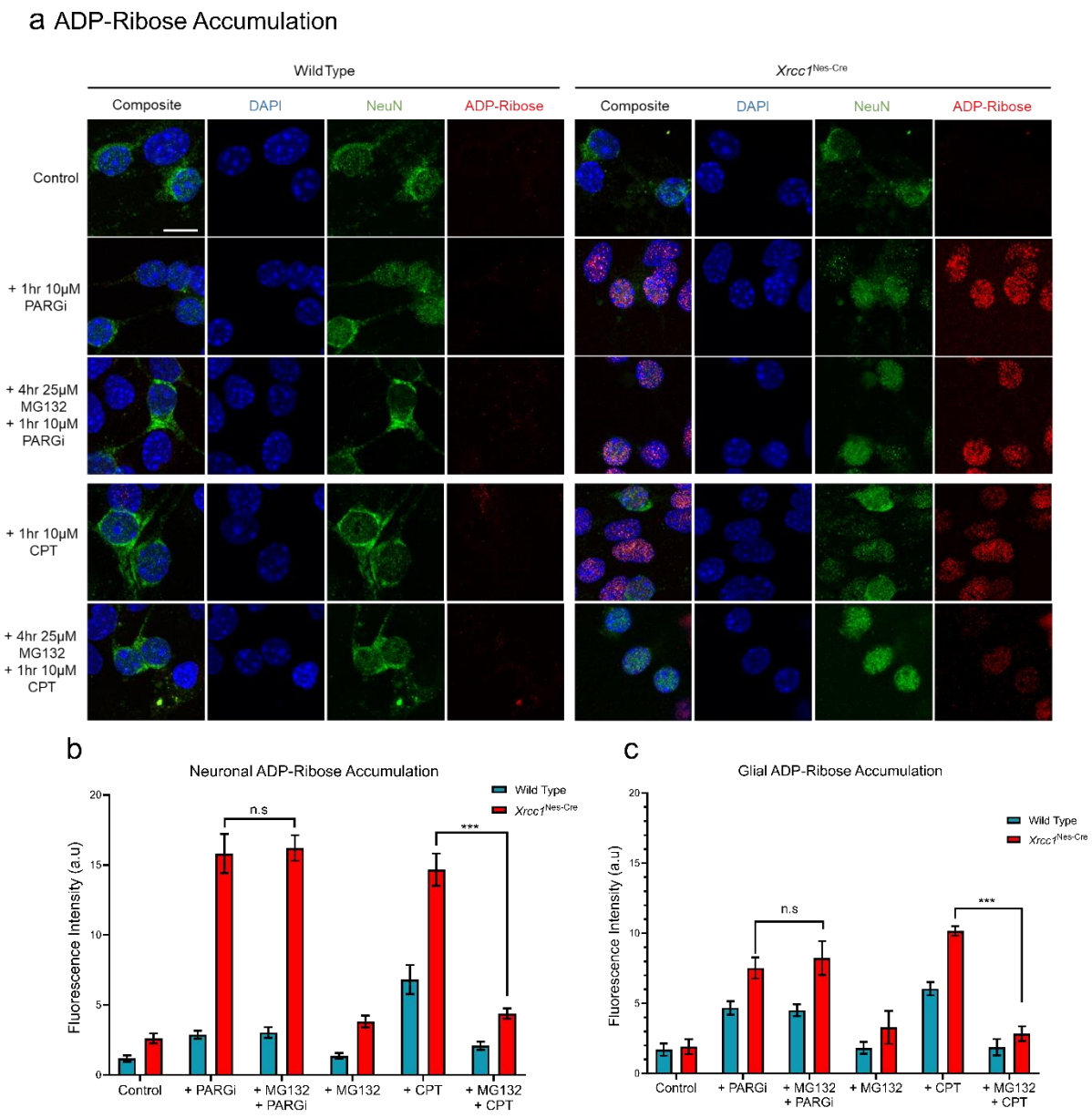

Figure 3.13 *Inhibition of TOP1cc Degradation by the Proteasome Does Not Rescue poly(ADP-ribose) Accumulation*. Indirect immunofluorescence of DIV6 hippocampal neurons cultured from p1-2 Wild Type and *Xrcc1*$^{Nes\text{-}Cre}$ mice. Cells were pre-treated for 4hrs with either the proteasome inhibitor MG132, or DMSO control prior to 1hr treatment with either a PARG inhibitor or CPT. MG132 treatment did not significantly reduce poly(ADP-ribose) accumulation following PARG inhibition, however the significant reduction in CPT induced PARP activity would indicate its efficacy in the inhibition of Top1cc degradation. Scale bar = 20μM. Quantification of poly(ADP-ribose) intensity in neuronal cells in B) where *** denotes significance, $p < 0.005$ by student's t.test. Quantification in glial cells in C), where *** denotes significance, $p < 0.005$ by student's t.test. Data quantified from three replicates, > 90 cells quantified. Histograms show mean ± SEM.

Top1 regulates the breakage of a single strand of DNA to regulate torsional stress, by forming transient cleavage complexes in which Top1 is covalently linked to the 3' terminus of the single strand break (Wang, *et al*., 1971, Ashour, *et al*., 2015, Baranello, *et al*., 2016, Pommier, *et al*., 2016). These complexes are intrinsic in ordinary transcription, and are degraded by the proteasome, at which point Parp1 may identify the break and, in wild type cells, facilitate the recruitment of the SSBR machinery (Redinbo, *et al*., 1998, Lin, *et al*., 2008, Das, *et al*., 2016). In order to investigate whether the endogenously occurring DNA SSBs arise as a result of abortive Top1 activity, we pre-treated wild type and *Xrcc1*$^{Nes\text{-}Cre}$ hippocampal neurons with the 26s proteasome inhibitor MG132, prior to PARG inhibition. For Parp1 to recognise Top1-linked SSBs, the Top1cc must first be degraded by the proteasome, and as such will not induce PARP1 activity in the presence of MG132 (Lin, *et al*., 2008). Indeed, pre-treatment of hippocampal neurons with MG132 was sufficient to significantly reduce PARP1 activity induced by CPT, a Top1 poison which results in the genesis and stability of the Top1cc (Figure 3.13 A, B & C). However, MG132 pre-treatment did not suppress the elevated PARP1 activity in *Xrcc1*$^{Nes\text{-}Cre}$ neurons or glia, indicating that the source of endogenous DNA SSBs is unlikely to be a result of abortive Top1 activity (Figure 3.13 A, B & C).

3.2.10 Inhibition of Nitric Oxide Synthesis suppresses the elevated poly(ADP-ribose) in *Xrcc1*$^{Nes\text{-}Cre}$ Hippocampal Neurons

Since Top1-linked DNA SSBs are unlikely to be the source of endogenous damage in *Xrcc1*$^{Nes\text{-}Cre}$ hippocampal neurons, I investigated a separate means by which neuronal processes may underlie this elevated Parp1 activity. Nitric Oxide ($^{\bullet}NO$) is a key signalling molecule in the brain, regulating the intrinsic excitability of neuronal cells and directly acting in the maintenance of synaptic plasticity (Steinert, Chernova and Forsythe, 2010, Chachlaki and Prevot, 2020). In the brain, this molecule is generated by neuronal Nitric Oxide Synthase (nNOS), a calcium-calmodulin controlled enzyme which generates $^{\bullet}NO$ predominantly from L-arginine and NADPH (Zhou and Zhu, 2009). In conjunction with the superoxide anion, $O_2^{\bullet-}$, $^{\bullet}NO$ forms peroxynitrite, a reactive nitrogen species (Burney, *et al*., 1999). In DNA, purine nucleotides are prone to oxidation and the formation of adducts; one such being 8-nitroguanine in the presence of peroxynitrite, which is rapidly depurinated to form abasic sites, which will ultimately result in DNA SSBs following their removal by Ape proteins (Yermilov, *et al*., 1995, Ohshima, *et al*., 2006, Thakur, *et al*., 2014). Peroxynitrite also results in the oxidation of deoxyribose, resulting in DNA SSBs through the direct degradation of the DNA sugar backbone (ul Islam, *et al*., 2015).

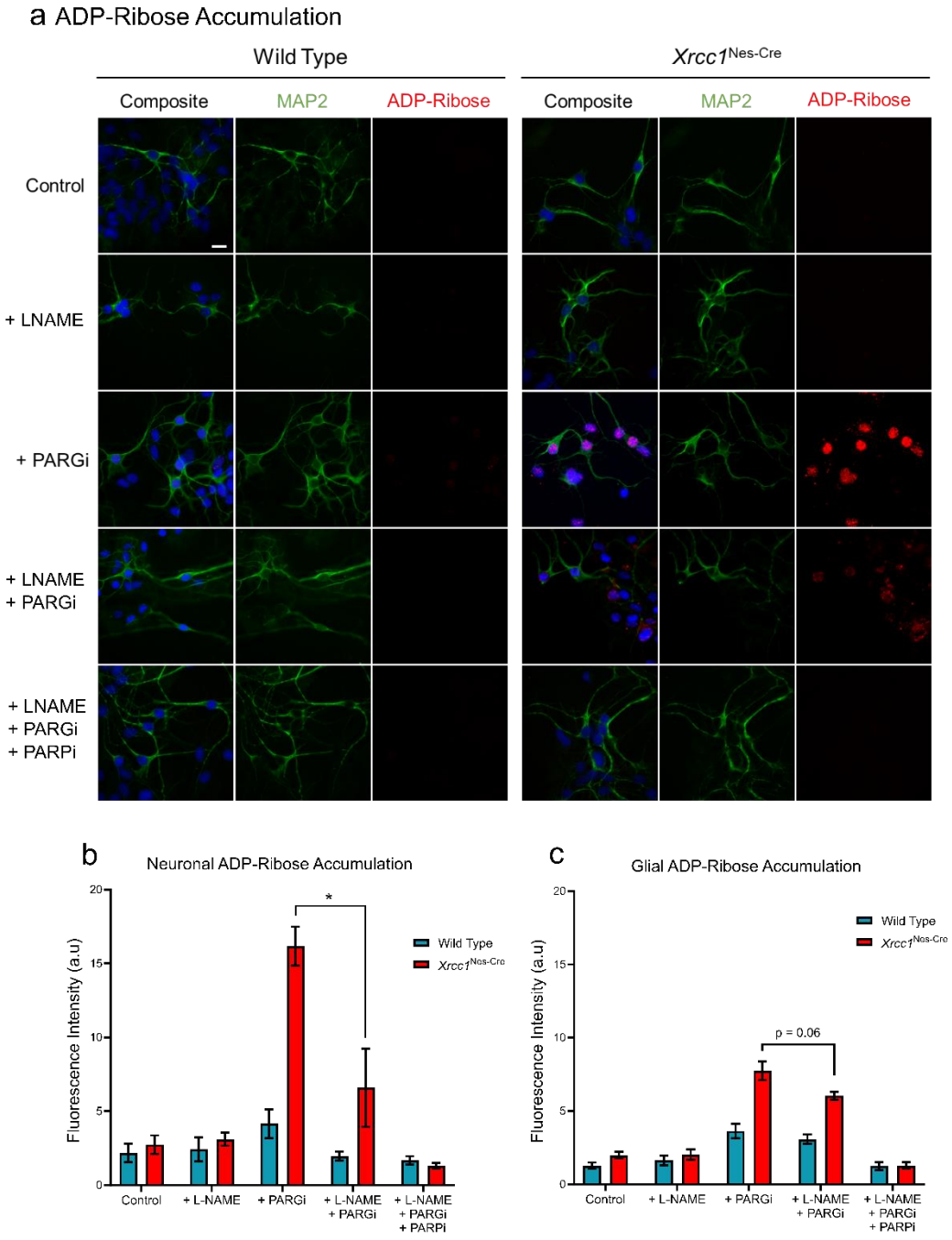

Figure 3.14 *nNOS Inhibition Rescues poly(ADP-ribose) Accumulation in Xrcc1*$^{Nes\text{-}Cre}$ *Hippocampal Neurons*. Cells were cultured from p1-2 Wild Type and *Xrcc1*$^{Nes\text{-}Cre}$ mouse pups. Cells were imaged at DIV6 and stained for NeuN and ADP-Ribose. Cells were pre-treated with 100μM nNOS inhibitor L-NAME, 5μM PARP inhibitor, both, or vehicle control for 4 hrs prior to 1 hr treatment with PARG inhibitor. Pre-treatment with L-NAME was sufficient to significantly reduce poly(ADP-ribose) accumulation in *Xrcc1*$^{Nes\text{-}Cre}$ hippocampal neurons. Wild Type n = 3, > 90 cells, *Xrcc1*$^{Nes\text{-}Cre}$ n = 3, > 90 for all treatments. Scale bar = 20μM. Quantified in neuronal cells (NeuN positive) in B), where * denotes $p < 0.05$ by student's t-test. Quantified in glial cells (NeuN negative) in C), where the reduction afforded by L-NAME in PARG inhibitor induced poly(ADP-ribose) accumulation is not significant, $p = 0.06$ by student's t.test. Data from three replicates, > 90 cells quantified. Histograms show mean ± SEM.

To investigate whether neuronal ˙NO signalling may underlie the elevated induction of endogenous DNA SSBs in *Xrcc1*$^{Nes\text{-}Cre}$ hippocampal neurons, I pre-treated cells with the nNOS inhibitor L-NAME for 4hrs prior to PARG inhibition. L-NAME was sufficient to greatly reduce poly(ADP-ribose) accumulation in *Xrcc1*$^{Nes\text{-}Cre}$ neuronal cells, suggesting that a fraction of the endogenous SSBs arising in *Xrcc1*$^{Nes\text{-}Cre}$ hippocampal neurons are the result of ˙NO induced RNS (Figure 3.14 A & B). Interestingly, I did not see a significant reduction in poly(ADP-ribose) accumulation in non-neuronal cells following L-NAME pre-treatment (Figure 3.14 C), consistent with the comparative lack of ˙NO synthesis in non-neuronal cells (Yuste, *et al*., 2015). However, evidence has suggested that ˙NO diffusion between neuronal cells and glia may result in peroxynitrite accumulation in peripheral cells, and as such may be a cause of endogenous SSB formation in cells absent nNOS (Haselden, *et al*., 2020). ˙NO has been implicated in numerous disorders, such as AD, PD, and ALS; however, the contribution of ˙NO to these conditions is typically confined to the genesis of neuroinflammation, rather than the pathology being a direct result of RNS induced DNA SSBs (Togo, Katsuse, and Iseki, 2004).

3.2.11 The Additional Deletion of *Ape1* Does Not Rescue poly(ADP-ribose) Accumulation in *Xrcc1*$^{Nes\text{-}Cre}$ Hippocampal Neurons

Having highlighted a potential role for ˙NO in the genesis of endogenous DNA SSBs in our neuronal model, I reasoned that radical-dependent base modification, and subsequent AP site formation may underlie endogenous SSB formation in *Xrcc1*-deficient models. Following this, I posited that the additional deletion of Ape1 would halt the formation of these SSBs, thereby reducing Parp1 activity. Ape1 is a multifunctional enzyme that acts to incise the DNA backbone at AP sites, so that these lesions may be replaced by undamaged nucleotides during BER (Whitaker and Freudenthal, 2018).

To investigate this hypothesis, *Xrcc1*$^{LoxP/LoxP}$ mice were crossed with *Ape1*$^{LoxP/Loxp}$ mice, along with the introduction of the nestin-cre driver, enabling the setup of breeding pairs capable of producing both *Ape1*$^{Nes\text{-}Cre}$ and *Ape1*$^{Nes\text{-}Cre}$/*Xrcc1*$^{Nes\text{-}Cre}$ mouse pups. The *Ape1*$^{Nes\text{-}Cre}$ mouse is similarly characterised by the degeneration of the cerebellum and juvenile mortality, however this is the result of the loss of thermoregulation following the selective death of serotonergic neurons, rather than terminal seizures (Illuzzi, *et al*., 2018). Hippocampal neurons were cultured from p1-2 *Ape1*$^{Nes\text{-}Cre}$/*Xrcc1*$^{Nes\text{-}Cre}$ mouse pups prior to their treatment at DIV6. Interestingly, however, neurons from double knockout mice exhibited drastic cell death, with fewer

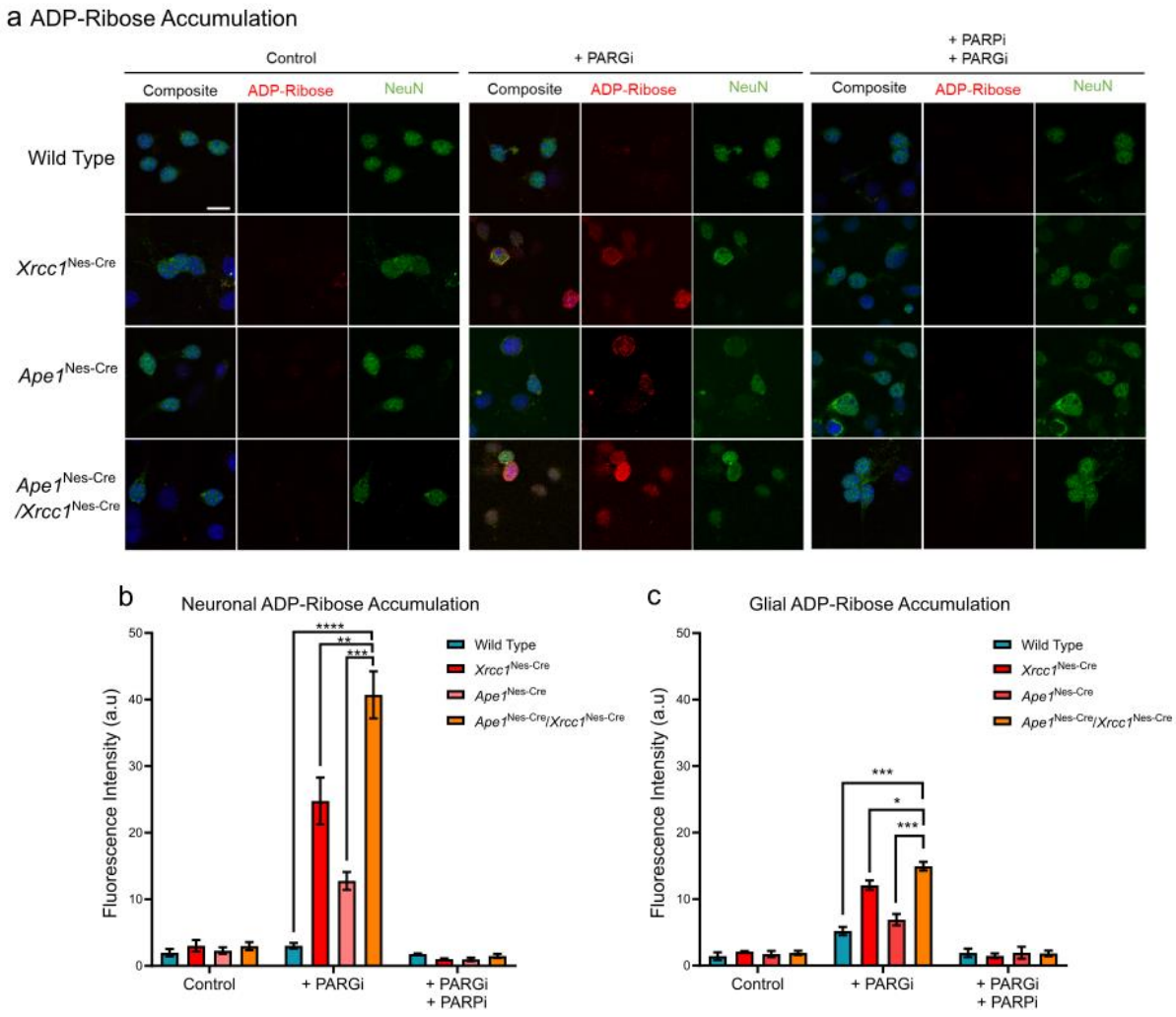

Figure 3.15 *The Additional Deletion of Ape1 Does Not Rescue poly(ADP-ribose) Accumulation.* Cells were cultured from p1-2 Wild Type, *Xrcc1*$^{Nes\text{-}Cre}$, *Ape1*$^{Nes\text{-}Cre}$, and *Ape1*$^{Nes\text{-}Cre}$/*Xrcc1*$^{Nes\text{-}Cre}$ mouse pups. Cells were imaged at DIV6 and stained for NeuN and ADP-Ribose. Cells were pre-treated with 5μM PARP inhibitor or DMSO control for 4 hrs prior to 1 hr treatment with PARG inhibitor. Additional deletion of *Ape1* did not rescue accumulation, but rather increased poly(ADP-ribose) intensity in *Xrcc1*$^{Nes\text{-}Cre}$ neurons. Single *Ape1* deletion also induced significant accumulation of poly(ADP-ribose). Wild Type n = 3, > 90 cells, *Xrcc1*$^{Nes\text{-}Cre}$ n = 3, > 90, *Ape1*$^{Nes\text{-}Cre}$ n = 3, > 90, *Ape1*$^{Nes\text{-}Cre}$/*Xrcc1*$^{Nes\text{-}Cre}$ n = 3, > 50 cells. Neuronal viability was noticeably decreased in *Ape1*$^{Nes\text{-}Cre}$/*Xrcc1*$^{Nes\text{-}Cre}$ cultures. Scale bar = 20μM. Quantified in neuronal cells (NeuN positive) in B), one way ANOVA where $p < 0.001$, followed by Tukey's post hoc comparison where significance is denoted by ** where $p < 0.01$, *** where $P < 0.005$, and **** where $P < 0.001$. Glial (NeuN Negative) quantification in C, one way ANOVA where $p < 0.001$, followed by post hoc comparisons as above where * denoted $p < 0.05$, and *** denotes $p < 0.005$. Histograms show mean ± SEM.

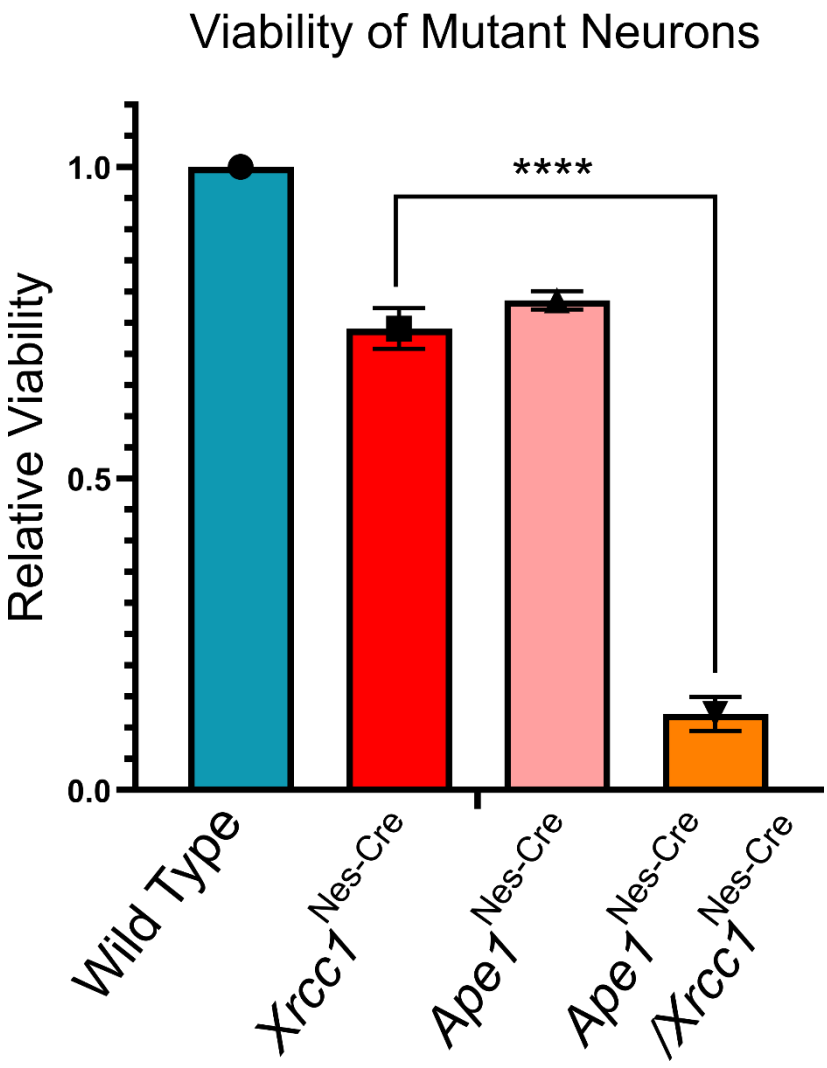

Figure 3.16 *Decreased Viability of Ape1$^{Nes\text{-}Cre}$/Xrcc1$^{Nes\text{-}Cre}$ Hippocampal Neurons.* Hippocampal neurons were cultured from p1-2 mouse pups and plated at a density of 100,000 cells per well. At DIV6 cell were stained for NeuN, a neuronal marker, and counted in comparison to the wild type control, represented in the histogram as viability relative to wild type. Significance is denoted as **** where $p < 0.001$ by student's t-test. Histogram shows mean ± SEM. Data from three individual replicates.

than 1% of plated cells surviving to treatment, at which point we increased plating density. When plated at 100,000 cells/well, there was a greater degree of survival, however there was a roughly 90% reduction in viability compared to wild type cells, indicating significant cell death (Figure 3.16).

Still, we aimed to investigate whether the absence of Ape1 would limit SSB formation through the impaired genesis of abasic sites. Following an increase in plating density, we treated wild type, *Ape1*$^{Nes\text{-}Cre}$, *Xrcc1*$^{Nes\text{-}Cre}$, and *Ape1*$^{Nes\text{-}Cre}$/*Xrcc1*$^{Nes\text{-}Cre}$ hippocampal neurons with a PARG inhibitor. Interestingly, we note elevated Parp1 activity in all three mutant cell lines (Figure 3.15 A & B). Partial elevation of Parp1 activity in *Ape1*$^{Nes\text{-}Cre}$ neurons was unexpected, given that the deletion of *Ape1* should result in an inability to incise abasic sites, but should not result in SSB formation (Illuzzi, *et al*., 2018). *Ape1*$^{Nes\text{-}Cre}$/*Xrcc1*$^{Nes\text{-}Cre}$ hippocampal neurons exhibited an even greater accumulation of poly(ADP-ribose) than in *Xrcc1*$^{Nes\text{-}Cre}$ cells, suggesting that the formation of endogenous DNA SSBs in *Xrcc1*$^{Nes\text{-}Cre}$ neurons is not Ape1 dependent.

3.3 Discussion

One of the more puzzling elements of SSBR-related pathology is their almost exclusively neurological phenotype. Hereditary defects in SSBR result in cerebellar degeneration and ataxia and, unlike in the case of disorders of DSBR (such as AT), are not commonly associated with an increased incidence of cancer (Caldecott, 2008). There are several theories as to why disorders of SSBR present in this way. The brain is a highly metabolically active organ, and as such may be more prone to ROS induced DNA-SSBs that might accumulate over cell lifespan (Caldecott, 2008, Watts, *et al*., 2018). Neuronal cells are highly transcriptionally active, in part due to activity-dependent alterations to protein expression. This transcription is intrinsically linked to DNA repair, as both Top1 and Top2 are required for the transcription of long, neuronal genes (King, *et al*., 2013, Stott, *et al*., 2021). Similarly, the longevity of neuronal cells may play a role; with some exceptions, there is very little turnover of neurons in the brain, and neurons are unique in their longevity (Magrassi, *et al*., 2013). As such, this longevity may facilitate the accumulation of DNA SSBs in the cell to a point of criticality that could not be reached in the lifespan of a mitotic cell. Previously, the majority of investigations of SSBR-related pathology had occurred in mitotic cells which, for the above reasons, are perhaps an unsuitable model for the investigation of a neurological phenotype. As such, we sought to establish a neuronal cell autonomous model of endogenous Parp1 activity to investigate the incidence of DNA SSBs in post-mitotic cells, in hopes of better understanding the mechanisms underlying SSBR-related neuropathology.

Previous studies of mitotic cells had indicated that the deletion of *XRCC1* resulted in defective DNA-SSBR, where induction of DNA damage by exogenous damaging agents resulted in elevated poly(ADP-ribose) accumulation, indicating that PARP1 was retained at unresolved breaks in SSBR-deficient cells (Hoch, *et al*., 2017). The further discovery that the conditional deletion of *Xrcc1* resulted in Parp1-dependent juvenile mortality and the accumulation of poly(ADP-ribose) in the mouse brain presented compelling evidence that endogenously occurring DNA-damage could result in pronounced neuropathology (Hoch, *et al*., 2017, Komulainen, *et al*., 2021). However, while *Parp1* deletion was sufficient to rescue many aspects of this phenotype, chemical manipulation by PARP inhibitors seemingly did not (likely through either difficulty in accessing cells, or maintaining PARP inhibition), further highlighting the need for a cell autonomous model by which we could further study the effect of *Xrcc1* deletion in neuronal cells *in vitro* (Komulainen, E. unpublished observations).

Upon establishing that hippocampal neurons cultured from *Xrcc1*$^{Nes\text{-}Cre}$ mice were, indeed, characterised by defective SSBR (Figure 3.3 and Figure 3.4), we sought to investigate whether they replicated the accumulation of poly(ADP-ribose) at sites of endogenous damage that was observed in the mouse brain. While we did not observe this accumulation in untreated cells, treatment with the PARG inhibitor (which stabilises poly(ADP-ribose) chains on autoribosylated Parp1) facilitated the large-scale accumulation of poly(ADP-ribose) in neuronal nuclei within only 1 hour (Figure 3.6). This highly dynamic accumulation is indicative of the scale of Parp1 activity at sites of unresolved endogenous DNA-damage in Xrcc1-deficient cells. Interestingly, pre-treatment of cells with a PARP inhibitor was sufficient to completely remove this accumulation, indicating that the accumulation we observe is the constitutive synthesis of nascent polymer at sites of endogenous damage, rather than previously synthesised poly(ADP-ribose). Of further note is the discrepancy between neurons and co-cultured glial cells; where there is a greater accumulation of poly(ADP-ribose) accumulation in post-mitotic cells, perhaps indicating that neurons exhibit elevated steady-state levels of endogenous DNA-damage (Figure 3.6 B & C). In some non-neuronal cells, we do observe highly elevated poly(ADP-ribose) accumulation, however these are present in both wild type and *Xrcc1*$^{Nes\text{-}Cre}$ glia, and likely represent Parp1 activation at unligated Okazaki fragments during S-phase (Hanzlikova, *et al*., 2018). The elevated steady-state level of poly(ADP-ribosylation) in neurons is of particular interest, due to the question of the exclusively neurological phenotype characteristic of hereditary defects in SSBR. Following these observations, we cultured hippocampal neurons from *Parp1*$^{+/-}$/*Xrcc1*$^{Nes\text{-}Cre}$ and *Parp1*$^{-/-}$/*Xrcc1*$^{Nes\text{-}Cre}$ mice which, when treated with the PARG inhibitor, replicated either the partial or total rescue of poly(ADP-ribose) accumulation that we see in the mouse brain, further establishing the validity of our cellular model (Figure 3.7) (Komulainen, *et al*., 2021).

One of the key features of the *Xrcc1*$^{Nes\text{-}Cre}$ mouse model is the degeneration of the cerebellum, accompanying cell death in the granule layer, as well as the selective death of cerebellar interneurons (Lee, *et al*., 2009). While the death of interneurons is p53 dependent and, as such, likely occurring during development, cell death in the cerebellum may underlie the progressive ataxia that characterises the *Xrcc1*$^{Nes\text{-}Cre}$ mouse (Lee, *et al*., 2009). Despite this, cell death in the hippocampus (the other main structure in which we observe elevated poly(ADP-ribose) accumulation) has not been observed. Strikingly, however, upon culturing hippocampal neurons from *Xrcc1*$^{Nes\text{-}Cre}$ mice, we observed significantly reduced viability of neuronal cells in comparison to wild type. This phenotype could be rescued by the additional deletion of one or both alleles

of *Parp1*, as well as by chronic co-incubation with a PARP inhibitor (Figure 3.8). Interestingly, PARP inhibitor treatment provided greater rescue than deletion, perhaps due to a lack of selectively for Parp1 over Parp2/3. While we have yet to observe hippocampal death *in vivo*, Parp1-dependent death *in vitro* indicates the toxicity of poly(ADP-ribose) accumulation in neuronal cells. Repletion of cellular NAD+ did not rescue the spontaneous cell death observed in *Xrcc1*$^{Nes\text{-}Cre}$ hippocampal neurons, however it did significantly rescue PARG inhibitor sensitivity, indicating that when poly(ADP-ribose) accumulates to a point of criticality, cell death occurs due to NAD+ depletion, but that this is not the case at endogenous levels (Figure 3.9 and Figure 3.12). These data may provide mechanistic insight into cell death observed in other structures of the mouse brain *in vivo*, as well as provide compelling support for the utilisation of PARP inhibitors in the treatment of SSBR-related neuropathology.

The elevated accumulation of poly(ADP-ribose) in post-mitotic cells and selective death of neurons *in vitro* each support the conclusion that neuronal cells are characterised by an elevated steady-state level of endogenous damage compared to glial cells (Figure 3.6). It is well established that neuronal cells exhibit elevated transcriptional demand, however through inhibition of cleavage complex degradation, we show that abortive Top1 activity is unlikely to be the source of this damage (Figure 3.13). This is perhaps unsurprising, given that in comparison to the *Xrcc1*$^{Nes\text{-}Cre}$ mouse, the *Tdp1*$^{-/-}$ mouse, which is characterised by an inability to repair Top1-linked SSBs, displays a much milder phenotype, though it does exhibit a gradual decrease in brain volume and a sensitivity to Top1 poisons (Katyal, *et al*., 2007). We reasoned that a separate source of endogenous DNA-SSBs might be ˙NO signalling. ˙NO signalling is a critical process in neuronal cells and is involved in the regulation of many key processes, such as LTP (Chachlaki and Prevot, 2020). ˙NO signalling does, however, result in the production of RNS, capable of attacking DNA and resulting in SSB induction (Ohshima, *et al*., 2006, ul Islam, *et al*., 2015). Upon inhibition of nNOS (the enzyme responsible to the production of ˙NO in neurons), we note a significant decrease in poly(ADP-ribose) accumulation in *Xrcc1*$^{Nes\text{-}Cre}$ hippocampal neurons (Figure 3.14 A & B). The observation that nNOS inhibition is capable of rescuing poly(ADP-ribose) accumulation is significant, as it provides a compelling explanation for the elevated accumulation of poly(ADP-ribose) in neuronal nuclei in comparison to glia, which do not utilise ˙NO to the same extent (Yuste, *et al*., 2015). This data may improve our understanding of the neurological phenotype associated with hereditary defects in SSBR, as it provides an exclusively neuronal mechanism by which SSB induction may contribute to the *Xrcc1*$^{Nes\text{-}Cre}$ phenotype.

To further investigate this induction, neurons were cultured from a newly created strain of *Ape1*$^{Nes\text{-}Cre}$/*Xrcc1*$^{Nes\text{-}Cre}$ mice. We reasoned that the RNS-dependent production of DNA adducts would likely be processed by Ape1, an endonuclease which processes the AP site prior to Parp1 recruitment (Caldecott, 2008, Whitaker and Freudenthal, 2018). Interestingly, however, we observed an even greater accumulation of poly(ADP-ribose) in these double knockout cells (Figure 3.15). Further, *Ape1*$^{Nes\text{-}Cre}$/*Xrcc1*$^{Nes\text{-}Cre}$ mice exhibited a similar phenotype to the *Xrcc1*$^{Nes\text{-}Cre}$ mouse, and displayed near total death of neurons *in vitro* (Figure 3.16). This result is perhaps unsurprising, given that both *Xrcc1*$^{Nes\text{-}Cre}$ and *Ape1*$^{Nes\text{-}Cre}$ mouse pups are notably small and feeble at birth, and that the *Ape1*$^{Nes\text{-}Cre}$/*Xrcc1*$^{Nes\text{-}Cre}$ was born at a sub-mendelian rate, indicating possible death during development. Those *Ape1*$^{Nes\text{-}Cre}$/*Xrcc1*$^{Nes\text{-}Cre}$ mice that were born and not cultured at p1-2 were assessed for lifespan, and did not demonstrate any increase in longevity, but rather died or were culled within the range expected of both mutant strains (Komulainen, Badman, and Ju, unpublished observations). Interestingly, single knockout *Ape1*$^{Nes\text{-}Cre}$ hippocampal neurons also exhibit elevated poly(ADP-ribose) accumulation in the presence of PARG inhibitor. Ape1 has a wide variety of both RNA and DNA substrates, and there is much yet unknown about the interactions between Ape1 and these targets. The depletion of Ape1 in neurons has been shown to result in an accumulation of ROS and RNS due to glutamate excitotoxicity, which may underlie the elevated poly(ADP-ribose) that we observe in *Ape1*$^{Nes\text{-}Cre}$/*Xrcc1*$^{Nes\text{-}Cre}$ hippocampal neurons (Yang, *et al*., 2010). One possible mechanism by which Parp1 activity might follow Ape1 deletion is through the collision of transcriptional polymerases with SSBs at abasic sites, which may induce poly(ADP-ribosylation) (Zhou and Doetsch, 1993).

I had thought that, should the majority of endogenous DNA SSBs be the result of $^{\bullet}$NO-derived radicals, then the resultant base modification would ultimately be processed by Ape1. I propose that, either a separate protein is involved in the processing of these $ONOO^-$ induced modifications, or that the damage being caused is due to the direct oxidation of the DNA sugar moiety, rather than base modification (ul Islam, *et al*., 2015). The repair of SSBs induced by direct oxidation would not be directly dependent on Ape1 and, as such, we would not expect to see any decrease in poly(ADP-ribose) accumulation in *Ape1*$^{Nes\text{-}Cre}$/*Xrcc1*$^{Nes\text{-}Cre}$ hippocampal neurons (Caldecott, 2008, Cadet, *et al*., 2017). Elevated Parp1 activity might also be linked to the spontaneous hydrolysis of elevated abasic sites, or perhaps the use of a bifunctional glycosylase (an APE1-independent BER mechanism) (Wiederhold, *et al*., 2004, Greenberg, 2014). Interestingly, nNOS only partially rescued poly(ADP-ribose) accumulation, with both hippocampal neurons and glia still retaining some degree of elevated Parp1 activity. This

residual activity may represent a separate mechanism by which endogenous DNA SSBs occur in Xrcc1-deficient models. Perhaps these remaining breaks are due to ROS generated during cellular metabolism.

A consistent observation made during these experiments is that many aspects of the *Xrcc1*$^{Nes\text{-}Cre}$ neuronal phenotype can be rescued by PARP inhibition. Notably, the inhibition of Parp1 is protective against neuronal death *in vitro*, consistent with the ablation of poly(ADP-ribose) accumulation following PARP inhibitor treatment. These data highlight the therapeutic potential of PARP inhibitors in the treatment of XRCC1-related neuropathology and may have further applications in the treatment of other hereditary defects of SSBR. The development of PARP inhibitors that do not engage in PARP trapping, but rather phenocopy *PARP1* deletion is, however, required for limiting potential toxicity.

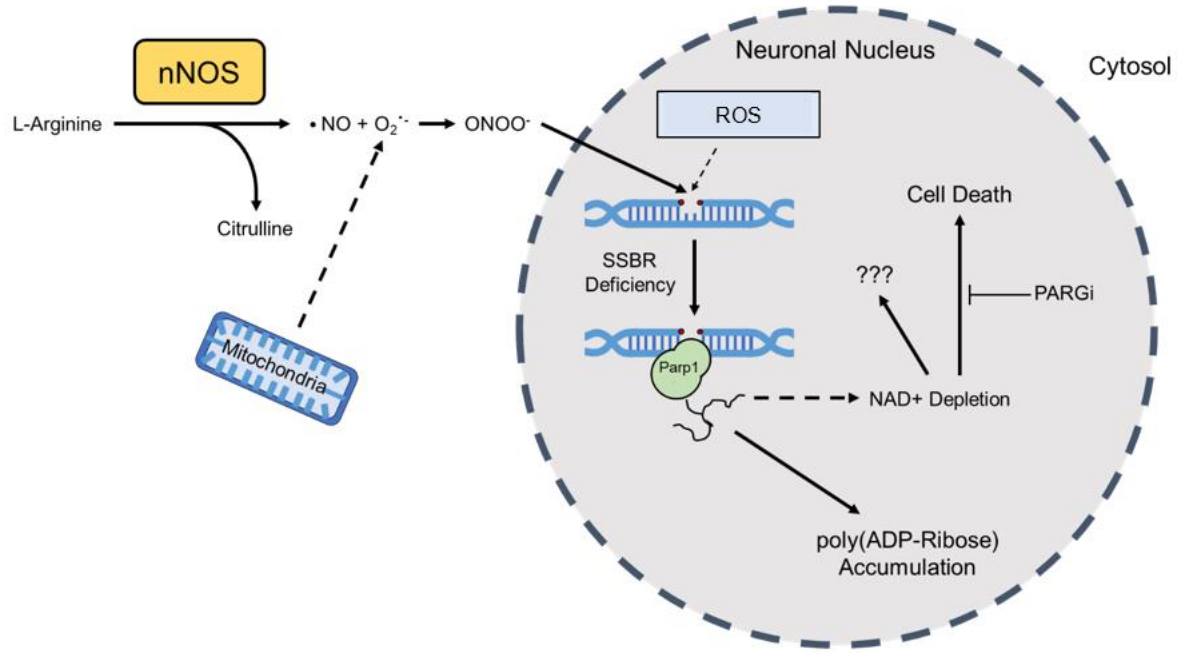

Figure 3.18 *A Model of Endogenous DNA Damage in the Xrcc1-Deficient Neuron*. Our data suggests that a significant portion of the endogenously occurring DNA SSBs occurring in *Xrcc1*$^{Nes\text{-}Cre}$ hippocampal neurons are the result of nitric oxide dependent production of RNS. We propose that these RNS induce DNA SSBs, likely through oxidation of the sugar moiety. It is likely that SSBs are also being generated concurrently through ongoing cellular processes, such as ROS generated during metabolism. Following this attack, Parp1 localises to the unresolved break, whereupon it is retained; continuously synthesising poly(ADP-ribose) in the absence of Xrcc1. As the break goes unrepaired, poly(ADP-ribose) accumulation leads to the depletion of cellular NAD+ which, in cells unable to recycle poly(ADP-ribose) due to PARG inhibition, is cytotoxic.

3.3.1 Conclusion

Xrcc1$^{Nes\text{-}Cre}$ hippocampal neurons represent a cell autonomous model of endogenous DNA damage and Parp1 activation that replicates elements of the phenotype associated with the *Xrcc1*$^{Nes\text{-}Cre}$ mouse. The accumulation of poly(ADP-ribose) in *Xrcc1*$^{Nes\text{-}Cre}$ neurons following PARG inhibition indicates that *Xrcc1* deletion results in an elevated, steady state level of endogenously arising DNA SSBs and subsequent Parp1 activity. We highlight elevated poly(ADP-ribose) in neuronal cells, compared to proliferative glia, perhaps indicating an elevated degree of endogenous SSB induction, and providing a potential explanation for the exclusively neurological phenotype associated with hereditary defects in SSBR. The Parp1 activity associated with these breaks results in elevated neuronal death *in vitro,* providing a possible explanation for the cell death observed in certain structures of the *Xrcc1*$^{Nes\text{-}Cre}$ brain. We propose that a fraction of these breaks, and the subsequent activation of Parp1, are the result of $^{\bullet}$NO signalling, a critical process in neurons resulting in the production of reactive nitrogen species, the inhibition of which is sufficient to largely reduce poly(ADP-ribose) in the neuronal nucleus (Figure 3.18). Both the accumulation of nuclear poly(ADP-ribose) and the spontaneous cell death observed in *Xrcc1*$^{Nes\text{-}Cre}$ hippocampal neurons can be also be rescued by the deletion or inhibition of Parp1, suggesting potential therapeutic application in the treatment of XRCC1 dependent neurodegeneration.

4. Chapter Four – Results: PARP1 Dependent, Aberrant Presynaptic Calcium Signalling in Xrcc1-Deficient Hippocampal Neurons

4.1 Introduction and Aims

As demonstrated in the previous chapter, the deletion of *Xrcc1* in mouse hippocampal neurons results in the accumulation of unrepaired, endogenous DNA SSBs, and subsequently the increased synthesis of poly(ADP-ribose) by Parp1. Furthermore, I detected elevated poly(ADP-ribose) accumulation in post-mitotic neurons when compared to co-cultured glia, indicating that this defect is enhanced in neurons. Endogenous DNA SSBs may occur through a variety of mechanisms, some of which are linked to neuronal function, such as their induction by RNS, a by-product of NO signalling, and through glutamatergic excitotoxicity (Didier, *et al*., 1996, Yang, *et al*., 2011, Radi, 2013, Radi, 2018). Similarly, the excessive metabolic demand that characterises nervous tissue may result in an elevated degree of endogenous SSB induction (Caldecott, 2008, Vakharia, *et al*., 2018, Murata, *et al*., 2019).

One of the most striking elements of the *Xrcc1*$^{Nes\text{-}Cre}$ phenotype is the incidence of intractable seizures. The *Xrcc1*$^{Nes\text{-}Cre}$ mouse lifespan is dictated by the prevalence of these seizures (Komulainen, *et al*., 2021). The exact mechanism of death is unclear, although it likely occurs due to cardiac or respiratory disruption; much like in human Sudden Unexpected Death During Epilepsy (SUDEP) (Komulainen, *et al*., 2021). Despite this, AOA-XRCC1 has yet to result in seizures in a human patient, presenting primarily with cerebellar degeneration and progressive ataxia, though this may be indicative of patients retaining residual XRCC1 activity (Hoch, *et al*., 2017). Interestingly, patients with MCSZ, a disorder related to mutations in the SSBR protein PNKP exhibit epileptic seizures and delayed motor development (Shen, *et al*., 2010).

The synapse is the functional unit of neuronal connectivity, a junction through which neuronal communication can occur. Following an action potential, presynaptic membrane depolarisation results in the opening of voltage gated Ca^{2+} channels (VGCC) (Südhof, 2012). The subsequent influx of ionic Ca^{2+} through these presynaptic calcium channels in the presynaptic terminal is a key step in the translation of an electrical impulse into neurotransmitter release across the synapse for signal propagation (Südhof, 2012). Following this highly localised, transient increase in presynaptic [Ca^{2+}], membrane fusion of vesicles rapidly occurs (Sabatini and Regehr, 1996). Synaptic vesicles are not functionally uniform, a fact discovered in 1961, following observations by Birks and MacIntosh that synaptic vesicles in the cat sympathetic ganglia, noting that some vesicles were not as readily released as others. Neurotransmitters are stored at

the synapse in the readily releasable vesicle pool (RRP), bound to the cell membrane by SNARE proteins, which mediate vesicle fusion, effectively docked at the presynaptic terminal and primed for release (Kaeser and Regehr, 2017). Beyond the RRP, the recycling pool constitutes 10-20% of synaptic vesicles, and is recruited once the RRP has been depleted, upon moderate stimulation (Rizzoli and Betz, 2005). The remaining vesicles make up the resting, or reserve pool, which are reluctant to release; doing so only following high-frequency stimulation, ones the recycling pool is depleted (Denker, *et al*., 2011).

The transient elevation of presynaptic [Ca^{2+}] results in the binding of Ca^{2+} to synaptotagmin, displacing complexin; which acts as a fusion clamp inhibiting spontaneous vesicle release, from the SNARE complex (Li, *et al*., 1995, Yu, *et al*., 2018). The result of this process is that, following the invasion of an action potential into the nerve terminal, an increase in presynaptic [Ca^{2+}] precedes vesicle fusion and, ultimately, the release of neurotransmitter-containing vesicles across the presynaptic membrane. As such, alterations of presynaptic calcium homeostasis would result in deregulation of synaptic transmission (Scullin, *et al*., 2012, Atlas, 2013). Further, residual presynaptic [Ca^{2+}] regulates release probability, as well as paired-pulse facilitation, a means by which repetitive impulses increase the strength of postsynaptic potentials (Mongillo, Barak, and Tsodyks, 2008, Scullin, *et al*., 2012). The relationship between [Ca^{2+}] at the presynaptic terminal and release probability is highly non-linear, with small increases in ionic calcium resulting in large-scale alterations in vesicle exocytosis (Heidelberger, *et al*., 1994, Sakaba and Neher, 2001). The deregulation of Ca^{2+} signalling is implicated in the pathology of several neurodegenerative disorders, such as AD and PD (Schapira, 2013, Popugaeva, *et al*., 2017). Recently, Parp1-dependent deregulated calcium homeostasis in cerebellar PCs was found to underlie the pathology of the SCA7 mouse (Stoyas, *et al*., 2020) In summary, the transient rise in intracellular [Ca^{2+}] occurs downstream from action potential-evoked presynaptic depolarisation, and upstream from neurotransmitter release. As such, presynaptic calcium flux is a pivotal event enabling rapid information signalling in the brain.

The influx of calcium into the presynaptic terminal does not occur exclusively through external sources. Internal stores, including the endoplasmic reticulum (ER), mitochondria, and acidic Ca^{2+} stores, such as lysosomes, play a crucial role in the regulation of the spatial and temporal dynamics of Ca^{2+} signalling (Padamsey, *et al*., 2018). Sarcoplasmic/Endoplasmic Reticulum Ca^{2+}ATPases (SERCAs) maintain calcium concentration in the ER lumen at three orders of magnitude higher than cytosolic [Ca^{2+}] (Meldolesi and Pozzan, 1998, Shen, *et al*., 2011). The release of Ca^{2+} from the ER is

regulated by either IP3Rs, which are activated by the presence of Ca^{2+} and inositol triphosphate, or ryanodine receptors (RyRs), which are activated by cADPR (Lanner, *et al*., 2010, Karagas and Vankatachalam, 2019). SERCAs act to uptake Ca^{2+} into the lumen of the ER, buffering presynaptic [Ca^{2+}] following activity evoked influx (Scullin and Partridge, 2010). Mitochondrial calcium release occurs through the opening of the mitochondrial permeability transition pore (MPTP), facilitated by an increase in mitochondrial [Ca^{2+}] (Mnatsakanyan, *et al*., 2017). The mitochondria also play a key role in the shaping of the presynaptic Ca^{2+} signal; their hyperpolarised resting membrane potential (-180 mV) facilitates the rapid sequestration of Ca^{2+} across an electrochemical gradient (Contreras, *et al*., 2010, Zorova, *et al*., 2011). Acidic Ca^{2+} stores, such as lysosomes, also sequester Ca^{2+} through a H^+ gradient generated by H^+-ATPase and Ca^{2+}/H^+ exchange (Morgan, *et al*., 2010). This sequestered Ca^{2+} can be released from acidic stores via the second messenger, NAADP, although the mechanism through which this occurs is unclear (Galione, *et al*., 2010). The deregulation of Ca^{2+} release and sequestration from intracellular stores has been implicated in the pathology of several neurodegenerative conditions, such as AD and PD, spinocerebellar ataxia, and epilepsy (Liu, *et al*., 2009, Feng and Yang, 2017, Britti, *et al*., 2018, Purroy, *et al*., 2018, Yap and Smith, 2019). The various means by which Ca^{2+} release and sequestration can be regulated, and the consequence of mutation in proteins involved in this regulation, emphasise the intricacy of calcium signalling, which enables the fine tuning required for information processing in the brain.

In this chapter, I aim to characterise the effects of *Xrcc1* deletion and subsequent Parp1 hyperactivation on presynaptic calcium signalling. Given that *Xrcc1*$^{Nes\text{-}Cre}$ hippocampal neurons exhibit elevated steady-state levels of poly(ADP-ribosylation), replicating the poly(ADP-ribose) accumulation I observe in the mutant mouse brain, I sought to examine whether synaptic manifestations of the *Xrcc1*$^{Nes\text{-}Cre}$ seizure phenotype could be identified in cells. To do so, I adopted a sensitive optical readout approach based on expression of SyGCaMP6f; a synaptically targeted, genetically encoded calcium indicator (GECI). This allowed me to quantify the effects of *Xrcc1* deletion on presynaptic calcium changes at the level of individual synaptic terminals, allowing me to test for a cellular signalling correlate of the *Xrcc1*$^{Nes\text{-}Cre}$ seizure phenotype.

4.2 Results

4.2.1 Investigating Calcium Signalling at the Presynaptic Terminal of Wild Type Hippocampal Neurons

GCaMP is an optical reporter of calcium flux, consisting of circularly permutated EGFP, connected C-terminally to Calmodulin and N-terminally to the M13 domain of Myosin light chain kinase (the sequence targeted by Calmodulin). Following increased [Ca^{2+}] and the subsequent binding of Ca^{2+} to the reporter, the Ca^{2+} dependent interactions of Calmodulin-M13 induce conformational alterations to cpEGFP, resulting in GFP fluorescence (Nakai, Ohkura, and Imoto, 2001). For the purposes of investigating presynaptic Ca^{2+} fluctuations, I utilised a fast variant of GCaMP fused to synaptophysin, a ubiquitous synaptic vesicle protein, known as SyGCaMP6f (Figure 4.1 A) (Dreosti, *et al*., 2009). To utilise such a reporter, I generated dissociated hippocampal cultures from wild type and, following optimisation of the reporter, mutant mouse pups (Figure 4.1 B i). Ordinarily, primary hippocampal cultures will be maintained in the presence of cytosine arabinoside (AraC), which inhibits DNA synthesis and limits the proliferation of co-cultured glial cells (Patel, *et al*., 1988). However, this treatment results in single-strand breakage, and so in order to avoid the induction of DNA damage in *Xrcc1*$^{Nes\text{-}Cre}$ neurons, I did not treat our hippocampal neurons with AraC (Geller, *et al*., 2001, Owen, *et al*., 2021). Neurons were infected from DIV6/7, with an MOI of 100, and incubated until DIV15-17 prior to recording. Neurons were recorded at this age as synaptogenesis and maturation occur roughly two weeks after plating. Following this, neurons were transferred to an imaging chamber consisting of two, parallel platinum wires positioned 10mm apart, across which a voltage of 22.5V was applied. Initially, I established the efficacy of the reporter in demonstrating activity evoked Ca^{2+} transients in wild type puncta. To do so, cells were bathed in EBS designed to physiologically mimic the extracellular environment, albeit containing the NMDA and AMPA receptor antagonists AP-v and CNQX (at 50 µM and 20 µM concentrations respectively) both to inhibit spontaneous action potential induction, as well as limit network feedback.

Once optimal expression of SyGCaMP6f was achieved (Figure 4.1 B ii), wild type neurons were exposed to field stimulation (10 x 1 ms square wave pulses, frequency: 20 Hz), corresponding to 10 action potentials (APs), repeated three times. These stimulus parameters are known to evoke a Ca^{2+} rise that drives the recruitment of vesicles in the readily releasable pool; the subset of synaptic vesicles immediately available to undergo fusion, allowing us to assess the physiologically relevant signalling response at each synaptic terminal. Synaptic regions of interest (ROIs) were determined

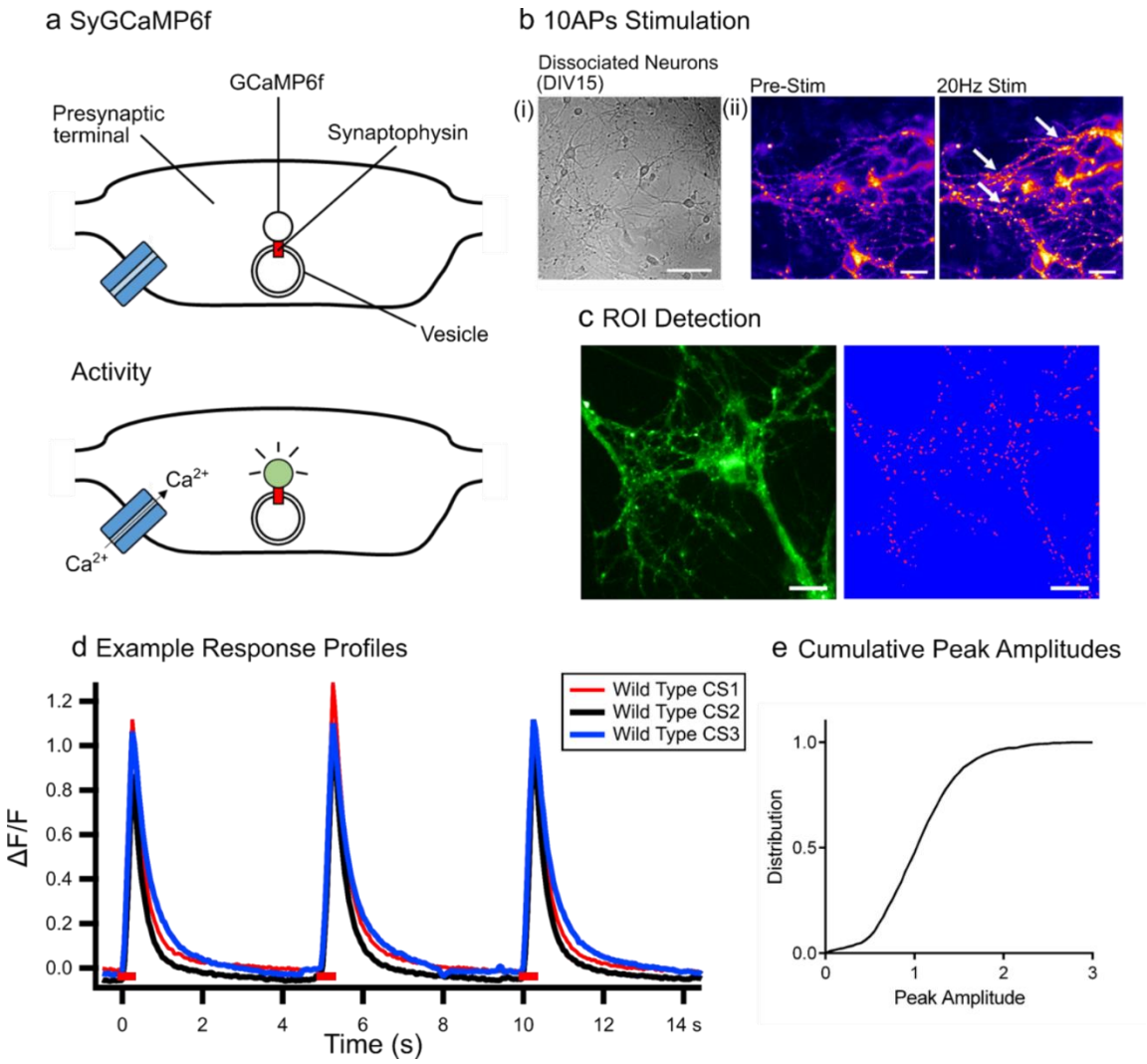

Figure 4.1 *Characterisation of SyGCaMP6f Responses in Wild Type Hippocampal Neurons.* A) Cartoon schematic illustration of SyGCaMP6f targeting and action. B) (i) Representative brightfield image of dissociated, wild type hippocampal neurons used. Scale bar, 100µM. (ii) false-colour SyGCaMP expressing hippocampal neurons prior to and following 10Aps, 20Hz freq. stimulation. Arrows highlight example regions of fluorescence intensity flux. Scale bar, 20µM. C) automated IGOR overlay of recording highlighting synaptic regions of interest (ROIs), i.e responsive synapses. D) Example traces from three individual recordings, following 10AP stimulation of wild type hippocampal neurons cultured from three separate animals. Red bars along x-axis represent the starting point and duration of stimulation. E) Cumulative distribution of response amplitudes following stimulation. Peak amplitudes represent maximal ΔF/F values of responses to stimulation in wild type hippocampal neurons from three, individual animals.

using the SARFIA Igor Pro plugin, using correlates of STDEV between proximal pixels, facilitating the automated and non-subjective identification of responsive synapses (Figure 4.1 C). Utilising this reporter expression approach, I demonstrated transient increases in fluorescence at the synapse characteristic of activity evoked Ca^{2+} flux at the wild type presynaptic terminal, reported as mean responses from coverslips of neurons cultured from three different wild type mouse pups (Figure 4.1 D and 4.1 E). Having validated the baseline characteristics of wild type activity evoked Ca^{2+} influx, I next sought to investigate presynaptic Ca^{2+} signalling in *Xrcc1*$^{Nes\text{-}Cre}$ hippocampal neurons.

4.2.2 Alterations to Presynaptic Ca^{2+} Signalling in Dissociated *Xrcc1*$^{Nes\text{-}Cre}$ Hippocampal Neurons

Wild type and *Xrcc1*$^{Nes\text{-}Cre}$ hippocampal neurons expressing SyGCaMP6f were subjected to 10AP field stimulations, with the fluorescence change measured in SyGCaMP6f positive puncta. Following repeated trains of 10AP stimuli, Wild Type SyGCaMP6f positive puncta exhibited transient changes in fluorescence, indicative of stimulation induced presynaptic calcium influx (Figure 4.1 D, Figure 4.2 A and B). I chose to subject neurons to three repeats of 10APs for two reasons; to investigate the consistency of the responses, and to explore the possibility of activity-dependent effects, such as whether depression following initial stimulation was notably different between genotype and treatment groups. Strikingly, the amplitude of activity-evoked responses in *Xrcc1*$^{Nes\text{-}Cre}$ puncta was ~2 fold higher than that of wild type synapses, consistent with a much greater Ca^{2+} influx following stimulation. I did not observe any obvious and consistent difference between the initial, secondary, and tertiary stimulus responses. I further report a significant elevation in the total Ca^{2+} flux combined from the three responses, determined by measuring the area under the curve for each profile (Figure 4.2 C). As individual synapses cannot necessarily be considered independent replicates, a comparison between coverslips provides a more robust quantification of differences. In representing data by coverslip, I also highlight responses of strikingly large amplitude and duration in *Xrcc1*$^{Nes\text{-}Cre}$ synaptic puncta (Figure 4.3).

Given that calcium signalling is a critical step in the rapid processing of information in the brain, a 2-fold increase in the amplitude of activity-evoked calcium transients could have dramatic consequences for network activity in the brain. I propose that this aberrant presynaptic calcium flux represents a signalling defect in the *Xrcc1*$^{Nes\text{-}Cre}$ brain, providing a possible explanation for the seizures that characterise this mouse model. The hippocampal neurons in the above experiments were stimulated in EBS

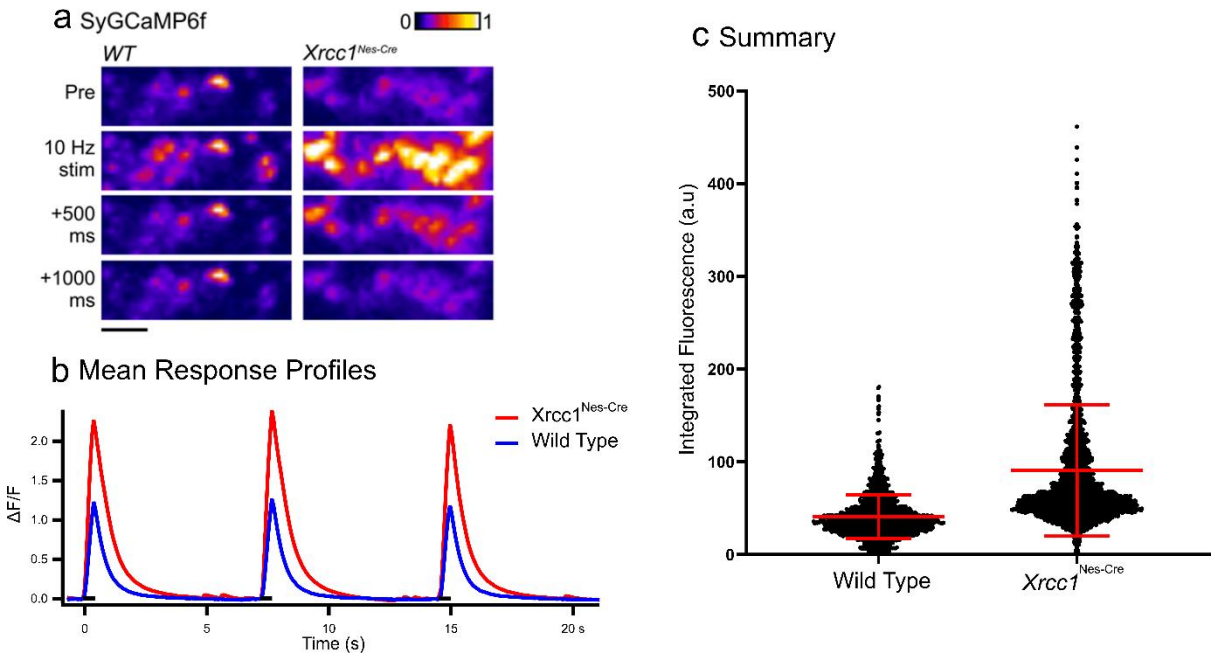

Figure 4.2 *Deregulated Presynaptic Calcium Signalling in Xrcc1$^{Nes-Cre}$ Hippocampal Neurons.* Investigations of wild type and mutant hippocampal neurons infected at DIV6 with SyGCaMP6f expressing AAV, prior to further incubation. A) Representative images of fluorescence responses in synaptic terminals expressing SyGCaMP6f to 10 AP (10 Hz) stimulation in DIV15-17 dissociated hippocampal neurons derived from wild type and *Xrcc1*$^{Nes-Cre}$ mouse pups. Scale bar: 5 µm. B) Mean SyGCaMP6f responses to three rounds of 10 APs stimulation from mice of the following genotypes; Wild Type (n = 1946 synapses, 9 coverslips, 3 animals) in blue, *Xrcc1*$^{Nes-Cre}$ (n = 3313 synapses, 12 coverslips, 4 animals) in red. Response profiles plotted as ΔF/F, fluorescence intensity flux. Black bars along x-axis represent the starting point and duration of stimulation C) Integrated Fluorescence as calculated by area under the curve in B), where one data point represents a single, recorded synapse. Mean and Standard Deviation represented in red.

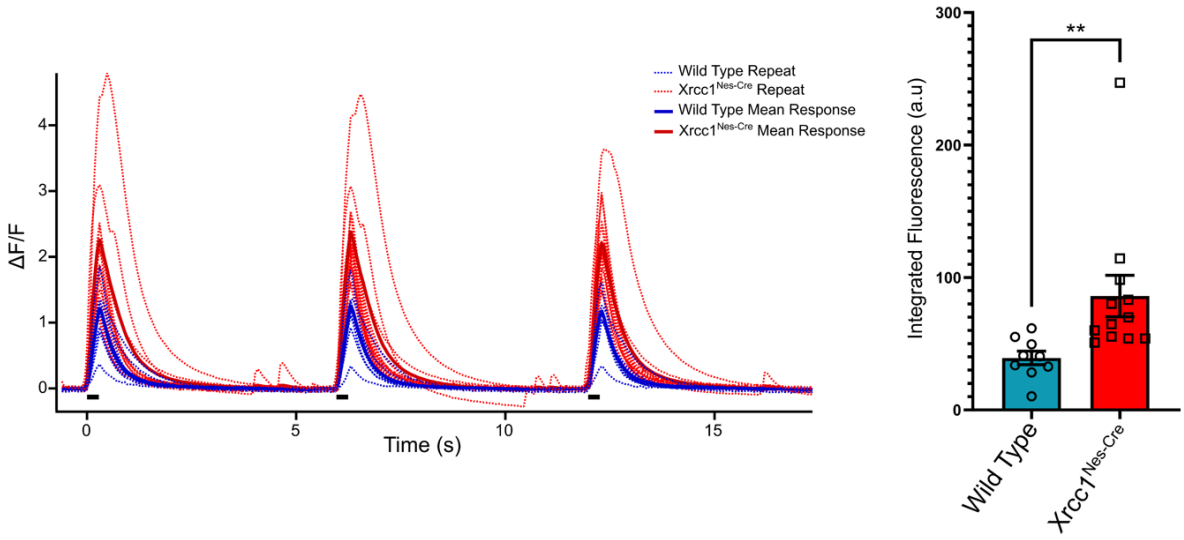

Figure 4.3 *By Coverslip Analysis of Deregulated Presynaptic Calcium Signalling in Xrcc1*$^{Nes\text{-}Cre}$ *Hippocampal Neurons.* Left: SyGCaMP6f responses from individual replicate coverslips, wild type (3 mice) in blue, *Xrcc1*$^{Nes\text{-}Cre}$ (4 mice) in red. Dotted traces represent individual replicates, continuous traces represent mean response as seen in Figure 4.2. Response profiles plotted as ΔF/F, fluorescence intensity flux. Black bars along x-axis represent the starting point and duration of stimulation. Right: Integrated fluorescence Integrated Fluorescence as calculated by area under the curve in B), where one data point represents mean responses from individual replicate coverslips. Histogram shows mean ± SEM, significance denoted as ** where $p < 0.01$ (as reported by post-hoc Tukey-Kramer comparison of means identifying between group significance following one way ANOVA ($p < 0.0033$) test with data from further genetic backgrounds).

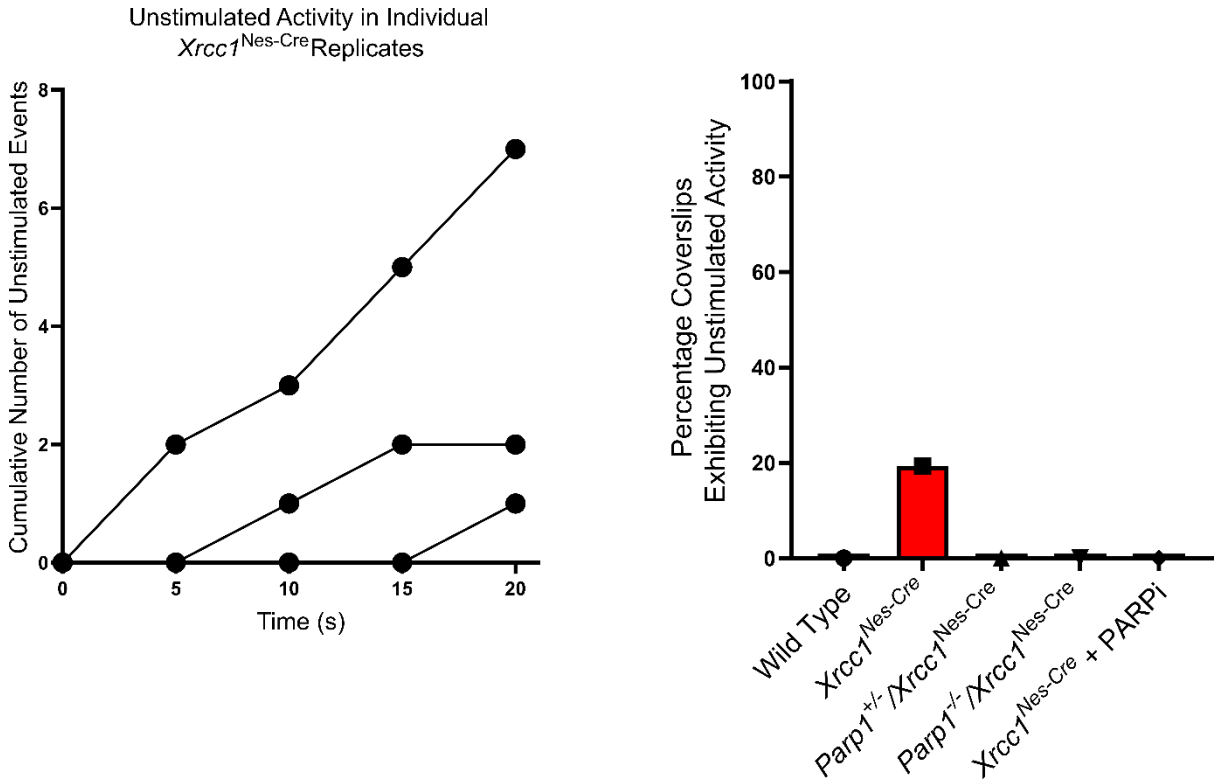

Figure 4.4 *Unstimulated Activity in Xrcc1$^{Nes\text{-}Cre}$ Hippocampal Neurons.* Left: Graph showing cumulative, unstimulated events in three separate, individual recordings on *Xrcc1*$^{Nes\text{-}Cre}$ hippocampal neurons. These replicates are highlighted due to the presence of these unstimulated events, but do not represent the whole data set. Right: Percentage of individual replicates wherein unstimulated activity was recorded. Unstimulated activity was only observed in *Xrcc1*$^{Nes\text{-}Cre}$ hippocampal neurons and was absent from all other genotypes and treatments.

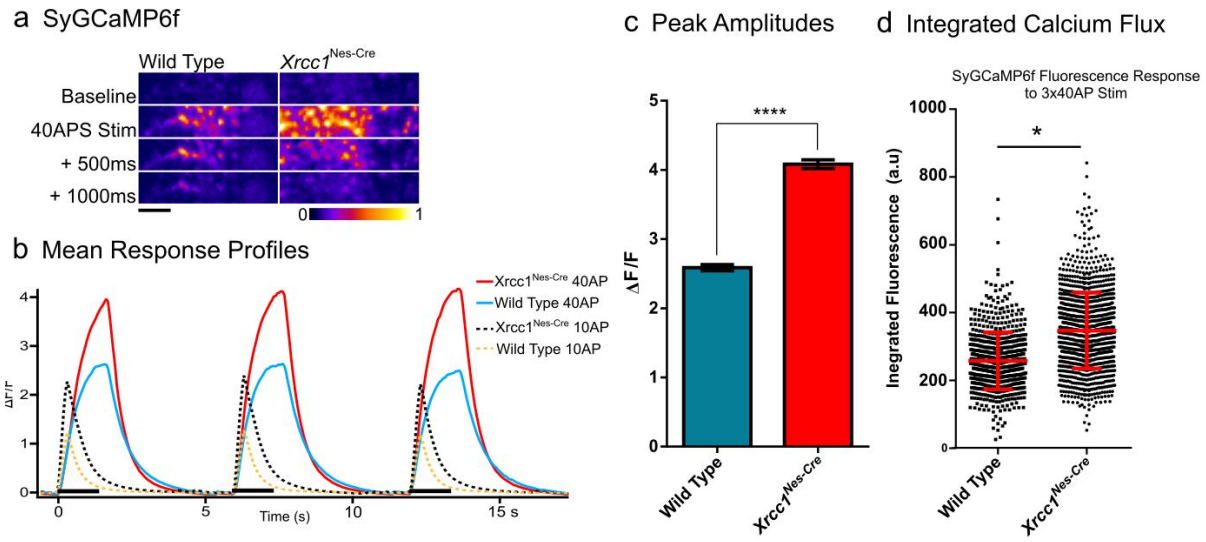

Figure 4.5 *Increased Stimulation Exacerbates Aberrant Presynaptic Calcium Phenotype of Xrcc1*$^{Nes\text{-}Cre}$ *Hippocampal Neurons.* Wild type and mutant hippocampal neurons were infected as previously before being stimulated with repeated trains of 40AP stimuli. A) Representative images of fluorescence responses in synaptic terminals expressing SyGCaMP6f to 40AP (10Hz) stimulation in DIV15-17 dissociated hippocampal neurons cultured from wild type and *Xrcc1*$^{Nes\text{-}Cre}$ mouse pups. Scale bar = 5μM. B) Mean SyGCaMP6f responses to three rounds of 40APs stimulation in wild type (726 synapses, 5 coverslips, 3 animals), and *Xrcc1*$^{Nes\text{-}Cre}$ (1229 synapses, 7 coverslips, 3 animals) hippocampal neurons. Overlaid in dotted lines are mean response profiles of wild type and *Xrcc1*$^{Nes\text{-}Cre}$ hippocampal neurons to 10AP stimuli for reference, as reported in Figure 4.2. Response profiles plotted as ΔF/F, fluorescence intensity flux. C) Integrated fluorescence as calculated by area under the curve in B), where one data point represents a single, recorded synapse. Mean and Standard Deviation represented in red, significance denoted where $p < 0.05$ (as reported by students T-test).

containing AMPA and NMDA receptor blockers, which inhibit most unstimulated/spontaneous signalling. Nonetheless, it was striking to see that, in some cases, *Xrcc1*$^{Nes\text{-}Cre}$ hippocampal synapses were still prone to unstimulated (signalling during the decay of a previous, activity evoked transient) event activity (as can be seen in (Figure 4.3, where further, small peaks appear late into the decay of the evoked Ca^{2+} transient, and Figure 4.4). This suggests that *Xrcc1*$^{Nes\text{-}Cre}$ hippocampal neurons may be more prone to spontaneous activity, a sensitivity which could, in turn, relate to increased seizure-like activity in the brain. Given that these unstimulated events were independent of AMPA/NMDAR activity, they could potentially correspond to the release of Ca^{2+} from intracellular stores.

Previous studies of the SCA7 mouse model have implicated Parp1-dependent aberrant Ca^{2+} signalling in a model of progressive cerebellar ataxia. While the *Xrcc1*$^{Nes\text{-}Cre}$ mouse is characterised by cerebellar degeneration and ataxia, we have previously reported the cause of juvenile mortality to be terminal seizures (Komulainen, *et al*., 2021). It is interesting to note that seizures are not as ubiquitous a symptom of hereditary SSBR disorders as cerebellar degeneration (mutations in PNKP may result in the manifestation of seizures, however this is not universal), and have yet to be reported in the limited cohort of patients with *XRCC1* mutation. The currently reported patients do retain some functionality of the *XRCC1* protein, however, which may underlie the discrepancy between comparatively long-lived human patients, and the conditional knockout mouse. Despite this discrepancy, these data represent a synaptic model of elevated activity that may underlie the terminal seizures characteristic of the *Xrcc1*$^{Nes\text{-}Cre}$ mouse.

To further investigate this newly discovered synaptic phenotype, I increased the stimulation from 10 to 40APs to see if this phenomenon was replicated at higher intensity stimulation. I showed that repeated trains of field stimulation at this higher intensity replicate the elevated amplitude of evoked Ca^{2+} transients in *Xrcc1*$^{Nes\text{-}Cre}$ hippocampal neurons (Figure 4.5). Interestingly, the increased stimulation that was applied to the cells was sufficient in both cases to cause a plateau in Ca^{2+} flux, indicating maximal release at the synapse (Figure 4.5 B). In *Xrcc1*$^{Nes\text{-}Cre}$ synapses, this plateau occurred following a much greater initial release of Ca^{2+}, perhaps indicating an increased sensitivity to stimulation, or perhaps that alterations in calcium homeostasis result in an increased releasable pool of Ca^{2+} at the synapse, which could translate to the inappropriate release of neurotransmitter.

A separate interpretation of this result could be that we are observing probe saturation. SyGCaMP6f is a high affinity Ca^{2+} probe with an equilibrium dissociation constant (Kd) of 0.22μM ± 0.01 at 20°C (Helassa, *et al*., 2016). Industrial testing has shown linear increases in the dynamic range of the SyGCaMP6f up to 40AP stimulation at 20Hz frequency (de Oliveira Borges, 2017). The experiments performed in Figure 4.5 are done under stimulation parameters at the upper limits of the detection capacity of the reporter. While we may be able to achieve relative comparisons between genotypes at this stimulation, given the plateau in intensity observed under these conditions the potential for probe saturation makes it difficult to draw robust conclusions as to the concentration of Ca^{2+} at the presynaptic terminal, as this may underlie prolonged signals and slow decay.

4.2.3 Genetic Rescue of Aberrant Presynaptic Ca^{2+} Signalling in *Xrcc1*$^{Nes\text{-}Cre}$ Hippocampal Neurons by the Additional Deletion of Parp1

Previous data has highlighted that the hyperactivation of the SSB sensor protein *Parp1* causes the accumulation of poly(ADP-ribose) in *Xrcc1*$^{Nes\text{-}Cre}$ neurons both *in vitro* and in the whole brain (Figure 3.5 and Figure 3.6). It has been reported that the additional deletion of one or both alleles of *Parp1* is sufficient to prevent both the excessive accumulation of nuclear poly(ADP-ribose) (Figure 3.7), and the juvenile mortality associated with *Xrcc1*$^{Nes\text{-}Cre}$ mice, with *Parp1*$^{-/-}$/*Xrcc1*$^{Nes\text{-}Cre}$ and with *Parp1*$^{-/-}$/*Xrcc1*$^{Nes\text{-}Cre}$ exhibiting an 8-fold and 25-fold increase in lifespan respectively (Komulainen, *et al*., 2021). Given that *Parp1*$^{-/-}$/*Xrcc1*$^{Nes\text{-}Cre}$ mice do not exhibit seizures, and that the deletion of *Parp1* also rescues the spontaneous death observed in cultured *Xrcc1*$^{Nes\text{-}Cre}$ hippocampal neurons (Figure 3.8), I reasoned that perhaps cells cultured from *Parp1*$^{+/-}$/*Xrcc1*$^{Nes\text{-}Cre}$ and *Parp1*$^{-/-}$/*Xrcc1*$^{Nes\text{-}Cre}$ mice may not exhibit aberrant presynaptic Ca^{2+} signalling. Indeed, I found that the additional deletion of *Parp1* suppresses activity-evoked Ca^{2+} influx at *Xrcc1*$^{Nes\text{-}Cre}$ hippocampal synaptic puncta to wild type levels (Figure 4.6 and Figure 4.7) (Komulainen, *et al*., 2021). This ablation of aberrant presynaptic Ca^{2+} signalling provides a potential mechanism for the rescue of lifespan seen in *Parp1*$^{-/-}$/*Xrcc1*$^{Nes\text{-}Cre}$ mice, as these mice do not exhibit the terminal seizures observed in *Xrcc1*$^{Nes\text{-}Cre}$ mice during the first few weeks of life. Interestingly, the deletion of only one allele of *Parp1,* as in the *Parp1*$^{+/-}$/*Xrcc1*$^{Nes\text{-}Cre}$ mouse, partially rescued aberrant presynaptic signalling, both in terms of peak amplitude and total calcium flux, consistent with the intermediate accumulation of poly(ADP-ribose) in both *Parp1*$^{+/-}$/*Xrcc1*$^{Nes\text{-}Cre}$ neurons and the *Parp1*$^{+/-}$/*Xrcc1*$^{Nes\text{-}Cre}$ brain (Figure 3.2.7, Figure 4.6, and Figure 4.7) (Komulainen, *et al*., 2021). It is unclear whether *Parp1*$^{+/-}$/*Xrcc1*$^{Nes\text{-}Cre}$ mice exhibit seizures later in life, however the partial rescue of aberrant presynaptic calcium

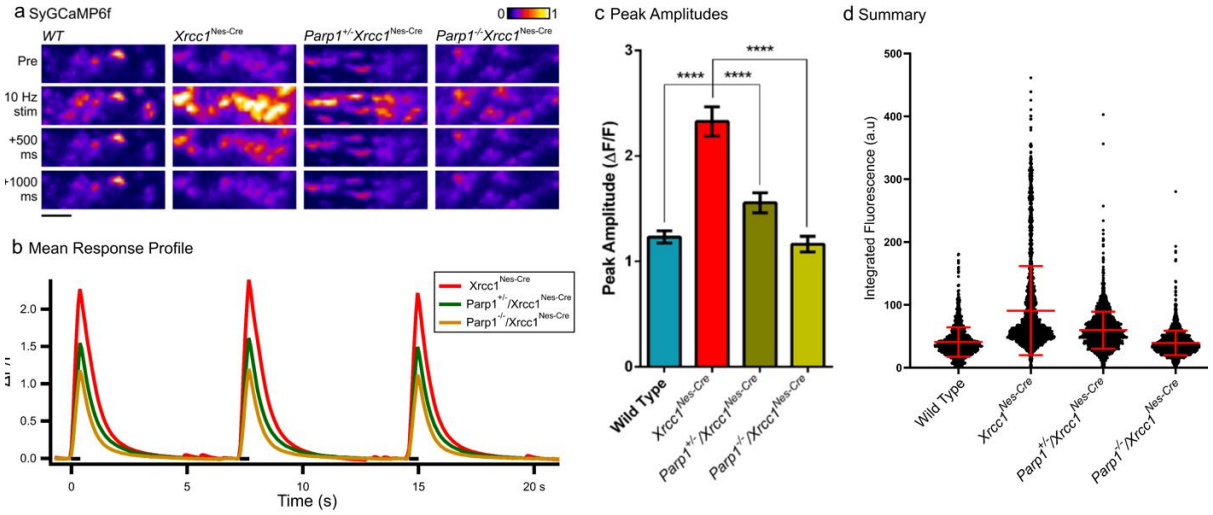

Figure 4.6 *The Impact of Additional Parp1 Deletion on Aberrant Presynaptic Calcium Signalling in Xrcc1$^{Nes\text{-}Cre}$ Hippocampal Neurons*. Investigations of mutant hippocampal neurons infected as above with SyGCaMP6f expressing AAV, prior to further incubation. A) Representative images of fluorescence responses in synaptic terminals expressing SyGCaMP6f to 10 AP (10 Hz) stimulation in DIV15-17 dissociated hippocampal neurons derived from wild type and mutant mice, including those with the additional deletion of the SSB sensor protein *Parp1*. Scale bar: 5 µm. B) Mean SyGCaMP6f responses to three rounds of 10 APs stimulation from mice of the following genotypes: *Xrcc1$^{Nes\text{-}Cre}$* (n = 3313 synapses, 12 coverslips, 4 animals), *Parp1$^{+/-}$/Xrcc1$^{Nes\text{-}Cre}$* (n = 2272 synapses, 9 coverslips, 3 animals) in green, and *Parp1$^{-/-}$/Xrcc1$^{Nes\text{-}Cre}$* (n = 2122, 11, 3) in yellow. Response profiles plotted as ΔF/F, fluorescence intensity flux. Black bars along x-axis represent the starting point and duration of stimulation. C) Mean peak amplitudes taken from individual synaptic recordings, **** denotes significance where $p < 0.001$, as reported by multiple T-tests. D) Integrated Fluorescence as calculated by area under the curve in B), and in Figure 4.2. Mean and Standard Deviation represented in red. Due to the limitations and rarity associated with hippocampal culture of mice from multiple genetic backgrounds, data are pooled from multiple cultures, and recorded in each instance with at least a wild type control.

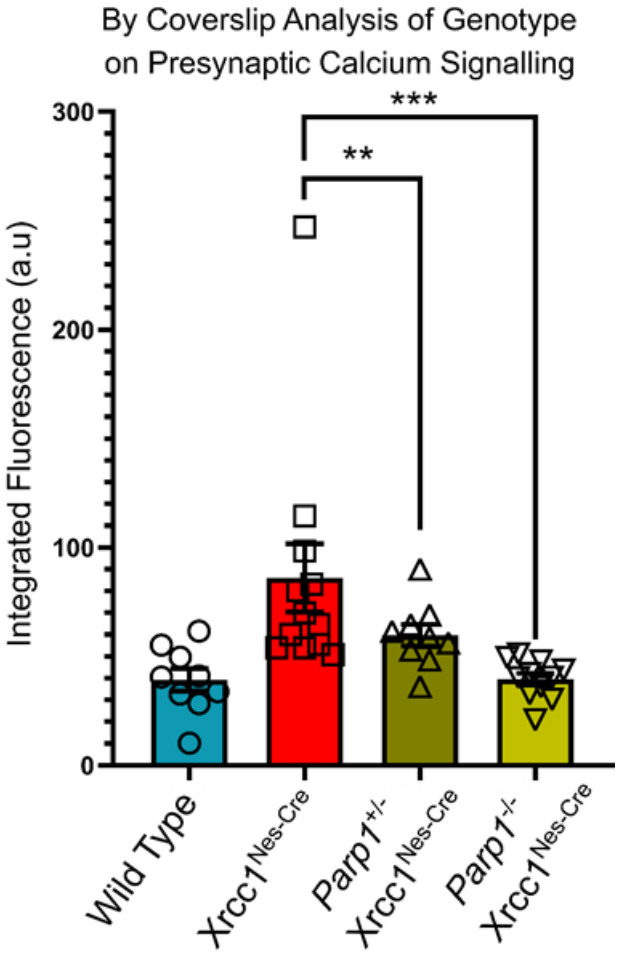

Figure 4.7 By Coverslip Analysis of Deregulated Presynaptic Calcium Signalling in *Parp1*$^{+/-}$/*Xrcc1*$^{Nes\text{-}Cre}$ and *Parp1*$^{-/-}$/*Xrcc1*$^{Nes\text{-}Cre}$ Hippocampal Neurons. Integrated Fluorescence as calculated by area under the curve in 4.2.3.1 where one data point represents responses from individual replicate coverslips. Histogram shows mean ± SEM, significance denoted as ** where $p < 0.01$, *** where $p < 0.005$ (as reported by post-hoc Tukey-Kramer comparison of means identifying between group significance following one way ANOVA ($p < 0.0033$)). Due to the limitations and rarity associated with hippocampal culture of mice from multiple genetic backgrounds, data are pooled from multiple cultures, and recorded in each instance with at least a wild type control.

signalling may underlie the rescue observed both in seizure-like activity *ex vivo*, and the extension of their lifespan (Komulainen, *et al*., 2021). A further point to note is the absence of unstimulated activity in *Parp1* deleted neurons, as opposed to that seen in the *Xrcc1*$^{Nes\text{-}Cre}$ cells, as these cells do not exhibit additional peaks of unstimulated activity during signal decay (Figure 4.4). While this network activity is notably rare in *Xrcc1*$^{Nes\text{-}Cre}$ hippocampal neurons, occurring following roughly 20% of recorded stimulations, they were not observed in either *Parp1*$^{+/-}$/*Xrcc1*$^{Nes\text{-}Cre}$ and *Parp1*$^{-/-}$/*Xrcc1*$^{Nes\text{-}Cre}$ cells, suggesting that this unstimulated activity is a result of Parp1 hyperactivation.

These data suggest that Parp1 activity at sites of irreparable, endogenous SSBs, results in elevated activity-evoked Ca^{2+} signalling at presynaptic terminals. To my knowledge, this is the first data to suggest a mechanistic link between DNA single strand breaks, Parp1, and aberrant Ca^{2+} signalling at the synapse, and may provide insight into the intractable seizures and subsequent shortened lifespan of the *Xrcc1*$^{Nes\text{-}Cre}$ mouse.

4.2.4 Investigating the Efficacy of PARP Inhibitors in the Treatment of Aberrant Presynaptic Ca^{2+} Signalling in *Xrcc1* Deleted Hippocampal Neurons

Following this genetic rescue, I aimed to investigate whether clinically available PARP inhibitors could be utilised to rescue the observed presynaptic phenotype. Previous studies of *Xrcc1*$^{Nes\text{-}Cre}$ mice have suggested that clinically available PARP inhibitors, many of which trap Parp1 at the DNA break, are ineffective in rescuing organism lifespan, and do not phenocopy the deletion of *Parp1* (Komulainen, unpublished) (Murai, *et al*., 2012). Utilising our cellular model of elevated synaptic activity, I chronically administered *Xrcc1*$^{Nes\text{-}Cre}$ hippocampal neurons with 1µM KU0058948, a highly potent inhibitor of both Parp1 and Parp2, for 9-11 consecutive days prior to recording, following their infection with SyGCaMP6f (Murai, *et al*., 2012). Interestingly, chronic PARP inhibition was sufficient to suppress activity-evoked Ca^{2+} transients to wild type levels in *Xrcc1*$^{Nes\text{-}Cre}$ puncta, with both peak amplitude and total evoked calcium release being significantly reduced (Figure 4.8 and Figure 4.9), without affecting those evoked in wild type neurons (Figure 4.8 C). Further, chronic PARP inhibition suppressed the partially elevated Ca^{2+} response in *Parp1*$^{+/-}$/*Xrcc1*$^{Nes\text{-}Cre}$ neurons, suggesting that the retention of one allele of *Parp1*, and the resultant elevated poly(ADP-ribose) accumulation, underlies the partially elevated presynaptic Ca^{2+} signalling observed in heterozygous knockout cells, and that the ablation of this accumulation rescues this residual defect (Figure 4.10). As observed in the *Parp1*$^{+/-}$/*Xrcc1*$^{Nes\text{-}Cre}$ and *Parp1*$^{-/-}$/*Xrcc1*$^{Nes\text{-}Cre}$ neurons, the continuous incubation with the PARP inhibitor rescued unstimulated activity in *Xrcc1*$^{Nes\text{-}Cre}$ hippocampal neurons (Figure 4.4).

The data suggests that PARP inhibition is sufficient to rescue Parp1-dependent synaptic dysfunction in *Xrcc1*$^{Nes\text{-}Cre}$ hippocampal neurons *in vitro,* indicating the potential viability for their use in the treatment of XRCC1-linked disease.

4.2.5 Parp1-Dependent Slowing of [Ca^{2+}] Decay in *Xrcc1*$^{Nes\text{-}Cre}$ Hippocampal Neurons

By normalising the amplitudes of mean responses to one another, I was able to highlight a further element of the *Xrcc1*$^{Nes\text{-}Cre}$ synaptic phenotype; the increased duration of signal decay, or calcium reuptake at the synapse (Figure 4.11). Deficits in decay rate

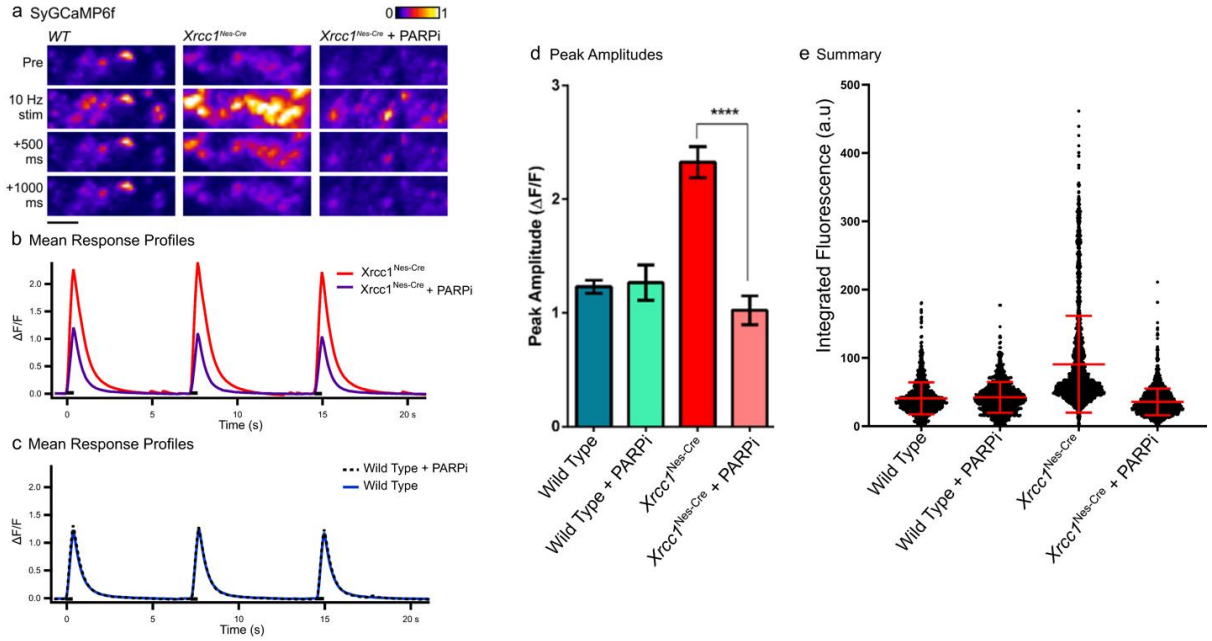

Figure 4.8 *The Impact of PARP Inhibition on Aberrant Presynaptic Calcium Signalling in Xrcc1*$^{Nes\text{-}Cre}$ *Hippocampal Neurons*. Investigations of mutant hippocampal neurons infected as above with SyGCaMP6f expressing AAV, prior to chronic incubation with a PARP inhibitor. A) Representative images of fluorescence responses in synaptic terminals expressing SyGCaMP6f to 10 AP (10 Hz) stimulation in DIV15-17 dissociated hippocampal neurons derived from wild type and *Xrcc1*$^{Nes\text{-}Cre}$ mouse pups. Scale bar: 5 µm. B) and C) Mean SyGCaMP6f responses to three rounds of 10 APs stimulation in Wild Type control, Wild Type PARP inhibitor treated (1264 synapses, 6 coverslips, 3 animals) in dotted black, *Xrcc1*$^{Nes\text{-}Cre}$ control (n = 3313 synapses, 12 coverslips, 4 animals) and *Xrcc1*$^{Nes\text{-}Cre}$ PARP inhibitor treated (2231 synapses, 9 coverslips, 3 animals) in purple. Response profiles plotted as ΔF/F, fluorescence intensity flux. Black bars along x-axis represent the starting point and duration of stimulation D) Mean peak amplitudes taken from individual synaptic recordings, **** denotes significance where $p < 0.001$, as reported by Student's t-test. E) Integrated Fluorescence as calculated by area under the curve in B). Mean and Standard Deviation represented in red.

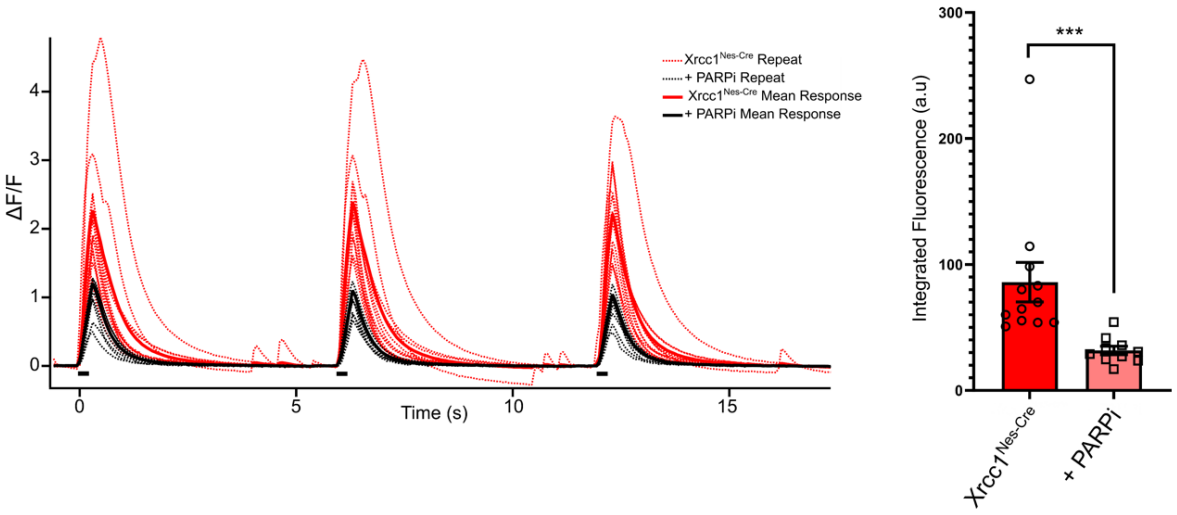

Figure 4.9 *By Coverslip Analysis of Deregulated Presynaptic Calcium Signalling in PARP Inhibitor Treated Xrcc1$^{Nes\text{-}Cre}$ Hippocampal Neurons*. Left: SyGCaMP6f responses from individual replicate coverslips, *Xrcc1*$^{Nes\text{-}Cre}$ control (4 mice) in red, and PARP inhibitor treated (3 mice) in black. Dotted traces represent individual replicates, continuous trace represents mean response as seen in Figure 4.8. Response profiles plotted as ΔF/F, fluorescence intensity flux. Black bars along x-axis represent the starting point and duration of stimulation. Right: Integrated fluorescence Integrated Fluorescence as calculated by area under the curve in B), where one data point represents responses from individual replicate coverslips. Histogram shows mean ± SEM, significance denoted as *** where $p < 0.005$ (as reported by post-hoc Tukey-Kramer comparison of means identifying between group significance following one way ANOVA ($p < 0.0033$) test with data from further genetic backgrounds).

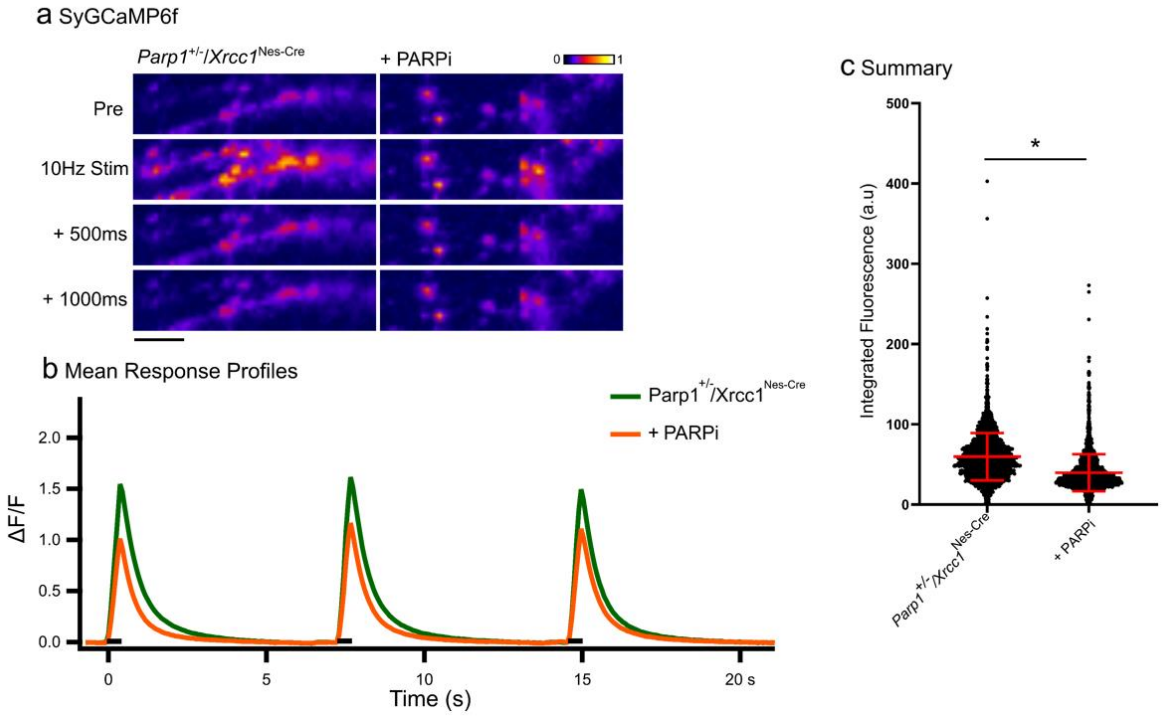

Figure 4.10 *The Impact of PARP Inhibition on Residual Aberrant Presynaptic Calcium Signalling in Parp1$^{+/-}$/Xrcc1$^{Nes-Cre}$ Hippocampal Neurons*. Investigations of mutant hippocampal neurons infected as above with SyGCaMP6f expressing AAV, prior to chronic incubation with a PARP inhibitor. A) Representative images of fluorescence responses in synaptic terminals expressing SyGCaMP6f to 10 AP (10 Hz) stimulation in DIV15-17 dissociated hippocampal neurons derived from *Parp1$^{+/-}$/Xrcc1*$^{Nes-Cre}$ mouse pups. Scale bar: 5 µm. B) Mean SyGCaMP6f responses to three rounds of 10 APs stimulation in *Parp1$^{+/-}$/Xrcc1*$^{Nes-Cre}$ control (2272 synapses, 9 coverslips, 3 animals) in green, and *Parp1$^{+/-}$/Xrcc1*$^{Nes-Cre}$ PARP inhibitor treated (1805 synapses, 8 coverslips, 3 animals) in orange. Response profiles plotted as ΔF/F, fluorescence intensity flux. Black bars along x-axis represent the starting point and duration of stimulation. C) Integrated Fluorescence as calculated by area under the curve in B). Mean and Standard Deviation represented in red, significance denoted as * where $p < 0.05$ (as reported by post-hoc Tukey-Kramer comparison of means identifying between group significance following one way ANOVA ($p < 0.0033$)).

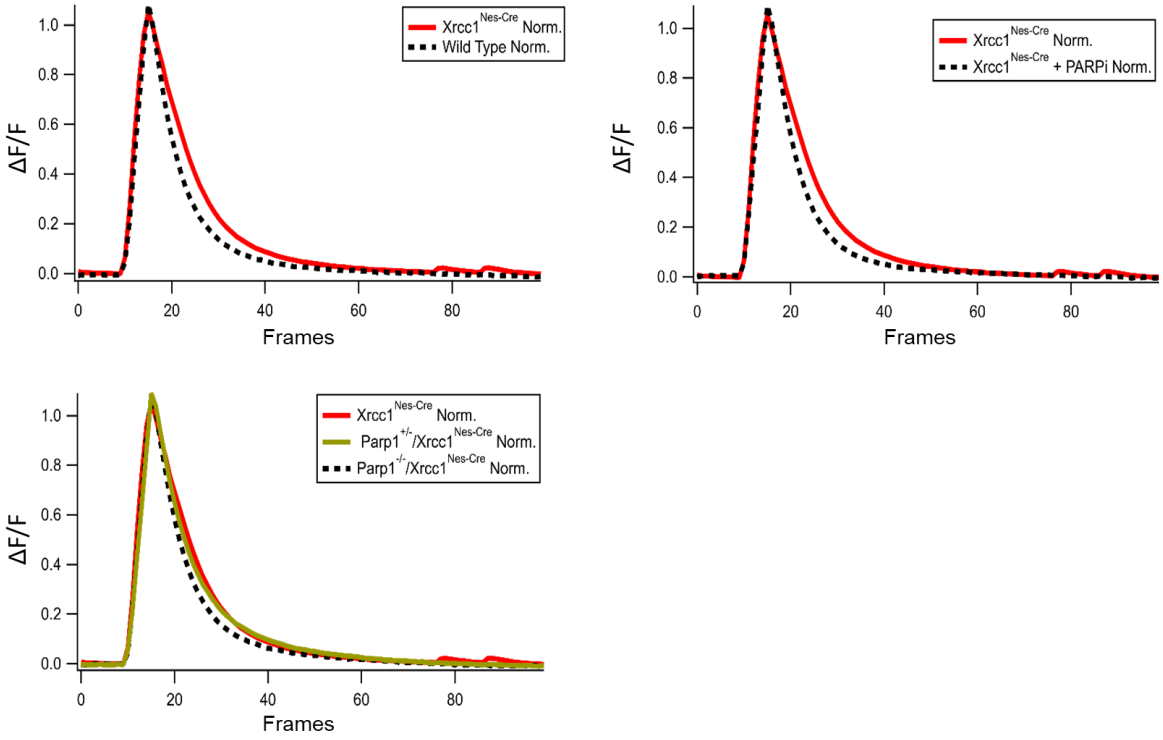

Figure 4.11 *Normalisation of Peak Amplitudes Highlights Elongated Decay Rate of Xrcc1$^{Nes\text{-}Cre}$ Ca^{2+} Transients.* Traces were each normalised to equivalent amplitudes to investigate length of decay rate. Amplitude represented as ΔF/F. Frames of response videos represented on the x axis. Data was pooled from all responses shown in 4.2, 4.6, and 4.8. Traces were overlayed, and show the slight, Parp1-dependent elongation of decay rate characteristic of activity-evoked Ca^{2+} transients in *Xrcc1*$^{Nes\text{-}Cre}$ hippocampal neurons.

unrelated to amplitude may reflect alterations in the machinery that regulate Ca^{2+} balance in the cell, such as the sequestration of calcium by Ca^{2+} ATPase pumps in the ER, or through mitochondrial voltage-dependent anion channels (VDAC), which facilitate the rapid reuptake of Ca^{2+} , modulating the amplitude and duration of cytosolic Ca^{2+} signalling (Vos, *et al*., 2010, Vandecaetsbeek, *et al*., 2011). This is potentially important because a delayed rate at which Ca^{2+} is removed from the presynaptic terminal could impact on the likelihood of future signal induction, especially given the highly non-linear relationship between [Ca^{2+}] and the probability of vesicle fusion; and that the presence of calcium at the presynaptic terminal can result in the increased efficiency of Ca^{2+} currents in subsequent evoked neurotransmitter release (Heidelberger, *et al*., 1994, Sakaba and Neher, 2001). Interestingly, this decreased decay rate is rescued by the deletion of either one or both alleles of *Parp1*, as well as by chronic PARP inhibition with KU0058948 (Figure 4.11), potentially implicating Parp1-dependent alterations to the mechanisms of calcium buffering and sequestration. This elongated decay rate may explain the presence of the unstimulated, AMPA/NMDA independent activity occurring exclusively in *Xrcc1*$^{Nes\text{-}Cre}$ hippocampal neurons. The release of calcium from intracellular stores is partially linked to calcium concentration, as both the IP3R mediated release of calcium from the ER and the opening of the MPTP are calcium dependent.

4.2.6 Acute Modulation of poly(ADP-ribose) Levels Does Not Alleviate the Synaptic Phenotype in *Xrcc1*$^{Nes\text{-}Cre}$ Hippocampal Neurons

I next sought to investigate the mechanism by which Parp1 activity might result in aberrant presynaptic Ca^{2+} signalling. To do so, SyGCaMP6f expressing hippocampal neurons were acutely treated for 1 hr with 10µM PARPi, which was washed out immediately prior to recording. Previously, I have showed that acute pre-treatment with a PARP inhibitor for 1 hr was sufficient to prevent the elevated accumulation of poly(ADP-ribose) at sites of DNA SSBs in the presence of a PARG inhibitor, indicating that polymer synthesis is constitutive and ongoing in *Xrcc1*$^{Nes\text{-}Cre}$ hippocampal neurons (Figure 3.6). However, an acute, 1 hr treatment with PARP inhibitor had no effect on the amplitude of activity-evoked presynaptic Ca^{2+} signalling in *Xrcc1*$^{Nes\text{-}Cre}$ hippocampal (Figure 4.12 A and B). This suggests that an acute increase in poly(ADP-ribose) is not sufficient to trigger aberrant presynaptic Ca^{2+} signalling, but rather it is likely the consequence of constitutive Parp1 activity for prolonged periods at sites of endogenous DNA SSBs in neurons. As such, aberrant presynaptic Ca^{2+} signalling can be chemically rescued through chronic, rather than acute, PARP inhibition (Figure 4.8 and Figure 4.12).

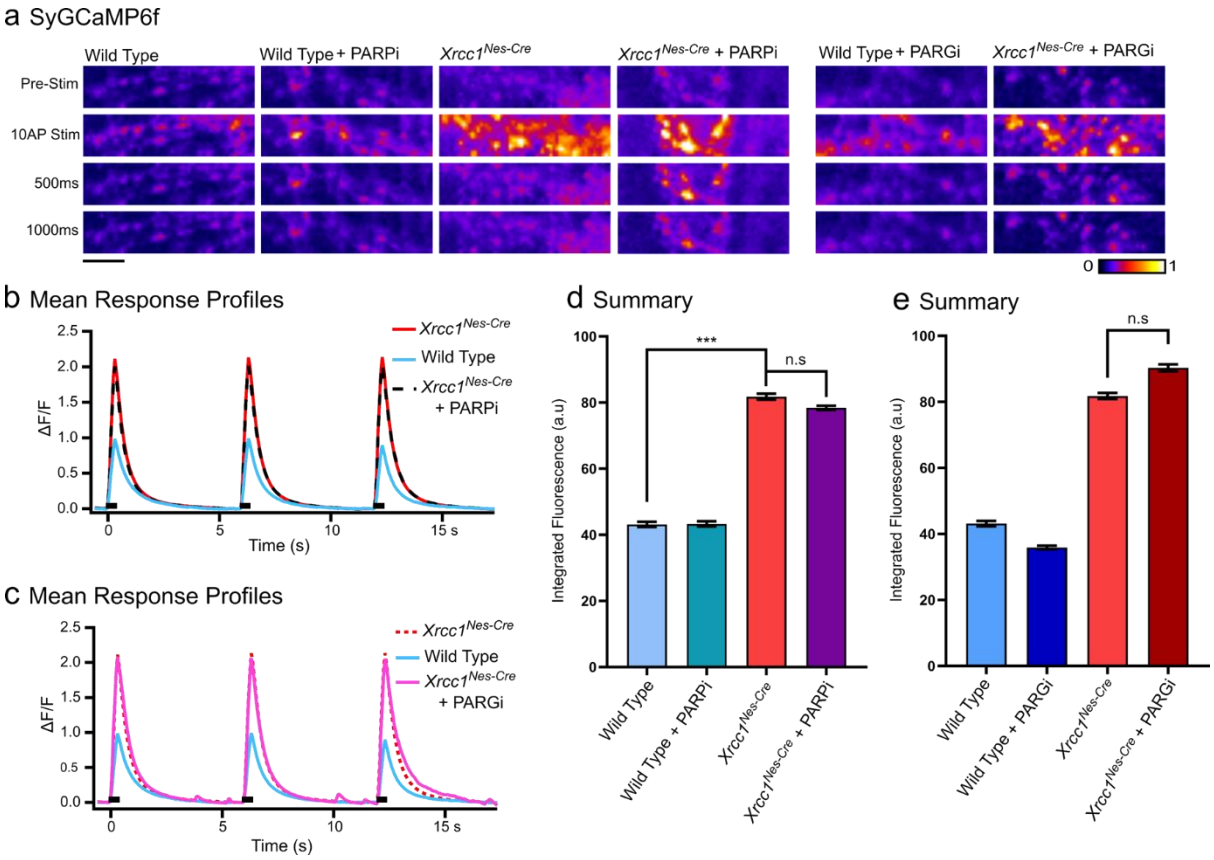

Figure 4.12 *The Acute Presence of poly(ADP-Ribose) Residues Does Not Result in Aberrant Presynaptic Calcium Signalling in Xrcc1*$^{Nes\text{-}Cre}$ *Hippocampal Neurons*. Investigations of mutant hippocampal neurons infected as above with SyGCaMP6f expressing AAV, prior to acute incubation with PARP and PARG inhibitors. A) Representative images of fluorescence responses in synaptic terminals expressing SyGCaMP6f to 10 AP (10 Hz) stimulation in DIV15-17 dissociated hippocampal neurons derived from wild type and *Xrcc1*$^{Nes\text{-}Cre}$ mouse pups, additionally treated for 1Hr with either a PARP or PARG inhibitor. Scale bar: 5 µm. B) and C) Mean SyGCaMP6f responses to three rounds of 10 APs stimulation from wild type control (n = 1541 synapses, 5 coverslips, 3 animals) in blue, *Xrcc1*$^{Nes\text{-}Cre}$ control (2635 synapses, 8 coverslips, 3 animals) in red, *Xrcc1*$^{Nes\text{-}Cre}$ PARP inhibitor treated (2278 synapses, 7 coverslips, 3 animals) in dotted black, and *Xrcc1*$^{Nes\text{-}Cre}$ PARG inhibitor treated (2359 synapses, 8 coverslips, 3 animals) in pink. Response profiles plotted as ΔF/F, fluorescence intensity flux. Black bars along x-axis represent the starting point and duration of stimulation. D) Mean Integrated Fluorescence as calculated by area under the curve in B) and C). Mean and SEM represented in red, $p > 0.05$ by Student's T-Test indicates non-significant data.

To confirm that the acute presence of poly(ADP-ribose) at sites of endogenous DNA-damage is not the source of elevated, aberrant presynaptic Ca^{2+} signalling, I treated cells with 10µM PARGi for 1 hr. I have shown that this acute treatment results in the accumulation of nuclear poly(ADP-ribose) in *Xrcc1*$^{Nes\text{-}Cre}$ cells (Figure 3.6), but found that this had no significant effect on the amplitude of activity-evoked Ca^{2+} transients in either wild type or mutant hippocampal neurons (Figure 4.12 C and E). This result confirms the previous hypothesis that the aberrant calcium signalling observed in *Xrcc1*$^{Nes\text{-}Cre}$ hippocampal neurons is unrelated to the acute presence of poly(ADP-ribose), and more likely a result of its constitutive synthesis by Parp1.

Taken together, our findings suggest that it is not the toxicity of poly(ADP-ribose) itself that results in aberrant Ca^{2+} signalling, and this provides further insight into the mechanism that is driving this deregulation. Chronic poly(ADP-ribosylation) may interfere with the transcription of genes regulating Ca^{2+} homeostasis, such as voltage-gated calcium channels, some of which have been implicated in the aetiology of spinocerebellar ataxia and epilepsy (Giunti, *et al*., 2015, Sintas, *et al*., 2017, Indelicato and Boesch, 2021). Similarly, the constitutive synthesis of poly(ADP-ribose) might also result in the chronic depletion of cellular NAD+. Consistent with this, the *Xrcc1*$^{Nes\text{-}Cre}$ brain is characterised by a significant decrease in NAD+ (Komulainen, *et al*., 2021).

4.2.7 Supplementation of *Xrcc1*$^{Nes\text{-}Cre}$ Hippocampal Neurons with the NAD+ Precursor NMN Partially Rescues Aberrant Presynaptic Ca^{2+} Signalling

I have previously shown that the supplementation with the NAD+ precursor NMN is sufficient to rescue PARG inhibitor toxicity in *Xrcc1*$^{-/-}$ RPE-1 cells, and previous studies have implicated NAD+ depletion in PARP1 mediated cell death (Figure 3.2) (Alano, *et al*., 2010). Further, brain NAD+ levels are significantly decreased in the *Xrcc1*$^{Nes\text{-}Cre}$ mouse (Komulainen, *et al*., 2021). Given the importance of NAD+ in the cell, and the rescue associated with NAD+ repletion in the Parp1-mediated deregulation of calcium homeostasis in the SCA7 mouse, I examined next whether NAD+ supplementation might restore normal Ca^{2+} signalling in *Xrcc1*$^{Nes\text{-}Cre}$ neurons (Stoyas, *et al*., 2020). To investigate this, I supplemented wild type and *Xrcc1*$^{Nes\text{-}Cre}$ hippocampal neurons expressing SyGCaMP6f with NMN for 9-11 days prior to recording. I observed that supplementation of cells with 500µM NMN partially suppressed the amplitude of activity-evoked Ca^{2+} transients in *Xrcc1*$^{Nes\text{-}Cre}$ hippocampal neurons (Figure 4.13). These data suggest that PARP1 hyperactivation at sites of endogenous DNA damage may trigger aberrant presynaptic Ca^{2+} signalling through the chronic depletion of cellular NAD+. It is interesting to note that NAD+ repletion achieved only partial rescue, reducing the

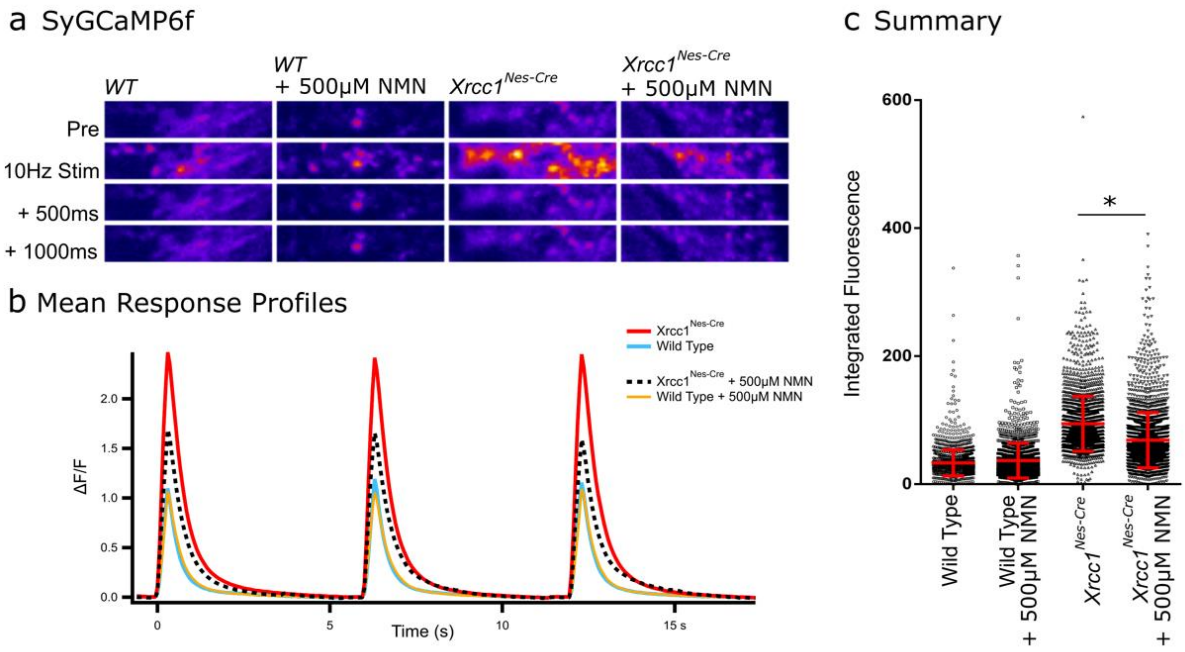

Figure 4.13 *The Impact of NAD+ Repletion on Aberrant Presynaptic Calcium Signalling in Xrcc1*$^{Nes\text{-}Cre}$ *Hippocampal Neurons*. Investigations of wild type and mutant hippocampal neurons infected as above with SyGCaMP6f expressing AAV, prior to chronic incubation with the NAD+ precursor NMN. A) Representative images of fluorescence responses in synaptic terminals expressing SyGCaMP6f to 10 AP (10 Hz) stimulation in DIV15-17 dissociated hippocampal neurons derived from wild type and *Xrcc1*$^{Nes\text{-}Cre}$ mouse pups. B) Mean SyGCaMP6f responses to three rounds of 10 APs stimulation in Wild Type control (1870 synapses, 8 coverslips, 3 animals), and NMN treated (1976 synapses, 8 coverslips, 3 animals) in orange, *Xrcc1*$^{Nes\text{-}Cre}$ control (n = 2163 synapses, 9 coverslips, 3 animals) and NMN treated (2602 synapses, 11 coverslips, 3 animals) in dotted black. Response profiles plotted as ΔF/F, fluorescence intensity flux. Black bars along x-axis represent the starting point and duration of stimulation. C) Integrated Fluorescence as calculated by area under the curve in B), Mean and Standard Deviation represented in red, significance denoted as * where $p < 0.05$ as reported by Student's t-test.

amplitude of activity-evoked transcripts to roughly 1.5-fold that of wild type hippocampal neurons. I suggest that this may be explained by the limitations of cellular NMN uptake, or the highly dynamic nature of poly(ADP-ribose) accumulation in *Xrcc1*$^{\text{Nes-Cre}}$ hippocampal neurons (Figure 3.6).

4.3 Discussion

The *Xrcc1*$^{Nes\text{-}Cre}$ mouse suffers intractable seizures that represent the primary limiting factor in its lifespan (Komulainen, *et al*., 2021). In chapter 3, I highlighted an elevated steady-state level of endogenous DNA SSBs in *Xrcc1*$^{Nes\text{-}Cre}$ hippocampal neurons, which exhibit an increased accumulation of nuclear poly(ADP-ribose). This Parp1-dependent accumulation in *Xrcc1*$^{Nes\text{-}Cre}$ hippocampal neurons replicated previous observations of poly(ADP-ribose) accumulation in the mouse hippocampus (Komulainen, *et al*., 2021). Given this accumulation, I aimed to investigate whether our cellular model of endogenous DNA SSBs could further be used to investigate signalling correlates of the *Xrcc1*$^{Nes\text{-}Cre}$ seizure phenotype at a synaptic level.

Alterations to Ca^{2+} homeostasis are found in several neurodegenerative diseases, such as Alzheimer's disease, Huntington's disease, and Spinocerebellar Ataxia (Small, 2009, Kasumu and Bezprozvanny, 2012, Kolobkova, *et al*., 2017, Stoyas, *et al*., 2020). The SCA7 mouse model is characterised by progressive cerebellar ataxia that has been linked to Parp1/NAD+ dependent aberrant Ca^{2+} signalling (Stoyas, *et al*, 2020). I identified a *Parp1* dependent manifestation of seizure-like activity in dissociated *Xrcc1*$^{Nes\text{-}Cre}$ hippocampal neurons; using SyGCaMP6f, demonstrating the increased amplitude of activity-evoked presynaptic Ca^{2+} transients (Figure 4.2, Figure 4.6 and Figure 4.8). To our knowledge, this is the first evidence to demonstrate a direct link between endogenous, nuclear DNA damage, Parp1 hyperactivation and alterations to synaptic signalling, and provides a cellular signalling correlate for the terminal seizures observed in the *Xrcc1*$^{Nes\text{-}Cre}$ mouse. The additional deletion of *Parp1* rescues the *Xrcc1*$^{Nes\text{-}Cre}$ mouse lifespan ~8-fold in *Parp1*$^{-/-}$/*Xrcc1*$^{Nes\text{-}Cre}$ mice, and ~25 fold in *Parp1*$^{+/-}$/*Xrcc1*$^{Nes\text{-}Cre}$ mice (Komulainen, *et al*., 2021). This data would suggest that the absence of Parp1 rescues the synaptic defect underlying this juvenile mortality, thereby greatly extending mouse lifespan. Interestingly, the intermediate rescue of both poly(ADP-ribose) accumulation, and excessive activity-evoked Ca^{2+} transients afforded by the heterozygous deletion of *Parp1* is sufficient to rescue lifespan.

PARP inhibitors are used clinically to treat a variety of cancers, their efficacy linked to their ability to trap PARP1 on DNA (Murai, *et al*., 2012, Sachdev, *et al*., 2019). While PARP inhibitors have been unable to significantly improve the lifespan of the *Xrcc1*$^{Nes\text{-}Cre}$ mouse (Komulainen, unpublished), I show here that PARP inhibition replicates Parp1 deletion in our cellular model, resulting in a reduction in amplitude of activity-evoked Ca^{2+} transients to the level which I observed in wild type hippocampal neurons (Figure 4.8 and Figure 4.9). While there are major limitations related to the

treatment of SSBR pathologies through PARP inhibition, namely an absence of clinically available, non-trapping inhibitors, these data would suggest that PARP inhibition might have potential as a viable therapy for XRCC1-mediated disease, as well as other SSBR-linked seizure pathologies, such as MCSZ, a disorder caused by mutations in *PNKP* (Shen, *et al,* 2010). Interestingly, while I show that chronic inhibition of Parp1 can rescue aberrant presynaptic Ca^{2+} signalling in *Xrcc1*$^{Nes\text{-}Cre}$ hippocampal cells, the fact that acute inhibition (which I have shown to ablate poly(ADP-ribose) accumulation in the cell) does not, would indicate that synaptic dysfunction is a consequence of long-term Parp1 activation, and likely unrelated to the acute presence of poly(ADP-ribose) at sites of endogenous DNA SSBs (Figure 4.12). Limitations in the treatment of *Xrcc1*$^{Nes\text{-}Cre}$ mice may be linked to the ability for PARP inhibitors to effectively cross the BBB, the toxicity associated with Parp1 trapping in the nervous system (potentially resulting in the stalling of transcriptive polymerases), and difficulties in the maintenance of inhibition; we show that poly(ADP-ribose) accumulation is highly dynamic and may require continuous administration of PARP inhibitors to effectively limit accumulation (Figure 3.6) (Shen, *et al*., 2015). The development of PARP inhibitors that limit PARP trapping and more closely phenocopy *Parp1* deletion might decrease the toxicity associated with PARP inhibitor treatment in mice. The administration of a PARP inhibitor *in vitro* affords an ideal cellular environment to test the efficacy of Parp1 inhibition on synaptic defects. Overcoming these obstacles in intact brain would be a major advancement in our understanding of the therapeutic potential of PARP inhibitors in XRCC1-mediated disease. Recently, successful maintenance of Parp1 inhibition has been shown to suppress seizure-like activity in the *ex vivo Xrcc1*$^{Nes\text{-}Cre}$ hippocampus (Komulainen, *et al*., 2021).

There are several potential mechanisms through which alterations to presynaptic calcium signalling could occur. Given that the amplitude of activity-evoked calcium transients is increased in *Xrcc1*$^{Nes\text{-}Cre}$ hippocampal neurons, perhaps this reflects the deregulated activity of neuronal ion channels. VGCCs are responsible for the influx of extracellular calcium following depolarisation (Atlas, 2013). The deregulated activity of VGCCs could explain the rapid influx of Ca^{2+} into the presynaptic terminal, and mutations in genes encoding VGCCs have been linked to both epilepsy and ataxia (Atlas, 2013, Morino, *et al*., 2015, Rajakulendran and Hanna, 2016). It is possible that the elevated influx of Ca^{2+} is a result of elongated depolarisation of the neuronal membrane, which could result in the persistent opening of VGCCs. Prolonged depolarisation could be linked to the deregulation of voltage gated K^+ channels (VGKCs) that facilitate the efflux of K^+ from the cell and, following an action potential, restore the membrane from a

depolarised level back to its resting potential (Köhling and Wolfart, 2016, Benarroch, 2021). In humans, VGKCs are encoded by 40 genes, mutations in many of which result in epilepsy and ataxia phenotypes (Lai and Yan, 2006). One notable VGKC is the large conductance calcium-activated potassium (BK) channel, which acts to transmit large volumes of K^+ ions across the membrane (Kshatri, *et al*., 2018). BK channels open in response to both electrical stimulation and increased cytosolic [Ca^{2+}], and function to restore the depolarised membrane to resting potential, thereby influencing the timing of membrane recovery following an action potential (Kshatri, *et al*., 2018). BK channels were found to be downregulated in the SCA7 mouse model, potentially implicating a role in the cerebellar calcium dyshomeostasis that characterises the ataxic mouse (Stoyas, *et al*., 2020). Due to the role of BK channels in restoring resting membrane potential, they are key regulators of neuronal excitability, and mutations in BK channels have been shown to result in a variety of phenotypes, including ataxia and epilepsy (Du, *et al*., 2005, Du, *et al*., 2020). Another potential source of irregularity in membrane excitability are voltage gated sodium channels (VGSCs), which are critical for the generation and propagation of APs throughout the neuron (de Lera Ruiz and Kraus, 2015). While VGSCs predominantly function in the depolarisation of the membrane, the persistent Na^+ current (leakage of a small percentage of Na^+ ions through inactivated channels) during the repolarising downstroke of an action potential contributes to neuronal excitability (Wengert and Patel, 2021). Alterations to the persistent Na^+ current result in aberrant excitability and have been linked to epilepsy (Hargus, *et al*., 2010).

The defective activity of any of these channels could result in the elevated influx of presynaptic calcium observed in *Xrcc1*$^{Nes\text{-}Cre}$ hippocampal neurons, either through direct (i.e the deregulation of VGCC activity resulting in the elevated influx of extracellular Ca^{2+}) or indirect means (through the elongation of depolarisation and subsequent increase in neuronal excitability), and mutations in many of the genes encoding these channels result in ataxia and epilepsy phenotypes similar to that which we observe in the *Xrcc1*$^{Nes\text{-}Cre}$ mouse. There are, as such, many different candidate proteins that could underlie the elevated activity-evoked calcium transients observed in *Xrcc1*$^{Nes\text{-}Cre}$ hippocampal neurons. To investigate whether the defect underlying aberrant presynaptic calcium signalling in these neurons is related to ion channels dysfunction, we should investigate the expression of these channels in the *Xrcc1*$^{Nes\text{-}Cre}$ hippocampus. For such a purpose, RNA sequencing is likely the most suitable method, as it will allow the high-throughput screening of genes encoding ion channels in the brain, which will be covered in the following chapter.

Another mechanism by which this dyshomeostasis may occur could be through deregulation of Ca^{2+} release from organelles, as well as sequestration and buffering mechanisms. The release of Ca^{2+} from the mitochondria occurs primarily through the Ca^{2+} dependent opening of the mitochondrial permeability transition pore, which allows the rapid efflux of small molecules (Mnatsakanyan, *et al*., 2017). Both the deregulation of the MPTP, and mutations in proteins facilitating mitochondrial Ca^{2+} uptake have been linked to ataxia and neurodegeneration (Logan, *et al*., 2014, Kalani, *et al*., 2018). The release of Ca^{2+} from the ER occurs primarily through IP3Rs, which facilitate the release of ER-calcium in the presence of both calcium and inositol triphosphate, and RyRs, which are activated by cADPr (the NAD+ dependent synthesis of which is catalysed by CD38) (Padamsey, *et al*., 2018, Hogan, *et al*., 2019). Both IP3Rs and RyRs have been implicated in cerebellar ataxia and epilepsy (Matsumoto, *et al*., 1996, Liu, *et al*., 2009, Kushnit, *et al*., 2018). Intracellular organellar calcium stores, such as the ER, mitochondria, and acidic lysosomes, also act to buffer and sequester ionic calcium at the presynaptic terminal, allowing the spatial and temporal modulation of the calcium signal (Padamsey, *et al*., 2018). The presynaptic terminal is rich in mitochondria which, when hyperpolarised, facilitate the sequestration of cytosolic calcium via a uniporter across the electrochemical gradient (Datta and Jaiswal, 2021). Similarly, the ER acts to sequester cytosolic Ca^{2+} through SERCAs, Ca^{2+}-ATPases which maintain the $[Ca^{2+}]$ in the ER lumen (Karagas and Vankatachalam, 2019). Given that the relationship between $[Ca^{2+}]$ and release probability is highly non-linear, the effects of defective buffering and sequestration could have drastic consequences upon further stimulation (Heidelberger, *et al*., 1994, Sakaba and Neher, 2001). To examine whether defective mechanisms of buffering and sequestration may underpin the Ca^{2+} dyshomeostasis and elongation of Ca^{2+} transient decay rate in *Xrcc1*$^{Nes\text{-}Cre}$ hippocampal neurons, we could utilise optical reporters to investigate Ca^{2+} dynamics in organelles. To investigate whether the influx and efflux of Ca^{2+} in the mitochondria may be deregulated in *Xrcc1*$^{Nes\text{-}Cre}$ hippocampal neurons, future work could involve the utilisation of Rhod-2/AM, a Ca^{2+} sensitive dye (Lopez-Manzaneda, *et al*., 2021). Similarly, we could utilise CatchER to investigate the dynamics of Ca^{2+} flux in the ER (Tang, *et al*., 2011). Through these dyes, we could investigate whether the organelle mediated release or sequestration of Ca^{2+} upon stimulation is deregulated in *Xrcc1*$^{Nes\text{-}Cre}$ hippocampal neurons. We could further utilise these dyes to investigate the source of unstimulated Ca^{2+} signalling in *Xrcc1*$^{Nes\text{-}Cre}$ hippocampal neurons; given that Ca^{2+} release from both the mitochondria and ER are Ca^{2+} dependent, perhaps the excessive activity evoked influx of Ca^{2+} results in smaller, spontaneous Ca^{2+} release events from organelles (Padamsey, *et al*., 2018).

Previous work in mitotic, human RPE-1 cells has demonstrated that *XRCC1*-dependent sensitivity to PARG inhibition could be rescued via the repletion of NAD+ with the precursor NMN. Stoyas, *et al*., suggested that the aberrant Ca^{2+} signalling underlying the cerebellar pathology of the SCA7 mouse was a result of cellular NAD+ depletion, proposing that the limited bioavailability of the molecule resulted in the inhibition of SIRT1. SIRT1 is an NAD+ dependent, nuclear deacetylase, which works to deacetylate transcription factors involved in regulating the expression of genes linked to longevity and cellular homeostasis (Elibol and Kilic, 2018). While SIRT1 and PARP1 have a similar affinity for NAD+, given that the induction of DNA-damage can significantly increase PARP1 levels, elevated endogenous SSBs will likely result in PARP1 outcompeting SIRT1 for use of the co-factor, which likely explains the significantly decreased levels of NAD+ in the *Xrcc1*$^{Nes\text{-}Cre}$ brain (Mendelsohn and Larrick, 2017, Komulainen, *et al*., 2021). One target of SIRT1 is PGC-1α, which is a further regulator of several genes involved in Ca^{2+} homeostasis, such as *ITPR1*; which encodes the IP3 receptor, and *CACNA1G*, which encodes $Ca_v3.1$, a low-voltage activated, t-type calcium channel primarily found in the cerebellum and thalamic neurons, and linked to progressive ataxia, but still expressed in the hippocampus (Rodgers, *et al*., 2005, Gao, *et al*., 2012, Stoyas, *et al*., 2020). In the case of the SCA7 mouse, both NAD+ repletion and SIRT1 overexpression are sufficient to rescue the aberrant calcium signalling that characterises the model (Stoyas, *et al*., 2020). CD38 also utilises NAD+ as a cofactor, catalysing the synthesis of both cADPr and NAADP from NAD+ and nicotinic acid respectively, both of which act as second messengers to modulate cytosolic [Ca^{2+}] via its release from organelles, such as the ER (Hogan, *et al*., 2019, Guerreiro, *et al*., 2020). Through the supplementation of the NAD+ precursor, NMN, I show significant suppression of elevated activity-evoked Ca^{2+} transients, suggesting that NAD+ depletion by chronic poly(ADP-ribosylation) may be partly responsible for aberrant Ca^{2+} signalling in *Xrcc1*$^{Nes\text{-}Cre}$ hippocampal neurons (Figure 4.13).

To investigate the effects of NAD+ repletion in the *Xrcc1*$^{Nes\text{-}Cre}$ mouse, I undertook a small pilot study investigating the impact of intraperitoneal NMN administration. Mice were injected daily with either 30µg/kg NMN, 50µg/kg NMN, or a PBS control. Our pilot study failed to identify any clear indication of the efficacy of NMN administration in the elongation of the *Xrcc1*$^{Nes\text{-}Cre}$ lifespan, with all treated mice reaching humane endpoint by p21, within the range expected of the *Xrcc1*$^{Nes\text{-}Cre}$ mouse (data not shown). While we did not directly observe seizures in NMN treated mice, they continued to exhibit profound ataxia and progressive weight loss characteristic of the *Xrcc1*$^{Nes\text{-}Cre}$ mouse (Badman, J. Komulainen, E. unpublished observations). The limitations of this treatment may be

similar to those of PARP inhibitor administration, perhaps the uptake of NMN into the brain is limited in capacity and cannot keep up with the critical demand for NAD+ in cells that are constitutively synthesising poly(ADP-ribose). Regardless, we cannot, as yet, conclude whether NAD+ may have therapeutic applications in the treatment of Xrcc1-linked pathology

In future, to further investigate the synaptic phenotype of *Xrcc1*$^{Nes\text{-}Cre}$ hippocampal neurons, separate optical reporters should be employed. These reporters, such as SypHy (a pHluorin based reporter that enables the visualisation of vesicle exo- and endocytosis through pH-linked fluorescence change) and iGluSnFr (a fluorescence-based reporter of synaptic glutamate transmission), may highlight the downstream consequences of aberrant presynaptic calcium signalling on vesicle fusion and neurotransmitter release (Hempel, *et al*., 2011, Marvin, *et al*., 2013, Jackson and Burrone, 2016, Marvin, *et al*., 2018). Both vesicle fusion and neurotransmitter release are key elements of synaptic signalling, and as such may provide greater insight into the synaptic irregularities that underlie the *Xrcc1*$^{Nes\text{-}Cre}$ seizure phenotype. We are, however, limited in scope by the inherent sensitivity of dissociated *Xrcc1*$^{Nes\text{-}Cre}$ hippocampal neurons. As I have previously reported, *Xrcc1*$^{Nes\text{-}Cre}$ hippocampal neurons exhibit spontaneous death *in vitro*, and my previous attempts made to induce expression of SypHy and iGluSnFr resulted in the total death of cultured mutant neurons. It is, as yet, unclear why I was able to achieve consistent expression of SyGCaMP6f in viable *Xrcc1*$^{Nes\text{-}Cre}$ neurons, while other reporters resulted in cell death. Another reporter of interest would be PSDGCaMP6f, an indicator of postsynaptic calcium flux (NMDAr mediated postsynaptic calcium signalling is a key regulator of activity-dependent plasticity and, by extension, the excitability of neuronal systems); however, this again resulted in the death of *Xrcc1*$^{Nes\text{-}Cre}$ hippocampal cultures (Topolnik and Camiré, 2019). Given the infrequent acquisition of cultured, mutant neurons, future work on separate optical reporters might be more viable in wild type neurons, with *Xrcc1* knocked down, or in IPSCs expressing the disease mutation associated with AOA-*XRCC1*. This would, however, still be limited in scope; as the AOA-XRCC1 patients retain a residual degree of XRCC1 function, a factor which may explain the absence of seizures in disease patients when compared to the *Xrcc1*$^{Nes\text{-}Cre}$ mouse, which has total deletion of the protein in brain (Hoch, *et al*., 2017).

4.3.1 Conclusion

Following from the observation that dissociated *Xrcc1*$^{Nes\text{-}Cre}$ hippocampal neurons exhibited elevated steady-state levels of endogenous DNA SSBs, as in the *Xrcc1*$^{Nes\text{-}Cre}$ mouse brain; I sought to investigate whether synaptic signalling correlates of the *Xrcc1*$^{Nes\text{-}Cre}$ seizure phenotype could be identified *in vitro*. To do so, I utilised a genetically encoded, optical reporter of calcium flux to highlight aberrant, presynaptic calcium signalling in *Xrcc1*$^{Nes\text{-}Cre}$ hippocampal neurons, providing a compelling potential explanation for the seizures observed in the mutant mouse, as well as being, to our knowledge, the first mechanistic link between endogenous DNA damage, Parp1 activation, and synaptic dysfunction. Genetic rescue of this synaptic phenotype via the deletion of *Parp1* may underlie the absence of observed seizure activity and subsequent drastic increase in lifespan associated with both the *Parp1*$^{+/-}$*/Xrcc1*$^{Nes\text{-}Cre}$ and *Parp1*$^{-/-}$*/Xrcc1*$^{Nes\text{-}Cre}$ mouse (Komulainen, *et al*., 2021). I propose that this phenotype may, in part, be caused by the depletion of cellular NAD+ through the continuous synthesis of poly(ADP-ribose) and highlight partial rescue through the administration of the NAD+ precursor, NMN. A separate, though not mutually exclusive, possible mechanism underlying this synaptic phenotype could be through Parp1-dependent alterations to transcription, and subsequent alteration to the expression of proteins critical in the regulation of neuronal signalling and calcium homeostasis. Finally, I note the efficacy of PARP inhibition in the treatment of this observed synaptic phenotype, and as such again highlight the potential viability of PARP inhibitors in the treatment of *XRCC1*-mediated neurodegeneration. The data in this chapter therefore contribute to our understanding of SSBR mediated neuropathology and may have consequences for its treatment in future.

5. Chapter Five: Results – Altered Gene Expression in the *Xrcc1*$^{Nes\text{-}Cre}$ Mouse Brain

5.1 Introduction and Aims

PARP1 is a ubiquitous nuclear enzyme that, alongside facilitating the recruitment of the SSBR machinery, acts in the regulation of gene expression due to its interaction with chromatin (Kraus, 2008, Matveeva, *et al*., 2019). Chromatin is comprised of arrays of nucleosomes (a section of DNA tightly wrapped around histone octamers) and nucleosome binding proteins that function to regulate gene expression by regulating RNA Pol II loading at gene promoters and facilitating the initiation of transcription from transcription start sites (TSS) (Kulaeva, *et al*., 2007, Nagai, *et al*., 2017). PARP1 binds the nucleosome, promoting alterations to chromatin structure to facilitate the regulation of gene expression through changes to nucleosome spacing (Sultanov, *et al*., 2017, Thomas, *et al*., 2019). While the enzymatic activity of PARP1 is predominantly linked to autoribosylation, numerous other targets of transribosylation have been described, such as core histones, linker histone, and numerous other proteins involved in the regulation of gene expression (Kraus and Hottiger, 2013). poly(ADP-ribosylation) of SNF2 Family ATPase Amplified in Liver Cancer 1 (ALC1) results in the formation of a stable ALC1:PARP1 intermediate that acts to regulate nucleosome remodelling (Gottschalk, *et al*., 2012, Ooi, *et al*., 2021). Autoribosylation further acts to regulate the effects of PARP1 on the transcriptome, as highly ribosylated PARP1 is limited in its ability to bind nucleosomes, with the high turnover of poly(ADP-ribose) facilitating a dual role for active PARP1 in the regulation of transcription and in the repair of DNA damage (Beneke, 2012, Muthurajan, *et al*., 2014). Through the regulation of histone acetylation, PARP1 can also regulate posttranslational covalent modification of the nucleosome core, further impacting chromatin organisation and, subsequently, gene expression (Verdone, *et al*., 2015, Ciccarone, *et al*., 2017).

The poly(ADP-ribosylation) of sequence-specific DNA binding factors further enables the direct regulation of transcription by PARP1 (Pahi, *et al*., 2020). The inherently labile nature of poly(ADP-ribose) modification has made the identification of poly(ADP-ribosyl)ated substrates difficult (Bock and Chang, 2016). SMAD3 and SMAD4 are known substrates of PARP1 (Dahl, *et al*., 2014). SMAD3/4 are poly(ribosyl)ated by PARP1, resulting in the dissociation of the SMAD complex from DNA, attenuating SMAD-specific gene expression, thereby acting in the indirect regulation of TGF-β signalling (downstream effectors of which include regulators of cell death and differentiation) (Lönn, *et al*., 2010, Dahl, *et al*., 2014). Similarly, the poly(ADP-

ribosylation) of NELF (negative elongation factor) promotes its release from stalled RNA Pol II to facilitate RNA production and elongation (Gibson, *et al*., 2016). The interaction of PARP1 with transcription factors is not always the result of poly(ADP-ribosylation), as PARP1 has been reported to bind two separate motifs of the FOXO1 (Forkhead box O1) promoter, a transcription factor critical in the regulation of many cellular processes, such as gluconeogenesis and apoptosis, in a polymerase independent manner (Tikhanovich, *et al*., 2013, Tian, *et al*., 2020). In response to DNA damage, poly(ADP-ribosylation) leads to the recruitment of both repressive polycomb and NuRD complexes, regulators of gene transcription, to facilitate repair (Chou, *et al*., 2010, Hoffman and Spengler, 2019, Piunti and Shilatifard, 2021). From these studies, it is clear that PARP1 plays a key role in the regulation of gene expression, either by structural alteration of the nucleosome or by posttranslational modification of transcription factors. In the case of Xrcc1 deficiency, we propose that the hyperactivation of Parp1 at sites of endogenous DNA damage may interfere with the intrinsic role of Parp1 in the regulation of transcription.

In *Xrcc1*$^{Nes\text{-}Cre}$ hippocampal neurons, I detected the Parp1/NAD+ dependent deregulation of synaptic signalling. NAD+ is a co-factor of Parp1, utilised in the synthesis of poly(ADP-ribose) (Murata, *et al*., 2019). Previous studies of the *Xrcc1*$^{Nes\text{-}Cre}$ brain have identified a ~50% reduction in total brain NAD+ (Komulainen, *et al*., 2021). NAD+ is used as a co-factor by several other proteins in the cell, one such being SIRT1. The sirtuins are a family of ADP-ribosyltransferases and NAD+ dependent protein deacetylases, functioning as critical regulators of metabolism, senescence, and the cell stress response (Elibol and Kilic, 2018). SIRT1 has been shown to regulate chromatin structure through the NAD+ dependent deacetylation of core histones (Zhang and Kraus, 2010, Bosch-Presegue and Vaquero, 2015). Similarly, SIRT1 facilitates histone and DNA CpG methylation to repress transcription via the recruitment of nuclear enzymes to chromatin, suggesting a broad function in epigenetic regulation (Rifai, *et al*., 2018, Li, *et al*., 2020). SIRT1 also functions to deacetylate many transcription factors and coregulators (Zhang and Kraus, 2010). These targets are varied and contribute to the heterogeneous nature of epigenetic regulation by Sirtuins. For example, the NAD+ dependent deacetylation of PGC-1α results in the co-activation of various transcription factors, such as FOXO1, resulting in the regulation of numerous cellular processes, such as gluconeogenesis, mitochondrial biosynthesis, and cellular respiration (Tikhanovich, *et al*., 2014, Zhou, *et al*., 2017).

Alterations in the Sirt1/PGC-1α signalling pathway have been linked to synaptic failure in AD models (Panes, *et al*., 2020). The key regulator of SIRT1 function is the

cellular energy state, specifically NAD+ metabolism, as the decreased bioavailability of NAD+ (or, it has been proposed, the elevated presence of nicotinamide (NAM), a byproduct of PARP1 and SIRT1 activity), inhibits the activity of SIRT1 (Imai and Guarente, 2016). Recently, Stoyas *et al*., proposed that Parp1-dependent NAD+ depletion in the SCA7 mouse model preceded the reduced activity of Sirt1 and, subsequently, the decreased expression of several genes involved in calcium homeostasis, downstream of transcription factors containing Sirt1 binding sites. In the SCA7 mouse, both the overexpression of Sirt1 and treatment with the NAD+ precursor nicotinamide riboside (NR) resulted in the partial elongation of mouse lifespan, and the reversal of calcium-dependent motor impairments (Stoyas, *et al*., 2020).

A further mechanism by which Xrcc1 deficient cells might exhibit deregulated transcription is through the challenges faced by transcriptive polymerases, such as RNA Pol II, in bypassing unrepaired SSBs. The induction of oxidative DNA damage in nuclear extracts has been shown to inhibit RNA Pol II progression, indicating that the elevated presence of DNA SSBs in cells might result in deregulated transcription (Kathe, *et al*., 2004). Interestingly, the ability of RNA Pol II to bypass breaks appears to be dependent on 3' end chemistry of the lesion, with the chemistry of the 5' end lesion being of seemingly little importance (Sordet, *et al*., 2008, Neil, *et al*., 2012). Similarly, SSBs introduced at AP sites result in stalled polymerase progression (Zhou and Doetsch, 1993). Bulky 3' lesions are sufficient to induce transcriptional arrest. These bulky lesions include the Top1cc and 3'-phosphoglycolates formed by radical-mediated cleavage of DNA and processed by TDP1 and APE1, respectively (Parsons, *et al*., 2004, Zhou, *et al*., 2005, Sordet, *et al*., 2008). The ability of certain forms of SSB to induce transcription arrest could be relevant to Xrcc1-deficient cells, particularly neurons, as they may continue to accumulate unrepaired breaks across their lifespan, potentially resulting in the stalling of RNA Pol II during transcription. Wu, *et al*., recently identified site-specific SSBs at sites of neuronal enhancers in Xrcc1 deficient rat and human neurons. They propose that these site-specific breaks may be the result of active demethylation (the epigenetic modification of CpG enriched sites via the TET-dependent progressive oxidation of 5-methylcytosine through TDG1 initiated BER and the formation of XRCC1-associated SSB intermediates) (He, *et al*., 2011, Wu and Zhang, 2017). Increasing evidence has suggested that active demethylation in the brain is dependent on neuronal activity, and tenfold more frequent in neuronal cells, possible explaining the appearance of site-specific SSBs predominantly in neuronal enhancers (Kraucionis and Heintz, 2009, Bayraktar and Kreutz, 2018, Wu, *et al*., 2021). Recently, PARP1 activation as a consequence of XRCC1 loss was found to directly result in transcription inhibition during

BER, by promoting the excessive recruitment and activity of ubiquitin protease USP3, resulting in decreased levels of monoubiquitinated histones required for transcription regulation (Adamowicz, *et al*., 2021). These data have identified PARP1-dependent alterations to transcription in cells lacking XRCC1 and support the notion that aberrant transcription may be identified in the *Xrcc1*$^{Nes\text{-}Cre}$ brain.

PARP1 is capable of regulating transcription through many mechanisms, such as direct interaction with the nucleosome, and through the posttranslational modification of histones and transcriptional regulators. Similarly, the potential downstream consequences of poly(ADP-ribosylation), such as NAD+ may interfere with ordinary transcription. Given these roles of PARP1 in the regulation of transcription, we propose that hyperactivity of Parp1 associated with Xrcc1 deficiency may result in alterations to transcription in the *Xrcc1*$^{Nes\text{-}Cre}$ brain. The aim of this chapter is to investigate whether aberrant gene expression in the brain might underlie the episodic ataxia and terminal seizures that characterise the *Xrcc1*$^{Nes\text{-}Cre}$ mouse, as well as the aberrant presynaptic calcium signalling identified in cultured *Xrcc1*$^{Nes\text{-}Cre}$ hippocampal neurons. To do so, I examined the expression of numerous proteins involved in neuronal function and calcium homeostasis in the brain. Following this, using RNA sequencing, I investigated mRNA levels in the *Xrcc1*$^{Nes\text{-}Cre}$ hippocampus, to examine whether transcriptional alterations may contribute to the mouse phenotype.

5.2 Results

5.2.1 Alterations in Protein Levels in the *Xrcc1*$^{Nes\text{-}Cre}$ Mouse Brain

Following the observation that *Xrcc1*$^{Nes\text{-}Cre}$ hippocampal neurons exhibit altered pre-synaptic calcium signalling, and with evidence of aberrant gene expression in separate models of cerebellar ataxia, I reasoned that alterations in protein expression might underlie defective signalling in the *Xrcc1*$^{Nes\text{-}Cre}$ mouse brain (Stoyas, *et al*., 2020) (Figure 4.2). To investigate this, I first verified that *Xrcc1*$^{Nes\text{-}Cre}$ mice were lacking Xrcc1 in whole brain extracts, and that Parp1 was expressed in these extracts but absent from those in which the *Parp1* gene was additionally deleted (Figure 5.1). Following this, mice were sacrificed at p15, at which point their brains were dissected into cortices, cerebella, and hippocampi which were snap frozen in liquid nitrogen prior to protein lysates being fractionated by SDS-PAGE and immunoblotted with appropriate antibodies.

5.2.1.1 IP3R

Alongside intractable seizures, the *Xrcc1*$^{Nes\text{-}Cre}$ mouse is characterised by progressive ataxia. Ataxia is highly heterogeneous, with several mutations known to result in cerebellar ataxia phenotypes (Pilotto and Saxena, 2018, Bird, 2019). Inositol triphosphate receptors (IP3R) are membrane glycoproteins that act as Ca^{2+} channels upon binding inositol triphosphate, leading to the release of calcium from intracellular stores (Foskett, *et al*., 2007, Paknejad and Hite, 2018). Mutations in *ITPR1*, which encodes IP_3R1, the main neuronal isoform of the receptor, result in the autosomal dominantly inherited spinocerebellar ataxias, SCA15 and SCA29 (Marelli, *et al*., 2011, Zambonin, *et al*., 2017). IP3R1 expression is 7-fold lower in the cerebellum of human AT patients (Lee, *et al*., 2021). Recently, a mouse model was reported in which DNA polymerase β (POLβ) and *Atm* deletion resulted in profound ataxia and juvenile mortality, purportedly due to the deregulation of *Itpr1* transcription and the subsequent effects of IP_3R1 loss in cerebellum, possibly due to the impact on calcium homeostasis (Kim, *et al*., 2020). Further, IP_3 related alterations to cytosolic calcium are linked to both SCA2 and SCA3 (Bezprozvanny, 2010). IP_3R1 is most abundantly expressed in cerebellar PCs, where its role in the modulation of Ca^{2+} release from intracellular stores regulates dendritic spine morphology and the maintenance of cerebellar circuitry, however it is expressed across the brain (Sugaware, *et al*., 2013, Segal and Korkotia, 2014). In the mouse hippocampus, genetic deletion of IP3K-A, a protein kinase responsible for the regulation of inositol triphosphate signalling, results in pronounced synaptic plasticity defects, likely the result of deregulation of the cytosolic calcium pool

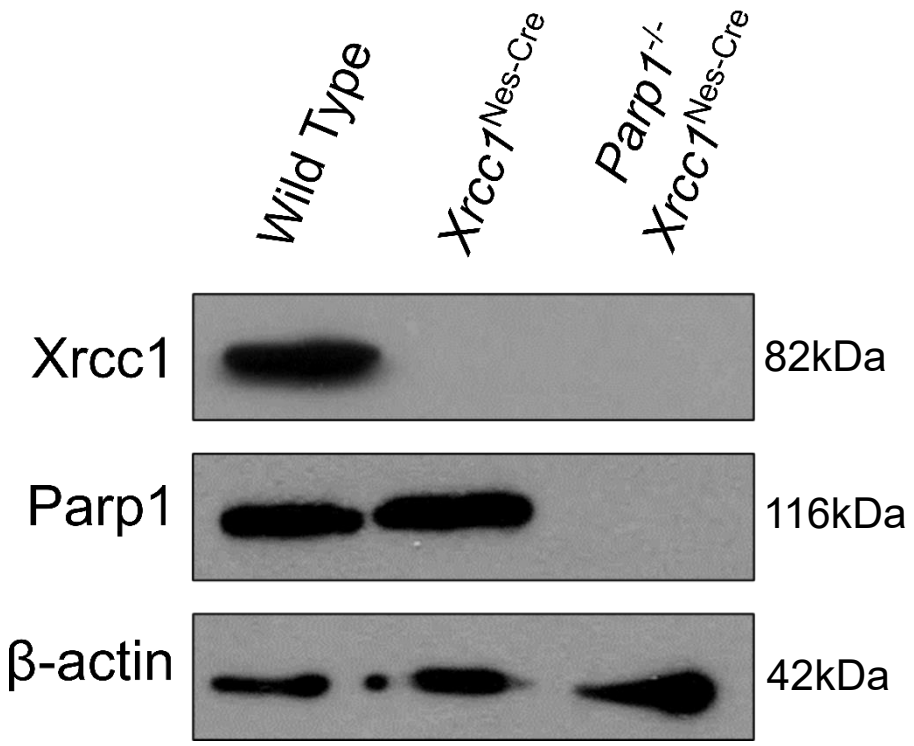

Figure 5.1 *Confirmation of Xrcc1 and Parp1 deletion in mutant mice*. Western blot analysis of Xrcc1 and Parp1 expression in whole brain extracts taken from p15 wild type, *Xrcc1*$^{Nes\text{-}Cre}$ and *Parp1*$^{-/-}$/*Xrcc1*$^{Nes\text{-}Cre}$ mice. β-actin used as loading control.

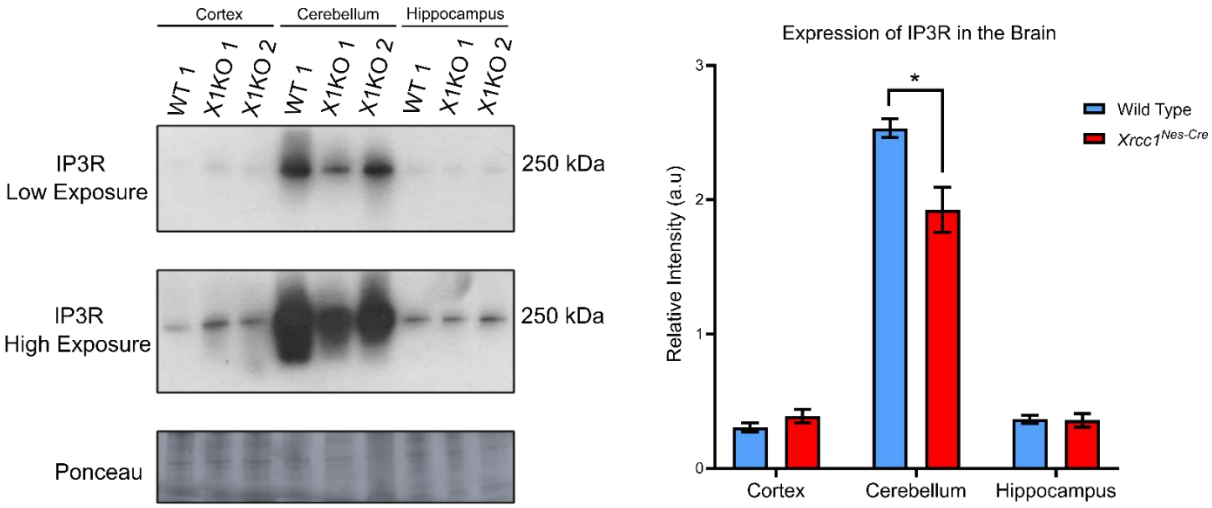

Figure 5.2 *Decreased Levels Inositol Triphosphate Receptors in the Xrcc1*$^{Nes\text{-}Cre}$ *Cerebellum.* Left: Western blot analysis of IP3R in cortical, cerebellar, and hippocampal tissues taken from p15 wild type and *Xrcc1*$^{Nes\text{-}Cre}$ mice, highlighting decreased IP3R in the *Xrcc1*$^{Nes\text{-}Cre}$ cerebellum. Blots shown are representative of 1 wild type and 2 separate *Xrcc1*$^{Nes\text{-}Cre}$ brains. Ponceau S staining served as a loading control. Right: Quantification of IP3R expression in cortical, cerebellar, and hippocampal tissues from wild type and *Xrcc1*$^{Nes\text{-}Cre}$ brains, n = 3 mice, blot images from remaining brains not shown in (A). Statistical significance is denoted as * where $p < 0.05$ by student's t-test. Histogram shows mean ± SEM.

(Choi, *et al*., 2018). Indeed, overexpression of IP3K-A kinase results in the amplification of vesicle pool size, and an increase in evoked presynaptic release probability (Choi, *et al*., 2018). Given that I have demonstrated aberrant presynaptic calcium signalling in cultured *Xrcc1*$^{Nes\text{-}Cre}$ hippocampal neurons, I wondered if alterations in calcium homeostasis may underlie the cerebellar ataxia that characterises the *Xrcc1*$^{Nes\text{-}Cre}$ mouse, which could be linked to defective InsP3 signalling.

For the above reasons, I proposed that I might observe alterations in IP3R expression in *Xrcc1*$^{Nes\text{-}Cre}$ mouse brain, and that such an alteration might underlie elements of both progressive cerebellar ataxia and aberrant presynaptic calcium signalling. Following lysis and immunoblotting of *Xrcc1*$^{Nes\text{-}Cre}$ cortical, cerebellar, and hippocampal samples. I observed a significant reduction in the level of the 250kDa IP3R isoform in the *Xrcc1*$^{Nes\text{-}Cre}$ cerebellum (Figure 5.2). IP3R expression was not altered in either cortical or hippocampal tissue. The reduced expression of IP3R is interesting, as it may explain certain elements of the *Xrcc1*$^{Nes\text{-}Cre}$ phenotype, such as cerebellar ataxia, given the ubiquity of IP3R deregulation in cerebella ataxia phenotypes (Bezprozvanny, 2010).

5.2.1.2 GRID2IP

Following the discovery that the cerebella of *Xrcc1*$^{Nes\text{-}Cre}$ mice exhibit decreased expression of IP3R, I sought to investigate the expression of further proteins involved in the regulation of PC signalling. Glutamate Receptor Ionotropic Delta 2 Interacting Protein (GRID2IP) is involved in the regulation of GRID signalling, expressed exclusively at parallel fibre PC synapses (Miyagi, *et al*., 2002, Takeuchi, *et al*., 2008). The name is a misnomer, as GRID signalling is unrelated to glutamate, with their endogenous ligand suggested to be D-serine which, upon binding, induces conformational changes required for non-ionotropic signalling (Chin, *et al*., 2020). GRID and GRID2IP are predominantly expressed in PCs, and function in the regulation of motor co-ordination, synaptogenesis, and synaptic plasticity (Takeuchi, *et al*., 2008, Ichikawa, *et al*., 2016). Mutations in *Grid2* result in the ‘lurcher’ mouse, characterised by defective co-ordination and ataxia as a result of apoptotic PC death (Vogel, *et al*., 2007, Zanjani, *et al*., 2009). In humans, *GRID2* mutation is linked to progressive ataxia, ocular motor apraxia, and lower motor neuron involvement, demonstrating striking similarity to several conditions associated with hereditary defects in SSBR, including patients harbouring mutations in XRCC1 (Coutelier, *et al*., 2015, Hoch, *et al*., 2017, Veeranpandiyan, *et al*., 2017). While the function of GRID2IP is somewhat unclear, it appears to facilitate the surface expression of GRID2 at parallel fibre PC synapses (Matsuda, *et al*., 2006).

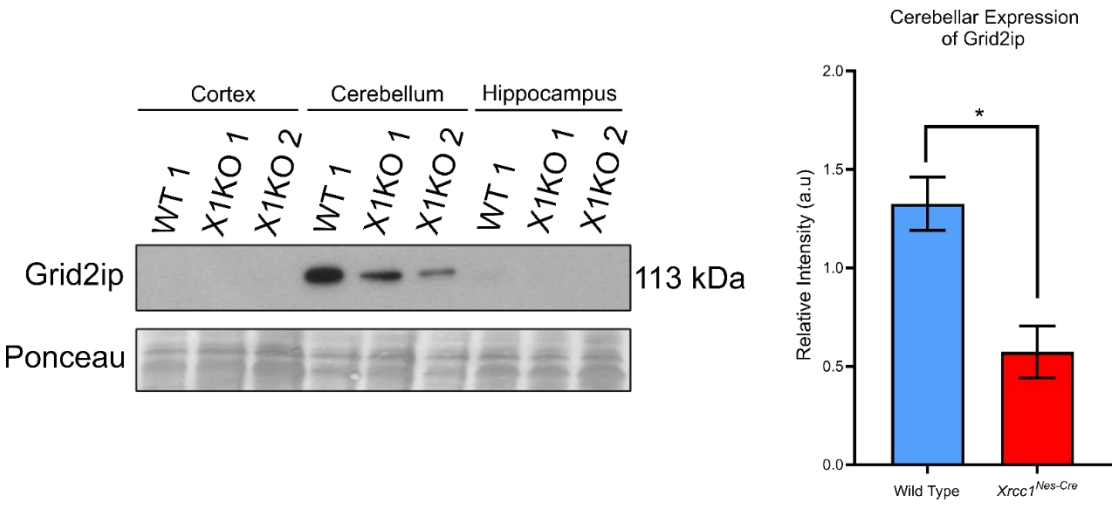

Figure 5.3 *Decreased Levels of Grid2ip in Xrcc1$^{Nes-Cre}$ Cerebellum.* Left: Western blot analysis of Grid2ip (Delphilin) in cortical, cerebellar, and hippocampal tissues taken from p15 wild type and *Xrcc1*$^{Nes-Cre}$ mice, demonstrating decreased Grid2ip in the *Xrcc1*$^{Nes-Cre}$ cerebellum. Blots shown are representative of 1 wild type and 2 separate *Xrcc1*$^{Nes-Cre}$ brains. Right: Quantification of Grid2ip in cerebellar tissue from wild type and *Xrcc1*$^{Nes-Cre}$ brains, n = 3 mice, blot images from remaining brains not shown in (A). Statistical significance is denoted as * where $p < 0.05$ by student's t-test. Histogram shows mean ± SEM.

As with IP3R, following blotting I observed that the levels of Grid2ip was significantly decreased in the cerebellum of the *Xrcc1*$^{Nes\text{-}Cre}$ mouse (Figure 5.3). Grid2ip is required for the surface expression of Grid2, mutations in which are associated with cerebellar ataxia. This decreased level may also underlie elements of the *Xrcc1*$^{Nes\text{-}Cre}$ ataxia phenotype, as defective Grid2 trafficking may interfere with the function of PC parallel fibre synapses. As Grid2ip expression is limited to cerebellar PCs, the decreased level of this protein would not explain the defects observed in hippocampal neurons.

5.2.1.3 Cacna1a

Having previously established that the seizures characterising the *Xrcc1*$^{Nes\text{-}Cre}$ mouse may reflect aberrant presynaptic calcium signalling in hippocampal neurons, I next examined levels of the protein Cacna1a, a which encodes the transmembrane pore-forming subunit of $Ca_{v2}2.1$, the P/Q Voltage Dependent Calcium Channel (Diriong, *et al*., 1995, Stampfl and Fee, 2021). $Ca_{v2}2.1$ is widely present throughout the brain, located at the presynaptic terminal, where it regulates the voltage-dependent entry of calcium into the presynaptic terminal following an action potential, preceding the fusion of neurotransmitter containing vesicles (He, *et al*., 2018, Mochida, 2019). I identified $Ca_{v2}2.1$ as a potential target due to the pathologies associated with mutations in *CACNA1A*, which encodes the channel, notably spinocerebellar ataxia type 6 (SCA6), episodic ataxia type 2 (EA2), and epilepsy with multiple seizure types (Giunti, *et al*., 2015, Sintas, *et al*., 2017, Indelicato and Boesch, 2021).

I detected a striking decrease in Cacna1a levels in the *Xrcc1*$^{Nes\text{-}Cre}$ cerebellum (Figure 5.4). The pore-forming subunit, Cacna1a, is required for $Ca_{v2}2.1$ function (Guida, *et al*., 2001). Mutations in *CACNA1A* are associated with SCA6 and increasing evidence has suggested that alterations in calcium signalling may be mechanistically linked to multiple forms of cerebellar ataxia. The decreased level of Cacna1a is consistent with the notion that deregulated calcium homeostasis in the cerebellum of the *Xrcc1*$^{Nes\text{-}Cre}$ mouse may contribute to the aetiology of its ataxia phenotype (Giunti, *et al*., 2015, Hisatsune, *et al*., 2018). Interestingly, I also detected a decrease in this protein in *Xrcc1*$^{Nes\text{-}Cre}$ cortex (Figure 5.4). The phenotype of the *Xrcc1*$^{Nes\text{-}Cre}$ mouse has, so far, indicated only the involvement of the cerebellum (progressive degeneration and ataxia) and the hippocampus (poly(ADP-ribose) accumulation linked to terminal seizures), however there is moderate accumulation of poly(ADP-ribose) in the *Xrcc1*$^{Nes\text{-}Cre}$ cortex (Komulainen, *et al*., 2021). I did not detect any significant change in levels of Cacna1a

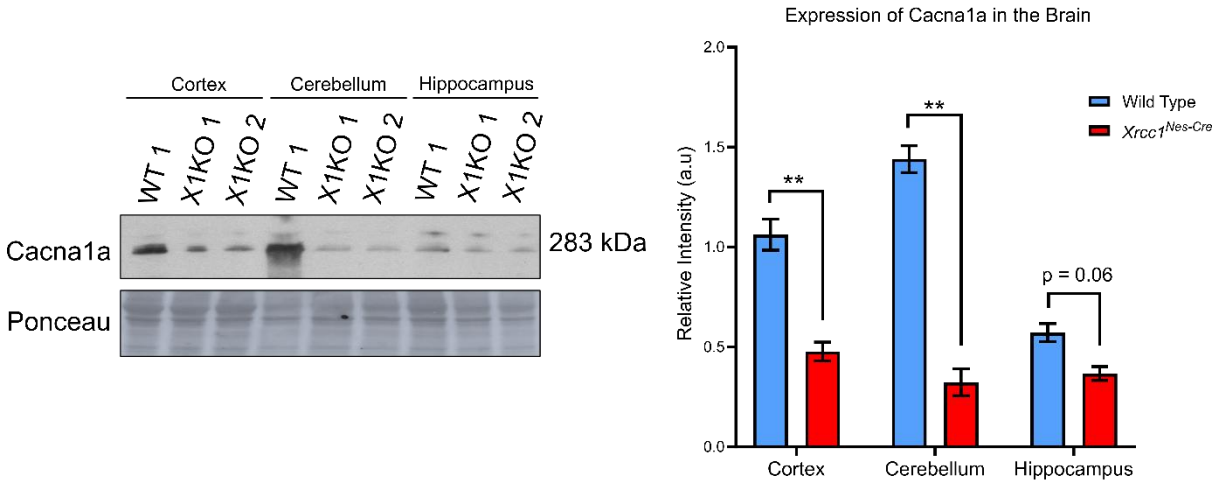

Figure 5.4 *Decreased Levels of Cacna1a in the Xrcc1$^{Nes-Cre}$ Cortex and Cerebellum.* Left: Western blot analysis of Cacna1a (P/Q Type voltage gated Ca^{2+} channel subunit α1) in cortical, cerebellar, and hippocampal tissues taken from p15 wild type and *Xrcc1*$^{Nes-Cre}$ mice, demonstrating the decreased levels of Cacna1a in the *Xrcc1*$^{Nes-Cre}$ cortex and cerebellum. Blots shown are representative of 1 wild type and 2 separate *Xrcc1*$^{Nes-Cre}$ brains. Right: Quantification of Cacna1a expression in cortical, cerebellar, and hippocampal tissues from wild type and *Xrcc1*$^{Nes-Cre}$ brains, n = 3 mice, blot images from remaining brains not shown in (A). Statistical significance is denoted as ** where $p < 0.01$ by student's t-test. Histogram shows mean ± SEM.

in *Xrcc1*$^{Nes\text{-}Cre}$ hippocampus, and as such it is unlikely to be related to the aberrant presynaptic calcium signalling observed in *Xrcc1*$^{Nes\text{-}Cre}$ hippocampal neurons.

5.2.1.4 DAGLα

Another protein that I sought to investigate was Diacylglycerol Lipase Alpha (DAGLα), a protein responsible for the biosynthesis of the endocannabinoid 2-arachidonoylglycerol, as well as the modulation of PC parallel fibre synapses (Yoshida, *et al*., 2006, Shonesy, *et al*., 2014). While *Dagla* null mice are viable, endocannabinoid-dependent retrograde synaptic transmission is absent from the hippocampus and cerebellum, and duplications at chromosome 11q12.2–11q12.3, which encode *DAGLA* are associated with spinocerebellar ataxia type 20 (SCA20) (Knight, *et al*., 2008, Asami, *et al*., 2010). Further, DAGLα has been found to differentially expressed in separate models of spinocerebellar ataxia, such as SCA1, SCA3, and SCA7 (Pflieger, *et al*., 2017). In the *Xrcc1*$^{Nes\text{-}Cre}$ mouse cerebellum, I observed significantly increased expression of DAGLα, (Figure 5.5). Elevated DAGLα levels in the cerebellum could contribute to the aberrant modulation of PC parallel fibre synapses, which may have consequences for the highly intricate signalling required for movement co-ordination and requires further investigation (Heck, *et al*., 2007).

5.2.2 RNA Sequencing Reveals Altered Gene Expression in the *Xrcc1*$^{Nes\text{-}Cre}$ Hippocampus

Following the discovery of abnormal protein levels in the *Xrcc1*$^{Nes\text{-}Cre}$ brain, particularly in the cerebellum, I sought to investigate the effects of *Xrcc1* deletion on gene expression in the hippocampus. Arguably, one of the most drastic elements of the *Xrcc1*$^{Nes\text{-}Cre}$ phenotype are the intractable seizures that, ultimately, result in shortened lifespan. Through my investigations of cultured *Xrcc1*$^{Nes\text{-}Cre}$ hippocampal neurons, I identified significant alterations to presynaptic calcium signalling that may underlie the seizures observed in the mouse. This signalling can be rescued both by the chronic inhibition of Parp1 in isolated hippocampal neurons, and partially with supplementation ofNAD+ precursors, possibly implicating NAD+ depletion as a cause of defective presynaptic signalling. The cellular energy state can regulate transcription through Sirt1 activity, and NAD+ depletion has shown to result in aberrant gene expression in the SCA7 mouse, which is rescued by either Sirt1 overexpression or NAD+ repletion (Imai and Guarente, 2016, Stoyas, *et al*., 2020).

To investigate whether alterations to gene expression may underlie defective signalling in the hippocampus, 3 wild type and 4 *Xrcc1*$^{Nes\text{-}Cre}$ mice from 3 different litters (1 mouse of each genotype per litter, with one litter providing 2 *Xrcc1*$^{Nes\text{-}Cre}$ pups) were

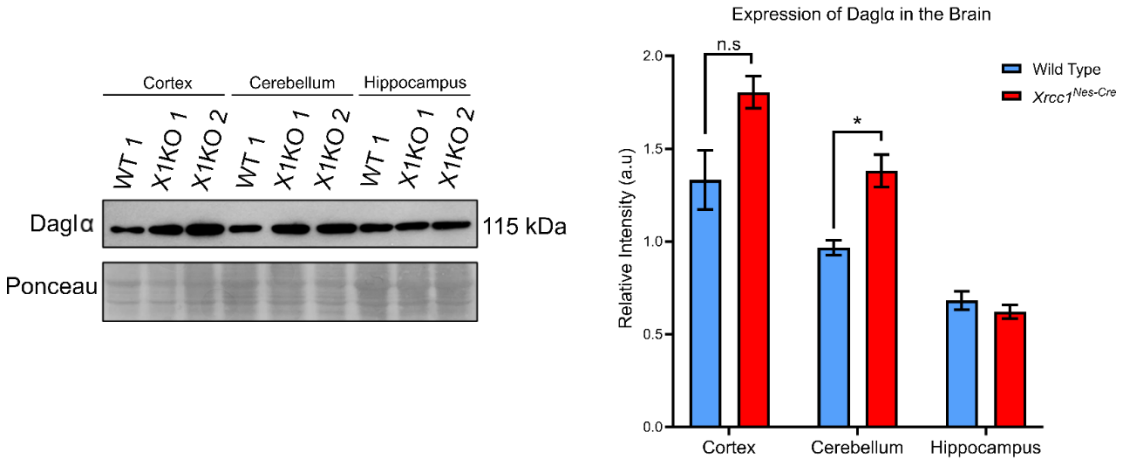

Figure 5.5 *Elevated Levels of Daglα in the Xrcc1*$^{Nes\text{-}Cre}$ *cerebellum.* Left: Western blot analysis of Daglα (Diacylglycerol Lipase α) expression in cortical, cerebellar, and hippocampal tissues taken from p15 wild type and *Xrcc1*$^{Nes\text{-}Cre}$ mice, demonstrating elevated levels of Daglα in the *Xrcc1*$^{Nes\text{-}Cre}$ cerebellum. Blots shown are representative of 1 wild type and 2 separate *Xrcc1*$^{Nes\text{-}Cre}$ brains. Right: Quantification of Daglα levels in cortical, cerebellar, and hippocampal tissues from wild type and *Xrcc1*$^{Nes\text{-}Cre}$ brains, n = 3 mice, blot images from remaining brains not shown in (A). Statistical significance is denoted as * where $p < 0.05$ by student's t-test. Histogram shows mean ± SEM.

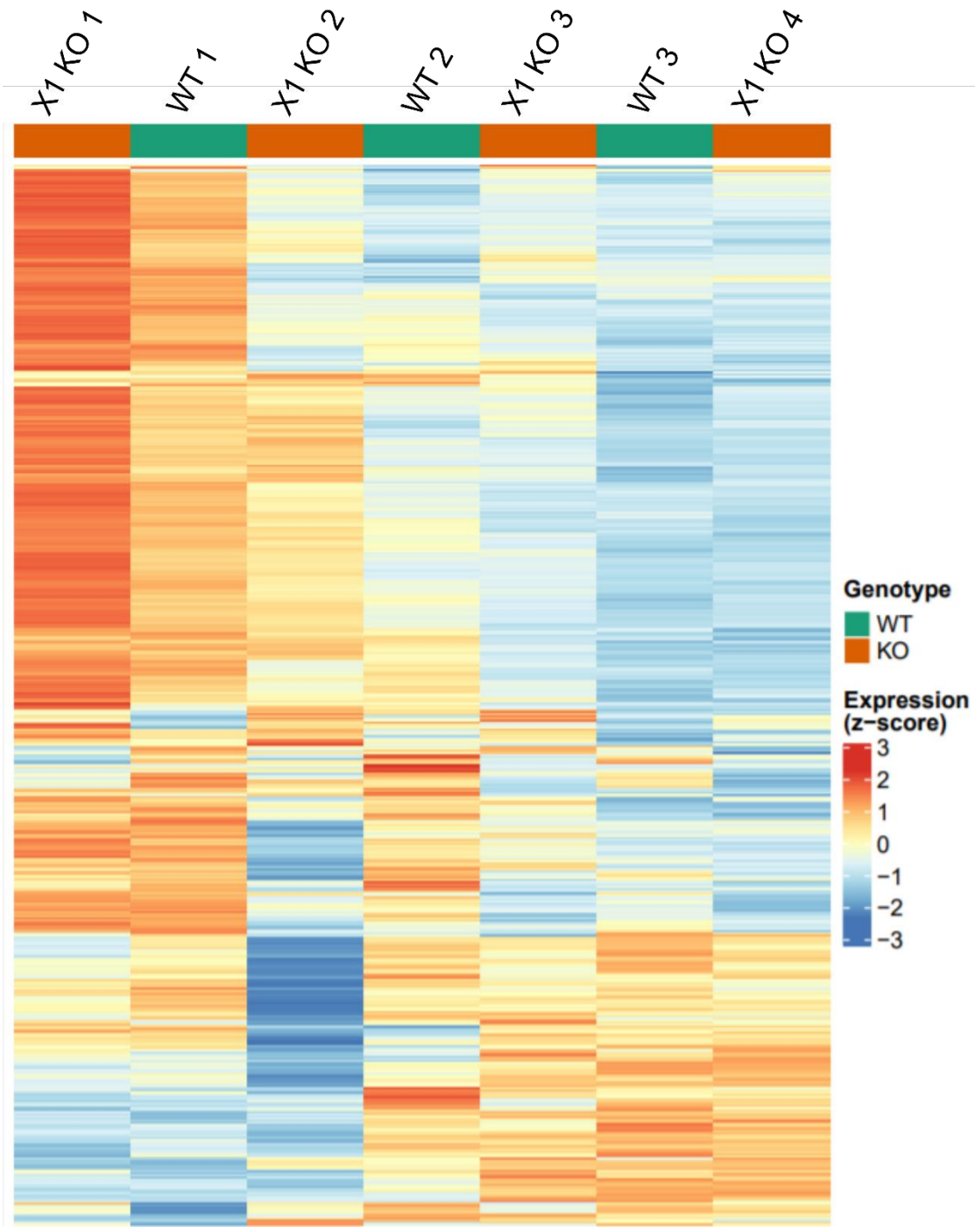

Figure 5.6 *RNA Sequencing Highlights Altered Transcription in the Xrcc1*$^{Nes\text{-}Cre}$ *Hippocampus*. RNA-Seq heatmap showing the expression z-scores calculated for the top 151 genes differentially expressed in the p15 *Xrcc1*$^{Nes\text{-}Cre}$ hippocampus. 151 differentially expressed genes (DEGs) were highlighted from 32,718 examined genes. DEGs are shown in red if expression is increased, and in blue if shown to be decreased following analysis. All genes presented were identified as significantly differentially expressed where $p < 0.05$. 3 wild type and 4 *Xrcc1*$^{Nes\text{-}Cre}$ mice from 3 separate litters were harvested for tissues, which were lysed prior to isolation and sequencing at the Institute of Molecular Genetics of the Czech Academy of Sciences (IMG).

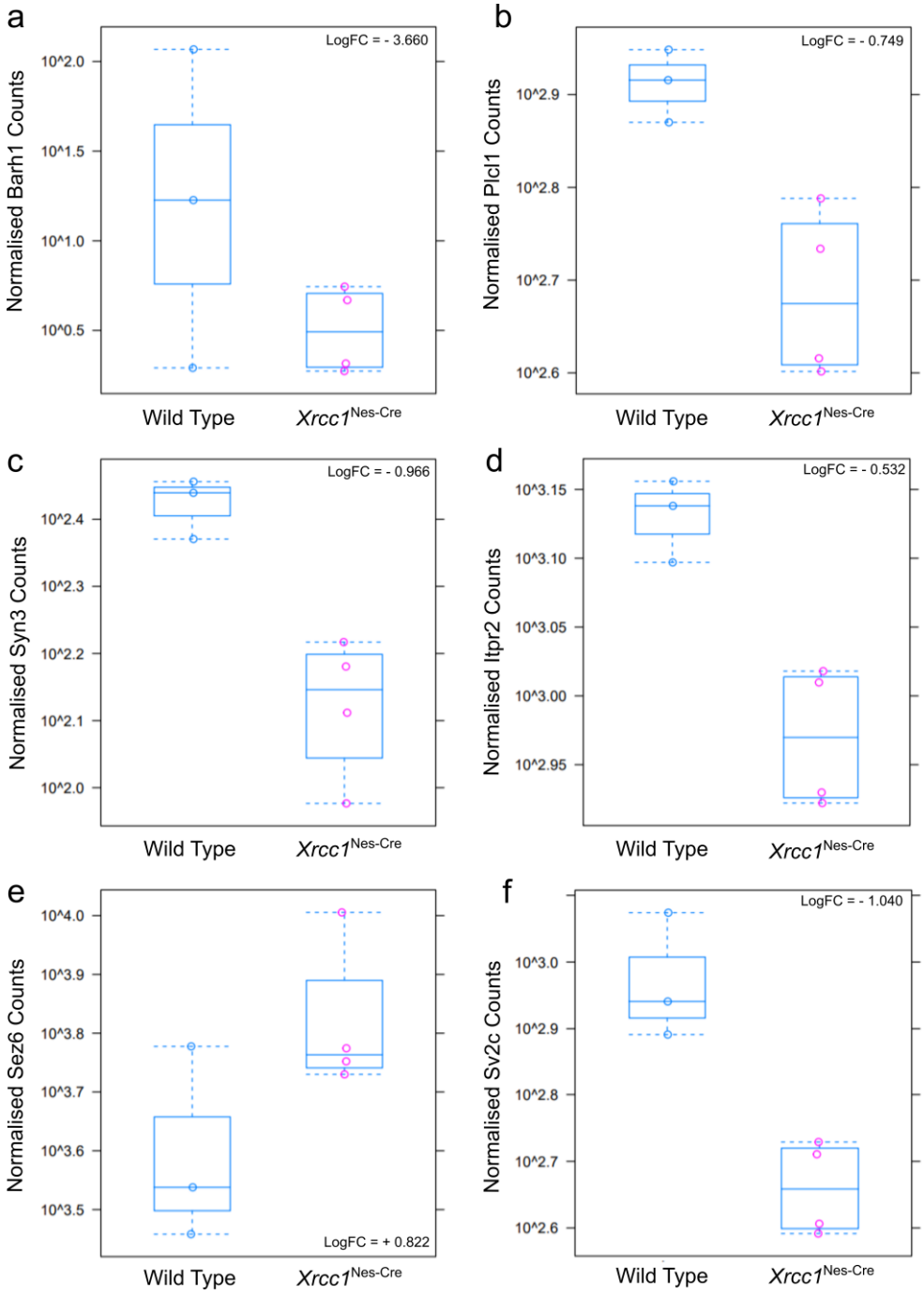

Figure 5.7 *Summary of Notable DEGs in the Xrcc1$^{Nes-Cre}$ Hippocampus*. Box and whisker plots highlighting the differential expression of several genes highlighted by RNA-seq. Expression of a) Barh1 ($p = 0.015$), b) Plcl1 ($p = 0.006$), c) Syn3 ($p = 0.014$), d) Itpr2 ($p = 0.04$), e) Sez6 ($p < 0.001$), and f) Sv2c ($p < 0.001$), determined to be significantly differentially expressed in the *Xrcc1*$^{Nes-Cre}$ hippocampus. Box and Whisker plots demonstrate central median, with upper and lower quartiles above and below. Dashed bars represent the upper and lower extremes within the data set. Genes were highlighted due to the strength of the effect (as in Barh1), or their potential relevance to the *Xrcc1*$^{Nes-Cre}$ phenotype (such as Syn3 and Itpr2). Box and whisker plots generated in R during analysis at IMG.

sacrificed, with tissue lysed and RNA extracted. RNA sequencing identified a number of genes with significant deregulation of their expression in *Xrcc1*$^{Nes\text{-}Cre}$ hippocampi (Figure 5.6). In total, 151 significant differentially expressed genes (DEGs) were identified (Table 5.2 and 5.3). Ranges of log fold change identified in significant DEGs were from the -3.660 Log2 fold change (Log2FC) decreased expression of Barh1 (BarH Like Homeobox, responsible for the regulation of neurotrophin expression, linked to cell survival, cerebellar dysfunction and medulloblastoma), to the +1.570 Log2FC increased expression of neurotensin (an endogenous neuroleptic linked to thermoregulation and cell protection following cerebral ischaemia) (Li, *et al*., 2004, Antonelli, *et al*., 2008) (Figure 5.7). Of potential interest in the aetiology of the *Xrcc1*$^{Nes\text{-}Cre}$ phenotype is another DEG downregulated in our RNAseq data, *Plcl1* (Log2FC = -0.749), which encodes phospholipase c-like 1 (Plcl1) (Figure 5.7 B). Plcl1 is associated with the turnover and trafficking of GABA(A) receptors to the plasma membrane, deletion of which in mice results in an epileptic phenotype (Kanematsu, *et al*., 2002, Zhu, *et al*., 2012). Mutations in *PLCL1* have also been associated with ASD and are considered a candidate for ultra-rare genetic epilepsy variants in humans (Epi25 Collaborative, 2019, Zheng, *et al*., 2021).

Another functionality seemingly deregulated in the *Xrcc1*$^{Nes\text{-}Cre}$ hippocampi is synaptic signalling. For example, I noted the significant downregulation of *Sv2c* (synaptic vesicle glycoprotein 2c, Log2FC = -1.040), expression of which is linked dopaminergic neuron function and is associated with the aetiology of PD (Dunn, *et al*., 2017) (Figure 5.7 F). Similarly highlighted is *Syn3* (synapsin 3, downregulated, Log2FC = -0.966), a member of the synapsin family, which encode neuronal phosphoproteins associated with vesicles, and which are known to regulate neurotransmitter release (Feng, *et al*., 2002) (Figure 5.7 C). Several genes highlighted are associated with seizure phenotypes, such as *Sez6* (seizure related 6, upregulated, Log2FC = +0.822), which is critical in cell-cell interactions and the facilitation of dendritic arborisation, as well as membrane trafficking of kainate receptor subunits (Gunnersen, *et al*., 2007, Pigoni, *et al*., 2020) (5.2.2.2 E). *SEZ6* is also a candidate gene for epilepsy, with mutations in *SEZ6* associated with febrile seizures (Mulley, *et al*., 2011). A further DEG identified in our RNAseq data is *Kcnj10*, which encodes for Kcnj10 (potassium inwardly rectifying channel, subfamily J, member 10, downregulated, Log2FC = -0.654), which is predominantly expressed in glial cells (Seifert, *et al*., 2009) (Table 5.3). Kcnj10 is an inwardly rectifying channel, facilitating influx of K^+ into glia, regulating special buffering of K^+ released by neurons during action potential propagation (Kucheryavykh, *et al*.,

2007). Mutations in *KCNJ10* are associated with both seizures and ataxia (Guo, *et al*., 2015, Zhang, *et al*., 2019).

5.2.2.1 Downregulation of Cadherin 1 in the *Xrcc1*$^{Nes\text{-}Cre}$ Hippocampus

Of further note was the significant downregulation of both Cadherin 1 (Cdh1, Log2FC = -2.15) and Cadherin Related Family Member 1 (Cdhr1, Log2FC = -0.799) (Figure 5.8 A & B). Cadherins are glycosylated transmembrane proteins which form adhesion complexes in many tissues, with notable roles in the regulation of synaptic and dendritic architecture, as well as the maintenance of plasticity (Seong, *et* al., 2015, Yamagata, *et* al., 2018). Mutations in genes encoding members of the cadherin family have been associated with several disorders, such as female-limited epilepsy and AD (Dibbens, *et al*., 2008, Leschyns'ka and Sytnyk, 2016). The deletion of N-Cadherin (Cadherin 2) results in decreased levels of Glu1A, an AMPA receptor subunit, and Postsynaptic density protein 95 (Psd-95), a postsynaptic scaffold protein (Nikitczuk, *et al*., 2014). N-Cadherin is also responsible for the regulation of presynaptic vesicle clustering (Stan, *et al*., 2012). Cadherin 1 is predominantly expressed in epithelial cells, key in the regulation of cell-cell adhesion through the formation and maintenance of adherens junctions (Pecina-Slaus, 2003, Bruner and Darksen, 2018). The deletion of Cadherin 1 in cultured cortical neurons results in a reduced density of dendritic, GABAergic inhibitory synapses, whereas glutamatergic synapses were not affected (Fiederling, *et al*., 2011).

The decreased expression of a protein required for the regulation of inhibitory synaptic signalling could contribute to the *Xrcc1*$^{Nes\text{-}Cre}$ phenotype, as any alteration in the balance of excitatory and inhibitory signalling in the brain could result in seizures (Fritschy, 2008). Other classical members of the cadherin superfamily (such as Cadherin 2, Cadherin 9, and Cadherin 10) are associated with neurodevelopmental disorders such as autism but were not found to be significantly differentially expressed in *Xrcc1*$^{Nes\text{-}Cre}$ hippocampal tissue (Wang, *et al*., 2009, Wang, *et al*., 2019). One possible mechanism for the decreased expression of Cadherin 1 in the *Xrcc1*$^{Nes\text{-}Cre}$ hippocampus is through the poly(ADP-ribosylation) of Smad4, which induces Cadherin 1 expression (Müller, *et al*., 2002, Reinacher-Schick, *et al*., 2004, Diab, *et al*., 2012). Smad4 is poly(ADP-ribosyl)ated by Parp1, leading to the dissolution of the Smad complex and the attenuation of Smad-linked gene expression (Lönn, *et al*., 2010, Dahl, *et al*., 2014). This Parp1-dependent effect might also explain the Cadherin 1 defects observed in the glaikit (Tdp1 homolog) knockout drosophila (Dunlop, *et al*., 2004).

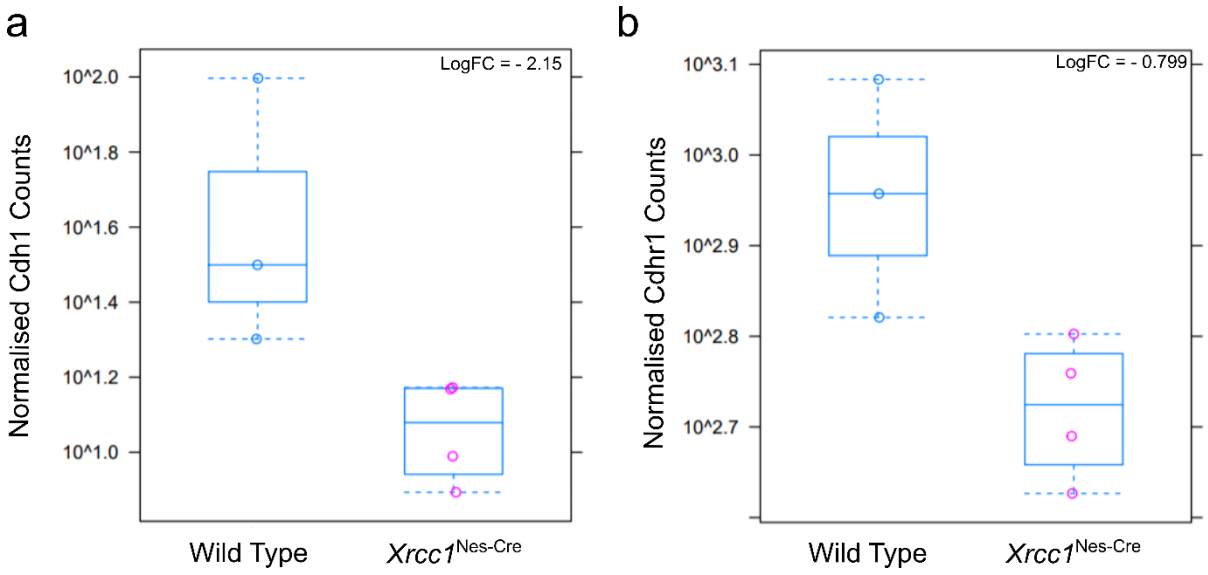

Figure 5.8 *Summary of Cell Adhesion and Synaptogenesis Related DEGs in the Xrcc1$^{Nes-Cre}$ Hippocampus.* Box and whisker plots highlighting the differential expression of several genes highlighted by RNA-seq. Expression of a) Cadherin 1 (Cdh1) (p = 0.02), and b) Cadherin Related Family Member 1 (Cdhr1) (p = 0.02) determined to be significantly differentially expressed in the *Xrcc1*$^{Nes-Cre}$ hippocampus. Box and Whisker plots demonstrate central median, with upper and lower quartiles above and below. Dashed bars represent the upper and lower extremes within the data set. Genes were highlighted due to their functions in cell adhesion and synaptogenesis, and their potential relevance to the *Xrcc1*$^{Nes-Cre}$ phenotype. Box and whisker plots generated in R during analysis at IMG.

5.2.2.2 Downregulation of Sema Family Proteins in the *Xrcc1*$^{Nes\text{-}Cre}$ Hippocampus

Of those investigated, several genes found to be downregulated in the *Xrcc1*$^{Nes\text{-}Cre}$ hippocampus were associated with the regulation of axon guidance, with significant alterations found in the expression of *Sema6a, Sema5a, Sema4d,* and *Sema3c*, which express Sema proteins (Figure 5.9). Semaphorins are a family of transmembrane or secreted proteins originally identified in the axonal growth cone (Koncina, *et al*., 2007, Hu and Zhu, 2018). Semaphorins are critical in the development of the nervous system, acting as cues to deflect neuronal growth away from inappropriate regions (Hu and Zhu, 2018). During neuronal development, Sema5a acts to negatively regulate synaptogenesis in hippocampal granule cells, and deletion of Sema5a results in elevated dendritic spine density and AMPA receptor synaptic responses (Duan, *et al*., 2014). In humans, mutations in *SEMA5A* are commonly associated ASD and intellectual impairment (Mosca-Voidron, *et al*., 2016). Recently, de novo germline mutations in *SEMA5A* were found in patients with early onset infantile epileptic encephalopathy (Wang, *et al*., 2019). Several Sema proteins are linked to ASD, likely through their function in promoting synaptogenesis and oligodendrocyte differentiation (Carulli, *et al*., 2021). Similarly, another DEG identified was *Ephb1*, which encodes ephrin receptor b1, mediators of Eph/ephrin interactions which also regulate directionality of the axonal growth curve (Robichaux, *et al*., 2014). Deletion of astrocytic Ephb1 results in the enhanced excitability of CA1 pyramidal neurons, increased dendritic spine density, and elevated amplitude of evoked NMDAR and AMPAR EPSCs, providing evidence for the role of ephrin signalling in the maintenance of the E/I balance (Nguyen, *et al*., 2020).

5.2.2.3 RNA Sequencing of *Xrcc1*$^{Nes\text{-}Cre}$ Hippocampi Reveals Overlap with Neuronal Enhancers Prone to Demethylation-Linked Breakage Highlighted by SARseq

Through studying human i^3 and rat neurons, Wu et al recently discovered that endogenous DNA SSBs are prone to clustering in certain regions of the genome. They proposed that these DNA SSBs represented endogenous damage that occurred in a site and cell type-specific manner (Wu, *et al*., 2021). Through genomic mapping, it was discovered that Xrcc1 loss resulted in deficient short-patch repair, and subsequently increased repair synthesis at sites of neuronal enhancers, providing a site and cell type-specific model of the effect of DNA SSBs on transcription. Synthesis Associated with Repair Sequencing (SARseq) peaks revealed the clustering of endogenous SSBs at CpG sites, prompting the hypothesis that active demethylation; the TET dependent progressive oxidation of 5-methylcytosine to (predominantly) 5-hydroxymethylcytosine through XRCC1-associated SSB intermediates accounted for these breaks

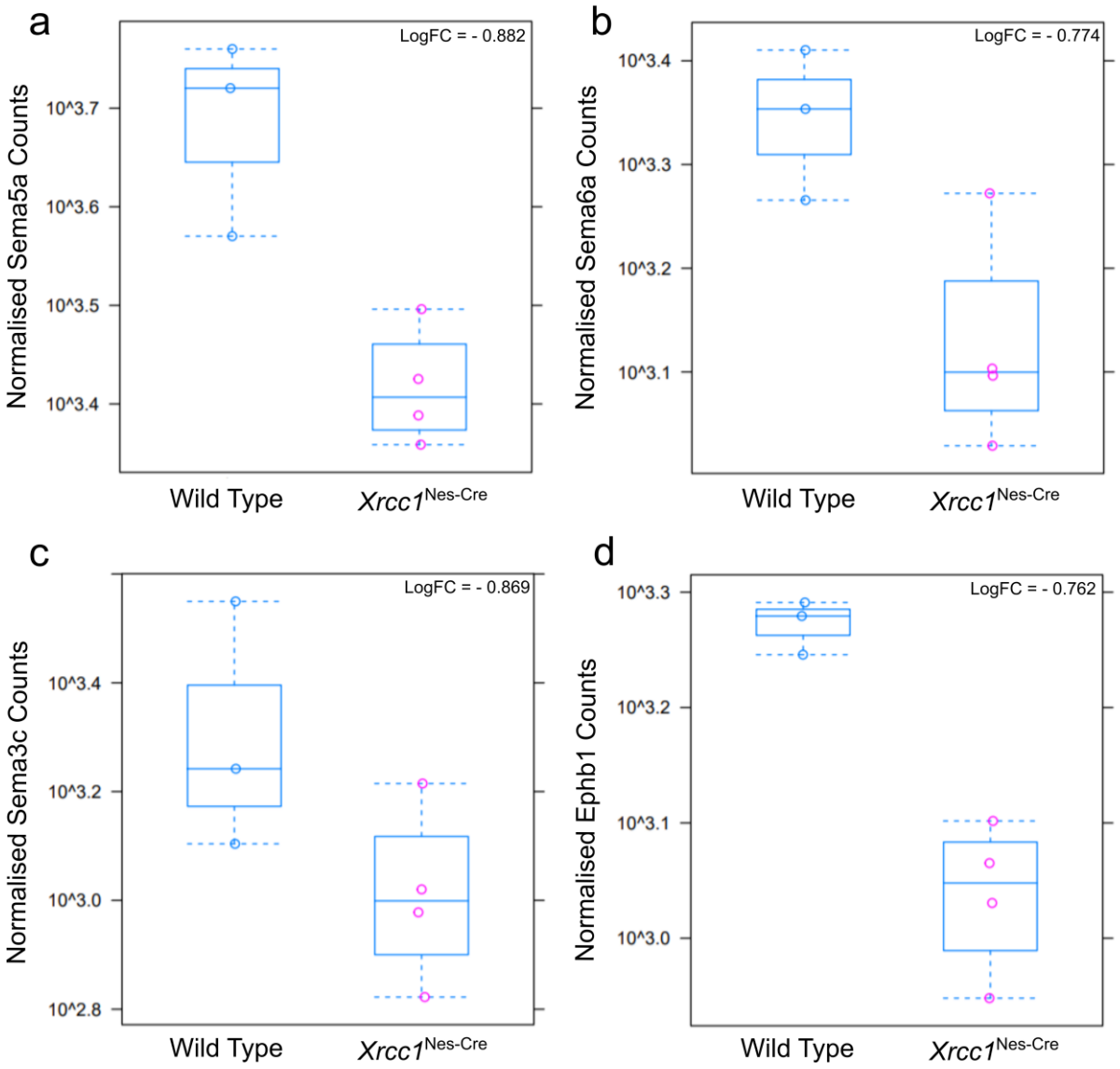

Figure 5.9 *Summary of Axonal Growth and Neurogenesis Related DEGs in the Xrcc1$^{Nes-Cre}$ Hippocampus*. Box and whisker plots highlighting the differential expression of several genes highlighted by RNA-seq. Expression of a) Semaphorin 5A (Sema5a) ($p < 0.001$), b) Semaphorin 6A (Sema6a) ($p < 0.001$), c) Semaphorin 3C (Sema3c) ($p = 0.002$) and d) Ephrin Type B Receptor 1 (Ephb1) ($p < 0.001$), determined to be significantly differentially expressed in the *Xrcc1*$^{Nes-Cre}$ hippocampus. Box and Whisker plots demonstrate central median, with upper and lower quartiles above and below. Dashed bars represent the upper and lower extremes within the data set. Genes were highlighted due to their functions in the development and guidance of axonal growth and neurogenesis, and their potential relevance to the *Xrcc1*$^{Nes-Cre}$ phenotype. Box and whisker plots generated in R during analysis at IMG.

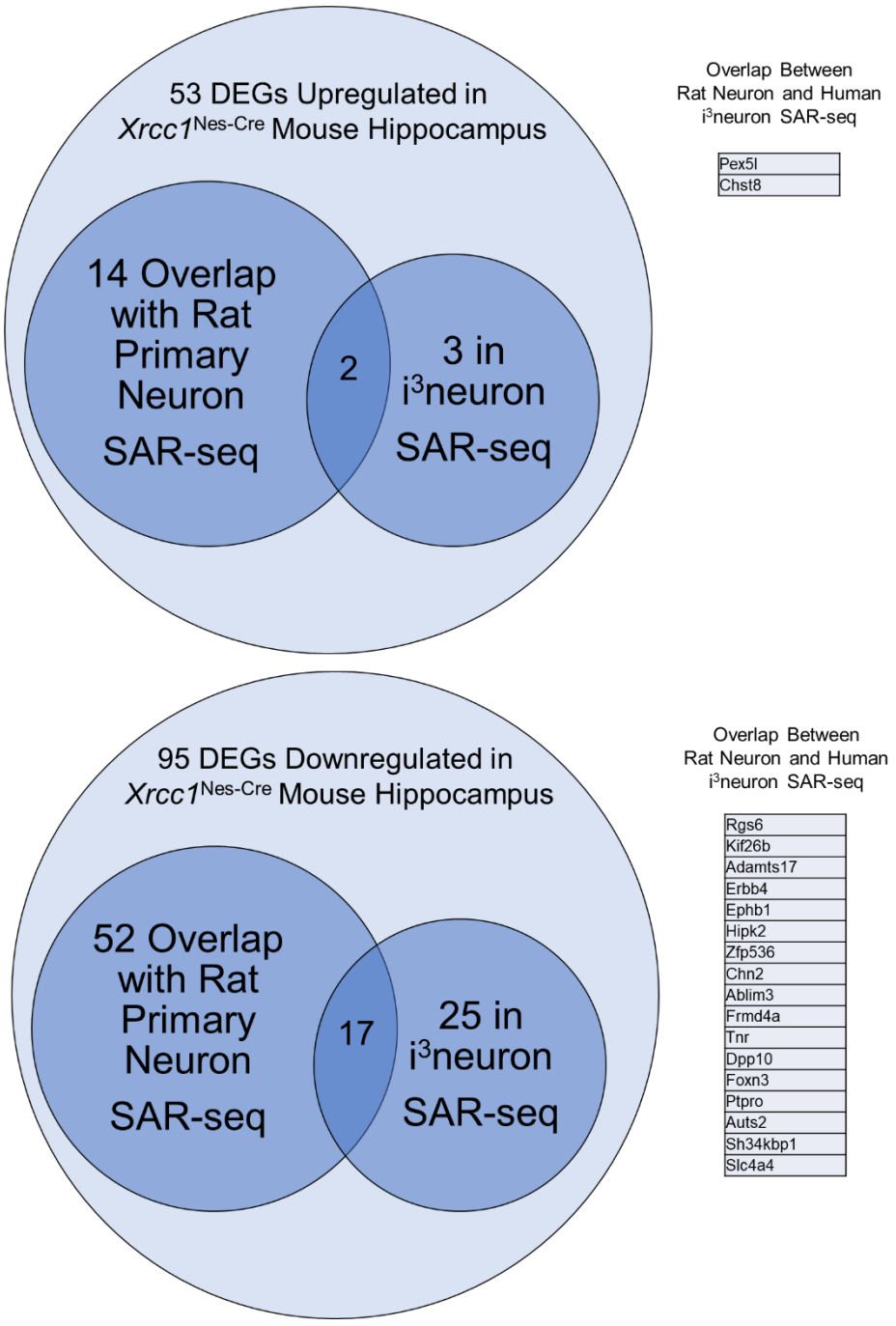

Figure 5.10 *The Overlap Between RNAseq and SARseq in Xrcc1 Deficient Models.* Two diagrams demonstrating the overlap between significantly differentially expressed genes in the *Xrcc1*$^{Nes\text{-}Cre}$ hippocampus and genes identified at neuronal enhancers affected by site-specific DNA SSBs (Wu, *et al*., 2021). Of the 53 significantly upregulated (above) genes identified in the *Xrcc1*$^{Nes\text{-}Cre}$ Hippocampus, 15 were highlighted by SARseq in rat and human i3 neurons, with 2 genes in both sets. Of the 95 significantly downregulated (below) genes, 60 had been highlighted by SARseq with an overlap of 17 genes. The comparison between RNAseq and SARseq data sets was not significant.

(Lio, *et al*., 2020, Wu, *et al*., 2021). The active demethylation of cytosine at CpG sites is tenfold more frequent in postmitotic neurons, likely the result of activity-driven epigenetic modification, and occurs primarily at enhancer regions (Kraucionis and Heintz, 2009, Lio, *et al*., 2020). With the discovery of frequent, endogenous DNA SSBs at sites of neuronal enhancers, Wu, *et al*., proposed that the accumulation of frequent, site-specific DNA damage, and the increased dependence on DNA repair synthesis gives rise to a potential deregulation of gene expression at break-associated loci.

Interestingly, many of the genes found to be significantly deregulated in the *Xrcc1*$^{Nes\text{-}Cre}$ mouse hippocampus corresponded to those identified by Wu *et al* as being at neuronal enhancers linked to site-specific DNA SSBs. In rat primary neurons, 22,196 SARseq peaks (sites identified as locations of site-specific breakage), overlapping with 5,202 mouse genes, 66 of which were found to be differentially expressed (52 downregulated, 14 upregulated) in the *Xrcc1*$^{Nes\text{-}Cre}$ hippocampus. This overlap was found to be insignificant (median overlap for 1000 random sets = 54, p = 0.104) (Wu, *et al*, 2021) (Figure 5.10). In human i^3 neurons, 39,253 SARseq peaks were identified, overlapping with 1,482 mouse genes, 28 of which were found to be differentially expressed (25 downregulated, 3 upregulated) in the *Xrcc1*$^{Nes\text{-}Cre}$ hippocampus. Again, this overlap was found to be insignificant (median overlap for 1000 random sets = 23, p = 0.274) (Wu, *et al*., 2021) (Figure 5.10). Despite the insignificant overlap between RNAseq and SARseq data sets, *Ephb1* was associated with SARseq peaks in both rat primary neurons and human i^3 neurons, with further representation of *Sema* genes in both data sets. *Syn3* and *Sez*6, two genes found downregulated in the *Xrcc1*$^{Nes\text{-}Cre}$ hippocampus and linked to synaptic transmission and seizure phenotypes, were also highlighted at SARseq peaks of rat primary neurons. *Itpr2* was also highlighted in both data sets, which may explain its frequent deregulation in DNA damage repair associated neurological phenotypes.

5.2.3 Validation of Highlighted Genes by qPCR

Finally, in order to validate the results of our RNA sequencing, we selected a subset of genes found to be significantly deregulated in the *Xrcc1*$^{Nes\text{-}Cre}$ mouse hippocampus. Genes were selected based on three main factors: the strength of the observed effect, the potential relevance of the gene in the aetiology of a seizure phenotype (such as genes involved in synaptic transmission, or those found to be mutated in epileptic disease), and their overlapping between RNAseq and SARseq data pools. Genes chosen for validation were *Syn3*, which encodes synapsin III, a protein involved in synaptic transmission and plasticity, and the epilepsy candidate genes *Sez6*

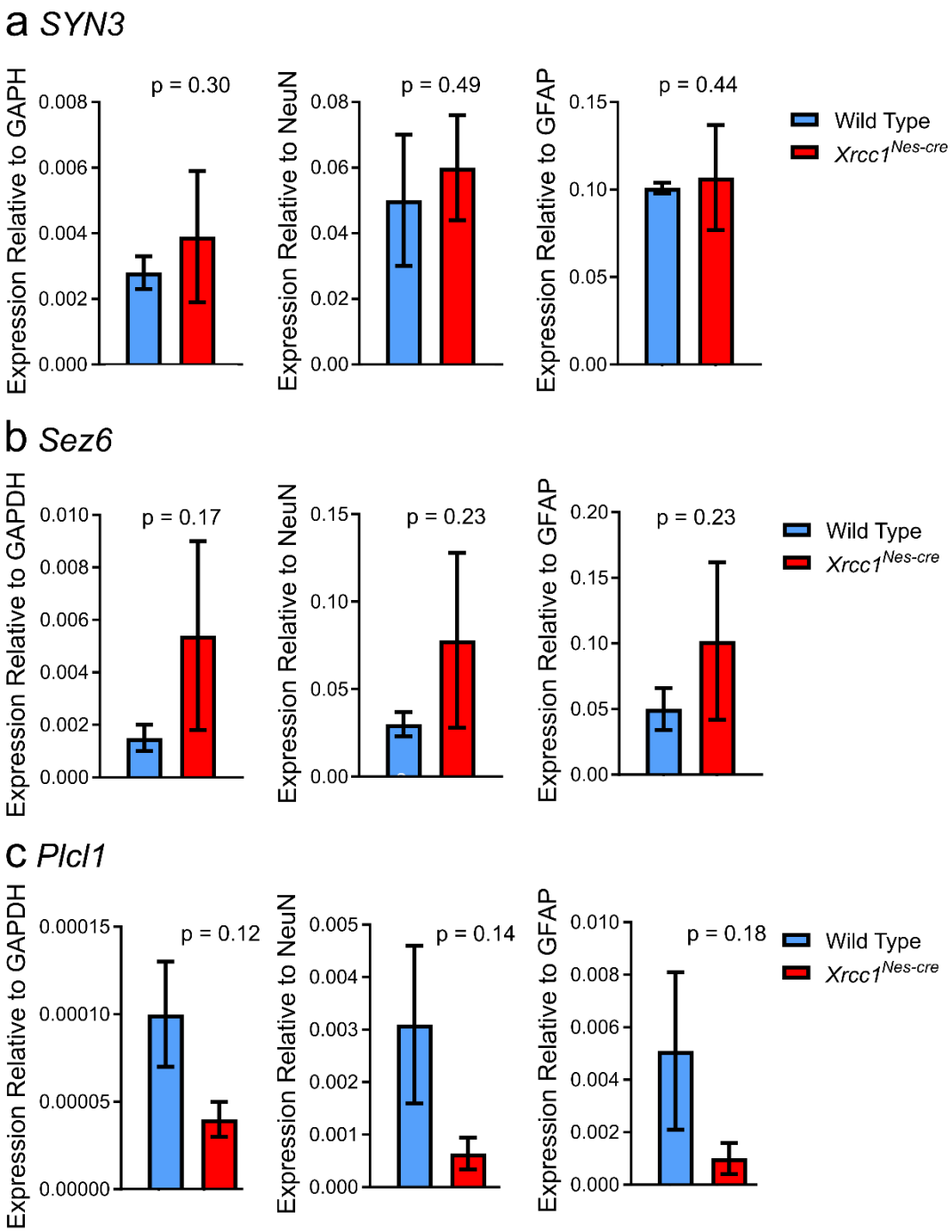

Figure 5.11 *RT-qPCR Validation of Genes Highlighted by RNAseq and SARseq in the Xrcc1*$^{Nes\text{-}Cre}$ *Hippocampus*. Hippocampal tissues were taken from p15 wild type (n = 3) and *Xrcc1*$^{Nes\text{-}Cre}$ (n = 4) mice. Tissue was lysed and RNA was isolated, prior to creation of cDNA libraries. RT-qPCR was performed on samples with primers designed against a) *Syn3*, b) *Sez6,* and c) *Plcl1*, genes which had been highlighted in both RNAseq and SARseq of Xrcc1 deficient models. Expression was measured by RT-qPCR in relation to the expression of three housekeeping genes, Left: *Gapdh*, Middle: *NeuN*, and Right: *Gfap*. Analysis was performed by student's t-test in relation to each of the housekeeping genes. None of the above validations were statistically significant.

and *Plcl1* (Feng, *et al*., 2002, Mulley, *et al*., 2011, Epi25 Collaborative, 2019). New hippocampal samples were taken from sacrificed mice, from which we extracted RNA and generated cDNA libraries. Our candidate genes were investigated relative to the expression of the housekeeping genes *Gapdh, NeuN,* and *Gfap.* We were unable to validate any of the chosen genes as being significantly deregulated by qPCR (Figure 5.11 A, B & C, Table 5.2 and 5.3). In most cases a general trend towards the effect observed in our RNAseq data was observed (Figure 5.11 A, B & C, Table 5.1).

Target Gene	Examiner	Result	Log2FC (RNAseq)	qPCR Rel. to WT
Syn3	JB	Not Validated	-0.966	1.22
Sez6	JB	Not Validated	+0.822	2.48
Plcl1	JB	Not Validated	-0.749	0.41
Sema5a	JB	Not Validated	-0.774	0.84
Itpr2	JB	Not Validated	-0.53	0.79
Tnr	JB	Not Validated	-0.635	1.03
Dcx	AM	Not Validated	-0.822	1.20
Draxin	AM	Not Validated	-1.17	0.89
Lrrc55	AM	Not Validated	-0.944	1.13
Erbb4	AM	Not Validated	-0.631	1.48

Table 5.1 *Validation of Target Genes by RT-qPCR*. The expression of target genes was measured relative to three, separate housekeeping genes by either Jack Badman (JB) or Alex McLoughlin (AM), with averages taken. No RNAseq result was significantly validated by RT-qPCR.

Symbol	Description	Log Fold Change	p Value
Cyb561	cytochrome b-561	0.582	2.27E-02
Pex5l	peroxisomal biogenesis factor 5-like	0.585	4.06E-02
Galnt9	polypeptide N-acetylgalactosaminyltransferase 9	0.587	1.99E-02
Egr4	early growth response 4	0.623	2.20E-02
Mal2	mal, T cell differentiation protein 2	0.624	2.23E-02
Rasal1	RAS protein activator like 1 (GAP1 like)	0.647	3.75E-03
Plpp6	phospholipid phosphatase 6	0.649	1.02E-02
Igfbp4	insulin-like growth factor binding protein 4	0.654	8.32E-04
Aldh1b1	aldehyde dehydrogenase 1 family, member B1	0.686	1.72E-02
Sst	somatostatin	0.692	6.85E-04
Junb	jun B proto-oncogene	0.697	1.05E-03
Chst8	carbohydrate sulfotransferase 8	0.701	2.88E-02
Snhg11	small nucleolar RNA host gene 11	0.702	2.75E-02
Slc5a5	solute carrier family 5 (sodium iodide symporter), member 5	0.713	4.35E-03
Grp	gastrin releasing peptide	0.731	1.83E-02
Hist1h1c	histone cluster 1, H1c	0.731	2.27E-02
Cotl1	coactosin-like 1 (Dictyostelium)	0.734	7.24E-04
Chrd	chordin	0.738	2.98E-02
Dusp5	dual specificity phosphatase 5	0.75	4.33E-03
Npas4	neuronal PAS domain protein 4	0.754	1.33E-02
Hrh3	histamine receptor H3	0.77	1.54E-02
AC149090.1	NULL	0.775	2.75E-02
Rasd1	RAS, dexamethasone-induced 1	0.784	1.83E-02
Mpped1	metallophosphoesterase domain containing 1	0.797	8.62E-06
Matn2	matrilin 2	0.817	9.70E-03
Sez6	seizure related gene 6	0.822	1.43E-06
Htr3a	5-hydroxytryptamine (serotonin) receptor 3A	0.828	2.24E-02
Nr4a1	nuclear receptor subfamily 4, group A, member 1	0.85	1.89E-05
Fibcd1	fibrinogen C domain containing 1	0.866	7.05E-03
Rprml	reprimo-like	0.869	7.15E-06
Gpr161	G protein-coupled receptor 161	0.873	1.25E-02
Fosb	FBJ osteosarcoma oncogene B	0.92	6.37E-03
Fezf2	Fez family zinc finger 2	0.975	8.57E-04
Pou3f1	POU domain, class 3, transcription factor 1	0.98	7.14E-08
Ptpru	protein tyrosine phosphatase, receptor type, U	0.986	2.34E-07
Lefty1	left right determination factor 1	1.05	6.88E-03
Nxph3	neurexophilin 3	1.06	3.75E-03
Rab26	RAB26, member RAS oncogene family	1.07	3.56E-04
Crym	crystallin, mu	1.09	1.17E-04
Ankrd63	ankyrin repeat domain 63	1.11	7.86E-04
Efcab6	EF-hand calcium binding domain 6	1.14	3.43E-03
Ccdc153	coiled-coil domain containing 153	1.15	7.05E-03
Gm34583	predicted gene, 34583	1.16	1.20E-02
Gpr101	G protein-coupled receptor 101	1.27	1.12E-03
Cort	cortistatin	1.31	2.53E-03
Ucma	upper zone of growth plate and cartilage matrix associated	1.31	3.35E-02
Stac	src homology three (SH3) and cysteine rich domain	1.32	7.12E-04
Spink8	serine peptidase inhibitor, Kazal type 8	1.36	2.27E-03
Tmem212	transmembrane protein 212	1.37	3.73E-02
Dlk1	delta like non-canonical Notch ligand 1	1.44	4.76E-03
Arhgap36	Rho GTPase activating protein 36	1.53	1.58E-04
Nts	neurotensin	1.57	1.05E-03
Rtl1	retrotransposon Gaglike 1	1.94	5.54E-04
Crygn	crystallin, gamma N	1.96	1.83E-02

Table 5.2 *Significant DEGs Identified in the Xrcc1$^{Nes\text{-}Cre}$ Hippocampus part 1*. Table showing genes identified as significantly upregulated by RNAseq, with LogFC and p value given.

Symbol	Description	Log Fold Change	p Value
Barhl1	BarH like homeobox 1	-3.66	1.55E-02
Pou4f1	POU domain, class 4, transcription factor 1	-3.18	9.15E-03
Irx2	Iroquois homeobox 2	-3.05	1.20E-02
Cdh1	cadherin 1	-2.15	2.81E-02
Plk5	polo like kinase 5	-1.65	1.70E-03
Smyd1	SET and MYND domain containing 1	-1.57	3.11E-02
Tac2	tachykinin 2	-1.32	3.18E-03
Igfbpl1	insulin-like growth factor binding protein-like 1	-1.26	6.43E-08
Prox1	prospero homeobox 1	-1.22	3.70E-07
Mobp	myelin-associated oligodendrocytic basic protein	-1.22	1.84E-06
Dsp	desmoplakin	-1.2	3.16E-05
Chrdl1	chordin-like 1	-1.19	3.59E-02
Plp1	proteolipid protein (myelin) 1	-1.18	3.59E-06
Draxin	dorsal inhibitory axon guidance protein	-1.17	3.90E-03
C1ql2	complement component 1, q subcomponent-like 2	-1.13	3.66E-07
Casr	calcium-sensing receptor	-1.13	1.65E-02
Otx2	orthodenticle homeobox 2	-1.1	1.62E-02
Ugt8a	UDP galactosyltransferase 8A	-1.07	1.23E-06
Rgs6	regulator of G-protein signaling 6	-1.06	2.31E-05
Sv2c	synaptic vesicle glycoprotein 2c	-1.04	1.58E-04
Enpp6	ectonucleotide pyrophosphatase/phosphodiesterase 6	-1.01	2.59E-06
Lpar1	lysophosphatidic acid receptor 1	-0.998	1.43E-06
Kif26b	kinesin family member 26B	-0.99	8.64E-06
Bcas1	breast carcinoma amplified sequence 1	-0.989	1.25E-05
Mal	myelin and lymphocyte protein, T cell differentiation protein	-0.981	2.67E-04
Adamts17	a disintegrin-like and metallopeptidase (reprolysin type) with thrombospondin type 1 motif, 17	-0.978	3.63E-04
Npnt	nephronectin	-0.975	1.70E-03
Stxbp6	syntaxin binding protein 6 (amisyn)	-0.968	1.28E-05
Car10	carbonic anhydrase 10	-0.966	7.86E-04
Syn3	synapsin III	-0.966	1.44E-02
Ermn	ermin, ERM-like protein	-0.964	1.87E-04
Ttc28	tetratricopeptide repeat domain 28	-0.956	1.23E-04
Lrrc55	leucine rich repeat containing 55	-0.944	1.38E-03
Fa2h	fatty acid 2-hydroxylase	-0.932	5.03E-03
Mex3a	mex3 RNA binding family member A	-0.911	4.45E-03
Xrcc1	X-ray repair complementing defective repair in Chinese hamster cells 1	-0.891	5.55E-03
Plekhh1	pleckstrin homology domain containing, family H (with MyTH4 domain) member 1	-0.891	1.76E-02
Acvr1c	activin A receptor, type IC	-0.89	4.10E-02
Opalin	oligodendrocytic myelin paranodal and inner loop protein	-0.886	2.15E-02
Sema5a	sema domain, seven thrombospondin repeats (type 1 and type 1-like), transmembrane domain (TM) and short cytoplasmic domain, (semaphorin) 5A	-0.882	1.86E-06
Thsd7a	thrombospondin, type I, domain containing 7A	-0.88	1.49E-04
Sema3c	sema domain, immunoglobulin domain (Ig), short basic domain, secreted, (semaphorin) 3C	-0.869	1.54E-03
Adarb2	adenosine deaminase, RNA-specific, B2	-0.852	6.34E-03
Dock10	dedicator of cytokinesis 10	-0.85	2.42E-04
Hhip	Hedgehog-interacting protein	-0.85	1.49E-02
Erbb3	erb-b2 receptor tyrosine kinase 3	-0.846	1.64E-02
Dcx	doublecortin	-0.822	3.75E-03
Cnksr3	Cnksr family member 3	-0.818	3.35E-02
Sox11	SRY (sex determining region Y)-box 11	-0.81	1.05E-03
Pdzd2	PDZ domain containing 2	-0.81	7.05E-03
Cdhr1	cadherin-related family member 1	-0.799	2.45E-02
Erbb4	erb-b2 receptor tyrosine kinase 4	-0.798	7.24E-04
Trim67	tripartite motif-containing 67	-0.783	5.99E-03
Sema6a	sema domain, transmembrane domain (TM), and cytoplasmic domain, (semaphorin) 6A	-0.774	8.68E-04
Cldn11	claudin 11	-0.773	3.73E-02
Scd1	stearoyl-Coenzyme A desaturase 1	-0.765	3.06E-05
Cemip2	cell migration inducing hyaluronidase 2	-0.763	1.49E-03
Neurod1	neurogenic differentiation 1	-0.763	2.90E-02
Ephb1	Eph receptor B1	-0.762	3.56E-04
Tspan2	tetraspanin 2	-0.76	3.06E-04
Plcl1	phospholipase C-like 1	-0.749	6.58E-03
Spata13	spermatogenesis associated 13	-0.748	1.99E-03
Steap2	six transmembrane epithelial antigen of prostate 2	-0.743	7.05E-03
Hipk2	homeodomain interacting protein kinase 2	-0.734	3.67E-03
Hmgcs1	3-hydroxy-3-methylglutaryl-Coenzyme A synthase 1	-0.728	1.58E-04
Zfp536	zinc finger protein 536	-0.71	7.00E-03
Fbxo7	F-box protein 7	-0.697	1.12E-03
Frmd4b	FERM domain containing 4B	-0.696	3.26E-02
Chn2	chimerin 2	-0.69	3.90E-03
Nfasc	neurofascin	-0.676	1.26E-04
Ppp1r16b	protein phosphatase 1, regulatory subunit 16B	-0.664	5.54E-04
Ablim3	actin binding LIM protein family, member 3	-0.662	4.20E-03
Hecw1	HECT, C2 and WW domain containing E3 ubiquitin protein ligase 1	-0.656	4.31E-02
Kcnj10	potassium inwardly-rectifying channel, subfamily J, member 10	-0.654	1.32E-02
Frmd4a	FERM domain containing 4A	-0.652	1.87E-03
Ick	intestinal cell kinase	-0.652	2.62E-03
Luzp2	leucine zipper protein 2	-0.643	2.48E-02
Tnr	tenascin R	-0.635	6.34E-03
Rragd	Ras-related GTP binding D	-0.632	1.55E-02
Igsf3	immunoglobulin superfamily, member 3	-0.632	2.16E-02
Erbin	Erbb2 interacting protein	-0.631	8.37E-03
Dpp10	dipeptidylpeptidase 10	-0.631	2.42E-02
Cyp51	cytochrome P450, family 51	-0.63	2.27E-03
Sema4d	sema domain, immunoglobulin domain (Ig), transmembrane domain (TM) and short cytoplasmic domain, (semaphorin) 4D	-0.629	1.73E-02
Foxn3	forkhead box N3	-0.628	3.31E-03
Gjc3	gap junction protein, gamma 3	-0.619	4.68E-02
Ptpro	protein tyrosine phosphatase, receptor type, O	-0.618	6.26E-03
Tns3	tensin 3	-0.605	2.28E-03
Abcd2	ATP-binding cassette, sub-family D (ALD), member 2	-0.602	3.97E-02
Tmem108	transmembrane protein 108	-0.601	1.91E-02
Gpr17	G protein-coupled receptor 17	-0.596	7.05E-03
Auts2	autism susceptibility candidate 2	-0.59	1.13E-02
Gnal	guanine nucleotide binding protein, alpha stimulating, olfactory type	-0.587	6.19E-03
Igfbp5	insulin-like growth factor binding protein 5	-0.585	2.79E-02
Epb41l2	erythrocyte membrane protein band 4.1 like 2	-0.582	3.90E-03

Table 5.3 *Significant DEGs Identified in the Xrcc1$^{Nes\text{-}Cre}$ Hippocampus part 2*. Table showing genes identified as significantly downregulated by RNAseq, with LogFC and p value given.

5.3 Discussion

The most well-established function of PARP1 is its role in DNA damage repair, which relies on the enzyme's ability to autoribosylate and facilitate the recruitment of the SSBR machinery (Chaudhuri and Nussenzweig, 2017). PARP1 does, however, act in the regulation of gene expression. The loading of PARP1 onto chromatin can regulate expression through the structural alteration of the nucleosome (Matveeva, *et al*., 2019). Similarly, PARP1 can regulate the expression of several genes through transribosylation, the posttranslational modification of proteins, such as transcription factors, via the covalent attachment of poly(ADP-ribose) residues, to alter both protein form and function (Pahi, *et al*., 2020). We further theorise that the hyperactivation of PARP1 will result in the depletion of NAD+, which will have further consequences of the activity of SIRT1, a major regulator of gene expression (Elibol and Kilic, 2018). It was for these reasons that I aimed to investigate whether Xrcc1 deficiency might result in transcriptional deregulation and may underlie certain aspects of the *Xrcc1*$^{Nes\text{-}Cre}$ mouse phenotype.

Hyperactivation of Parp1 has been proposed as a mechanism for the deregulation of transcription observed in the SCA7 mouse, wherein nuclear DNA damage results in the depletion of NAD+ and the subsequent inhibition of Sirt1 activity (Stoyas, *et al*., 2020). In the SCA7 mouse, the deregulated expression of genes involved in calcium homeostasis is thought to underlie progressive ataxia, a phenotype which can be reversed by either the overexpression of Sirt1 or the treatment with an NAD+ precursor (Stoyas, *et al*., 2020). In the *Xrcc1*$^{Nes\text{-}Cre}$ mouse, I detected Parp1/NAD+ dependent deregulated calcium homeostasis in hippocampal neurons, providing a compelling explanation for the seizures observed in the mouse model. As such, I first aimed to investigate whether proteins involved in calcium homeostasis might be differentially expressed. Recently, inositol 3-phosphate receptors have come to be strongly associated with hereditary cerebellar ataxia and are deregulated in both the SCA7 mouse and the Polβ/ATM double knockout ataxic mouse, amongst other models (Bezprozvanny, 2010, Marelli, *et al*., 2011, Zambonin, *et al*., 2017, Kim, *et al*., 2020, Stoyas, *et al*., 2020). I do identify a significant decrease in the expression of IP3R in the cerebellum of the *Xrcc1*$^{Nes\text{-}Cre}$ mouse, which may in part underlie the ataxia observed in the mouse, due to its role in the regulation of calcium homeostasis in cerebellar PCs (Figure 5.2). Similarly, I identify significantly decreased expression of Grid2ip in the cerebellum (Figure 5.3). Grid2ip is linked to synaptic activity in PCs, providing another potential mechanism by which deregulated signalling in the cerebellum may underlie the progressive ataxia characterising the *Xrcc1*$^{Nes\text{-}Cre}$ mouse (Takeuchi, *et al*., 2008,

Ichikawa, *et al*., 2016). Previous studies have, however, noted the selective death of fast-spiking PCs in the *Xrcc1*$^{Nes\text{-}Cre}$ cerebellum, which may account for this loss of cerebellar IP3R and Grid2ip expression (Hoch, *et al*., 2017, Komulainen, E. unpublished observations). Interestingly, I observed elevated DAGLα expression in cerebellum, where it is expressed in PC parallel fibres, which might contradict our belief that decreased expression is a result of PC death (Figure 5.5). Perhaps the remaining PCs express very high DAGLα levels, or perhaps the expression is increased in non-fast spiking PCs. We did observe a significant downregulation of *Itpr2*, the gene encoding one of the inositol 3-phosphate receptor variants, in the *Xrcc1*$^{Nes\text{-}Cre}$ hippocampus via RNA sequencing. *Itpr2* was also highlighted by SARseq in rat cotical neurons as being located at a neuronal enhancer susceptible to site-specific SSBs (Wu, *et al*., 2020) (Figure 5.6 and 5.7 D). Decreased expression of *Itpr2* could contribute to alterations to calcium signalling in *Xrcc1*$^{Nes\text{-}Cre}$ hippocampal neurons, as IP3R2 regulates the release of calcium from the endoplasmic reticulum (Wiel, *et al*., 2014).

I further investigated the protein levels of Cacna1a, a subunit $Ca_{v2}2.1$, a P/Q type voltage-gated calcium channel. I proposed that alterations in the expression of voltage-gated calcium channels might interfere with the entry of Ca^{2+} into the synapse. Again, I observed decreased levels of Cacna1a in the cerebellum (Figure 5.4). Several studies have implicated deregulated calcium signalling in many ataxia phenotypes, and our data would perhaps suggest alterations in calcium homeostasis in the cerebellum due to receptor expression may contribute to the ataxia associated with the *Xrcc1*$^{Nes\text{-}Cre}$ mouse. Further, I observed decreased Cacna1a levels in the cortex. The *Xrcc1*$^{Nes\text{-}Cre}$ mouse is primarily characterised by progressive cerebellar ataxia and hippocampal seizures; we have yet to identify any element of the phenotype associated with cortical involvement. While the accumulation of poly(ADP-ribose) is most apparent in the cerebellum and hippocampus, there is still elevated accumulation in the cortex of *Xrcc1*$^{Nes\text{-}Cre}$ mice (Komulainen, *et al*., 2021). In future, cortical neurons should be cultured and investigated for the presence of an aberrant presynaptic calcium signalling phenotype. It is interesting that we do not observe decreased expression of *Cacna1a* in hippocampal tissue. In fact, apart from *Itpr2*, we do not observe significant downregulation of any genes directly involved in calcium homeostasis through RNA sequencing (Figure 5.6, Table 5.2 and 5.3). It is unlikely that such a strong cellular phenotype would be the result of a relatively weak downregulation of *Itpr2*, perhaps the inherent variability between samples might mask the deregulation of other genes that could be involved in maintaining calcium homeostasis. The downregulation of *Kcnj10* could indirectly result in alterations to evoked calcium signalling. Kcnj10 is expressed predominantly in glia,

and acts to buffer K^+ following its efflux from neurons during the propagation of an action potential (Seifert, *et al*., 2009). Decreased glial potassium buffering could result in the inhibition of K^+ efflux from the neuron, prolonging neuronal repolarisation. Mutations in *KNJ10* are associated with epilepsy and ataxia phenotypes (Guo, *et al*., 2015, Zhang, *et al*., 2019).

Of the 151 genes significantly deregulated in the *Xrcc1*$^{Nes\text{-}Cre}$ mouse, 73 were identified by Wu, *et al*., as being at neuronal enhancers prone to demethylation associated site-specific SSBs (Figure 5.10). These site-specific breaks occur at sites of 5mC demethylation, a BER dependent process (Weber, *et al*., 2016). *Itpr2* was one gene found to be significantly downregulated in the *Xrcc1*$^{Nes\text{-}Cre}$ hippocampus, highlighted by SARseq, and also found to be decreased in *Xrcc1*$^{Nes\text{-}Cre}$ cerebellum, being the only investigated protein to be deregulated in all experiments. Similarly, *Sez6* and *Plcl1* were identified in both RNA sequencing and SARseq data sets. My previous work has identified nNOS-dependent RNS as the primary source of endogenous SSBs in *Xrcc1*$^{Nes\text{-}Cre}$ hippocampal neurons, as opposed to site-specific breaks caused by active demethylation (Figure 3.14). These two mechanisms are not mutually exclusive, as both processes exist separately in the cell, producing SSBs that will be irreparable in the absence of Xrcc1. The remainder of DEGs identified in *Xrcc1*$^{Nes\text{-}Cre}$ hippocampal tissues could be due to the toxic effect of Parp1 on transcription in Xrcc1-deficient cells (Adamowicz, *et al*., 2021). In the absence of Xrcc1, Parp1 activation at DNA damage results in decreased ubiquitylation of USP3 and the subsequent inhibition of transcription (Adamowicz, *et al.,* 2021). This general inhibition of transcription may explain why there is a greater emphasis on downregulation of genes in the *Xrcc1*$^{Nes\text{-}Cre}$ brain and may underlie the deregulated transcription of genes not found to be localised at neuronal enhancers, such as *Cadh1* (downregulated in RNAseq but not highlighted by SARseq).

The question of whether this transcriptional abnormality underlies the *Xrcc1*$^{Nes\text{-}Cre}$ phenotype is puzzling. The magnitude of the effects observed in our sequencing is, in most cases, relatively small. This may reflect the great deal of variation in expression between mice of the same genotype, as we were unable to validate any of our highlighted genes by qPCR, and as such we are unable to conclude if aberrant gene expression underlies the *Xrcc1*$^{Nes\text{-}Cre}$ phenotype at this time (Figure 5.11). Perhaps the heterogeneity in tissue samples could be resolved using single cell analysis. We did not note any clear explanation of the aberrant calcium signalling phenotype observed in *Xrcc1*$^{Nes\text{-}Cre}$ hippocampal neurons, and many of the DEGs were disparate in functionality. We do observe some degree of functional clustering; several genes encoding members of the semaphorin protein were found to be deregulated, perhaps indicating defective

axonal guidance in the *Xrcc1*$^{Nes\text{-}Cre}$ mouse that should be further investigated (Figure 5.9). The significant downregulation of Cadherin 1 is rather striking and could have critical consequences in the formation of inhibitory synapses. Interestingly, Cadherin 1 functionality is significantly impaired in the Tdp1 homolog glaikit knockout drosophila model (Figure 5.8) (Dunlop, *et al*., 2004). As such, the functionality of Cadherin 1 in the *Xrcc1*$^{Nes\text{-}Cre}$ is a highly exciting avenue for further investigation.

5.3.1 Conclusions

Xrcc1$^{Nes\text{-}Cre}$ mice exhibit significant alterations to the expression of several proteins involved in calcium homeostasis and PC signalling in the cerebellum (Figure 5.2 – 5.5). *Xrcc1*$^{Nes\text{-}Cre}$ hippocampi are characterised by aberrant gene expression (Figure 5.6). The magnitude of the observed effect on hippocampal gene expression is, however, relatively small and highly variable between mice of the same genotype and, as such, we are unable to conclude whether this aberrant expression underlies the seizures that typify the *Xrcc1*$^{Nes\text{-}Cre}$ mouse. We highlight Sema proteins and Cadherin 1 as exciting avenues for further investigation, proposing that the downregulation of these proteins may play a role in the aetiology of the *Xrcc1*$^{Nes\text{-}Cre}$ mouse phenotype. We did not, however, identify a clear mechanism underlying the deregulation of calcium signalling in *Xrcc1*$^{Nes\text{-}Cre}$ hippocampal neurons.

Chapter 6: General Discussion

The Role of Parp1 in Xrcc1-Linked Neuropathology

XRCC1 is a DNA repair scaffold protein critical for the efficient repair of SSBs (Caldecott, 2008, Andres, *et al*., 2015). The recruitment of XRCC1 is facilitated by the autoribosylation of PARP1, a SSB sensor (Masson, *et al*., 1998, Breslin, *et al*., 2015, Alemasova and Lavrik, 2019). Mutations in *XRCC1* are associated with AOA-XRCC1, which is characterised by progressive cerebellar degeneration and ataxia (Hoch, *et al*., 2017, O'Connor, *et al*., 2018). In mice, *Xrcc1* deletion is similarly associated with cerebellar dysfunction, alongside terminal seizures that limit mouse lifespan (Hoch, *et al*., 2017, Komulainen, *et al*., 2021). Hereditary defects in several proteins involved in SSBR are associated with neurodegeneration, but the mechanism behind this neurological involvement is unclear (Caldecott, 2008, McKinnon, 2017). Investigations of this phenomenon have mostly taken place in proliferating cell models and have demonstrated that, in the absence of XRCC1, endogenous DNA damage results in the hyperactivation of PARP1 and consequently elevated levels of poly(ADP-ribose) (Hanzlikova, *et al*., 2018) (Figure 3.1). In *Xrcc1*$^{Nes\text{-}Cre}$ mouse brain, elevated Parp1 activity similarly leads to elevated levels of poly(ADP-ribose), most notably in the hippocampus and cerebellum (Hoch, *et al*., 2017, Komulainen, *et al*., 2021). In this study, I investigated the effects of Xrcc1 deficiency in cultured post-mitotic neurons, providing for the first time a cell autonomous model for understanding the link between defects in SSBR, Parp1 hyperactivation, and neuronal dysfunction.

Endogenous SSBs can arise through a variety of mechanisms, such as by abortive TOP1 activity, as intermediates in BER, and by direct oxidation of the DNA sugar moiety (Pogozelski & Tullius, 1998, Caldecott, 2008, Andersen, *et al*., 2015, Li & Liu, 2016). The highly specialised function and morphology of brain may, in part, account for why the defect in SSBR and accumulation of poly(ADP-ribose) triggers dysfunction of the cerebellum and hippocampus in *Xrcc1*$^{Nes\text{-}Cre}$ mouse. For example, hippocampal function is highly reliant on NO signalling, which may result in the formation of reactive nitrogen species capable of inducing SSBs (Dinerman, *et al*., 1994, Niles, *et al*., 2006, Paul and Ekambaram, 2011, McLeod, *et al*., 2020). Alternatively, perhaps elevated active demethylation could underlie this selective accumulation, as this BER-dependent process is particularly prominent in both cerebellar and hippocampal neurons (Kraucionis and Heintz, 2009, Oliveira, 2016). To investigate the source of endogenous SSB damage, I cultured hippocampal neurons from *Xrcc1*$^{Nes\text{-}Cre}$ mice (See Chapter 3). While these cells exhibited elevated Parp1 activity following exposure to exogenous

damaging agents such as MMS and CPT, I did not detect elevated levels of poly(ADP-ribose) in untreated *Xrcc1*$^{Nes\text{-}Cre}$ hippocampal neurons, as a result of endogenous DNA damage. This was in contrast to the elevated level of poly(ADP-ribose) in detected in hippocampus and in other regions of the brain, *in vivo* (Komulainen, *et al*., 2021) (Figure 3.3, 3.4, and 3.5). Recently, Hanzlikova *et al*, demonstrated that elevated poly(ADP-ribose) can be detected in *XRCC1*$^{-/-}$ RPE-1 cells if incubated for short periods with PARG inhibitor, to prevent catabolism of the nascent polymer (also shown in Figure 3.1). Similarly, I detected elevated poly(ADP-ribose) accumulation in PARG inhibitor-treated *Xrcc1*$^{Nes\text{-}Cre}$ hippocampal neurons, confirming that these cells are indeed characterised by elevated endogenous damage and Parp1 activation (Figure 3.6). Interestingly, co-treatment with either a PARP or NAMPT inhibitor suppressed this activity, suggesting that elevated Parp1 activity is continuous in Xrcc1-deficient neuronal nuclei (Figure 3.6, Figure 3.11).

There are several mechanisms by which SSBs can occur (see 3.1). However, the predominantly neurological phenotype associated with hereditary defects in SSBR suggests that a neuronal specific mechanism, or a process more active in post-mitotic neurons, might underlie this damage. Consistent with this idea, lower levels of poly(ADP-ribose) were detected during incubation with PARG inhibitor in co-cultured, *Xrcc1*$^{Nes\text{-}Cre}$ glia (Figure 3.6). One possible source of endogenous SSBs in neurons is the abortive activity of TOP1. The expression of long genes, which are important for neuronal function, requires TOP1, which relieves torsional stress during transcription (King, *et al*., 2013). TOP1 function requires the transient nicking of DNA, and the formation of a reversible TOP1cc (Stewart, *et al*., 1998, Pommier, *et al*., 2006). Elevated levels of Top1ccs have been detected in murine models of AT and SCAN1, and the deletion of *Xrcc1* leads to the accumulation of Top1ccs in proliferative neural progenitor cells, and the cerebellum (Katyal, *et al*., 2014). Similarly, direct TOP1 poisoning (and the resultant accumulation of TOP1ccs) phenocopies the neuropathology associated with defective DDR (Katyal, *et al*., 2014). However, abortive TOP1 activity results in the formation of a detectable SSB only following proteasomal degradation of the abortive cleavage complex (El-Khamisy and Caldecott, 2006, Desai, *et al*., 2008). Importantly, I showed that *Xrcc1*$^{Nes\text{-}Cre}$ hippocampal neurons still exhibit elevated endogenous levels of poly(ADP-ribose) even if incubated in the presence of proteasome inhibitor, indicating that the underlying source of SSBs that trigger elevated PARP1 activity in *Xrcc1*$^{Nes\text{-}Cre}$ hippocampal neurons is not TOP1 activity (Figure 3.13).

The Contribution of Nitric Oxide to Parp1 Activation in *Xrcc1*$^{Nes\text{-}Cre}$ Hippocampal Neurons

Another, neuronal specific, mechanism by which endogenous SSBs may arise is through nitric oxide signalling. NO signalling is critical in synaptogenesis and the maintenance of synaptic plasticity (Dinerman, *et al*., 1994, Paul and Ekambaram, 2011, McLeod, *et al*., 2020). NO synthesis is also induced during glutamate excitotoxicity, wherein excessive stimulation results in postsynaptic calcium influx and the Ca^{2+} dependent activation of nNOS (Lewerenz and Maher, 2015, Wang and Swanson, 2020). The consequences of NO signalling are the production of RNS, which are capable of inducing SSBs through oxidation of either the DNA sugar moiety or nucleobases (Niles, *et al*., 2006, ul Islam, *et al*., 2015). Interestingly, I observed significant suppression of poly(ADP-ribose) accumulation in *Xrcc1*$^{Nes\text{-}Cre}$ hippocampal neurons treated with the nNOS inhibitor L-NAME (Figure 3.2.14). This suggests that NO signalling contributes to the SSBs that induce elevated PARP1 activity in *Xrcc1*$^{Nes\text{-}Cre}$ hippocampal neurons. Consistent with this idea, poly(ADP-ribose) levels were not significantly suppressed by L-NAME in glial cells, which do not utilise NO signalling to the same extent (Contestabile, *et al*., 2012) (Figure 3.2.14). The neuronal specific induction of SSBs following NO signalling provides a potential mechanism for the neurological phenotype associated with *Xrcc1* deletion. However, *Xrcc1*$^{Nes\text{-}Cre}$ hippocampal neurons do still exhibit significantly elevated levels of poly(ADP-ribose), indicating that NO signalling does not constitute all of the endogenous damage occurring in these cells (Figure 3.14). Perhaps the remainder of this damage occurs through ROS, as a consequence of cellular metabolism. Future experiments could involve the preincubation of *Xrcc1*$^{Nes\text{-}Cre}$ hippocampal neurons with ROS scavengers, such as ascorbic acid (Oh, *et al*., 2020). Alternatively, perhaps these residual SSBs are the result of active cytosine demethylation during epigenetic (re)modelling of the neural genome; a process that regulates the transcription profile/s that determine and maintain neural cell identity, and which involve the creation of SSB intermediates of BER, although we would expect Parp1 activation at these sites to be suppressed by *Ape1* deletion (Bayraktar and Kreutz, 2017, Wu and Zhang, 2017). Recently site-specific DNA SSBs were identified at sites of neuronal enhancers, the result of active demethylation at CpG sites, resulting in BER intermediates which could account for the Parp1 activity not suppressed by nNOS inhibition (Caldecott, 2020, Wu, *et al*., 2021).

The consequence of NO signalling is the production of $ONOO^-$, a RNS capable of attacking DNA (Radi, 2013, Radi, 2018). RNS-mediated base modification is repaired through BER, an Ape1-dependent process (Thakur, *et al*., 2014). However, *Ape1* deletion did not rescue poly(ADP-ribose) accumulation in *Xrcc1*$^{Nes\text{-}Cre}$ hippocampal

neurons (Figure 3.15). In fact, the deletion of *Ape1* resulted in elevated levels of poly(ADP-ribose). Perhaps this elevated Parp1 activity is linked to the collision of transcriptive polymerases with unresolved AP sites (Zhou and Doetsch, 1993). A separate mechanism for this activity could be due to the elevated formation of abortive TOP1ccs, which may be more likely to form due to proximity with existing lesions, such as AP sites (El-Khamisy and Caldecott, 2006). In order to further investigate this Parp1 activity in *Ape1*$^{Nes\text{-}Cre}$ neurons, future experiments would involve pre-treatment with either proteasome inhibitors, such as MG132, to prevent cleavage complex degradation, or transcription inhibitors such as DRB to prevent RNA polymerase collision. Further, the elevated steady state level of AP sites could lead to SSBs through spontaneous hydrolysis (Greenberg, 2014). Regardless, that deletion of *Ape1* did not suppress Parp1 activity in *Xrcc1*$^{Nes\text{-}Cre}$ neurons would suggest that nitrosative damage is not due to the modification of nucleobases, or at least is not being repaired by APE1 (Thakur, *et al*., 2014). Instead, I propose that $ONOO^-$ mediated oxidation of the DNA sugar may underlie the elevated incidence of DNA SSBs in *Xrcc1*$^{Nes\text{-}Cre}$ neuronal cells (Figure 6.1). $ONOO^-$ mediated oxidation of DNA may be linked to hereditary defects in PNKP, as it is required for end processing following sugar damage (Caldecott, 2008). By contrast, it is unlikely that this mechanism underpins the pathology of SCAN1, as $ONOO^-$ is not linked to elevated TOP1ccs.

Parp1 Dependent Cell Death in Xrcc1 Deficient Models

The deletion of both alleles of *Parp1* is sufficient to significantly rescue the *Xrcc1*$^{Nes\text{-}Cre}$ phenotype, resulting in the suppression of poly(ADP-ribose) accumulation and extending lifespan through the ablation of seizure activity (Komulainen, *et al*., 2021). Similarly, the deletion of *Parp1* is sufficient to prevent cerebellar degeneration and the death of cerebellar interneurons in the *Xrcc1*$^{Nes\text{-}Cre}$ mouse (Lee, *et al*., 2009, Komulainen, *et al*., 2021). Consistent with these observations, we show that the deletion of one or both alleles of *Parp1* is sufficient to suppress poly(ADP-ribose) levels in cultured *Xrcc1*$^{Nes\text{-}Cre}$ hippocampal neurons (Figure 3.7). Parp1-dependent cell death has not been observed in the *Xrcc1*$^{Nes\text{-}Cre}$ hippocampus, however cultured *Xrcc1*$^{Nes\text{-}Cre}$ hippocampal neurons do exhibit spontaneous death *in vitro* (Figure 3.8). Alongside suppression of elevated poly(ADP-ribose) levels, I noted that *Parp1*$^{+/-}$/*Xrcc1*$^{Nes\text{-}Cre}$ and *Parp1*$^{-/-}$/*Xrcc1*$^{Nes\text{-}Cre}$ cultures exhibited decreased cell death (Figure 3.7 and 3.8). The deletion of only one copy of *Parp1* resulted in a slightly higher level of rescue than seen in double knockout cells, perhaps consistent with the observation that *Parp1*$^{+/-}$/*Xrcc1*$^{Nes\text{-}Cre}$ mice live longer than their double knockout counterparts (Komulainen, *et al*., 2021). Perhaps one

functional copy of *Parp1* is sufficient to perform an as yet unidentified role in SSBR defective cells, while maintaining poly(ADP-ribose) at sub-pathological levels.

This spontaneous cell death could be rescued by an even greater degree by chronic administration of a PARP inhibitor (Figure 3.8). Similarly, I noted that *Xrcc1*$^{Nes\text{-}Cre}$ hippocampal neurons and glia were strikingly sensitive to PARG inhibition, which could also be rescued by *Parp1* deletion or inhibition (Figure 3.9 and Figure 3.10). This would indicate that the accumulation of significant quantities of poly(ADP-ribose) is capable of inducing cell death, and that neuronal cells are either more prone to this accumulation or are more sensitive to poly(ADP-ribose) toxicity. Interestingly, PARP inhibition rescued PARG inhibitor toxicity in glial cells (Figure 3.10). Proliferative. XRCC1 deficient cells are known to be sensitive to PARP inhibition, due to replication fork collapse and DSB formation (Ali, *et al*., 2020). This sensitivity occurs during replication, however, and in order to avoid overpopulation of glia, cells were cultured in serum free media to inhibit cell cycle progression (Chou and Langan, 2003, Horton, *et al*., 2014, Ali, *et al*., 2020).

Parp1-dependent cell death (parthanatos) is linked to several neurodegenerative diseases; however, it is unclear whether this occurs in the *Xrcc1*$^{Nes\text{-}Cre}$ mouse (Hivert, *et al*., 1998, Love, *et al*., 1999, Vis, *et al*., 2005, Kam, *et al*., 2020). Previous studies have indicated that parthanatotic death is linked to metabolic collapse, preceding the migration of AIF to the nucleus, and can be rescued by supplementation with either TCA substrates or NAD+ precursors (though some evidence has suggested it can occur independent of NAD+ levels) (Ying, *et al*., 2002, David, *et al*., 2009, Andrabi, *et al*., 2014, Fouquerel, *et al*., 2014). I observed that supplementation with NMN suppressed PARG inhibitor sensitivity in both *XRCC1*$^{-/-}$ RPE-1 cells and *Xrcc1*$^{Nes\text{-}Cre}$ hippocampal neurons (Figure 3.2, and 3.12). This would indicate that PARG inhibitor sensitivity is caused by the Parp1 dependent depletion of NAD+, however it is still unclear whether this represents parthanatotic cell death. In order to clarify the mechanism of cell death, I would need to confirm the translocation of AIF to the nucleus, as this is a prerequisite step in parthanatos (Fatokun, *et al*., 2014). I did not note any rescue of spontaneous neuronal death following chronic NMN administration, indicating that this cell death is unrelated to NAD+ depletion, and represents a separate, Parp1-dependent mechanism of toxicity (Figure 3.12). Immunofluorescent labelling of AIF would again allow us to investigate whether this spontaneous cell death is linked to parthanatos (Fatokun, *et al*., 2014). A separate mechanism underlying this cell death could be the deregulation of transcription. PARP1 is known to regulate transcription through the regulation of nucleosome structure, and direct modification of proteins such as the polycomb

repressive complex and transcription factors (Chou, *et al*., 2010, Lönn, *et al*., 2010, Matveeva, *et al*., 2019). Perhaps the elevated autoribosylation of Parp1 at sites of damage results in alterations to Parp1-dependent transcriptional regulation in *Xrcc1*$^{Nes\text{-}Cre}$ neurons. Recently, Adamowicz *et al* detected PARP1-dependent transcription inhibition in the absence of XRCC1 due to the decreased ubiquitylation of USP3. Perhaps Parp1-dependent transcription inhibition results in the decreased expression of genes required for neuronal function and survival in *Xrcc1*$^{Nes\text{-}Cre}$ hippocampal neurons.

Parp1 Hyperactivation Couples Endogenous SSBs to Alterations in Synaptic Signalling

Following my discovery that *Xrcc1*$^{Nes\text{-}Cre}$ derived hippocampal neurons recapitulate in vitro the endogenous poly(ADP-ribose) accumulation seen in *Xrcc1*$^{Nes\text{-}Cre}$ mouse brain (Figure 3.5 and Figure 3.6), I investigated the signalling defects in these neurons that might underlie the seizures that characterise this mouse model. To do this, I employed an optical reporter of presynaptic calcium flux, to measure synaptic functionality in cultured wild type and *Xrcc1*$^{Nes\text{-}Cre}$ neurons. SyGCaMP6f is a genetically encoded, engineered calcium indicator that functions through Ca^{2+} dependent interactions with calmodulin, leading to change in GFP fluorescence emission (Nakai, Ohkura, and Imoto, 2001) (Figure 4.1). The transient increase in [Ca^{2+}] at the presynaptic terminal is a key step in the conversion of an action potential to chemical transmission at the synapse, preceding the fusion of neurotransmitter containing vesicles (Südhof, 2012). I observed that, when stimulated, wild type neurons exhibited GFP fluorescence change characteristic of typical activity-evoked increase in pre-synaptic [Ca^{2+}] (Figure 4.1). Moreover, I observed a ~2-fold increase in response amplitude upon stimulation of *Xrcc1*$^{Nes\text{-}Cre}$ hippocampal neurons, indicating that Xrcc1 loss results in excessive activity-evoked Ca^{2+} influx (Figure 4.2).

The increased amplitude was partially or fully suppressed in neurons cultured from *Parp1*$^{+/-}$/*Xrcc1*$^{Nes\text{-}Cre}$ and *Parp1*$^{-/-}$/*Xrcc1*$^{Nes\text{-}Cre}$ mice respectively (Figure 4.6). This correlates with the degree to which poly(ADP-ribose) accumulation was suppressed in the brain and cultured neurons of these two genotypes (Komulainen, *et al*., 2021) (Figure 3.7). To my knowledge, this is the first data to demonstrate a mechanistic link between Parp1 activity and synaptic calcium signalling, providing a compelling potential explanation for the seizures observed in the *Xrcc1*$^{Nes\text{-}Cre}$ mouse. Consistent with this idea, the suppression of this calcium defect by deletion of one or both *Parp1* alleles also correlated with the level of suppression of seizure-like activity in *Parp1*$^{+/-}$/*Xrcc1*$^{Nes\text{-}Cre}$ and *Parp1*$^{-/-}$/*Xrcc1*$^{Nes\text{-}Cre}$ hippocampal sections, *ex vivo* (Komulainen, *et al*., 2021). The identification of a Parp1-dependent signalling correlate of the seizures exhibited by the

Xrcc1$^{Nes\text{-}Cre}$ mouse likely explains the increased lifespan associated with *Parp1*$^{+/-}$/*Xrcc1*$^{Nes\text{-}Cre}$ and *Parp1*$^{-/-}$/*Xrcc1*$^{Nes\text{-}Cre}$ mice (Komulainen, *et al*., 2021). We do not observe seizures in double knockout mice, consistent with the absence of elevated synaptic activity in *Parp1*$^{-/-}$/*Xrcc1*$^{Nes\text{-}Cre}$ cultured hippocampal neurons (Komulainen, *et al*., 2021) (Figure 4.6). While these mice do exhibit premature mortality, we believe that this is due to a separate requirement for Parp1 in the SSBR-defective brain and unrelated to seizure pathology. Similarly, we have yet to observe seizures in *Parp1*$^{+/-}$/*Xrcc1*$^{Nes\text{-}Cre}$ mice. This, however, is likely due to the challenges associated with long term observation of the mouse model. Given the elevated seizure like activity in the *ex vivo* *Parp1*$^{+/-}$/*Xrcc1*$^{Nes\text{-}Cre}$ hippocampus, and the elevated amplitude of activity evoked presynaptic Ca^{2+} transients, we believe that *Parp1*$^{+/-}$/*Xrcc1*$^{Nes\text{-}Cre}$ mice do exhibit terminal seizures later in life. I propose that the decreased accumulation of poly(ADP-ribose) in the *Parp1*$^{+/-}$/*Xrcc1*$^{Nes\text{-}Cre}$ mouse brain significantly delays the onset of these seizures, perhaps by reducing the severity of the *Xrcc1*$^{Nes\text{-}Cre}$ synaptic signalling phenotype.

To further confirm these findings, *Xrcc1*$^{Nes\text{-}Cre}$ neurons were treated chronically with the PARP inhibitor KU0058948, restoring activity-evoked Ca^{2+} transients to a waveform that was indistinguishable in amplitude and duration from those observed in wild type neurons (Figure 4.8, Figure 4.11). This outcome is strikingly different from the ineffectiveness of intraperitoneal administration of PARP inhibitors in rescuing mouse lifespan (Komulainen, E. Unpublished Observations). At present, it is unclear if this latter case is due to difficulties in the inhibitor crossing the blood-brain barrier, or an issue with maintenance of PARP inhibition. Perhaps *in vitro* administration simply provides the ideal cellular environment to test the effect of Parp1 inhibition on synaptic defects, which may explain this discrepancy with *in vivo* studies. Recently, the successful maintenance of PARP inhibition in the mouse brain was shown to rescue seizure like activity in the *ex vivo* hippocampus (Komulainen, *et al*., 2021). This, alongside the finding that PARP inhibitors can rescue signalling correlates of the *Xrcc1*$^{Nes\text{-}Cre}$ seizure phenotype *in vitro* highlight the therapeutic potential of PARP inhibitors in the treatment of *XRCC1*-linked neuropathology and, potentially, the treatment of other hereditary defects of SSBR associated with seizure phenotypes, such as MCSZ. The trapping of PARP1 by PARP inhibitors results in replication dependent cytotoxicity, which is not relevant to post-mitotic neurons (Rein, *et al*., 2015). However, the trapping of PARP1 can result in inhibition of transcription, which may result in altered expression of genes critical for neuronal function (Shen, *et al*., 2015). A similar caveat is inhibitor specificity, as several clinical PARP inhibitors do not selectively target PARP1, and often have additional effects on PARP2 (Murai, *et al*., 2012). The double knockout *Parp1* and *Parp2* is non-

viable (de Murcia, *et al*., 2012). Further, while PARP2 is responsible for a relatively small portion of poly(ADP-ribosylation) in the nucleus, it functions to protect against mitochondrial ROS induction and is active in brain following ischemia reperfusion, and so the consequences of off target effects by PARP inhibitors remain unclear (Kofler, *et al*., 2006, Janko, *et al*., 2021). As such, the development of less toxic, non-trapping, PARP1 specific inhibitors that phenocopy deletion would represent a significant step forward in the treatment of SSBR linked neuropathology.

Based on my data, I propose that Xrcc1 deficiency and Parp1 hyperactivation results in excessive Ca^{2+} flux at the presynaptic terminal, which may precipitate further damage induction (Figure 6.1). The initial source of damage is not yet fully understood but may be the result of non-pathological nitric oxide signalling, or perhaps ROS, which result in Parp1 hyperactivation and alterations to synaptic signalling. Given the intimate link between presynaptic Ca^{2+} and vesicle exocytosis, this is highly likely to drive elevated fusion of neurotransmitter containing vesicles, a hypothesis that could be directly tested using optical reporters of vesicle dynamics, such as sypHy (Royle, *et al*., 2008, Hempel, *et al*., 2011). In excitatory neurons, glutamate is the predominant neurotransmitter (Zhou and Danbolt, 2014). Excessive glutamate transmission results in excitotoxicity, through the elevated influx of Ca^{2+} into the postsynaptic terminal (Andrabi, *et al*., 2011, Lewerenz and Maher, 2015). Further optical reporters, such as iGluSnFr and PSD-GCaMP could be used to investigate glutamate transmission and postsynaptic calcium flux respectively (Marvin, *et al*., 2018, Topolnik and Camiré, 2019). Previously, I attempted to utilise these optical reporters, however the inherent sensitivity of *Xrcc1*$^{Nes\text{-}Cre}$ hippocampal neurons resulted in cell death and, as such, the reporters could not be expressed. Elevated postsynaptic Ca^{2+} influx results in the increased calmodulin/nNOS dependent synthesis of nitric oxide (Burney, *et al*., 1999, Zhou and Zhu, 2009). Perhaps the nNOS dependent activation of Parp1; downstream of aberrant presynaptic Ca^{2+} signalling, and subsequent excessive activity results in the NO dependent accumulation of poly(ADP-ribose). To investigate this, pretreatment of hippocampal neurons with NMDAr blockers prior to PARG inhibition would highlight the contribution of glutamate excitotoxicity to Parp1 activation. Perhaps non-pathological NO signalling and ROS result in a feedback loop of Parp1 activation and the deregulation of presynaptic Ca^{2+} signalling which, in turn, stimulates NO synthesis and the induction of further damage.

Having discovered that Xrcc1 loss results in Parp1-dependent, excessive, activity-evoked Ca^{2+} influx, I sought to investigate the mechanistic link between nuclear poly(ADP-ribose) accumulation and signalling irregularities at the synapse. Due to the

elevated synthesis of poly(ADP-ribose), there is a ~ 50% reduction in total NAD+ in the *Xrcc1*$^{Nes\text{-}Cre}$ brain (Komulainen, *et al*., 2021). NAD+ is utilised as a co-factor by several enzymes, notably Sirt1 and CD38 (Pehar, *et al*., 2018).. Interestingly, NAD+ repletion was sufficient to partially suppress the elevated response amplitudes in *Xrcc1*$^{Nes\text{-}Cre}$ synapses, indicating that the depletion of NAD+ by Parp1 may contribute to the deregulation of presynaptic Ca^{2+} signalling (Figure 4.13).

Sirt1 is an NAD+ dependent deacetylase, which acts to regulate the expression of several genes involved in cellular homeostasis and longevity (Elibol and Kilic, 2018, Herskovitzs, *et al*., 2018). Decreased NAD+ bioavailability has been shown to affect the expression of genes encoding regulators of Ca^{2+} homeostasis in a model of cerebellar ataxia, the SCA7 mouse, through the inhibition of Sirt1 (Stoyas, *et al*., 2020). Perhaps the depletion of NAD+ by Parp1 results in Sirt1 inhibition and altered transcription in *Xrcc1*$^{Nes\text{-}Cre}$ hippocampal neurons, which may underlie aberrant presynaptic Ca^{2+} signalling. In order to investigate whether the depletion of NAD+ in Xrcc1 deficient hippocampal neurons results in aberrant transcription, future work would involve RNA-sequencing of NMN treated cells. A further mechanism by which NAD+ depletion may result in deregulation of synaptic Ca^{2+} signalling is through CD38. CD38 is an enzyme responsible for the NAD+ dependent synthesis of cADPr, which facilitates the release of calcium from intracellular stores (Hogan, *et al*., 2019). cADPr functions in the activation of ryanodine receptors, which are deregulated in SCA2. Perhaps NAD+ depletion results in the inhibition of CD38, decreased cADPr synthesis, and subsequent alterations to ER calcium release in *Xrcc1*$^{Nes\text{-}Cre}$ hippocampal neurons. The possibility that the deregulation of CD38 might underlie the aberrant presynaptic calcium signalling in Xrcc1 deficient neurons could be tested in future experiments using optical reporters of ER calcium dynamics, such as CatchER, following chronic NAD+ supplementation (Tang, *et al*., 2011).

<u>The Effect of *Xrcc1* Deletion on Transcription in the Hippocampus</u>

Given that NAD+ depletion has been shown to result in an alteration in gene expression, and that PARP1 was recently shown to inhibit transcription in the absence of XRCC1, I questioned whether the *Xrcc1*$^{Nes\text{-}Cre}$ mouse exhibited deregulated transcription (Stoyas, *et al*., 2020, Adamowicz, *et al*., 2021). I identified altered levels of several proteins involved in calcium signalling in the *Xrcc1*$^{Nes\text{-}Cre}$ cerebellum but did not see any significant changes in hippocampal tissues (Figures 5.2 and Figure 5.4). RNA sequencing of *Xrcc1*$^{Nes\text{-}Cre}$ hippocampal tissue did, however, identify significant differential expression of 151 genes (Figure 5.6). Of these genes, there was a degree of

crossover with those identified by Wu *et al*., as being at locations of neuronal enhancers prone to active demethylation and site-specific DNA breakage, however this crossover was not significant (Figure 5.10). Interestingly, the majority of DEGs identified by RNA-sequencing of *Xrcc1*$^{Nes\text{-}Cre}$ were downregulated – consistent with the PARP1-dependent inhibition of transcription in the absence of XRCC1 due to decreased USP3 ubiquitylation (Adamowicz, *et al*., 2021).

The degree to which the DEGs identified in *Xrcc1*$^{Nes\text{-}Cre}$ hippocampi varied from the wild type was small, with the majority of significantly deregulated genes differing by a factor between Log2FC -1 and 1 (Tables 5.2 and 5.3). We were unable to significantly validate any highlighted DEGs by qPCR, however. This may reflect the relatively small magnitude of the observed effects, as well as the small sample size and high degree of variability between samples. In order to fully examine whether these targets can be validated by qPCR, I would next need to increase the sample size, as in most cases the result replicated the trend observed in our RNA-seq data set (Table 5.1). Perhaps the combined effect of the deregulated expression of many of these proteins contributes in some way to the *Xrcc1*$^{Nes\text{-}Cre}$ phenotype. Notably, several DEGs identified in the *Xrcc1*$^{Nes\text{-}Cre}$ hippocampus are linked to neuronal signalling (Tables 5.2 and 5.3). One such DEG is Cdh1, which encodes Cadherin 1 (downregulated in *Xrcc1*$^{Nes\text{-}Cre}$ hippocampus, Log2FC = -0.799). The deletion of Cadherin 1 results in decreased density of GABAergic inhibitory synapses, which could result in a deregulation of the E/I balance and result in altered network activity (Fritschy, 2008, Fiederling, *et al*., 2011). Similarly, Kcnmj10 (downregulated in *Xrcc1*$^{Nes\text{-}Cre}$ hippocampus, Log2FC = -0.654), which acts to buffer cytosolic K^+ and modulate action potential propagation, may also contribute to network signalling defects (Kucheryavykh, *et al*., 2007, Guo, *et al*., 2015, Zhang, *et al*., 2019).

Beyond Parp1 hyperactivation and NAD+ depletion, the presence of unresolved SSBs may also result in defective transcription, as transcriptive polymerases may stall at sites of damage (Kathe, *et al*., 2004). Perhaps alterations to transcription might also underlie elements of the phenotype associated with the *Parp1*$^{+/-}$/*Xrcc1*$^{Nes\text{-}Cre}$ and *Parp1*$^{-/-}$/*Xrcc1*$^{Nes\text{-}Cre}$ mice, which are SSBR deficient and still exhibit early mortality. It is important to investigate next whether there is significant deregulation of transcription in the aged *Parp1*$^{+/-}$/*Xrcc1*$^{Nes\text{-}Cre}$ and *Parp1*$^{-/-}$/*Xrcc1*$^{Nes\text{-}Cre}$ mice compared to wild type, and whether this may underlie elements of their phenotype.

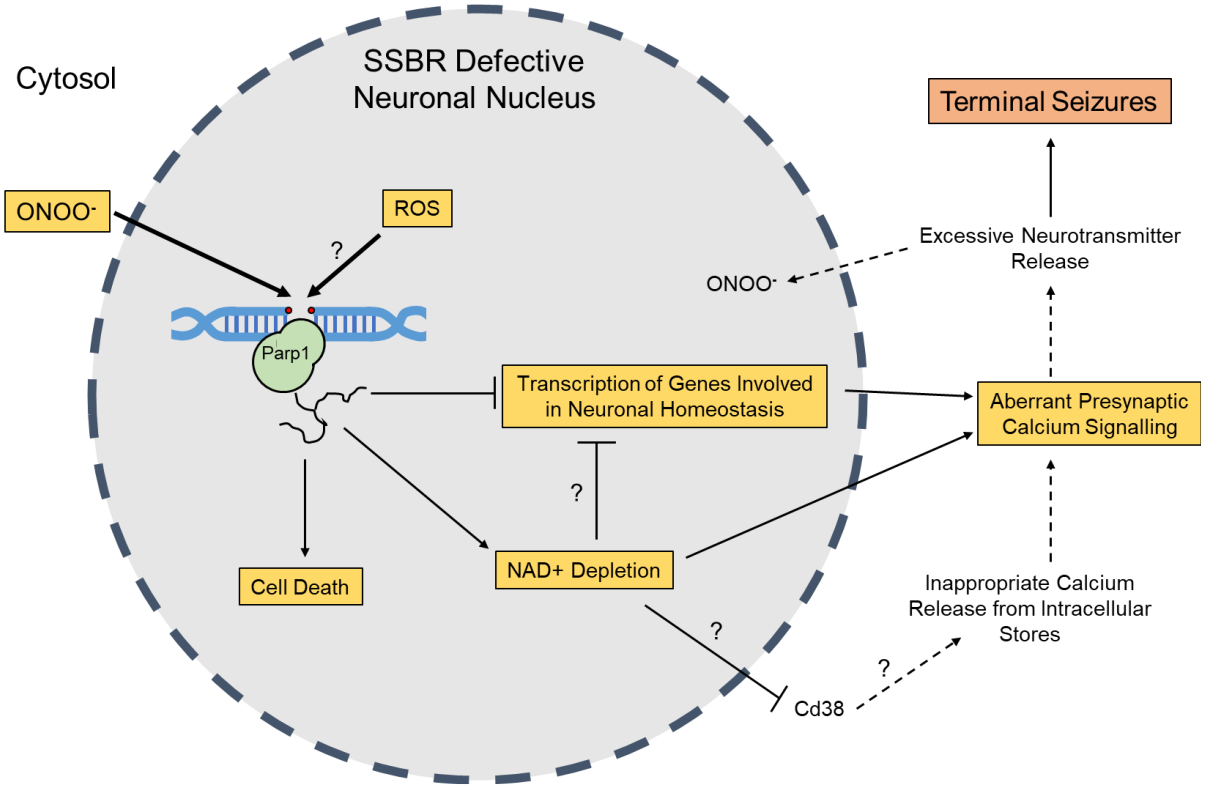

Figure 6.1 *A Model of Endogenous SSBs and Parp1 Activation Leading to Terminal Seizures in Xrcc1*$^{Nes\text{-}Cre}$ *mice*. Processes involved in neuronal homeostasis, such as NO signalling and metabolism result in the formation of a SSB, activating Parp1. In Xrcc1-deficient neurons, the repair of this SSB is delayed, leading to constitutive poly(ADP-ribose) synthesis. Elevated levels of poly(ADP-ribose) result in cell death, as well as the depletion of cellular NAD+. Parp1 activation also results in the inhibition of transcription, resulting in the altered expression of genes involved in the maintenance of neuronal homeostasis, such as Cdh1 and Itpr2. This, along with NAD+ depletion, contributes to aberrant presynaptic calcium signalling. Excessive activity evoked presynaptic calcium signalling in SSBR defective hippocampal neurons likely results in inappropriate vesicle fusion and neurotransmitter release, resulting in further induction of nitrosative DNA damage and providing a compelling explanation for the terminal seizures that characterise the *Xrcc1*$^{Nes\text{-}Cre}$ mouse.

6.1 Model and Concluding Remarks

My studies of *Xrcc1*$^{Nes\text{-}Cre}$ hippocampal neurons have revealed that, in the absence of Xrcc1, Parp1 hyperactivity at sites of endogenous SSBs results in the accumulation of poly(ADP-ribose) in the nucleus (Figure 6.1). I propose that in neuronal cells, a fraction of this damage occurs due to nitric oxide signalling and the production of $ONOO^-$, an RNS capable of inducing damage to DNA, with the remainder likely being due to ROS, a by-product of metabolism (Figure 6.1). $ONOO^-$ mediated damage may occur as a by-product of non-pathological nitric oxide signalling, or as a result of glutamate excitotoxicity. Parp1 is recruited to these breaks, whereupon it begins to continuously synthesise nascent poly(ADP-ribose). This accumulation of poly(ADP-ribose) may disrupt cellular homeostasis through the depletion of NAD+ (Figure 6.1). The consequence of Parp1 hyperactivation is the selective death of neurons *in vitro,* and the deregulation of presynaptic calcium signalling, which may result in further damage due to excessive glutamate release, both of which can be suppressed by the deletion or inhibition of Parp1 (Figure 6.1). I propose that this deregulation of presynaptic Ca^{2+} represents a signalling correlate of the seizures that characterise the *Xrcc1*$^{Nes\text{-}Cre}$ mouse. I show that supplementation with NAD+ precursors is sufficient to partially rescue the elevated amplitude of activity evoked Ca^{2+} transients in *Xrcc1*$^{Nes\text{-}Cre}$ hippocampal neurons, indicating that Parp1-dependent NAD+ depletion may contribute to this phenotype. It is unclear whether the partial rescue is due inefficient uptake of NMN, or if the remaining signalling defect is due to a separate, Parp1-dependent mechanism, such as the deregulation of transcription. I show that loss of Xrcc1 results in aberrant gene expression in the mouse brain, which may also contribute to the phenotype associated with the *Xrcc1*$^{Nes\text{-}Cre}$ mouse. These data contribute to our understanding of XRCC1-linked neuropathology, the contribution of PARP1 to neurodegeneration, and the therapeutic potential of PARP inhibitors in the treatment of SSBR-linked disease.

7 - References:

1) Abbotts, R. Wilson III, DM. (2017). Coordination of DNA Single Strand Break Repair. *Free Radical Biology and Medicine*. 107, 228-44.

2) Adamowicz, M. Hailstone, RM. Demin, AA. Komulainen, E. Hanzlikova, H. Brazina, J. Gautam, A. Wells, SE. Caldecott, KW. (2021). XRCC1 protects transcription from toxic PARP1 activity during DNA base excision repair. *Nature Cell Biology*. 23 (12), 1287-98.

3) Ahel, I. Rass, U. El-Khamisy, SF. Katyal, S. Clements, PM. Mckinnon, PJ. Caldecott, KW. West, SC. (2006). The neurodegenerative disease protein aprataxin resolves abortive DNA ligation intermediates. *Nature*. 443 (7112), 713-6.

4) Alano, CC. Garnier, P. Ying, W. Higashi, Y. Kauppinen, TM. Swanson, RA. (2010). NAD+ Depletion Is Necessary and Sufficient forPoly(ADP-ribose) Polymerase-1-Mediated Neuronal Death. *The Journal of Neuroscience*. 30 (8), 2967-78.

5) Alderton, GK. Joenje, H. Varon, R. Borglum, AD. Jeggo, PA. O'Driscoll, M. (2004). Seckel syndrome exhibits cellular features demonstrating defects in the ATR-signalling pathway. *Human Molecular Genetics*. 13 (24), 3127-38.

6) Alemasova, EE. Lavrik, OI. (2019). Poly(ADP-ribosylation) by PARP1: reaction mechanism and regulatory proteins. *Nucleic Acids Research*. 47 (8), 3811-27.

7) Alexander, JL. Orr-Weaver, TL. (2016). Replication fork instability and the consequences of fork collisions from rereplication. *Genes and Development*. 30 (20), 2241-52.

8) Ali, AEA. Jukes, RM. Pearl, LH. Oliver, AW. (2009). Specific recognition of a multiply phosphorylated motif in the DNA repair scaffold XRCC1 by the FHA domain of human PNK. *Nucleic Acids Research*. 37 (5), 1701-12.

9) Ali, F. Kwan, AC. (2019). Interpreting in vivo calcium signals from neuronal cell bodies, axons, and dendrites: a review. *Neurophotonics*. 7 (1), 011402.

10) Ali, R. Alabdullah, M. Alblihy, A. Miligy, I. Mesquita, KA. Chan, SYT. Mosely, P. Rakha, EA. Madhusudan, S. (2020). PARP1 blockade is synthetically lethal in XRCC1 deficient sporadic epithelial ovarian cancers. *Cancer Letters*. 469, 124-33.

11) Allgayer, J. Kitsera, N. von der Lippen, C. Epe, B. Khobta, A. (2013). Modulation of base excision repair of 8-oxoguanine by the nucleotide sequence. *Nucleic Acids Research*. 41 (18), 8559-71.

12) Amé, JC. Rolli, V. Schreiber, V. Niedergang, C. Apiou, F. Decker, P. Muller, S. Hoger, T. Menissier-de Murcia, J. de Murcia, G. (1999). PARP-2, A Novel Mammalian DNA Damage-dependent Poly(ADP-ribose) Polymerase. *The Journal of Biological Chemistry*. 274 (25), 17860-8.

13) Anand, KS. Dhikav. (2012). Hippocampus in health and disease: An overview. *Annals of Indian Academy of Neurology*. 15 (4), 239-46.

14) Andersen, SL. Sloan, RS. Petes, TD. Jinks-Robertson, S. (2015). Genome-Destabilizing Effects Associated with Top1 Loss or Accumulation of Top1 Cleavage Complexes in Yeast. *PLoS Genetics*. 11 (4), e1005098.

15) Andrabi, SA. Kang, HC. Haince, JF. Lee, YI. Zhang, J. et al. (2011). Iduna protects the brain from glutamate excitotoxicity and stroke by interfering with poly(ADP-ribose) polymer-induced cell death. *Nature Medicine*. 17 (6), 692-9.

16) Andrabi, SA. Umanah, GKE. Chang, C. Stevens, DA. Kauppagounder, SS. Gagne, JP. Poirier, GG. Dawson, VL. Dawson, TM. (2014). Poly(ADP-ribose) polymerase-dependent energy depletion occurs through inhibition of glycolysis. *Proceedings of the National Academy of Sciences of the United States of America*. 111 (28), 10209-14.

17) Andres, SN. Schellenberg, MJ. Wallace, BD. Tumbale, P. Williams, RS. (2015). Recognition and repair of chemically heterogeneous structures at DNA ends. *Environmental and Molecular Mutagenesis*. 56 (1), 1-21.

18) Antonelli, T. Tomasini, MC. Fournier, J. Mazza, R. Tanganelli, S. Pirondi, S. Fuxe, K. Ferraro, L. (2008). Neurotensin Receptor Involvement in the Rise of Extracellular Glutamate Levels and Apoptotic Nerve Cell Death in Primary Cortical Cultures after Oxygen and Glucose Deprivation. *Cerebral Cortex*. 18 (8), 1748-57.

19) Antolin, AA. Ameratunga, M. Banerji, U. Clarke, PA. Workman, P. Al-Lazikani, B. (2020). The kinase polypharmacology landscape of clinical PARP inhibitors. *Scientific Reports*. 2585 (10).

20) Anttinen, A. Koulu, L. Nikoskelainen, E. Portin, R. Kurki, T. et al. (2008). Neurological symptoms and natural course of xeroderma pigmentosum. *Brain*. 131 (8), 1979-89.

21) Arancio, O. Kiebler, M. Lee, CJ. Lev-Ram, V. Tsien, RY. Kandel, ER. Hawkins, RD. (1996). Nitric oxide acts directly in the presynaptic neuron to produce long-term potentiation in cultured hippocampal neurons. *Cell*. 87 (6), 1025-35.

22) Asami, T. Yamazaki, M. Hashimotodani, Y. Uchigashima, M. Kawata, S. et al. (2010). The Endocannabinoid 2-Arachidonoylglycerol Produced by Diacylglycerol Lipase α Mediates Retrograde Suppression of Synaptic Transmission. *Neuron*. 65 (3), 320-7.

23) Ashizawa, T. Xia, G. (2016). Ataxia. *Continuum (American Academy of Neurology)*. 22 (4), 1208-26.

24) Ashour, ME. Atteya, R. El-Khamisy, SF. (2015). Topoisomerase-mediated chromosomal break repair: an emerging player in many games. *Nature Reviews Cancer*. 15 (3), 137-51.

25) Atkin, ND. Raimer, HM. Wang, YH. (2019). Broken by the Cut: A Journey into the Role of Topoisomerase II in DNA Fragility. *Genes*. 10 (791), 31614794.

26) Atlas, D. (2013). The voltage-gated calcium channel functions as the molecular switch of synaptic transmission. *Annual Reviews in Biochemistry*. 82, 607-35.

27) Attwell, D. Mehta, AR. (2021). Anatomy embroiders function in Purkinje cells. *Neurology*. 20 (10), 973.

28) Azarm, K. & Smith, S. Nuclear PARPs and genome integrity. (2020). Gene Dev 34, 285–301

29) Ba, X. Boldogh, I. (2018). 8-Oxoguanine DNA glycosylase 1: Beyond repair of the oxidatively modified base lesions. *Redox Biology*. 14, 669-78.

30) Badura, A. De Zeeuw, CI. (2017). Cerebellar Granule Cells: Dense, Rich and Evolving Representations. *Current Biology*. 27 (11), 415-8.

31) Balasubramanian, B. Pogozelski, WK. Tullius, TD. (1998). DNA strand breaking by the hydroxyl radical is governed by the accessible surface areas of the hydrogen atoms of the DNA backbone. *Proceedings of the National Academy of Sciences of the United States of America*. 95, 9738-43.

32) Baranello, L. Wojtowicz, D. Cui, K. Devaiah, BN. Chung, HJ. et al. (2016). RNA Polymerase II Regulates Topoisomerase 1 Activity to Favor Efficient Transcription. *Cell*. 165 (2), 357-71.

33) Bargiela, D. Shanmugarajah, P. Lo, C. Blakely, EM. Taylor, RW. Horvath, R. Wharton, S. Chinnery, PF. Hadjivassiliou, M. (2015). Mitochondrial pathology in progressive cerebellar ataxia. *Cerebellum & Ataxias*. 2 (16), 1-5.

34) Bayraktar, G. Kreutz, MR. (2017). Neuronal DNA Methyltransferases: Epigenetic Mediators between Synaptic Activity and Gene Expression?. *The Neuroscientist*. 24 (2), 171-85.

35) Bayraktar, G. Kreutz, MR. (2018). The Role of Activity-Dependent DNA Demethylation in the Adult Brain and in Neurological Disorders. *Frontiers in Molecular Neuroscience*. 11, 1-7.

36) Beard, WA. Horton, JK. Prasad, R. Wilson, SH. (2019). Eukaryotic Base Excision Repair: New Approaches Shine Light on Mechanism. *Annual Review of Biochemistry*. 88, 137-62.

37) Beaudin, M. Matilla-Duenas, A. Soong, BW. Pedroso, JL. Barsottini, OG. et al. (2019). The Classification of Autosomal Recessive Cerebellar Ataxias: a Consensus Statement from the Society for Research on the Cerebellum and Ataxias Task Force. *Cerebellum*. 18 (6), 1098-125.

38) Beckman, JS. Beckman, TW. Chen, J. Marshall, PA. Freeman, BA. (1990). Apparent hydroxyl radical production by peroxynitrite: implications for endothelial injury from nitric oxide and superoxide. *Proceedings of the National Academy of Sciences of the United States of America*. 87 (4), 1620-4.

39) Beernink, PT. Hwang, M. Ramirez, . Murphy, MB. Doyle, SA. Thelen, MP. (2005). Specificity of Protein Interactions Mediated by BRCT Domains of the XRCC1 DNA Repair Protein. *Journal of Biological Chemistry*. 280 (34), 30206-13.

40) Benarroch, E. (2021). What Is the Role of Potassium Channels in Ataxia? *Neurology*. 97 (20), 938-41.

41) Beneke, S. (2012). Regulation of chromatin structure by poly(ADP-ribosylation). *Frontiers in Genetics*. 3 (169), 1-16.

42) Berti, M. Chaudhuri, AR. Thangavel, S. Gomathinayagam, S. Kenig, S. et al. (2013). Human RECQ1 promotes restart of replication forks reversed by DNA topoisomerase I inhibition. *Nature Structural and Molecular Biology*. 20 (3), 347-54.

43) Betle, MS. Reinicke, KE. Bey, EA. Spitz, DR. Boothman, DA. (2006). Calcium-dependent Modulation of Poly(ADP-ribose) Polymerase-1 Alters Cellular Metabolism and DNA Repair. *Journal of Biological Chemistry*. 281 (44), 33684-96.

44) Bezprozvanny, I. (2010). Inositol 1,4,5-tripshosphate receptor, calcium signaling and polyglutamine expansion disorders. *Current Topics in Membranes*. 66, 323-41.

45) Bianco, PR. Lyubchenko, YL. . (2017). SSB and the RecG DNA helicase: an intimate association to rescue a stalled replication fork. *Protein Science*. 26 (4), 638-49.

46) Bird, TD. (2019). Hereditary Ataxia Overview. *GeneReviews*.

47) Birks, R., and MacIntosh, F. C. (1961). Acetylcholine metabolism of a sympathetic ganglion. *The Canadian Journal of Biochemical Pharmacology.* 39, 787–827.

48) Blackford, AN. Jackson, SP. (2017). ATM, ATR, and DNA-PK: The Trinity at the Heart of the DNA Damage Response. *Molecular Cell*. 66 (6), 801-17.

49) Blenn, C. Althaus, FR. Malanga, M. (2006). Poly(ADP-ribose) glycohydrolase silencing protects against H2O2-induced cell death. *Biochemical Journal*. 396 (3), 419-29.

50) Bliss, TVP. Cooke, SF. (2011). Long-term potentiation and long-term depression: a clinical perspective. *Clinics*. 66, 3-17.

51) Bock, FJ. Chang, P. (2016). New directions in poly(ADP-ribose) polymerase biology. *The FEBS Journal*. 283 (22), 4017-31.

52) Boehler, C. Gauthier, LR. Mortusewicz, O. Biard, DS. Saliou, JM. (2011). Poly(ADP-ribose) polymerase 3 (PARP3), a newcomer in cellular response to DNA damage and mitotic progression. *Proceedings of the National Academy of Sciences of the United States of America*. 108 (7), 2783-8.

53) Bohio, AA. Sattout, A. Wang, R. Wang, K. Sah, RK. Guo, X. Zeng, X. Ke, Y. Boldogh, I. Ba, X. (2019). c-Abl-Mediated Tyrosine Phosphorylation of PARP1 Is Crucial for Expression of Proinflammatory Genes. *Journal of Immunology*. 203 (6), 1521-31.

54) Borrego-Soto, G. Ortiz-Lopez, R. Rojas-Martinez, A. (2015). Ionizing radiation-induced DNA injury and damage detection in patients with breast cancer. *Genetics and Molecular Biology*. 38 (4), 420-32.

55) Bosch-Presegue, L. Vaquero, A. (2015). Sirtuin-dependent epigenetic regulation in the maintenance of genome integrity. *The FEBS Journal*. 282 (9), 1745-67.

56) Boussios, S. Abson, C. Moschetta, M. Rassy, E. Karathanasi, A. Bhat, T. Ghumman, F. Sheriff, M. Pavlidis, N. (2020). Poly (ADP-Ribose) Polymerase Inhibitors: Talazoparib in Ovarian Cancer and Beyond. *Drugs Research and Development*. 20 (2), 55-73.

57) Bouwman, P. Aly, A. Escandell, JM. Pieterse, M. Bartkova, J. et al. (2010). 53BP1 loss rescues BRCA1 deficiency and is associated with triple-negative and BRCA-mutated breast cancers. *Nature Structural and Molecular Biology*. 17 (6), 688-95.

58) Branco, T. Staras, K. (2009). The probability of neurotransmitter release: variability and feedback control at single synapses. *Nature Reviews Neuroscience*. 10, 373-83.

59) Bras, J. Alonso, I. Barbot, C. Costa, MM. Darwent, L. Orme, T. Sequeiros, J. Hardy, J. Coutinho, P. Guerreiro, R. (2015). Mutations in PNKP Cause Recessive Ataxia with Oculomotor Apraxia Type 4. *The American Journal of Human Genetics*. 96 (3), 474-9.

60) Bredt, DS. Snyder, SH. (1994). Nitric oxide: a physiologic messenger molecule. *Annual Review of Biochemistry*. 63, 175-95.

61) Breslin, C. Hornyak, P. Ridley, A. Rulten, SL. Hanzlikova, H. Oliver, AW. Caldecott, KW. (2015). The XRCC1 phosphate-binding pocket binds poly (ADP-ribose) and is required for XRCC1 function. *Nucleic Acids Research*. 43 (14), 6934-44.

62) Britti, E. Delaspre, F. Tamarit, J. Ros, J. (2018). Mitochondrial calcium signalling and neurodegenerative diseases. *Neuronal Signalling*. 2 (4), NS20180061.

63) Brooks, SC. Adhikary, S. Rubinson, EH. Eichman, BF. (2013). Recent Advances in the Structural Mechanisms of DNA Glycosylases. *Biochimica et Biophysica Acta*. 1834 (1), 247-71.

64) Bruner, HC. Darksen, PWB. (2018). Loss of E-Cadherin-Dependent Cell–Cell Adhesion and the Development and Progression of Cancer. *Cold Spring Harbour Perspectives in Biology*.68 (10), 3645-54.

65) Bryant, HE. Petermann, E. Schultz, N. Jemth, AS. Loseva, O. Issaeva, N. Johansson, F. Fernandez, S. McGlynn, P. Helleday, T. (2009). PARP is activated at stalled forks to

mediate Mre11-dependent replication restart and recombination. *EMBO Journal*. 17 (28), 2601-15.

66) Bryant, HE. Schultz, N. Thomas, HD. Parker, KM. Flower, D. Lopez, E. Kyle, S. Meuth, M. Curtin, NJ. Helleday, T. (2005). Specific killing of BRCA2-deficient tumours with inhibitors of poly(ADP-ribose) polymerase. *Nature*. 7035 (434), 913-7.

67) Burger, W. Burge, M. (2008). Digital image processing : an algorithmic introduction using Java, New York, Springer.

68) Burney, S. Caulfield, JL. Niles, JC. Wishnok, JS. Tannenbaum, SR. (1999). The chemistry of DNA damage from nitric oxide and peroxynitrite. *Mutation Research*. 424 (1-2), 37-49.

69) Bushart, DD. Chopra, R. Singh, V. Murphy, GG. Wulff, H. Shakkottar, VG. (2018). Targeting potassium channels to treat cerebellar ataxia. *Annals of Clinical and Translational Neurology*. 5 (3), 297-314.

70) Buzun, K. Bielawska, A. Bielawski, K. Gornowicz, A. (2020). DNA topoisomerases as molecular targets for anticancer drugs. *Journal of Enzyme Inhibition and Medicinal Chemistry*. 35 (1).

71) Cadet, J. Davies, KJA. Medeiros, MHG. Di Mascio, P. Wagner, JR. (2017). Formation and repair of oxidatively generated damage in cellular DNA. *Free Radical Biology and Medicine*. 107, 13-34.

72) Caglayan, M. Batra, V. Sassa, A. Prasad, R. Wilson, SH. (2014). Role of pol β in complementing aprataxin deficiency during abasic site base excision repair. *Nature Structural and Molecular Biology*. 21 (5), 497-99.

73) Caglayan, M. Batra, VK. Sassa, A. Prasad, R. Wilson, SH. (2014). Role of polymerase β in complementing aprataxin deficiency during abasic-site base excision repair. *Nature Structural and Molecular Biology*. 21 (5), 497-9.

74) Caglayan, M. Horton, JK. Prasad, R. Wilson, SH. (2015). Complementation of aprataxin deficiency by base excision repair enzymes. *Nucleic Acids Research*. 43 (4), 2271-81.

75) Caldecott, KW. (2008). Single-strand break repair and genetic disease. *Nature Reviews Genetics*. 9, 619-31.

76) Caldecott, KW. (2020). Mammalian DNA base excision repair: Dancing in the moonlight. *DNA Repair*. 93 (102921), 1-4.

77) Caldecott, KW. McKeown, CK. Tucker, JD. Ljungquist, S. Thompson, LH. (1994). An interaction between the mammalian DNA repair protein XRCC1 and DNA ligase III. *Molecular and Cellular Biology*. 14 (1), 68-76.

78) Caldecott, KW. Tucker, JD. Stanker, LH. Thompson, LH. (1995). Characterization of the XRCC1-DNA ligase III complex in vitro and its absence from mutant hamster cells. *Nucleic Acids Research*. 23 (23), 4836-43.

79) Caldecott, KW. Tucker, JD. Thompson, LH. (1992). Construction of human XRCC1 minigenes that fully correct the CHO DNA repair mutant EM9.. *Nucleic Acids Research*. 20 (17), 4575-9.

80) Cannan, WJ. Pederson, DS. (2016). Mechanisms and Consequences of Double-strand DNA Break Formation in Chromatin. *Journal of Cell Physiology*. 231 (1), 3-14.

81) Cappelli, E. Taylor, R. Cevasco, M. Abbondandolo, A. Caldecott, KW. Frosina, G. (1997). Involvement of XRCC1 and DNA Ligase III Gene Products in DNA Base Excision Repair. *Journal of Biological Chemistry*. 272 (38), 23970-5.

82) Carroll, J. Page, TKW. Chiang, SC. Kalmar, B. Bode, D. Greensmith, L. McKinnon, PJ. Thorpe, JR. Hafezparast, M. El-Khamisy, SF. (2015). Expression of a pathogenic mutation of SOD1 sensitizes aprataxin-deficient cells and mice to oxidative stress and triggers hallmarks of premature ageing. *Human Molecular Genetics*. 24 (3), 828-40.

83) Carulli, D. de Winter, F. Verhaagen, J. (2021). Semaphorins in Adult Nervous System Plasticity and Disease. *Frontiers in Synaptic Neuroscience*. 13. 672891.

84) Castellotti, B. Mariotti, C. Rimoldi, M. Fancellu, R. Plumari, M. et al. (2011). Ataxia with oculomotor apraxia type1 (AOA1): novel and recurrent aprataxin mutations, coenzyme Q10 analyses, and clinical findings in Italian patients. *Neurogenetics*. 12 (3), 193-201.

85) Ceni, C. Pochon, N. Villaz, M. Muller-Steffner, H. Schuber, F. Baratier, J. de Waard, M. Ronjat, M. Moutin, MJ. (2006). The CD38-independent ADP-ribosyl cyclase from mouse brain synaptosomes: a comparative study of neonate and adult brain. *The Biochemical Journal*. 395 (2), 417-26.

86) Chachlaki, K. Prevot, V. (2020). Nitric oxide signalling in the brain and its control of bodily functions. *British Journal of Pharmacology*. 177 (24), 5437-58.

87) Chakarov, S. Petkova, R. Russev, GC. Zhelev, N. (2014). DNA damage and mutation. Types of DNA damage. *Biodiscovery*. 11, 1.

88) Chambliss, KL. Hinson, DD. Malaspina, P. Novelletto, A. Jakobs, C. Gibson, KM. (1998). Two exon-skipping mutations as the molecular basis of succinic semialdehyde dehydrogenase deficiency (4-hydroxybutyric aciduria). *The American Journal of Human Genetics*. 63 (2), 399-408.

89) Chambon, P. Weill, JD. Mandel, P. (1963). Nicotinamide mononucleotide activation of new DNA-dependent polyadenylic acid synthesizing nuclear enzyme. *Biochemical and Biophysical Research Communication*. 11 (2), 39-43.

90) Chapman, JD. Gagne, JP. Poirier, GG. Goodlett, DR. (2013). Mapping PARP-1 Auto-ADP-ribosylation Sites by Liquid Chromatography–Tandem Mass Spectrometry. *Journal of Proteome Research*. 12 (4), 1868-80.

91) Chatterjee, N. Walker, GC. (2017). Mechanisms of DNA damage, repair and mutagenesis. *Environmental and Molecular Mutagenesis*. 58 (5), 235-63.

92) Chaudhuri, AR. Callen, E. Ding, X. Gogola, E. Duarte, AA. (2016). Replication Fork Stability Confers Chemoresistance in BRCA-deficient Cells. *Nature*. 535 (7612), 382-7.

93) Chaudhuri, AR. Hashimoto, Y. Herrador, R. Neelson, KJ. Fachinetti, D. Bermejo, R. Cocito, A. Costanzo, V. Lopes, M. (2012). Topoisomerase I poisoning results in PARP-mediated replication fork reversal. *Nature Structural and Molecular Biology*. 19 (4), 417-23.

94) Chaudhuri, AR. Nussenzweig, A. (2017). The multifaceted roles of PARP1 in DNA repair and chromatin remodelling. *Nature Reviews Molecular Cell Biology*. 18 (10), 610-21.

95) Chen, J. Li, X. Xu, S. Zhang, M. Wu, Z. Zhang, X. Xu, Y. Chen, Y. (2020). Delayed PARP-1 Inhibition Alleviates Post-stroke Inflammation in Male Versus Female Mice: Differences and Similarities. *Frontiers in Cellular Neuroscience*. 14 (76), 1-12.

96) Chin, AC. Yovanno, RA. Wied, TJ. Gershman, A. Lau, AY. (2020). D-Serine Potently Drives Ligand-Binding Domain Closure in the Ionotropic Glutamate Receptor GluD2. *Structure*. 28 (10), 1168-78.

97) Choi, B. Lee, HW. Mo, S. Kim, JY. Kim, HW. et al. (2018). Inositol 1,4,5-trisphosphate 3-kinase A overexpressed in mouse forebrain modulates synaptic transmission and mGluR-LTD of CA1 pyramidal neurons. *PLOS one*. 13 (4). E0193859.

98) Choi, DW. (2020). Excitotoxicity: Still Hammering the Ischemic Brain in 2020. *Frontiers in Neuroscience*. 14, 579953.

99) Chou, DM. Adamson, B. Dephoure, NE. Tan, X. Nottke, AC. Hurov, KE. Gygi, SP. Claiacovo, MP. Elledge, SJ. (2010). A chromatin localization screen reveals poly (ADP ribose)-regulated recruitment of the repressive polycomb and NuRD complexes to sites of DNA damage. *Proceedings of the National Academy of Sciences of the United States of America*. 107 (43), 18475-80.

100) Chou, RC. Langan, TJ. (2003). In vitro synchronization of mammalian astrocytic cultures by serum deprivation. *Brain Research. Brain Research Protocols*. 11 (3), 162-7.

101) Choudhuri, S. Garg, NJ. (2020). PARP1-cGAS-NF-κB pathway of proinflammatory macrophage activation by extracellular vesicles released during Trypanosoma cruzi infection and Chagas disease. *PLOS Pathogens*. 16 (4). E1008474.

102) Ciccarone, F. Zampieri, M. Caiafa, P. (2017). PARP1 orchestrates epigenetic events setting up chromatin domains. *Seminars in Cell and Developmental Biology*. 63, 123-34.

103) Cleaver, JE. (1968). Defective repair replication of DNA in xeroderma pigmentosum. *Nature*. 218 (5142), 652-6.

104) Cleaver, JE. Bootsma, D. (1975). Xeroderma Pigmentosum: Biochemical and Genetic Characteristics. *Annual Review of Genetics*. 9, 19-38.

105) Coddington, JW. Hurst, JK. Lymar, SV. (1999). Hydroxyl Radical Formation during Peroxynitrous Acid Decomposition. *Journal of the American Chemical Society*. 121 (11), 2438-43.

106) Cohen-Armon, M. Yeheskel, A. Pascal, JM. (2019). Signal-induced PARP1-Erk synergism mediates IEG expression. *Signal Transduction and Targeted Therapy*. 4 (8), 1-8.

107) Coma, M. Guix, FX. Uribesalgo, I. Espuna, G. Sole, M. Andreu, D. Munoz, FJ. (2005). Lack of oestrogen protection in amyloid-mediated endothelial damage due to protein nitrotyrosination. *Brain*. 128 (7), 1613-21.

108) Contestabile, A. Monti, B. Polazzi, E. (2012). Neuronal-glial Interactions Define the Role of Nitric Oxide in Neural Functional Processes. *Current Neuropharmacology*. 10 (4), 303-10.

109) Contreras, L. Drago, I. Zampese, E. Pozzan, T. (2010). Mitochondria: the calcium connection. *Biochimica et Biophysica Acta*. 1797 (6-7), 607-18.

110) Cooke, MS. Evans, MD. Dizdaroglu, M. Lunec, J. (2003). Oxidative DNA damage: mechanisms, mutation, and disease. *The FASEB Journal*. 17 (10), 1195-214.

111) Coutelier, M. Burglen, L. Mundwiller, E. Abada-Bendib, M. Rodriguez, D. et al. (2015). GRID2 mutations span from congenital to mild adult-onset cerebellar ataxia. *Neurology*. 84 (17), 1751-9.

112) Covarrubias, AJ. Perrone, R. Grozio, A. Verdin, E. (2021). NAD+ metabolism and its roles in cellular processes during ageing. *Nature Reviews Molecular Cell Biology*. 22, 119-41.

113) Cox, MM. Goodman, MF. Kreuzer, KN. Sherratt, DJ. Sandler, SJ. Marians, KJ. (2000). The importance of repairing stalled replication forks. *Nature*. 404 (6773), 37-41.

114) Cozzi, A. Cipriani, G. Fossati, S. (2006). Poly(ADP-ribose) Accumulation and Enhancement of Postischemic Brain Damage in 110-kDa Poly(ADP-ribose) Glycohydrolase Null Mice. *Journal of Cerebral Blood Flow & Metabolism*. 26 (5), 684-95.

115) Crow, JF. (2000). The origins, patterns and implications of human spontaneous mutation. *Nature Reviews Genetics*. 1 (1), 40-7.

116) Culmsee, C. Mattson, MP. (2005). p53 in neuronal apoptosis. *Biochemical and Biophysical Research Communication*. 331 (3), 761-77.

117) Cuneo, MJ. London, RE. (2010). Oxidation state of the XRCC1 N-terminal domain regulates DNA polymerase β binding affinity. *Proceedings of the National Academy of Sciences of the United States of America*. 107 (15), 6805-10.

118) Dahl, M. Maruei, V. Lonn, P. Papoutsoglou, P. Zieba, A. et al. (2014). Fine-tuning of Smad protein function by poly(ADP-ribose) polymerases and poly(ADP-ribose) glycohydrolase during transforming growth factor β signaling. *PLOS one*. 9 (8). E103651

119) D'amours, D. Desnoyers, S. D'Silva, I. Poirier, GG. (1999). Poly(ADP-ribosylation) reactions in the regulation of nuclear functions. *The Biochemical Journal*. 342 (2), 249-68.

120) Danhauser, K. Alhaddad, B. Makowski, C. Piekutowska-Abramczuk, D. Syrbe, S. et al. (2018). Bi-allelic ADPRHL2 Mutations Cause Neurodegeneration with Developmental Delay, Ataxia, and Axonal Neuropathy. *The American Journal of Human Genetics*. 103 (5), 817-25.

121) Dantzer, F. Schreiber, V. Niedergang, C. Trucco, C. Flatter, E. De La Rubia, G. Oliver, J. Rolli, V. Menissier-de Murcia, J. de Murcia, G. (1999). Involvement of poly(ADP-ribose) polymerase in base excision repair. *Biochimie*. 81 (1-2), 69-75.

122) Das, SK. Rehman, I. Ghosh, A. Sengupta, S. Majumdar, P. Jana, B. Das, BB. (2016). Poly(ADP-ribose) polymers regulate DNA topoisomerase I (Top1) nuclear dynamics and camptothecin sensitivity in living cells. *Nucleic Acids Research*. 44 (17), 8363-75.

123) Date, H. Igarashi, S. Sano, Y. Takahashi, T. Takahashi, T. Takano, H. Tsuji, S. Nishizawa, M. Onodera, O. (2004). The FHA domain of aprataxin interacts with the C-terminal region of XRCC1. *Biochemical and Biophysical Research Communication*. 325 (4), 1279-85.

124) Datta, K. Suman, S. Kallakury, BVS. Fornace Jr, AJ. (2012). Exposure to Heavy Ion Radiation Induces Persistent Oxidative Stress in Mouse Intestine. *PLOS one*. 7 (8). E42224.

125) Datta, S. Jaiswal, M. (2021). Mitochondrial calcium at the synapse. *Mitochondrion*. 59, 135-53.

126) Daugas, E. Susin, SA. Zamzani, N. Ferri, KF. Irinopoulou, T. et al. (2000). Mitochondrio-nuclear translocation of AIF in apoptosis and necrosis. *The FASEB Journal*. 14, 729-39.

127) David, KK Andrabi, SA. Dawson, TM. Dawson, VL. (2009). Parthanatos, a messenger of death. *Frontiers in Biosciences*. 14, 1116-28.

128) Davis, AJ. Chen, DJ. (2013). DNA double strand break repair via non-homologous end-joining. *Translational Cancer Research*. 2 (3), 130-43.

129) Davis, L. Maizels, N. (2014). Homology-directed repair of DNA nicks via pathways distinct from canonical double-strand break repair. *Proceedings of the National Academy of Sciences of the United States of America*. 111 (10), 924-32.

130) Dawicki-McKenna, JM. Langelier, MF. DeNizio, JE. Riccio, AA. Cao, CD. Karch, KR. McCauley, M. Steffen, JD. Black, BE. Pascal, JM. (2015). PARP-1 Activation Requires Local Unfolding of an Autoinhibitory Domain. *Molecular Cell*. 60 (5), 755-68.

131) Dawson, TM. Dawson, VL. (2017). Mitochondrial Mechanisms of Neuronal Cell Death: Potential Therapeutics. *Annual Review of Pharmacology and Toxicology*. 57, 437-54.

132) de Lager, TL. Cockrell, AE. Du Plessis, SS. (2017). Ultraviolet Light Induced Generation of Reactive Oxygen Species. *Advances in Experimental Medicine and Biology*. 997, 15-23.

133) de Lera Ruiz, M. Kraus, RL. (2015). Voltage-Gated Sodium Channels: Structure, Function, Pharmacology, and Clinical Indications. *Journal of Medicinal Chemistry*. 58 (18), 7093-118.

134) de Murcia, JM. Ricoul, M. Tartier, L. Niedergang, C. Hube, A. et al. (2003). Functional interaction between PARP-1 and PARP-2 in chromosome stability and embryonic development in mouse. *EMBO Journal*. 22 (9), 2255-63.

135) Dedon, PC. (2008). The chemical toxicology of 2-deoxyribose oxidation in DNA. *Chemical Research in Toxicology*. 28 (1), 206-19.

136) Demin, AA. Hirota, K. Tsuda, M. Adamowicz, M. Hailstone, R. et al. (2021). XRCC1 prevents toxic PARP1 trapping during DNA base excision repair. *Molecular Cell*. 81 (14), 3018-30.

137) Demple, B. Herman, T. Chen, DS. (1991). Cloning and expression of APE, the cDNA encoding the major human apurinic endonuclease: Definition of a family of DNA repair enzymes. *Proceedings of the National Academy of Sciences of the United States of America*. 99, 11450-4.

138) Denker, A. Krohnert, K. Buckers, J. Neher, E. Rizzoli, SO. (2011). The reserve pool of synaptic vesicles acts as a buffer for proteins involved in synaptic vesicle recycling. *Proceedings of the National Academy of Sciences of the United States of America*. 108 (41), 17183-8.

139) Diab, A. Nikolopoulou-Stamati, P. Katostaras, T. Safioleas, M. Kostakis, A. Athanassiadou, P. Liossi-loakeim, A. Marinos, G. Konstantopoulos, K. (2012). Expression of Smad4, E-cadherin and beta-catenin in advanced colorectal cancer: a retrospective study. *Journal of BUON*. 17 (1), 92-6.

140) Dianova, II. Sleeth, KM. Allinson, SL. Parsons, JL. Breslin, C. Caldecott, KW. Dianov, GL. (2004). XRCC1–DNA polymerase β interaction is required for efficient base excision repair. *Nucleic Acids Research*. 32 (8), 2550-5.

141) Dibbens, LM. Tarpey, PS. Hynes, K. Bayly, MA. Scheffer, IE. et al. (2008). X-linked protocadherin 19 mutations cause female-limited epilepsy and cognitive impairment. *Nature Genetics*. 40 (6), 776-81.

142) Didier, M. Bursztajn, S. Adamec, E. Passani, L. Nixon, RA. Coyle, JT. Wei, JY. Berman, SA. (1996). DNA strand breaks induced by sustained glutamate excitotoxicity in primary neuronal cultures. *The Journal of Neuroscience*. 16 (7), 2238-50.

143) Dinerman, JL. Dawson, TM. Schell, MJ. Snowman, A. Snyder, SH. (1994). Endothelial nitric oxide synthase localized to hippocampal pyramidal cells: implications for synaptic plasticity. *Proceedings of the National Academy of Sciences of the United States of America*. 91 (10), 4214-8.

144) Diriong, S. Lory, P. Williams, ME. Ellis, SB. Harpold, MM. Taviaux, S. (1995). Chromosomal Localization of the Human Genes for α1A, α1B, and α1E Voltage-Dependent Ca2+ Channel Subunits. *Genomics*. 30 (3), 605-9.

145) Dizdaroglu, M. Jaruga, P. (2012). Mechanisms of free radical-induced damage to DNA. *Free Radical Research*. 46 (4), 382-419.

146) Dolphin, AC. Lee, A. (2020). Presynaptic calcium channels: specialized control of synaptic neurotransmitter release. *Nature Reviews Neuroscience*. 21, 213-29.

147) Donahue, BA. Yin, S. Taylor, JS. Reines, D. Hanawalt, PC. (1994). Transcript cleavage by RNA polymerase II arrested by a cyclobutane pyrimidine dimer in the DNA template. *Proceedings of the National Academy of Sciences of the United States of America*. 91 (18), 8502-6.

148) Du, W. Bautista, JF. Yang, H. Diez-Sampedro, A. You, SA. et al. (2005). Calcium-sensitive potassium channelopathy in human epilepsy and paroxysmal movement disorder. *Nature Genetics*. 37 (7), 733-8.

149) Du, X. Carvalho-de-souza, JL. Wei, C. Carrasquel-ursulaez, W. Lorenzo, Y. et al. (2020). Loss-of-function BK channel mutation causes impaired mitochondria and progressive cerebellar ataxia. *Proceedings of the National Academy of Sciences of the United States of America*. 117 (11), 6023-34.

150) Duan, Y. Wang, SH. Song, J. Mironova, Y. Ming, GL. Kolodkin, AL. Giger, RJ. (2014). Semaphorin 5A inhibits synaptogenesis in early postnatal- and adult-born hippocampal dentate granule cells. *eLife*. 3. E04390.

151) Dubois, NC. Hofmann, D. Kaloulis, K. Bishop, JM. Trumpp, A. (2006). Nestin-Cre transgenic mouse line Nes-Cre1 mediates highly efficient Cre/loxP mediated recombination in the nervous system, kidney, and somite-derived tissues. *Genesis*. 44 (8), 355-60.

152) Dugger, BN. Dickson, DW. (2017). Pathology of Neurodegenerative Diseases. *Cold Spring Harbour Perspectives in Biology*. 9 (7). E028035.

153) Dumitrache, LC. McKinnon, PJ. (2016). Polynucleotide Kinase-Phosphatase (PNKP) Mutations and Neurologic Disease. *Mechanisms of Ageing and Development*. 161 (A), 121-9.

154) Dumitrache, LC. Shimada, M. Downing, SM. Kwak, YD. Li, Y. Illuzzi, JL. Russell, HR. Wilson III, DM. McKinnon, PJ. (2018). Apurinic endonuclease-1 preserves neural genome integrity to maintain homeostasis and thermoregulation and prevent brain tumors. *Proceedings of the National Academy of Sciences of the United States of America*. 115 (52), 12285-94.

155) Dumont, E. Monari, A. (2015). Understanding DNA under oxidative stress and sensitization: the role of molecular modeling. *Frontiers in Chemistry*. 3 (43), 1-15.

156) Dunlop, J. Morin, X. Corominas, M. Serras, F. Tear, G. (2004). glaikit is essential for the formation of epithelial polarity and neuronal development. *Current Biology*. 14 (22), 2039-45.

157) Dunn, AR. Stout, KA. Ozawa, M. Lohr, Hoffman, CA. (2017). Synaptic vesicle glycoprotein 2C (SV2C) modulates dopamine release and is disrupted in Parkinson disease. *Proceedings of the National Academy of Sciences of the United States of America*. 114 (11), 2253-62.

158) Dziadkowiec, KN. Gasiorowska, E. Nowak-Markwitz, E. Jankowska, A. (2016). PARP inhibitors: review of mechanisms of action and BRCA1/2 mutation targeting. *Prz Menopauzalny*. 15 (4), 215-9.

159) Eckle, VS. Shcheglovitov, A. Vitko, I. Dey, D. Yap, CC. Winckler, B. Perez-Reyes, E. (2014). Mechanisms by which a CACNA1H mutation in epilepsy patients increases seizure susceptibility. *Journal of Physiology*. 592 (4), 795-809.

160) Eliasson, MJL. Huang, Z. Ferrante, RJ. Sasamata, M. Molliver, ME. Snyder, SH. Moskowitz, MA. (1999). Neuronal nitric oxide synthase activation and peroxynitrite formation in ischemic stroke linked to neural damage. *Journal of Neuroscience*. 19 (14), 5910-8.

161) Eliasson, MJL. Sampei, K. Mandir, AS. Hurn, PD. Traystman, RJ. et al. (1997). Poly(ADP-ribose) polymerase gene disruption renders mice resistant to cerebral ischemia. *Nature Medicine*. 3, 1089-95.

162) Elibol, B. Kilic, U. (2018). High Levels of SIRT1 Expression as a Protective Mechanism Against Disease-Related Conditions. *Frontiers in Endocrinology*. 9 (614), 1-7.

163) El-Khamisy, SF. Caldecott, KW. (2006). TDP1-dependent DNA single-strand break repair and neurodegeneration. *Mutagenesis*. 21 (4), 219-24.

164) El-Khamisy, SF. Saifi, GM. Weinfeld, M. Johansson, F. Helleday, T. Lupski, JR. Caldecott, KW. (2005). Defective DNA single-strand break repair in spinocerebellar ataxia with axonal neuropathy-1. *Nature*. 434 (7029), 108-13.

165) Epi25 Collaborative. (2019). Ultra-Rare Genetic Variation in the Epilepsies: A Whole-Exome Sequencing Study of 17,606 Individuals. *The American Journal of Human Genetics*. 105, 267-82.

166) Errichiello, E. Zagnoli-Vieira, G. Rizzi, R. Garavelli, L. Caldecott, KW. Zuffardi, O. (2020). Characterization of a novel loss-of-function variant in TDP2 in two adult patients with spinocerebellar ataxia autosomal recessive 23 (SCAR23). *Journal of Human Genetics*. 65, 1135-41.

167) Eustermann, S. Wu, WF. Langelier, MF. Yang, JC. Easton, LE. Riccio, AA. Pascal, JM. Neuhaus, D. (2015). Structural Basis of Detection and Signaling of DNA Single-Strand Breaks by Human PARP-1. *Molecular Cell*. 60 (5), 742-52.

168) Farmer, H. McCabe, N. Lord, CJ. Tutt, ANJ. Johnson, DA. et al. (2005). Targeting the DNA repair defect in BRCA mutant cells as a therapeutic strategy. *Nature*. 434 (7035), 917-21.

169) Fathers, C. Drayton, RM. Solovieva, S. Bryant, HE. (2012). Inhibition of poly(ADP-ribose) glycohydrolase (PARG) specifically kills BRCA2-deficient tumor cells. *Cell Cycle*. 11 (5), 990-7.

170) Fatokun, AA. Dawson, VL. Dawson, TM. (2014). Parthanatos: mitochondrial-linked mechanisms and therapeutic opportunities. *British Journal of Pharmacology*. 171, 2000-16.

171) Feng, J. Chi, P. Blanpied, TA. Xu, Y. Magarinos, AM. et al. (2002). Regulation of Neurotransmitter Release by Synapsin III. *The Journal of Neuroscience*. 22 (11), 4372-80.

172) Feng, L. Gonf, KW. Wang, J. Wang, W. Chen, J. (2013). RIF1 counteracts BRCA1-mediated end resection during DNA repair. *The Journal of Biological Chemistry*. 288 (16), 11135-43.

173) Feng, X. Koh, DW. (2013). Roles of Poly(ADP-ribose) Glycohydrolase in DNA Damage and Apoptosis. *International Review of Cell and Molecular Biology*. 304 (5), 227-81.

174) Feng, X. Yang, J. (2016). Lysosomal Calcium in Neurodegeneration. *Messenger*. 51 (1-2), 56-66.

175) Fiederling, A. Ewert, R. Andreyeva, A. Jungling, K. Gottmann, K. (2011). E-cadherin is required at GABAergic synapses in cultured cortical neurons. *Neuroscience Letters*. 501 (3), 167-72.

176) Finkel, T. Serrano, M. Blasco, MA. (2007). The common biology of cancer and ageing. *Nature*. 448 (7155), 767-74.

177) Fleming, AM. Burrows, CJ. (2013). G-Quadruplex Folds of the Human Telomere Sequence Alter the Site Reactivity and Reaction Pathway of Guanine Oxidation Compared to Duplex DNA. *Chemical Research in Toxicology*. 26 (4), 593-607.

178) Flett, FJ. Ruksenaite, E. Armstron, LA. Bharati, S. Carloni, R. Morris, ER. Mackay, L. Interthal, H. Richardson, JM. (2018). Structural basis for DNA 3′-end processing by human tyrosyl-DNA phosphodiesterase 1. *Nature Communications*. 9 (24), 1-13.

179) Foskett, JK. White, C. Cheung, KH. Mak, DD. (2007). Inositol Trisphosphate Receptor Ca2+ Release Channels. *Physiology Reviews*. 87 (2), 593-658.

180) Fouad, YA. Aanei, C. (2017). Revisiting the hallmarks of cancer. *American Journal of Cancer Research*. 7 (5), 1016-36.

181) Fouquerel, E. Goellner, EM. Yu, Z. Gagne, JP. de Moura, MB. et al. (2014). ARTD1/PARP1 Negatively Regulates Glycolysis by Inhibiting Hexokinase 1 Independent of NAD+ Depletion. *Cell Reports*. 8 (6), 1819-31.

182) Frade, JM. Ovejero-Benito, MC. (2015). Neuronal cell cycle: the neuron itself and its circumstances. *Cell Cycle*. 14 (5), 712-20.

183) Friel, D. Tsien, R. (1994). An FCCP-sensitive Ca2+ store in bullfrog sympathetic neurons and its participation in stimulus-evoked changes in [Ca2+]i. *Journal of Neuroscience*. 14 (7), 4007-24.

184) Fritschy, JM. (2008). Epilepsy, E/I Balance and GABAA Receptor Plasticity. *Frontiers in Molecular Neuroscience*. 1 (5), 1-6.

185) Fujikake, N. Shin, M. Shimizu, S. (2018). Association Between Autophagy and Neurodegenerative Diseases. *Frontiers in Neuroscience*. 12 (255), 1-11.

186) Galione, A. Morgan, AJ. Arredouani, A. Davis, LC. Rietdorf, K. Ruas, M. Parrington, J. (2010). NAADP as an intracellular messenger regulating lysosomal calcium-release channels. *Biochemical Society Transactions*. 38 (6), 1424-31.

187) Gao, Z. Todorov, B. Barrett, CF. van Dorp, S. Ferrari, MD. van den Maagdenberg, Arn MJM. De Zeeuw, CI. Hoebeek, FE. (2012). Cerebellar Ataxia by Enhanced CaV2.1 Currents Is Alleviated by Ca2+-Dependent K+-Channel Activators in Cacna1aS218L Mutant Mice. *The Journal of Neuroscience*. 32 (44), 15533-46.

188) Garcia-Diaz, B. Barca, E. Balreira, A. Lopez, LC. Tadesse, S. Krishna, S. Naini, A. Mariotti, C. Castellotti, B. Quinzii, CM. (2015). Lack of aprataxin impairs mitochondrial functions via downregulation of the APE1/NRF1/NRF2 pathway. *Human Molecular Genetics*. 24 (16), 4516-29.

189) Garthwaite, J. Charles, SL. Chess-Williams, R. (1988). Endothelium-derived relaxing factor release on activation of NMDA receptors suggests role as intercellular messenger in the brain. *Nature*. 336, 385-88.

190) Geller, HM Cheng, KY. Goldsmith, NK. Romero, AA. Zhang, AL. Morris, EJ. Grandison, L. (2001). Oxidative stress mediates neuronal DNA damage and apoptosis in response to cytosine arabinoside. *Journal of Neurochemistry*. 78, 265-75.

191) Ghosh, SH. Becker, K. Huang, H. Salazar, TD. Chai, G. et al. (2018). Biallelic Mutations in ADPRHL2, Encoding ADP-Ribosylhydrolase 3, Lead to a Degenerative Pediatric Stress-Induced Epileptic Ataxia Syndrome. *The American Journal of Human Genetics*. 103 (3), 431-9.

192) Gibbs-Seymour, I. Fontana, P. Rack, JGM. Ahel, I. (2016). HPF1/C4orf27 Is a PARP-1-Interacting Protein that Regulates PARP-1 ADP-Ribosylation Activity. *Molecular Cell*. 62 (3), 432-42.

193) Gibson, BA. Zhang, Y. Jiang, H. Hussey, KM. Shrimp, JP. Lin, H. Schwede, F. Yu, Y. Kraus, WL. (2016). Chemical genetic discovery of PARP targets reveals a role for PARP-1 in transcription elongation. *Science*. 353 (6294), 45-50.

194) Giunti, P. Mantuano, E. Frontali, M. Veneziano, L. (2015). Molecular mechanism of Spinocerebellar Ataxia type 6: glutamine repeat disorder, channelopathy and transcriptional dysregulation. The multifaceted aspects of a single mutation. *Frontiers in Cellular Neuroscience*. 9 (36), 1-5.

195) Gogola, E. Duarte, A. Ruiter, JR de. Wiegant, WW. Schmid, JA. et al. (2016). Selective Loss of PARG Restores PARylation and Counteracts PARP Inhibitor-Mediated Synthetic Lethality. *Cancer Cell*. 33 (6), 1078-93.

196) Gomez-Herreros, F. Schuurs-Hoeijmakers, JHM. McCormack, M. Greally, MT. Rulten, S. et al. (2014). TDP2 protects transcription from abortive topoisomerase activity and is required for normal neural function. *Nature Genetics*. 46, 516-21.

197) Gottschalk, AJ. Trivedi, RD. Conaway, JW. Conaway, RC. (2012). Activation of the SNF2 Family ATPase ALC1 by Poly(ADP-ribose) in a Stable ALC1·PARP1·Nucleosome Intermediate. *Journal of Biological Chemistry*. 287 (52), 43527-32.

198) Gravells, P. Grant, E. Smith, KM. James, DI. Bryant, HE. (2017). Specific killing of DNA damage-response deficient cells with inhibitors of poly(ADP-ribose) glycohydrolase. *DNA Repair*. 52, 81-91.

199) Greenberg, MM. (2014). Abasic and Oxidized Abasic Site Reactivity in DNA: Enzyme Inhibition, Cross-linking, and Nucleosome Catalyzed Reactions. *Accounts of Chemical Research*. 47 (2), 646-55.

200) Gruol, D. Manto, M. Haines, D. (2012). Ca2+ Signaling in Cerebellar Purkinje Neurons. *Cerebellum*. 11 (3), 605-8.

201) Grundy, GJ. Polo, LM. Zeng, Z. Rulten, SL. Hoch, NC. et al. (2016). PARP3 is a sensor of nicked nucleosomes and monoribosylates histone H2BGlu2. *Nature Communications*. 12404, 1-12.

202) Guerreiro, S. Privat, AL. Bressac, L. Toulorge, D. (2020). CD38 in Neurodegeneration and Neuroinflammation. *Cells*. 9 (2), 471.

203) Guida, S. Trettel, F. Pagnutti, S. Mantuano, E. Tottene, A. et al. (2001). Complete Loss of P/Q Calcium Channel Activity Caused by a CACNA1A Missense Mutation Carried by Patients with Episodic Ataxia Type 2. *The American Journal of Human Genetics*. 68 (3), 759-64.

204) Gunnersen, JM. Kim, MH. Fuller, SJ. de Silva, M. Britto, JM. et al. (2007). Sez-6 proteins affect dendritic arborization patterns and excitability of cortical pyramidal neurons. *Neuron*. 56 (4), 621-39.

205) Guo, JU. Su, Y. Zhong, C. Ming, GL. Song, H. (2011). Hydroxylation of 5-Methylcytosine by TET1 Promotes Active DNA Demethylation in the Adult Brain. *Cell*. 145 (3), 423-34.

206) Guo, Y. Yan, KP. Qu, Q. Qu, J. Chen, ZG. et al. (2015). Common Variants of KCNJ10 Are Associated with Susceptibility and Anti-Epileptic Drug Resistance in Chinese Genetic Generalized Epilepsies. *PLOS one*. 10 (4), 1-11.

207) Hagam S. Kanno, A. Morita, N. Jin, S. Matoba, K. Ozawa, T. Ozaki, M. (2021). Poly(ADP-ribose) Polymerase (PARP) is Critically Involved in Liver Ischemia/reperfusion-injury. *The Journal of Surgical Research*. 14 (270), 124-38.

208) Haince, JF. Ouellet, ME. McDonald, D. Hendzel, MJ. Poirier, GG. (2006). Dynamic relocation of poly(ADP-ribose) glycohydrolase isoforms during radiation-induced DNA damage. *Biochemica et Biophysica Acta*. 1763 (2), 226-37.

209) Hakem, R. (2008). DNA-damage repair; the good, the bad, and the ugly. *EMBO Journal*. 27 (4), 589-605.

210) Hanai, S. Kanai, M. Ohashi, S. Okamoto, K. Yamada, M. Takahashi, H. Miwa, M. (2004). Loss of poly(ADP-ribose) glycohydrolase causes progressive neurodegeneration in Drosophila melanogaster. *Proceedings of the National Academy of Sciences of the United States of America*. 101 (1), 82-6.

211) Hanzlikova, H. Kalasova, I. Demin, AA. Pennicott, LW. Cihlarova, Z. Caldecott, KW. (2018). The Importance of Poly(ADP-ribose) Polymerase as a Sensor of Unligated Okazaki Fragments during DNA Replication. *Molecular Cell*. 71, 319-31.

212) Hanzlikova, H. Prokhorova, E. Krejcikova, K. Cihlarova, Z. Kalasova, I. et al. (11). Pathogenic ARH3 mutations result in ADP-ribose chromatin scars during DNA strand break repair. *Nature Communications*. 2020 (3391), 1-13.

213) Hargus, NJ. Merrick, EC. Nigam, A. Kalmar, CL. Baheti, AR. Bertram EH 3rd. Patel, MK. (2010). Temporal lobe epilepsy induces intrinsic alterations in Na channel gating in layer II medial entorhinal cortex neurons. *Neurobiology of Disease*. 41 (2), 361-76.

214) Harris, JL. Jakob, B. Taucher-Scholz, G. Dianov, GL. Becherel, OJ. Lavin, MF. (2009). Aprataxin, poly-ADP ribose polymerase 1 (PARP-1) and apurinic endonuclease 1 (APE1) function together to protect the genome against oxidative damage. *Human Molecular Genetics*. 18 (21), 4102-17.

215) Harrision, D. Gravells, P. Thompson, R. Bryant, HE. (2020). Poly(ADP-ribose) Glycohydrolase (PARG) vs. Poly(ADP-ribose) Polymerase (PARP) – Function in Genome Maintenance and Relevance of Inhibitors for Anti-cancer Therapy. *Frontiers in Molecular Biosciences*. 7. 1-21.

216) Haselden, W. Kedarasetti, RT. Drew, PJ. (2020). Spatial and temporal patterns of nitric oxide diffusion and degradation drive emergent cerebrovascular dynamics. *PLOS Computational Biology*. 16 (7), 1-42.

217) Hassa, PO. Haenni, SS. Elser, M. Hottiger, MO. (2006). Nuclear ADP-Ribosylation Reactions in Mammalian Cells: Where Are We Today and Where Are We Going? *Microbiology and Molecular Biology Reviews*. 70 (3), 789-829.

218) Hayyan, M. Hashim, MA. Al Nashelf, IM. (2016). Superoxide Ion: Generation and Chemical Implications. *Chemical Reviews*. 116, 3029-85.

219) Hazra, TP. Izumi, T. Boldogh, I. Imhoff, B. Kow, YW. Jaruga, P. Dizdaroglu, M. Mitra, S. (2002). Identification and characterization of a human DNA glycosylase for repair of modified bases in oxidatively damaged DNA. *Proceedings of the National Academy of Sciences of the United States of America*. 99 (6), 3523-8.

220) He, R. Zhang, J. Yu, Y. Jizi, L. Wang, W. Li, M. (2018). New Insights Into Interactions of Presynaptic Calcium Channel Subtypes and SNARE Proteins in Neurotransmitter Release. *Frontiers in Molecular Neuroscience*. 11 (213), 1-11.

221) He, YF. Li, BZ. Li, Z. Liu, P. Wang, Y. et al. (2011). Tet-Mediated Formation of 5-Carboxylcytosine and Its Excision by TDG in Mammalian DNA. *Science*. 333 (6047), 1303-7.

222) Heck, DDH. Thach, WT. Keating, JG. (2007). On-beam synchrony in the cerebellum as the mechanism for the timing and coordination of movement. *Proceedings of the National Academy of Sciences of the United States of America*. 104 (18), 7658-63.

223) Heidelberger, R. Heinemann, C. Neher, E. Matthews, G. (1994). Calcium dependence of the rate of exocytosis in a synaptic terminal. *Nature*. 371 (6497), 513-5.

224) Helassa, N. Podor, B. Fine, A. Török, K. (2016). Design and mechanistic insight into ultrafast calcium indicators for monitoring intracellular calcium dynamics. *Scientific Reports*. 6 (6), 38276.

225) Hempel, CM. Sivul, M. Levenson, JM. Rose, DM. Li, B. Sirianni, AC. Xia, E. Ryan, TA. Gerber, DJ. Cottrell, JR. (2011). A System for Performing High Throughput Assays of Synaptic Function. *PLOS one*. 6 (10). E25999.

226) Herbst, WA. Deng, W. Wohlschlegel, JA. Achiro, JM. Martin, KC. (2021). Neuronal activity regulates the nuclear proteome to promote activity-dependent transcription. *Journal of Cell Biology*. 220 (12). 1-21.

227) Herskovitzs, AZ. Hunter, TA. Maxwell, N. Pereira, K. Whittaker, CA. Valdez, G. Guarente, LP. (2018). SIRT1 deacetylase in aging-induced neuromuscular degeneration and amyotrophic lateral sclerosis. *Aging Cell*. 17 (6). E12839.

228) Hirano, R. Interthal, H. Huang, C. Nakamura, T. Deguchi, K. et al. (2007). Spinocerebellar ataxia with axonal neuropathy: consequence of a Tdp1 recessive neomorphic mutation?. *EMBO Journal*. 26 (22), 4732-43.

229) Hisatsune, C. Hamada, K. Mikoshiba, K. (2018). Ca2+ signaling and spinocerebellar ataxia. *Biochimica et Biophysica Acta*. 1865 (11B), 1733-44.

230) Hivert, B. Cerruti, C. Camu, W. (1998). Hydrogen peroxide-induced motoneuron apoptosis is prevented by poly ADP ribosyl synthetase inhibitors. *NeuroReport*. 9 (8), 1835-8.

231) Hoch, N. Hanzlikova, H. Rulten, SL. Tetreault, M. Komulainen, E. et al. (2017). XRCC1 Mutation is Associated with PARP1 Hyperactivation and Cerebellar Ataxia. *Nature*. 541 (7635), 87-91.

232) Hoeijmakers, JH. (2009). DNA damage, aging, and cancer. *The New England Journal of Medicine*. 361 (15), 1475-85.

233) Hoffman, A. Spengler, D. (2019). Chromatin Remodeling Complex NuRD in Neurodevelopment and Neurodevelopmental Disorders. *Frontiers in Genetics*. 10, 1-21.

234) Hogan, KA. Chini, CCS. Chini, EN. (2019). The Multi-faceted Ecto-enzyme CD38: Roles in Immunomodulation, Cancer, Aging, and Metabolic Diseases. *Frontiers in Immunology*. 10 (1187). 1-12.

235) Horton, JK. Stefanick, DF. Prasad, R. Gassman, NR. Kedar, PS. Wilson, SH. (2014). Base excision repair defects invoke hypersensitivity to PARP inhibition. *Molecular Cancer Research*. 12 (8), 1128-39.

236) Hottiger, MO. Hassa, PO. Luscher, B. Schuler, H. Koch-Nolte, F. (2010). Toward a unified nomenclature for mammalian ADP-ribosyltransferases. *Trends in Biochemical Sciences*. 35 (4), 208-19.

237) Hou, Y. Lautrup, S. Cordonnier, S. Wang, Y. Croteau, DL. Zaval, E. et al. (2018). NAD+ supplementation normalizes key Alzheimer's features and DNA damage responses in a new AD mouse model with introduced DNA repair deficiency. *Proceedings of the National Academy of Sciences of the United States of America*. 115 (8), 1876-85.

238) Howard, MJ. Rodriguez, Y. Wilson, SH. (2017). DNA polymerase β uses its lyase domain in a processive search for DNA damage. *Nucleic Acids Research*. 45 (7), 3822-32.

239) Hoxha, E. Balbo, I. Miniaci, MC. Tempia, F. (2018). Purkinje Cell Signaling Deficits in Animal Models of Ataxia. *Frontiers in Synaptic Neuroscience*. 10, 1-17.

240) Hoxha, E. Tempia, F. Lippiello, P. Miniaci, MC. (2016). Modulation, Plasticity and Pathophysiology of the Parallel Fiber-Purkinje Cell Synapse. *Frontiers in Synaptic Neuroscience*. 8, 1-16.

241) Hu, S. Zhu, L. (2018). Semaphorins and Their Receptors: From Axonal Guidance to Atherosclerosis. *Frontiers in Physiology*. 9, 1-11.

242) Huang, CT. Huang, DY. Hu, CJ. Wu, D. Lin, WW. (2014). Energy adaptive response during parthanatos is enhanced by PD98059 and involves mitochondrial function but not autophagy induction. *Biochimica et Biophysica Acta*. 1843 (3), 531-43.

243) Huang, M. Verbeek, DS. (2019). Why do so many genetic insults lead to Purkinje Cell degeneration and spinocerebellar ataxia?. *Neuroscience Letters*. 688, 49-57.

244) Huang, SN. Pommier, Y. (2019). Mammalian Tyrosyl-DNA Phosphodiesterases in the Context of Mitochondrial DNA Repair. *International Journal of Molecular Sciences*. 20 (12), 3015.

245) Huie, RE. Padmaja, S. (1993). The reaction of no with superoxide. *Free Radical Research Communications*. 18 (4), 195-9.

246) Iarovaia, OV. Rubtsov, M. Ioudinkova, E. Tsfasman, T. Razin, SV. Vassetzky, YS. (2014). Dynamics of double strand breaks and chromosomal translocations. *Molecular Cancer*. 13 (249).

247) Ichikawa, R. Sakimua, K. Watanabe, M. (2016). GluD2 Endows Parallel Fiber–Purkinje Cell Synapses with a High Regenerative Capacity. *The Journal of Neuroscience*. 36 (17), 4846-58.

248) Ikejima, M. Noguchi, S. Yamashita, R. Ogura, T. Sugimura, T. Gill, DM. Miwa, M. (1990). The zinc fingers of human poly(ADP-ribose) polymerase are differentially required for the recognition of DNA breaks and nicks and the consequent enzyme activation. Other structures recognize intact DN. *Journal of Biological Chemistry*. 265 (35), 21907-13.

249) Imai, SI. Guarente, L. (2016). It takes two to tango: NAD+ and sirtuins in aging/longevity control. *Aging and Mechanisms of Disease*. 2 (16017), 1-6.

250) Indelicato, E. Boesch, S. (2021). From Genotype to Phenotype: Expanding the Clinical Spectrum of CACNA1A Variants in the Era of Next Generation Sequencing. *Frontiers in Neurology*. 12, 1-10.

251) Inoue, A. Zhang, Y. (2011). Replication-Dependent Loss of 5-Hydroxymethylcytosine in Mouse Preimplantation Embryos. *Science*. 334 (6053), 194.

252) Interthal, H. Champoux, JJ. (2011). Effects of DNA and protein size on substrate cleavage by human tyrosyl-DNA phosphodiesterase 1. *The Biochemical Journal*. 436 (3), 559-66.

253) Interthal, H. Chen, HJ. Champoux, JJ. (2005a). Human Tdp1 cleaves a broad spectrum of substrates, including phosphoamide linkages. *The Journal of Biological Chemistry*. 280 (43), 36518-28.

254) Interthal, H. Chen, HJ. Kehl-Fie, TE. Zotzmann, J. Leppard, JB. Champoux, JJ. (2005b). SCAN1 mutant Tdp1 accumulates the enzyme--DNA intermediate and causes camptothecin hypersensitivity. *The EMBO Journal*. 14 (12), 2224-33.

255) Isabelle, M. Moreel, X. Gagne, JP. Rouleau, M. Ethier, C. Gagne, P. Hendzel, MJ. Poirier, GG. (2010). Investigation of PARP-1, PARP-2, and PARG interactomes by affinity-purification mass spectrometry. *Proteome Science*. 8 (22). 885-8.

256) Ito, S. Shen, L. Dai, Q. Wu, SC. Collins, LB. Swenberg, JA. He, C. Zhang, Y. (2011). Tet Proteins Can Convert 5-Methylcytosine to 5-Formylcytosine and 5-Carboxylcytosine. *Science*. 333 (6047), 1300-3.

257) Jackson, MB. (2010). SNARE complex zipping as a driving force in the dilation of proteinaceous fusion pores. *The Journal of Membrane Biology*. 235 (2), 89-100.

258) Jackson, RE. Burrone, J. (2016). Visualizing Presynaptic Calcium Dynamics and Vesicle Fusion with a Single Genetically Encoded Reporter at Individual Synapses. *Frontiers in Synaptic Neuroscience*. 8 (21). 1-12.

259) Jacobs, AL. Schar, P. (2012). DNA glycosylases: in DNA repair and beyond. *Chromosoma*. 121 (1), 1-20.

260) James, DI. Smith, KM. Jordan, AM. Faiweather, EE. Griffiths, LA. et al. (2016). First-in-Class Chemical Probes against Poly(ADP-ribose) Glycohydrolase (PARG) Inhibit DNA Repair with Differential Pharmacology to Olaparib. *ACS Chemical Biology*. 11 (11), 3179-90.

261) Janko, L. Kovacs, M. Laczik, M. Sari, Z. Ujlaki, G. et al. (2021). Silencing of Poly(ADP-Ribose) Polymerase-2 Induces Mitochondrial Reactive Species Production and Mitochondrial Fragmentation. *Cells*. 10 (6), 1387.

262) Jiang, HY. Yang, Y. Zhang, YY. Xie, Z. Zhao, XY. Sun, Y. Kong, WJ. (2018). The dual role of poly(ADP-ribose) polymerase-1 in modulating parthanatos and autophagy under oxidative stress in rat cochlear marginal cells of the stria vascularis. *Redox Biology*. 14, 361-70.

263) Jilani, A. Ramotar, D. Slack, C. Ong, C. Yang, XM. Scherer, SW. Lasko, DD. (1999). Molecular cloning of the human gene, PNKP, encoding a polynucleotide kinase 3'-phosphatase and evidence for its role in repair of DNA strand breaks caused by oxidative damage. *The Journal of Biological Chemistry*. 274 (34), 24176-86.

264) Juarez, JC. Manuia, M. Burnett, ME. Betancourt, O. Boivin, B. Shaw, DE. Tonks, NK. Mazar, AP. Donate, F. (2008). Superoxide dismutase 1 (SOD1) is essential for H2O2-mediated oxidation and inactivation of phosphatases in growth factor signaling. *Proceedings of the National Academy of Sciences of the United States of America*. 105 (20), 7147-52.

265) Kaeser, PS. Regehr, WG. (2017). The readily releasable pool of synaptic vesicles. *Current Opinion in Neurobiology*. 43, 63-70.

266) Kalani, K. Yan, SF. Yan, SS. (2018). Mitochondrial permeability transition pore: a potential drug target for neurodegeneration. *Drug Discovery Today*. 23 (12), 1983-9.

267) Kalasova, I. Hanzlikova, H. Gupta, N. Li, Y. Altmuller, J. Reynolds, JJ. Stewart, GS. Wollnik, B. Yigit, G. Caldecott, KW. (2019). Novel PNKP mutations causing defective DNA strand break repair and PARP1 hyperactivity in MCSZ. *Neurology Genetics*. 5 (2). E320.

268) Kam, TI. Mao, X. Park, H. Chou, SC. Karuppagounder, SS. et al. (2018). Poly(ADP-ribose) drives pathologic α-synuclein neurodegeneration in Parkinson's disease. *Science*. 362 (6414). 2-27.

269) Kamiya, H. (2003). Mutagenic potentials of damaged nucleic acids produced by reactive oxygen/nitrogen species: approaches using synthetic oligonucleotides and nucleotides. *Nucleic Acids Research*. 31 (2), 517-31.

270) Kanematsu, T. Jang, IS. Yamaguchi, T. Nagahama, H. Yoshimura, K. et al. (2002). Role of the PLC-related, catalytically inactive protein p130 in GABA(A) receptor function. *EMBO Journal*. 21 (5), 1004-11.

271) Karagas, NE. Vankatachalam, K. (2019). Roles for the Endoplasmic Reticulum in Regulation of Neuronal Calcium Homeostasis. *Cells*. 8 (1232), 1-31.

272) Karpova, NN. Sales, AJ. Joca, SR. (2017). Epigenetic Basis of Neuronal and Synaptic Plasticity. *Current Topics in Medicinal Chemistry*. 7 (7), 771-93.

273) Kasamatsu, A. Nakao, M. Smith, BC. Comstock, LR. Ono, T. Kato, J. Denu, JM. Moss, J. (2011). Hydrolysis of O-acetyl-ADP-ribose isomers by ADP-ribosylhydrolase 3. *The Journal of Biological Chemistry*. 24 (286), 21110-7.

274) Kasumu, A. Bezprozvanny, Y. (2012). Deranged Calcium Signaling in Purkinje Cells and Pathogenesis in Spinocerebellar Ataxia 2 (SCA2) and Other Ataxias. *Cerebellum*. 11 (3), 630-9.

275) Kathe, SD. Shen, GP. Wallace, SS. (2004). Single-Stranded Breaks in DNA but Not Oxidative DNA Base Damages Block Transcriptional Elongation by RNA Polymerase II in HeLa Cell Nuclear Extracts. *Journal of Biological Chemistry*. 279 (18), 18511-20.

276) Katyal, S. El-Khamisy, SF. Russell, HR. Li, Y. Ju, L. Caldecott, KW. McKinnon, PJ. (2007). TDP1 facilitates chromosomal single-strand break repair in neurons and is neuroprotective in vivo. *EMBO Journal*. 26 (22), 4720-31.

277) Katyal, S. Lee, Y. Nitiss, KC. Downing, SM. Li, Y. Shimada, M. Zhao, J. Russell, HR. Petrini, JHJ. Nitiss, JL. McKinnon, PJ. (2014). Aberrant topoisomerase-1 DNA lesions are pathogenic in neurodegenerative genome instability syndromes. *Nature Neuroscience*. 17, 813-21.

278) Kauppinen, TM. Suh, SW. Higashi, Y. Berman, AE. Escartin, C. Won, SJ. Wang, C. Cho, SH. Gan, L. Swanson, RA. (2011). Poly(ADP-ribose)polymerase-1 modulates microglial responses to amyloid β. *Journal of Neuroinflammation*. 8 (152), 1-17.

279) Kawale, AS. Povirk, LF. (2018). Tyrosyl–DNA phosphodiesterases: rescuing the genome from the risks of relaxation. *Nucleic Acids Research*. 46 (2), 520-37.

280) Kiessling, V. Kreutzberger, AJB. Liang, B. Nyenhuis, SB. Seelheim, P. Castle, JD. Cafiso, DS. Tamm, LK. (2018). A molecular mechanism for calcium-mediated synaptotagmin-triggered exocytosis. *Nature Structural and Molecular Biology*. 25, 911-7.

281) Kim, J. Kim, K. Mo, JS. Lee, Y. (2020). Atm deficiency in the DNA polymerase β null cerebellum results in cerebellar ataxia and Itpr1 reduction associated with alteration of cytosine methylation. *Nucleic Acids Research*. 48 (7), 3678-91.

282) Kim, K. Pedersen, LC. Kirby, TW. DeRose, EF. London, RE. (2017). Characterization of the APLF FHA-XRCC1 phosphopeptide interaction and its structural and functional implications. *Nucleic Acids Research*. 45 (21), 12374-87.

283) King, I. Yandava, CN. Mabb, AM. Hsiao, JS. Huang, HS. (2013). Topoisomerases facilitate transcription of long genes linked to autism. *Nature*. 501, 58-62.

284) Kitsera, N. Gasteiger, K. Luhnsdorf, B. Allgayer, J. Epe, B. Carell, T. Khobya, A. (2014). Cockayne syndrome: varied requirement of transcription-coupled nucleotide excision repair for the removal of three structurally different adducts from transcribed DNA. *PLOS one*. 9 (4), E94405.

285) Kizilbash, SH. Gupta, SK. Chang, K. Kawashima, R. Parrish, KE. et al. (2017). Restricted Delivery of Talazoparib Across the Blood-Brain Barrier Limits the Sensitizing Effects of PARP Inhibition on Temozolomide Therapy in Glioblastoma. *Molecular Cancer Therapy*. 16 (12), 2735-46.

286) Klungland, A. Lindahl, T. (1997). Second pathway for completion of human DNA base excision-repair: reconstitution with purified proteins and requirement for DNase IV (FEN1). *EMBO Journal*. 16 (11), 3341-8.

287) Knight, MA. Hernandez, D. Diede, SJ. Dauwerse, HG. Rafferty, I. et al . (2008). A duplication at chromosome 11q12.2–11q12.3 is associated with spinocerebellar ataxia type 20. *Human Molecular Genetics*. 17 (24), 3847-53.

288) Koch, SC. Simon, N. Ebert, C. Carell, T. (2016). Molecular mechanisms of xeroderma pigmentosum (XP) proteins. *Quarterly Reviews of Biophysics*. 49. E5.

289) Kofler, J. Otsuka, T. Zhang, Z. Noppens, R. Grafe, MR. Koh, DW. Dawson, VL. de Mucia, JM. Hurn, PD. Traystman, RJ. (2006). Differential effect of PARP-2 deletion on

brain injury after focal and global cerebral ischemia. *Journal of Cerebral Blood Flow and Metabolism*. 26 (1), 135-41.

290) Koh, DW. Lawler, AM. Poitras, MF. Sasaki, M. Wattler, S. Nehls, MC. Stoger, T. Poirier, GG. Dawson, VL. Dawson, TM. (2004). Failure to degrade poly(ADP-ribose) causes increased sensitivity to cytotoxicity and early embryonic lethality. *Proceedings of the National Academy of Science of the United States of America*. 101 (51), 17699-704.

291) Kolobkova, YA. Vigont, VA. Shalygin, AV. Kaznacheyeva, EV. (2017). Huntington's Disease: Calcium Dyshomeostasis and Pathology Models. *Acta Naturae*. 9 (2), 34-46.

292) Komulainen, E. Badman, J. Rey, S. Rulten, S. Ju, L. Fennell, K. Kalasova, I. Ilievova, K. McKinnon, PJ. Hanzlikova, H. Staras, K. Caldecott, KW. (2021). Parp1 hyperactivity couples DNA breaks to aberrant neuronal calcium signalling and lethal seizures. *EMBO Reports*. 22 (5). E51851.

293) Koncina, E. Roth, L. Gonthier, B. Bagnard, D. (2007). Role of Semaphorins during Axon Growth and Guidance. *Axon Growth and Guidance*. 50-64.

294) Kourosh-Arami, M. Hosseini, N. Mohsenzadegan, M. Komaki, A. Joghataei, MT. (2020). Neurophysiologic implications of neuronal nitric oxide synthase. *Reviews in Neuroscience*. 31 (6), 617-36.

295) Kraucionis, S. Heintz, N. (2009). The nuclear DNA base, 5-hydroxymethylcytosine is present in brain and enriched in Purkinje neurons. *Science*. 324 (5929), 529-30.

296) Kraus, WL. (2008). Transcriptional Control by PARP-1: Chromatin Modulation, Enhancer-binding, Coregulation, and Insulation. *Current Opinion in Cell Biology*. 20 (3), 294-302.

297) Kraus, WL. Hottiger, MO. (2013). PARP-1 and gene regulation: Progress and puzzles. *Molecular Aspects of Medicine*. 34 (6), 1109-23.

298) Kreimeyer, A. Wielckens, K. Adamietz, P. Hilz, H. (1984). DNA repair-associated ADP-ribosylation in vivo. Modification of histone H1 differs from that of the principal acceptor proteins. *The Journal of Biological Chemistry*. 259 (2), 890-6.

299) Kress, C. Thomassin, H. Grange, T. (2006). Active cytosine demethylation triggered by a nuclear receptor involves DNA strand breaks. *Proceedings of the National Academy of Sciences of the United States of America*. 103 (30), 11112-7.

300) Krishnakumar, R. Kaus, WL. (2010). The PARP side of the nucleus: molecular actions, physiological outcomes, and clinical targets. *Molecular Cell*. 39 (1), 8-24.

301) Krokan, HE. Bjørås, M. (2013). Base Excision Repair. *Cold Spring Harbour Perspectives in Biology*. 5 (4), 12583.

302) Kruman, II. Wersto, RP. Cardozo-Pelaez, F. Smilenov, L. Chan, SL. Chrest, FJ. Emokpae Jr., R. Gorospe, M. Mattson, MP. (2004). Cell Cycle Activation Linked to Neuronal Cell Death Initiated by DNA Damage. *Neuron*. 41 (4), 549-61.

303) Krüger, A. Bürkle, A. Hauser, K. Magerich, A. (2020). Real-time monitoring of PARP1-dependent PARylation by ATR-FTIR spectroscopy. *Nature Communications*. 11 (2174), 1-15.

304) Kshatri, AS. Gonzalez-Hernandez, A. Giraldez, T. (2018). Physiological Roles and Therapeutic Potential of Ca2+ Activated Potassium Channels in the Nervous System. *Frontiers in Molecular Neuroscience*. 11, 1-18.

305) Kubota, Y. Nash, RA. Klungland, A. Schar, P. Barnes, DE. Lindahl, T. (1996). Reconstitution of DNA base excision-repair with purified human proteins: interaction between DNA polymerase beta and the XRCC1 protein. *EMBO Journal*. 15 (23), 6662-70.

306) Kucheryavykh, YV. Kucheryavykh, CG. Nichols, CG. Maldonado, HM. Baksi, K. Reichenback, A. Skatchkov, SN. Eaton, MJ. (2007). Downregulation of Kir4.1 inward rectifying potassium channel subunits by RNAi impairs potassium transfer and glutamate uptake by cultured cortical astrocytes. *Glia*. 55 (3), 274-81.

307) Kulaeva, OL. Gaykalova, D. Studitsky, VM. (2007). Transcription Through Chromatin by RNA polymerase II: Histone Displacement and Exchange. *Mutation Research*. 618 (1-2), 116-29.

308) Kushnit, A. Wajsberg, B. Maks, AR. (2018). Ryanodine receptor dysfunction in human disorders. *Biochimica et Biophysica Acta. Molecular Cell Research*. 1865 (11), 1687-97.

309) Kuzminov, A. (2001). Single-strand interruptions in replicating chromosomes cause double-strand breaks. *Proceedings of the National Academy of Sciences of the United States of America*. 98 (15), 8241-6.

310) Köhling, R. Wolfart, J. (2016). Potassium Channels in Epilepsy. *Cold Spring Harbour Perspectives in Medicine*. 6 (5). E022871.

311) Lai, HC. Yan, LY. (2006). The distribution and targeting of neuronal voltage-gated ion channels. *Nature Reviews Neuroscience*. 7, 548-62.

312) Lalla, R. Donmez, G. (2013). The role of sirtuins in Alzheimer's disease. *Frontiers in Aging Neuroscience*. 5 (16), 9.

313) Langelier, MF. Planck, JL. Roy, S. Pascal, JM. (2011). Crystal Structures of Poly(ADP-ribose) Polymerase-1 (PARP-1) Zinc Fingers Bound to DNA STRUCTURAL AND FUNCTIONAL INSIGHTS INTO DNA-DEPENDENT PARP-1 ACTIVITY. *Journal of Biological Chemistry*. 286 (12), 10690-701.

314) Langelier, MF. Planck, JL. Roy, S. Pascal, JM. (2012). Structural basis for DNA damage-dependent poly(ADP-ribosylation) by human PARP-1. *Science*. 336 (6082), 728-32.

315) Langelier, MF. Zandarashvili, L. Aguiar, PM. Black, BE. Pascal, JM. (2018). NAD+ analog reveals PARP-1 substrate-blocking mechanism and allosteric communication from catalytic center to DNA-binding domains. *Nature Communication*s. 9 (844), 1-13.

316) Lanner, JT. Georgiu, DK. Joshi, AD. Hamilton, SL. (2010). Ryanodine receptors: structure, expression, molecular details, and function in calcium release. *Cold Spring Harbour Perspectives in Biology*. 2 (11). E003996.

317) Lau, A. Tymianski, M. (2010). Glutamate receptors, neurotoxicity and neurodegeneration. *Pflugers Archiv. European Journal of Physiology*. 460 (2), 525-42.

318) Lavin, M. (2008). Ataxia-telangiectasia: from a rare disorder to a paradigm for cell signalling and cancer. *Nature Reviews Molecular Cell Biology*. 9, 759-69.

319) Le Ber, I. Moreira, MC. Rivaud-Pechoux, S. Chamayou, C. Ochsner, F. et al. (2003). Cerebellar ataxia with oculomotor apraxia type 1: clinical and genetic studies. *Brain*. 126 (12), 2761-72.

320) Leal, A. Bogantes-Ledezma, S. Ekici, AB. Uebe, S. Thiel, CT. et al. (2018). The polynucleotide kinase 3′-phosphatase gene (PNKP) is involved in Charcot-Marie-Tooth disease (CMT2B2) previously related to MED25. *Neurogenetics*. 19 , 215-25.

321) Lebedeva, NA. Rechkunova, NI. Ishchenko, AA. Saparbaev, M. Lavrik, OI. (2013). The mechanism of human tyrosyl-DNA phosphodiesterase 1 in the cleavage of AP site and its synthetic analogs. *DNA Repair*. 12 (12), 1037-42.

322) Ledesma, FP. El Khamisy, SF. Zuma, MC. Osbon, K. Caldecott, KW. (2009). A human 5'-tyrosyl DNA phosphodiesterase that repairs topoisomerase-mediated DNA damage. *Nature*. 461 (7264), 674-8.

323) Lee, JH. Man, MR. Kao, CH. Zhou, Y. Ryu, SW. Richards, AL. Coon, JJ. Paull, TT. (2018). ATM directs DNA damage responses and proteostasis via genetically separable pathways. *Science Signalling*. 11 (512). E5598.

324) Lee, JH. Paull, TT. (2021). Cellular functions of the protein kinase ATM and their relevance to human disease. *Nature Reviews Molecular Cell Biology*. 22, 796-814.

325) Lee, JH. Ryu, SW. Ender, NA. Paull, TT. (2021). Poly-ADP-ribosylation drives loss of protein homeostasis in ATM and Mre11 deficiency. *Molecular Cell*. 81, 1515-33.

326) Lee, SY. Kim, JH. (2015). Mechanisms underlying presynaptic Ca2+ transient and vesicular glutamate release at a CNS nerve terminal during in vitro ischaemia. *The Journal of Physiology*. 593 (13), 2793-806.

327) Lee, Y. Katyal, S. Li, Y. El-Khamisy, SF. Russell, HR. Caldecott, KW. McKinnon, PJ. (2009). The genesis of cerebellar interneurons and the prevention of neural DNA damage require XRCC1. *Nature Neuroscience*. 8 (12), 973-80.

328) Leegwater, PAJ. Yan, BQ. Steen, van der Steen, J. Mulders, J. Konst AAM. et al. (2001). Mutations of MLC1 (KIAA0027), Encoding a Putative Membrane Protein, Cause Megalencephalic Leukoencephalopathy with Subcortical Cysts. *The American Journal of Human Genetics*. 68 (4), 831-38.

329) Lent, R. Azevedo, FAC. Andrade-Moraes, CH. Pinto, AVO. (2012). How many neurons do you have? Some dogmas of quantitative neuroscience under revision. *European Journal of Neuroscience*. 35, 1-9.

330) Lenz, SAP. Kellie, JL. Wetmore, SD. (2015). Glycosidic Bond Cleavage in DNA Nucleosides: Effect of Nucleobase Damage and Activation on the Mechanism and Barrier. *The Journal of Physical Chemistry*. 8 (119), 15601-12.

331) Leshchyns'ka, I. Sytnyk, V. (2016). Synaptic Cell Adhesion Molecules in Alzheimer's Disease. *Neural Plasticity.* 1-10.

332) Levin, DS. McKenna, AE. Motycka, TA. Matsumoto, Y. Tomkinson, AE. (2000). Interaction between PCNA and DNA ligase I is critical for joining of Okazaki fragments and long-patch base-excision repair. *Current Biology*. 10 (15), 919-22.

333) Lewerenz, J. Maher, P. (2015). Chronic Glutamate Toxicity in Neurodegenerative Diseases—What is the Evidence?. *Frontiers in Neuroscience*. 9. 1-20.

334) Li, C. Ullrich, B. Zhang, JZ. Anderson, RG. Brose, N. Sudhof, TC. (1995). Ca(2+)-dependent and independent activities of neural and non-neural synaptotagmins. *Nature*. 375 (6532), 594-9.

335) Li, GM. (2008). Mechanisms and functions of DNA mismatch repair. *Cell Research*. 18, 85-98.

336) Li, M. Liu, Y. (2016). Topoisomerase I in Human Disease Pathogenesis and Treatments. *Genomics, Proteomics & Bioinformatics*. 14 (3), 166-71.

337) Li, T. Garcia-Gomez, A. Morante-Palacios, O. Ciudad, L. Ozkaramehmet, S. van Dijck, E. Rodriguez-Ubreva, J. Vaquero, A. Ballestar, E. (2020). SIRT1/2 orchestrate acquisition of DNA methylation and loss of histone H3 activating marks to prevent premature activation of inflammatory genes in macrophages. *Nucleic Acids Research*. 48 (2), 665-81.

338) Li, Z. Gu, TP. Weber, AR. Shen, JZ. Li, BZ. et al. (2015). Gadd45a promotes DNA demethylation through TDG. *Nucleic Acids Research*. 43 (8), 3986-97.

339) Liao, H. Ji, F. Helleday, T. Ying, S. (2018). Mechanisms for stalled replication fork stabilization: new targets for synthetic lethality strategies in cancer treatments. *EMBO Reports*. 19 (9). E46263.

340) Lin, CP. Ban, Y. Lyu, YL. Desai, SD. Liu, LF. (2008). A Ubiquitin-Proteasome Pathway for the Repair of Topoisomerase I-DNA Covalent Complexes. *Journal of Biological Chemistry*. 283 (30), 21074-83.

341) Lindahl, T. (362). Instability and decay of the primary structure of DNA. *Nature*. 1993, 709-15.

342) Lindahl, T. Barnes, DE. (2000). Repair of endogenous DNA damage. *Cold Spring Harbour Symposia on Quantitative Biology*. 65, 127-33.

343) Lio, CWJ. Yue, C. Lopez-Moyado, IF. Tahiliani, M. Aravind, L. Rao, A. (2020). TET methylcytosine oxidases: new insights from a decade of research. *Journal of Biosciences*. 45 (21), 1-22.

344) Liu, J. Tang, TS. Tu, H. Nelson, O. Herndon, E. Huynh, DP. Pulst, SM. Bezprozvanny, I. (2009). Deranged calcium signaling and neurodegeneration in spinocerebellar ataxia type 2. *The Journal of Neuroscience*. 29 (29), 9148-62.

345) Lodato, MA. Rodin, RE. Bohrson, CL. Coulter, ME. Barton, AR. et al. (2018). Aging and neurodegeneration are associated with increased mutations in single human neurons. *Science*. 359 (6375), 555-9.

346) Loeffler, PA. Cuneo, MJ. Mueller, GA. DeRose, EF. Gabel, SA. London, RE. (2011). Structural studies of the PARP-1 BRCT domain. *BMC Structural Biology*. 11 (37), 1-11.

347) Logan, CV. Szabadkai, G. Sharpe, JA. Parry, DA. Torelli, S. et al. (2014). Loss-of-function mutations in MICU1 cause a brain and muscle disorder linked to primary alterations in mitochondrial calcium signaling. *Nature Genetics*. 46, 188-93.

348) London, RE. (2015). The structural basis of XRCC1-mediated DNA repair. *DNA Repair*. 30, 90-103.

349) Lopez-Manzaneda, M. Franco-Espin, J. Tejero, R. Cano, R. Tabares, L. (2021). Calcium is reduced in presynaptic mitochondria of motor nerve terminals during neurotransmission in SMA mice. *Human Molecular Genetics*. 30 (8), 629-43.

350) Love, S. Barber, R. Wilcock, GK. (1999). Increased poly(ADP-ribosylation) of nuclear proteins in Alzheimer's disease. *Brain*. 122 (2), 247-53.

351) Lovejoy, CA. Cortez, D. (2009). Common mechanisms of PIKK regulation. *DNA Repair*. 8 (9), 1004-8.

352) Lu, M. Mani, RS. Karimi-Busheri, F. Fanta, M. Wang, H. Litchfeld, DW. Weinfeld, M. (2010). Independent mechanisms of stimulation of polynucleotide kinase/phosphatase

by phosphorylated and non-phosphorylated XRCC1. *Nucleic Acids Research*. 38 (2), 510-21.

353) Lönn, P. vander Heide, LP. Dahl, M. Hellman, U. Heldin, CH. Moustakas, A. (2010). PARP-1 attenuates Smad-mediated transcription. *Molecular Cell*. 40 (4), 521-32.

354) Ma, J. Wang, MD. (2016). DNA supercoiling during transcription. *Biophysical Reviews*. 8 (Supp. 1), 75-87.

355) Magrassi, L. Leto, K. Rossi, F. (2013). Lifespan of neurons is uncoupled from organismal lifespan. *Proceedings of the National Academy of Sciences of the United States of America*. 110 (11), 4374-79.

356) Maiti, A. Drohat, AC. (2011). Thymine DNA Glycosylase Can Rapidly Excise 5-Formylcytosine and 5-Carboxylcytosine POTENTIAL IMPLICATIONS FOR ACTIVE DEMETHYLATION OF CpG SITES. *286*. 2011 (41), 35334-8.

357) Mao, K. Chen, J. Yu, H. Li, H. Ren, Y. Wu, X. Wen, Y. Zou, F. Li, W. (2020). Poly (ADP-ribose) polymerase 1 inhibition prevents neurodegeneration and promotes α-synuclein degradation via transcription factor EB-dependent autophagy in mutant α-synucleinA53T model of Parkinson's. *Aging Cell*. 19 (6). E13163.

358) Marelli, C. van de Leemput, J. Johnson, J. Tison, F. Thauvin-Riboinet, C. et al. (2011). SCA15 Due to Large ITPR1 Deletions in a Cohort of 333 White Families with Dominant Ataxia. *Archives of Neurology*. 68 (5), 637-43.

359) Margalef, P. Kotsantis, P. Borel, V. Bellelli, R. Panier, S. Boulton, SJ. (2018). Stabilization of Reversed Replication Forks by Telomerase Drives Telomere Catastrophe. *Cell*. 172 (3), 439-53.

360) Markkanen, E. (2017). Not breathing is not an option: How to deal with oxidative DNA damage. *DNA Repair*. 59, 82-105.

361) Marques, M. Jangal, M. Wang, LC. Kazanets, A. da Silva, SD. et al. (2019). Oncogenic activity of poly (ADP-ribose) glycohydrolase. *Oncogene*. 38, 2177-91.

362) Martincorena, I. Campbell, PJ. (2015). Somatic mutation in cancer and normal cells. *Science*. 349 (6255), 1483-9.

363) Martire, S. Mosca, L. d'Erme, M. (2015). PARP-1 involvement in neurodegeneration: A focus on Alzheimer's and Parkinson's diseases. *Mechanisms of Ageing and Development*. 146 (148), 53-64.

364) Marvin, JS. Borghuis, BG. Tian, L. Cichon, J. Harnett, MT. et al. (2013). An optimized fluorescent probe for visualizing glutamate neurotransmission. *Nature Methods*. 10 (2), 162-70.

365) Marvin, JS. Scholl, B. Wilson, DE. Podgorski, K. Kazemipour, A. et al. (2018). Stability, affinity, and chromatic variants of the glutamate sensor iGluSnFR. *Nature Methods*. 15, 936-9.

366) Mashimo, M. Bu, X. Aoyama, K. Kato, J. Ishiwata-Endo, E. et al. (2019). PARP1 Inhibition Alleviates Injury In ARH3-deficient Mice And Human Cells. *JCL Insight*. 4 (4). E124519.

367) Masson, M. Niedergang, C. Schreiber, V. Muller, S. de Murcia, JD. de Murcia, G. (1998). XRCC1 is specifically associated with poly(ADP-ribose) polymerase and negatively regulates its activity following DNA damage. *Molecular and Cellular Biology*. 18 (6), 3563-71.

368) Matsuda, K. Matsuda, S. Gladding, CM. Yuzaki, M. (2006). Characterization of the δ2 Glutamate Receptor-bindingProtein Delphilin. *Journal of Biological Chemistry*. 281 (35), 25577-87.

369) Matsumoto, K. Nishimura, M. Onoe, T. Sakai, H. Urakawa, Y. Onda, T Yaegashi, N. (2019). PARP inhibitors for BRCA wild type ovarian cancer; gene alterations, homologous recombination deficiency and combination therapy. *Japanese Journal of Clinical Oncology*. 49 (8), 703-7.

370) Matsumoto, M. Nakagawa, T. Inoue, T. Nagata, E. Tanaka, K. et al. (1996). Ataxia and epileptic seizures in mice lacking type 1 inositol 1,4,5-trisphosphate receptor. *Nature*. 379 (6561), 168-71.

371) Matveeva, EA. Al-Tinawi, QMH. Rouchka, EC. Fondufe-Mittendorf, YN. (2019). Coupling of PARP1-mediated chromatin structural changes to transcriptional RNA polymerase II elongation and cotranscriptional splicing. *Epigenetics and Chromatin*. 12 (15), 1-18.

372) Mazzone, GL. Nistri, A. (2011). Effect of the PARP-1 inhibitor PJ 34 on excitotoxic damage evoked by kainate on rat spinal cord organotypic slices. *Cellular and Molecular Neurobiology*. 31 (3), 469-78.

373) McCullock, SD. Kunkel, TA. (2008). The fidelity of DNA synthesis by eukaryotic replicative and translesion synthesis polymerases. *Cell Research*. 18, 148-61.

374) McKie, SJ. Neuman, KC. Maxwell, A. (2021). DNA topoisomerases: Advances in understanding of cellular roles and multi-protein complexes via structure-function analysis. *BioEssays*. 43 (3). E2000286.

375) McKinnon, PJ. (2009). DNA Repair Deficiency and Neurological Disease. *Nature Reviews Neuroscience*. 10 (2), 100-12.

376) McKinnon, PJ. (2016). Topoisomerases and the regulation of neural function. *Nature Reviews Neuroscience*. 17, 673-9.

377) McKinnon, PJ. (2017). Genome integrity and disease prevention in the nervous system. *Genes and Development*. 31, 1180-94.

378) McLeod, F. Boyle, K. Mazo, A. Martin-Flores, N. Moe, TZ. Palomer, E. Gibb, AJ. Salinas, PC. (2020). Wnt Signaling Through Nitric Oxide Synthase Promotes the Formation of Multi-Innervated Spines. *Frontiers in Synaptic Neuroscience*. 12 (575863), 1-10.

379) Meffert, MK. Premack, BA. Schulman, H. (1994). Nitric oxide stimulates Ca2+-independent synaptic vesicle release. *Neuron*. 12 (6), 1235-44.

380) Mehta, A. Haber, JE. (2014). Sources of DNA double-strand breaks and models of recombinational DNA repair. *Cold Spring Harbour Perspectives in Biology*. 6 (9). E016428.

381) Meldolesi, J. Pozzan, T. (1998). The endoplasmic reticulum Ca2+ store: a view from the lumen. *Trends in Biochemical Science*. 23 (1), 10-4.

382) Mena, S. Ortega, A. Estrela, JM. (2009). Oxidative stress in environmental-induced carcinogenesis. *Mutation Research/Genetic Toxicology and Environmental Mutagenesis*. 674 (1-2), 36-44.

383) Mendelsohn, AR. Larrick, JW. (2017). The NAD+/PARP1/SIRT1 Axis in Aging. *Rejuvination Research*. 3 (20), 244-7.

384) Menon, RP. Nethisinghe, S. Faggiano, S. Vannocci, T. Rezaei, H. et al. (2013). The Role of Interruptions in polyQ in the Pathology of SCA1. *PLOS Genetics*. 9 (7). E1003648.

385) Messner, S. Altmeyer, M. Zhao, H. Pozivil, A. Roschitzki, B. Gehrig, P. Rutishauser, R. Huang, D. Caflisch, A. Hottiger, MO. (2010). PARP1 ADP-ribosylates lysine residues of the core histone tails. *Nucleic Acids Research*. 38 (19), 6350-62.

386) Meyer, RG. Meyer-Ficca, ML. Whatcott, CJ. Jacobson, EL. Jacobson, MK. (2007). Two small enzyme isoforms mediate mammalian mitochondrial poly(ADP-ribose) glycohydrolase (PARG) activity. *Experimental Cell Research*. 313 (13), 2920-36.

387) Min, A. Im, SA. Yoon, YK. Song, SH. Nam, HJ. et al. (2013). RAD51C-deficient cancer cells are highly sensitive to the PARP inhibitor olaparib. *Molecular Cancer Therapy*. 12 (6), 865-77.

388) Minnella, AM. Zhao, JX. Jiang, X. Jakobsen, E. Lu, F. et al. (2018). Excitotoxic superoxide production and neuronal death require both ionotropic and non-ionotropic NMDA receptor signaling. *Scientific Reports*. 8 (1), 17522.

389) Miyagi, Y. Yamashita, T. Fukaya, M. Sonoda, T. Okuno, T. et al. (2002). Delphilin: a novel PDZ and formin homology domain-containing protein that synaptically colocalizes

and interacts with glutamate receptor delta 2 subunit. *The Journal of Neuroscience*. 22 (3), 803-14.

390) Mnatsakanyan, N. Beutner, G. Porter, GA. Alavian, KN. Jonas, EA. (2017). Physiological roles of the mitochondrial permeability transition pore. *Journal of Bioenergetics and Biomembranes*. 49 (1), 13-25.

391) Mochida, S. (2019). Presynaptic Calcium Channels. *Internation Journal of Molecular Sciences*. 20 (9), 2217.

392) Mok, MCY. Campalans, A. Pillon, MC. Guarne, A. adicella, JP. Junop, MS. (2019). Identification of an XRCC1 DNA binding activity essential for retention at sites of DNA damage. *Scientific Reports*. 9 (1), 3095.

393) Mongillo, G. Barak, O. Tsodyks, M. (2008). Synaptic Theory of Working Memory. *Science*. 319 (5869), 1543-6.

394) Moor, NA. Lavrik, OI. (2018). Protein-Protein Interactions in DNA Base Excision Repair. *Biochemistry (Moscow)*. 83 (4), 411-22.

395) Morales, JC. Li, L. Fattah, F. Dong, Y. Bey, EA. Patel, M. Gao, J. Boothman, DA. (2014). Review of Poly (ADP-ribose) Polymerase (PARP) Mechanisms of Action and Rationale for Targeting in Cancer and Other Diseases. *Critical Reviews in Eukaryotic Gene Expression*. 24 (1), 15-28.

396) Moreira, MDC. Barbot, C. Tachi, N. Kozuka, N. Mendonca, P. Barros, J, Coutinho, P. Sequeiros, J. Koenig, M. (2001). Homozygosity Mapping of Portuguese and Japanese Forms of Ataxia-Oculomotor Apraxia to 9p13, and Evidence for Genetic Heterogeneity. *The American Journal of Human Genetics*. 68 (2), 501-8.

397) Morgan, AJ. Platt, FM. Lloyd-Evans, E. Galione, A. (2011). Molecular mechanisms of endolysosomal Ca2+ signalling in health and disease. *The Biochemical Journal*. 439 (3), 349-74.

398) Morino, H. Matsuda, Y. Muguruma, K. Miyamoto, R. Ohsawa, R. et al. (2015). A mutation in the low voltage-gated calcium channel CACNA1G alters the physiological properties of the channel, causing spinocerebellar ataxia. *Molecular Brain*. 8 (89), 1-9.

399) Moriya, M. (1993). Single-stranded shuttle phagemid for mutagenesis studies in mammalian cells: 8-oxoguanine in DNA induces targeted G.C-->T.A transversions in simian kidney cells. *Proceedings of the National Academy of Sciences of the United States of America*. 90 (3), 1122-6.

400) Mortusewicz, O. Ame, JC. Schreiber, V. Leonhardt, H. (2007). Feedback-regulated poly(ADP-ribosylation) by PARP-1 is required for rapid response to DNA damage in living cells. *Nucleic Acids Research*. 35 (22), 7665-75.

401) Mortusewicz, O. Fouquerel, E Ame, JC. Leonhardt, H. Schreiber, V. (2011). PARG is recruited to DNA damage sites through poly(ADP-ribose)- and PCNA-dependent mechanisms. *Nucleic Acids Research*. 39 (12), 5045-56.

402) Mosca-Voidron. AL. Gueneau, L. Huguet, G. Goldenberg, A. Henry, C. et al. (2016). A de novo microdeletion of SEMA5A in a boy with autism spectrum disorder and intellectual disability. *European Journal of Human Genetics*. 24, 838-43.

403) Mouret, S. Baudouin, C. Chaveron, M. Favier, A. Cadet, J. Douki, T. (2006). Cyclobutane pyrimidine dimers are predominant DNA lesions in whole human skin exposed to UVA radiation. *Proceedings of the National Academy of Sciences of the United States of America*. 103 (37), 13765-70.

404) Mulley, JC. Iona, X. Hodgson, B. Heron, SE. Berkovic, SF. Scheffer, IF. Dibbens, LM. (2011). The Role of Seizure-Related SEZ6 as a Susceptibility Gene in Febrile Seizures. *Neurology Research International*. 917565, 1-4.

405) Mullins, EA. Rodriguez, AA. Bradley, NP. Eichman, BF. (2019). Emerging Roles of DNA Glycosylases and the Base Excision Repair Pathway. *Trends in Biochemical Sciences*. 44 (9), 765-81.

406) Murai, J. Huang, SN. Das, BB. Renaud, A. Zhang, Y. Doroshow, JH. Ji, J. Takeda, S. Pommier, Y. (2012). Differential trapping of PARP1 and PARP2 by clinical PARP inhibitors. *Cancer Research*. 72 (21), 5588-99.

407) Murai, J. Huang, SH. Renaud, A. Zhang, Y. Ji, J. et al. (2014). Stereospecific PARP trapping by BMN 673 and comparison with olaparib and rucaparib. *Molecular Cancer Therapy*. 13 (2), 433-43.

408) Murata, MM. Kong, X. Moncada, E. Chen, Y. Imamura, H. Wang, P. Berns, MW. Yokomori, K. Digman, MA. (2019). NAD+ consumption by PARP1 in response to DNA damage triggers metabolic shift critical for damaged cell survival. *Molecular Biology of the Cell*. 30 (20), 2584-97.

409) Muthurajan, UM. Hepler, MRD. Hieb, AR. Clark, NJ. Kramer, M. Yao, T. Luger, K. (2014). Automodification switches PARP-1 function from chromatin architectural protein to histone chaperone. *Proceedings of the National Academy of Sciences of the United States of America*. 111 (35), 12752-7.

410) Müller, N. Reinacher-Schick, A. Baldus, S. van Hengel, J. Berx, G. Baar, A. van Roy, F. Schmiegel, W. Schwarte-Waldhoff, I. (2002). Smad4 induces the tumor suppressor E-cadherin and P-cadherin in colon carcinoma cellsSmad4 induces the tumor suppressor E-cadherin and P-cadherin in colon carcinoma cells. *Oncogene*. 21, 6049-58.

411) Nagai, S. Davis, RE. Mattei, PJ. Eagen, KP. Kornberg, RD. (2017). Chromatin potentiates transcription. *Proceedings of the National Academy of Sciences of the United States of America*. 11 (52), 1536-41.

412) Nakashima, M. Takano, K. Osaka, H. Aida, N. Tsurusaki, Y. Miyake, N. Saitsu, H. Matsmoto. (2014). Causative novel PNKP mutations and concomitant PCDH15 mutations in a patient with microcephaly with early-onset seizures and developmental delay syndrome and hearing loss. *Journal of Human Genetics*. 59 (8), 471-4.

413) Nanou, E. Lee, A. Catterall, WA. (2018). Control of Excitation/Inhibition Balance in a Hippocampal Circuit by Calcium Sensor Protein Regulation of Presynaptic Calcium Channels. *The Journal of Neuroscience*. 38 (18), 4430-40.

414) Narasimhan, P. Fujimura, M. Noshita, N. Chan, PH. (2003). Role of superoxide in poly(ADP-ribose) polymerase upregulation after transient cerebral ischemia. *Brain Research. Molecular Brain Research*. 113 (1-2), 28-36.

415) Neil, AJ. Belotserkovskii, BP. Hanawalt, PC. (2012). Transcription blockage by bulky end termini at single-strand breaks in the DNA template: differential effects of 5' and 3' adducts. *Biochemistry*. 51 (44), 8964-70.

416) Neitz, A. Mergia, E. Neubacher, U. Koesling, D. Mittmann, T. (2015). NO regulates the strength of synaptic inputs onto hippocampal CA1 neurons via NO-GC1/cGMP signalling. *Pflugers Archiv. European Journal of Physiology*. 467 (6), 1383-94.

417) Nguyen, AQ. Sutley, S. Koeppen, J. Mina, K. Woodruff, S. Hanna, S. Vengala, A. Hickmott, PW. Obenaus, A. Ethell, IM. (2020). Astrocytic Ephrin-B1 Controls Excitatory-Inhibitory Balance in Developing Hippocampus. *The Journal of Neuroscience*. 40 (36), 6854-71.

418) Nikitczuk, JS. Patil, SB. Maikainen-Ankney, BA. Scarpa, J. Shapiro, ML. Benson, DL. Huntley, GW. (2014). N-cadherin regulates molecular organization of excitatory and inhibitory synaptic circuits in adult hippocampus in vivo. *Hippocampus*. 24 (8), 943-62.

419) Niles, JC. Wishnok, JS. Tannenbaum, SR. (2006). Peroxynitrite-induced oxidation and nitration products of guanine and 8-oxoguanine: structures and mechanisms of product formation. *Nitric Oxide*. 14 (2), 109-21.

420) Noordermeer, SM. van Attikum, H. (2019). PARP Inhibitor Resistance: A Tug-of-War in BRCA-Mutated Cells. *Trends in Cell Biology*. 29 (10), 820-34.

421) O'Connor, E. Vndrovcova, J. Bugiardini, E. Chelban, V. Manole, A. et al. (2018). Mutations in XRCC1 cause cerebellar ataxia and peripheral neuropathy. *Journal of Neurology, Neurosurgery and Psychiatry*. 89 (11), 1230-2.

422) Oh, S. Kim, YJ. Lee, EK. Park, SW. Yu, HG. (2020). Antioxidative Effects of Ascorbic Acid and Astaxanthin on ARPE-19 Cells in an Oxidative Stress Model. *Antioxidants*. 9 (833), 1-15.

423) Ohshima, H. Sawa, T. Akaike, T. (2006). 8-nitroguanine, a product of nitrative DNA damage caused by reactive nitrogen species: formation, occurrence, and implications in inflammation and carcinogenesis. *Antioxidants and Redox Signalling*. 8 (5-6), 1033-45.

424) Oliveira, AMM. (2016). DNA methylation: a permissive mark in memory formation and maintenance. *Learning and Memory*. 23 , 587-93.

425) de Oliveira Borges, CFQ. (2017). Assaying synaptic function using geneticallyencoded optical reporters in the context of Alzheimer's disease. *Universidade de Coimbra*.

426) Ooi, SK. Sato, S. Tomomori-Sato, C. Zhang, Y. Wen, Z. Banks, CAS. Washburn, MP. Unruh, JR. Florens, L. Conaway, RC. Conaway, JW. (2021). Multiple roles for PARP1 in ALC1-dependent nucleosome remodeling. *Proceedings of the National Academy of Sciences of the United States of America*. 118 (36). E 2107277118.

427) Pacher, P. Szabo, C. (2008). Role of the Peroxynitrite-Poly(ADP-ribose) Polymerase Pathway in Human Disease. *The American Journal of Pathology*. 173 (1), 2-13.

428) Padamsey, Z. Foster, WJ. Emptage, NJ. (2018). Intracellular Ca2+ Release and Synaptic Plasticity: A Tale of Many Stores. *The Neuroscientist*. 1-17.

429) Pahi, ZG. Borsos, BN. Pantazi, V. Ujfaludi, Z. Pankotai, T. (2020). PARylation During Transcription: Insights into the Fine-Tuning Mechanism and Regulation. *Cancers*. 12 (183), 1-18.

430) Paiva, CN. Bozza, MT. (2014). Are Reactive Oxygen Species Always Detrimental to Pathogens? *Antioxidants & Redox Signalling*. 20 (6), 1000-37.

431) Paknejad, N. Hite, RK. (2018). Structural basis for the regulation of inositol trisphosphate receptors by Ca2+ and IP3. *Nature Structural and Molecular Biology*. 25, 660-8.

432) Pal, S. Sombati, S. Limbrick, DD. DeLorenzo, RJ. (1999). In vitro status epilepticus causes sustained elevation of intracellular calcium levels in hippocampal neurons. *Brain Research*. 851 (1-2), 20-31.

433) Palazzo, L. Leidecker, O. Prokhorova, E. Dauben, H. Matic, I. Ahel, I. (2018). Serine is the major residue for ADP-ribosylation upon DNA damage. *ELife*. 7. E34334.

434) Panes, JD. Godoy, PA. Silva-Grecchi, T. Celis, MT. Ramirez-Molina, O. et al. (2020). Changes in PGC-1α/SIRT1 Signaling Impact on Mitochondrial Homeostasis in Amyloid-Beta Peptide Toxicity Model. *Frontiers in Pharmacology*. 11, (709), 1-17.

435) Panier, S. Boulton, SJ. (2014). Double-strand break repair: 53BP1 comes into focus. *Nature Reviews Molecular Cell Biology*. 15, 7-18.

436) Park, H. Kam, TI. Dawson, TM. Dawson, VL. (2020). Poly (ADP-ribose) (PAR)-dependent cell death in neurodegenerative diseases. *International Review of Cell and Molecular Biology*. 353 (1), 1-29.

437) Park, H. Kang, JH. Lee, S. (2020). Autophagy in Neurodegenerative Diseases: A Hunter for Aggregates. *International Journal of Molecular Sciences*. 21 (9), 3369.

438) Parrish, KE. Cen, L. Murray, J. Calligaris, D. Kizilbash, S. et al. (2015). Efficacy of PARP inhibitor rucaparib in orthotopic glioblastoma xenografts is limited by ineffective drug penetration into the central nervous system. *Molecular Cancer Therapy*. 14 (12), 2735-43.

439) Parsons, JL. Dianova, II. Allinson, SL. Dianov, GL. (2005). DNA polymerase beta promotes recruitment of DNA ligase III alpha-XRCC1 to sites of base excision repair. *Biochemistry*. 44 (31), 10613-9.

440) Parsons, JL. Dianova, II. Finch, D. Tait, PS. Strom, CE. Helleday, T. Dianov, GL. (2010). XRCC1 phosphorylation by CK2 is required for its stability and efficient DNA repair. *DNA Repair*. 9 (7), 835-41.

441) Parsons, JL. Dianova, IL. Dianov, GL. (2004). APE1 is the major 3'-phosphoglycolate activity in human cell extracts. *Nucleic Acids Research*. 32 (12), 3531-6.

442) Patel, AG. Sarkaria, JN. Kaufmann, SH. (2011). Nonhomologous end joining drives poly(ADP-ribose) polymerase (PARP) inhibitor lethality in homologous recombination-deficient cells. *Proceedings of the National Academy of Sciences of the United States of America*. 108 (8), 3406-11.

443) Patel, AJ. Seaton, P. Hunt, A. (1988). A novel way of removing quiescent astrocytes in a culture of subcortical neurons grown in a chemically defined medium. *Brain Research*. 470 (2), 283-8.

444) Paucar, M. Halmgren, H. Taylor, M. Reynolds, JJ. Svenningsson, P. Press, R. Nordgren, A. (2016). Expanding the ataxia with oculomotor apraxia type 4 phenotype. *Neurology Genetics*. 2 (1). E49.

445) Paul, TT. (2015). Mechanisms of ATM Activation. *Annual Review of Biochemistry*. 84, 711-38.

446) Paul, V. Ekambaram, P. (2011). Involvement of nitric oxide in learning & memory processes. *The Indian Journal of Medical Research*. 133 (5), 471-8.

447) Pazzaglia, S. Pioli, C. (2020). Multifaceted Role of PARP-1 in DNA Repair and Inflammation: Pathological and Therapeutic Implications in Cancer and Non-Cancer Diseases. *Cells*. 9 (41).

448) Pecina-Slaus, N. (2003). Tumor suppressor gene E-cadherin and its role in normal and malignant cells. *Cancer Cell International*. 3 (17).

449) Pećina-Šlaus, N. Kafka, A. Salamon, I. Bukovac, A. (2020). Mismatch Repair Pathway, Genome Stability and Cancer. *Frontiers in Molecular Biosciences*. 7 (122), 1-12.

450) Pehar, M. Harlan, BA. Killoy, KM. Vargas, MR. (2018). Nicotinamide Adenine Dinucleotide Metabolism and Neurodegeneration. *Antioxidants & Redox Signalling*. 28 (18), 1652-68.

451) Pettitt, SJ. Krastev, DB. Brandsma, I. Drean, A. Song, F. et al. (2018). Genome-wide and high-density CRISPR-Cas9 screens identify point mutations in PARP1 causing PARP inhibitor resistance. *Nature Communications*. 9 (1), 1849.

452) Pfeiffer, P. Goedecke, W. Obe, G. (2000). Mechanisms of DNA double-strand break repair and their potential to induce chromosomal aberrations. *Mutagenesis*. 15 (4), 289-302.

453) Pflieger, LT. Dansithong, W. Paul, S. Scoles, DR. Figueroa, KP. Meera, P. Otis, TS. Facelli, JC. Pulst, SM. (2017). Gene co-expression network analysis for identifying modules and functionally enriched pathways in SCA2. *Human Molecular Genetics*. 26 (16), 3069-80.

454) Picón-Pagés, P. Garcia-Buendia, J. Munoz, FJ. (2019). Functions and dysfunctions of nitric oxide in brain. *Biochimica et Biophysica Acta (BBA) - Molecular Basis of Disease*. 1865 (8), 1949-67.

455) Pigoni, M. Hsia, HE. Hartmann, J. Njavro, JR. Shmueli, MD. (2020). Seizure protein 6 controls glycosylation and trafficking of kainate receptor subunits GluK2 and GluK3. *EMBO Journal*. 39 (15). E103457.

456) Pilotto, F. Saxena, S. (2018). Epidemiology of inherited cerebellar ataxias and challenges in clinical research. *Swiss Federation of Clinical Neurosciences*. 2 (2), 1-12.

457) Piskunova, TS. Yurova, MN. Ovsyannikov, AI. Semenchenko, AV. Zabezhinksi, MA. Popovich, IG. Wang, ZQ. Anisimov, VN. (2008). Deficiency in Poly(ADP-ribose) Polymerase-1 (PARP-1) Accelerates Aging and Spontaneous Carcinogenesis in Mice. *Current Gerontology and Geriatics Research*. 2008 (754190), 1-11.

458) Piunti, A. Shilatifard, A. (2021). The roles of Polycomb repressive complexes in mammalian development and cancer. *Nature Reviews Molecular Cell Biology*. 22, 326-45.

459) Plo, I. Liao, ZY. Barcelo, JM. Kohlhagen, G. Caldecott, KW. Weinfeld, M. Pommier, Y. (2003). Association of XRCC1 and tyrosyl DNA phosphodiesterase (Tdp1) for the repair of topoisomerase I-mediated DNA lesions. *DNA Repair*. 2 (10), 1087-100.

460) Plo, I. Liao, ZY. Barcelo, JM. Kohlhagen, G. Caldecott, KW. Weinfeld, M. Pommier, Y. (2003). Association of XRCC1 and tyrosyl DNA phosphodiesterase (Tdp1) for the repair of topoisomerase I-mediated DNA lesions. *DNA Repair*. 7 (2), 1087-100.

461) Plongthongkum, N. Diep, DH. Zhang, K. (2014). Advances in the profiling of DNA modifications: cytosine methylation and beyond. *Nature Reviews Genetics*. 15, 647-61.

462) Plosky, BS. Woodgate, R. (2004). Switching from high-fidelity replicases to low-fidelity lesion-bypass polymerases. *Current Opinion in Genetics and Development*. 14 (2), 113-9.

463) Poetsch, AR. (2020). The genomics of oxidative DNA damage, repair, and resulting mutagenesis. *Computational and Structural Biology Journal*. 18, 207-219.

464) Pogozelski, WK. Tullius, TD. (1998). Oxidative Strand Scission of Nucleic Acids: Routes Initiated by Hydrogen Abstraction from the Sugar Moiety. *Chemical Reviews*. 98 (3), 1089-108.

465) Polo, SE. Jackson, SP. (2011). Dynamics of DNA damage response proteins at DNA breaks: a focus on protein modifications. *Genes & Development*. 25 (5), 409-33.

466) Pommier, Y. Barcelo, JM. Rao, VA. Sordet, O. Jobson, AG. et al. (2006). Repair of topoisomerase I-mediated DNA damage. *Progress in Nucleic Acid Research and Molecular Biology*. 81, 179-229.

467) Pommier, Y. Huang, SN. Gao, R. Das, BB. Murai, J. Marchand, C. (2014). Tyrosyl-DNA-phosphodiesterases (TDP1 and TDP2). *DNA Repair*. 19, 114-29.

468) Pommier, Y. Sun, Y. Huang, SN. Nitiss, JL. (2016). Roles of eukaryotic topoisomerases in transcription, replication and genomic stability. *Nature Reviews Molecular Cell Biology*. 17, 703-21.

469) Popugaeva, E. Pchitskaya, E. Bezprozvanny, I. (2017). Dysregulation of neuronal calcium homeostasis in Alzheimer's disease - A therapeutic opportunity? *Biochemical and Biophysical Research Communication*. 483 (4), 998-1004.

470) Poulton, C. Oegama, R. Heijsman, D. Hoogeboom, J. Schot, R. et al. (2013). Progressive cerebellar atrophy and polyneuropathy: expanding the spectrum of PNKP mutations. *Neurogenetics*. 14 (1), 43-51.

471) Pourquier, P. Pilon, AA. Kohlhagen, G. Mazumder, A. Sharma, A. Pommier, Y. (1997b). Trapping of mammalian topoisomerase I and recombinations induced by damaged DNA containing nicks or gaps. Importance of DNA end phosphorylation and camptothecin effects. *The Journal of Biological Chemistry*. 272 (42), 26441-7.

472) Pourquier, P. Ueng, LM. Kohlhagen, G. Mazumder, A. Gupta, M. Kohn, KW. Pommier, Y. (1997a). Effects of uracil incorporation, DNA mismatches, and abasic sites

on cleavage and religation activities of mammalian topoisomerase I. *The Journal of Biological Chemistry*. 272 (12), 7792-6.

473) Purnell, MR. Whish, WJ. (1980). Novel inhibitors of poly(ADP-ribose) synthetase. *Biochemical Journal*. 185 (3), 775-7.

474) Purroy, R. Britti, E. Delaspre, F. Tamarit, J. Ros, J. (2018). Mitochondrial pore opening and loss of Ca 2+ exchanger NCLX levels occur after frataxin depletion. *Biochimica et Biophysica Acta. Molecular Basis of Disease*. 1864, 618-631.

475) Radi, R. (2013). Peroxynitrite, a Stealthy Biological Oxidant. *Journal of Biological Chemistry*. 288 (37), 26464-72.

476) Radi, R. (2018). Oxygen radicals, nitric oxide, and peroxynitrite: Redox pathways in molecular medicine. *Proceedings of the National Academy of Sciences of the United States of America*. 115 (23), 5839-48.

477) Rajakulendran, S. Hanna, MG. (2016). The Role of Calcium Channels in Epilepsy. *Cold Spring Harbour Perspectives in Medicine*. 6, 1-22.

478) Rasmussen, KD. Helin, K. (2016). Role of TET enzymes in DNA methylation, development, and cancer. *Genes and Development*. 30 (7), 733-50.

479) Redinbo, MB. Stewart, L. Kuhn, P. Champoux, JJ. Hol, WGJ. (1998). Crystal Structures of Human Topoisomerase I in Covalent and Noncovalent Complexes with DNA. *Science*. 279 (5356), 1504-13.

480) Rein, ID. Landsverk, KS. Micci, F. Patzke, S. Stokke, T. (2015). Replication-induced DNA damage after PARP inhibition causes G2 delay, and cell line-dependent apoptosis, necrosis and multinucleation. *Cell Cycle*. 14 (20), 3248-60.

481) Reinacher-Schick, A. Baldus, SE. Romdhana, B. Landsberg, S. Zapatka, M. Monig, SP. Holsher, AH. Dienes, HP. Schmiegel, Wolff. Schwarte-Waldhoff, I. (2004). Loss of Smad4 correlates with loss of the invasion suppressor E-cadherin in advanced colorectal carcinomas. *The Journal of Pathology*. 202 (2), 412-20.

482) Reisz, JA. Bansal, N. Qian, J. Zhao, W. Furdui, CM. (2014). Effects of Ionizing Radiation on Biological Molecules—Mechanisms of Damage and Emerging Methods of Detection. *Antioxidants and Redox Signalling*. 21 (2), 260-92.

483) Reynolds, JJ. El-Khamisy, SF. Katyal, S. Clements, P. McKinnon, PJ. Caldecott, KW. (2009). Defective DNA ligation during shortpatch singlestrand break repair in ataxia oculomotor apraxia 1. *Molecular and Cellular Biology*. 29 (5), 1354.

484) Reynolds, JJ. Walker, AK. Gilmore, EC. Walsh, CA. Caldecott, KW. (2012). Impact of PNKP mutations associated with microcephaly, seizures and developmental delay on enzyme activity and DNA strand break repair. *Nucleic Acids Research*. 40 (14), 6608-19.

485) Rifai, K. Judes, G. Idrissou, M. Daures, M. Bignon, YJ. Penault-Llorca, F. Bernard-Gallon, D. (2018). SIRT1-dependent epigenetic regulation of H3 and H4 histone acetylation in human breast cancer. *Oncotarget*. 9 (55), 30661-78.

486) Rizzoli, SO. Betz, WJ. (2005). Synaptic vesicle pools. *Nature Reviews Neuroscience*. 6, 57-69.

487) Robertson, AB. Klungland, A. Rognes, T. Leiros, I. (2009). Base excision repair: the long and short of it. *Cellular and Molecular Life Sciences*. 66, 981-93.

488) Robichaux, MA. Chenaux, G. Ho, HYH. Soskis, MJ. Dravis, C. Kwan, KY. Sestan, N. Greenberg, ME. Henkemeyer, M. Cowan, CW. (2014). EphB receptor forward signaling regulates area-specific reciprocal thalamic and cortical axon pathfinding. *Proceedings of the National Academy of Sciences of the United States of America*. 111 (6), 2188-93.

489) Rodgers JT. Lerin, C. Haas, W. Gygi, SP. Spiegelman, BM. Puigserver, P. (2005). Nutrient control of glucose homeostasis through a complex of PGC-1alpha and SIRT1. *Nature*. 434 (7029), 113-8.

490) Rose, M. Burgess, JT. O'Byrne, K. Richard, DJ. Bolderson, E. (2020). PARP Inhibitors: Clinical Relevance, Mechanisms of Action and Tumor Resistance. *Frontiers in Cell and Developmental Biology*. 8, 564601.

491) Rossi, MR. Anheim, M. Durr, A. Klein, C. Koenig, M. Synofzik, M. Marras, C, van de Warrenburg, BP. (2018). The genetic nomenclature of recessive cerebellar ataxias. *Movement Disorders*. 33 (7), 1057-76.

492) Roth, DB. Wilson, JH. (1988). Illegitimate recombination in mammalian cells. *Genetic Recombination*. ASM Press, 621-53.

493) Rothblum-Oviatt, C. Wright, J. Lefton-Greif, MA. McGrath-Morrow, SA. Crawford, TO. Lederman, HM. (2016). Ataxia telangiectasia: a review. *Orphanet Journal of Rare Diseases*. 11 (1), 159.

494) Roychoudhury, S. Pramanik, S. Harris, HL. Tarpley, M. Sarkar, A. et al. (2020). Endogenous oxidized DNA bases and APE1 regulate the formation of G-quadruplex structures in the genome. *Proceedings of the National Academy of Sciences of the United States of America*. 117 (21), 11409-20.

495) Royle, SJ. Granseth, B. Odermatt, B. Derevier, A. Lagnado, L. (2008). Imaging pHluorin-based probes at hippocampal synapses. *Methods Molecular Biology*. 457, 293-303.

496) Rubin, RD. Watson, PD. Duff, MC. Cohen, NJ. (2014). The role of the hippocampus in flexible cognition and social behavior. *Frontiers in Human Neuroscience*. 8 (742), 1-15.

497) Rueda, CB. Llorente-Folch, I. Traba, J. Amigo, I. Gonzalez-Sanchez, P. et al. (2016). Glutamate excitotoxicity and Ca2+-regulation of respiration: Role of the Ca2+ activated mitochondrial transporters (CaMCs). *Biochimica et Biophysica Acta*. 1857 (8), 1158-66.

498) Sabatini, BL. Regehr, WG. (1996). Timing of neurotransmission at fast synapses in the mammalian brain. *Nature*. 384 (6605), 170-2.

499) Sachdev, E. Tabatabai, R. Roy, V. Rimel, BJ. Mita, MM. (2019). PARP Inhibition in Cancer: An Update on Clinical Development. *Targeted Oncology*. 14 (6), 657-79.

500) Sakaba, T. Neher, E. (2001). Quantitative Relationship between Transmitter Release and Calcium Current at the Calyx of Held Synapse. *The Journal of Neuroscience*. 21 (2), 462-76.

501) Salerno, JC. Ray, K. Poulos, T. Li, H. Ghosh, DK. (2013). Calmodulin activates neuronal nitric oxide synthase by enabling transitions between conformational states. *FEBS Letters*. 587 (1), 44-7.

502) Santivasi, WL. Xia, F. (2014). Ionizing Radiation-Induced DNA Damage, Response, and Repair. *Antioxidants and Redox Signalling*. 21 (2), 251-9.

503) Schapira, AHV. (2013). Calcium dysregulation in Parkinson's disease. *Brain*. 136 (7), 2015-6.

504) Schellenberg, MJ. Tumbale, PP. Scott Williams, R. (2015). Molecular Underpinnings of Aprataxin RNA/DNA Deadenylase Function and Dysfunction in Neurological Disease. *Progress in Biophysics and Molecular Biology*. 117 (0), 157-65.

505) Schmidt, HH. Pollock, JS. Nakane, M. Forstermann, U. Murad, F. (1992). Ca2+/calmodulin-regulated nitric oxide synthases. *Cell Calcium*. 13 (6-7), 427-34.

506) Schonewille, M. Girasole, AE. Rostaing, P. Mailhes-Hamon, C. Ayon, A. Nelson, AB. Triller, A. Casado, M. De Zeeuw, CI. Bouvier, G. (2021). NMDARs in granule cells contribute to parallel fiber–Purkinje cell synaptic plasticity and motor learning. Proceedings of the National Academy of Sciences of the United States of America. 118 (37). E2102635118.

507) Schorge, S. van de Leemput, J. Singleton, A. Houlden, H. Hardy, J. (2010). Human ataxias: a genetic dissection of inositol triphosphate receptor (ITPR1)-dependent signaling. *Trends in Neuroscience*. 33 (5), 211-9.

508) Scullin, CS. Tafoya, LC. Wilson, MC. Partridge, LD. (2012). Presynaptic residual calcium and synaptic facilitation at hippocampal synapses of mice with altered expression of SNAP-25. *Brain Research*. 1431, 1-12.

509) Scullin. CS. Partridge, LD. (2010). Contributions of SERCA pump and ryanodine-sensitive stores to presynaptic residual Ca2+. *Cell Calcium*. 47 (4), 326-38.

510) Segal, M. Korkotia, E. (2014). Endoplasmic reticulum calcium stores in dendritic spines. *Frontiers in Neuroanatomy*. 8 (64), 1-7.

511) Seifert, G. Huttmann, K. Binder, DK. Hartmann, C. Wyczynski, A. Neusch, C. Steinhauser, C. (2009). Analysis of Astroglial K+ Channel Expression in the Developing Hippocampus Reveals a Predominant Role of the Kir4.1 Subunit. *The Journal of Neuroscience*. 29 (23), 7474-88.

512) Seong, E. Yuan, L. Arikkath, J. (2015). Cadherins and catenins in dendrite and synapse morphogenesis. *Cell Adhesion & Migration*. 9 (3), 202-13.

513) Shabbir, SH. (2015). DNA Repair Dysfunction and Neurodegeneration: Lessons From Rare Pediatric Disorders. *Journal of Child Neurology*. 31 (37), 392-6.

514) Sharifi, R. Morra, R. Appel, CD. Tallis, M. Chioza, B. et al. (2013). Deficiency of terminal ADP-ribose protein glycohydrolase TARG1/C6orf130 in neurodegenerative disease. *EMBO Journal*. 32 (9), 1225-37.

515) Shen, J. Gilmore, EC. Marshall, CA. Haddadin, M. Reynolds, JJ. (2010). Mutations in PNKP cause microcephaly, seizures and defects in DNA repair. *Nature Genetics*. 42 (3), 245-9.

516) Shen, WW. Frieden, M. Demaurex, N. (2011). Remodelling of the endoplasmic reticulum during store-operated calcium entry. *Biology of the Cell*. 103 (8), 365-80.

517) Shen, Y. Aoyagi-Scharber, M. Wang, B. (2015). Trapping Poly(ADP-Ribose) Polymerase. *The Journal of Pharmacology and Experimental Therapeutics*. 353 (3), 446-57.

518) Shimada, M. Dumitrache, LC. Russell, HR. McKinnon, PJ. (2015). Polynucleotide kinase-phosphatase enables neurogenesis via multiple DNA repair pathways to maintain genome stability. *The EMBO Journal*. 34 (19), 2465-80.

519) Shonesy, BC. Bluett, RJ. Tamikie, TS. Baldi, R. Hermanson, DJ. Kingsley, PJ. Marnett, LJ. Winder, DG. Colbran, RJ. Patel, S. (2014). Genetic Disruption of 2-Arachidonoylglycerol Synthesis Reveals a Key Role for Endocannabinoid Signaling in Anxiety Modulation. *Cell Reports*. 9 (5), 1644-53.

520) Singh, B. Monteil, A. Bidaud, I. Sugimoto, Y. Suzuki, T. et al. (2007). Mutational analysis of CACNA1G in idiopathic generalized epilepsy. Mutation in brief #962.. *Human Mutation*. 28 (5), 524-5.

521) Sintas, C. Carreno, O. Fernandez-Castillo, N. Corominas, R. Vila-Pueyo, M. et al. (2017). Mutation Spectrum in the CACNA1A Gene in 49 Patients with Episodic Ataxia. *Scientific Reports*. 7 (1), 2514.

522) Skalitzky, DJ. Marakovits, JT. Maegley, KA. Ekker, A. Yu, XH. et al. (2003). Tricyclic benzimidazoles as potent poly(ADP-ribose) polymerase-1 inhibitors. *Journal of Medicinal Chemistry*. 46 (2), 210-3.

523) Slade, D. Dunstan, MS. Barkauskaite, E. Weston, R. Lafite, P. Dixon, N. Ahel, M. Leys, D. Ahel, I. (2011). The structure and catalytic mechanism of a poly(ADP-ribose) glycohydrolase. *Nature*. 477 (7366), 616-20.

524) Small, DH. (2009). Dysregulation of calcium homeostasis in Alzheimer's disease. *Neurochemical Research*. 34 (10), 1824-9.

525) Smith, MA. Harris, PLR. Sayre, LM. Beckman, JS. Perry, G. (1997). Widespread peroxynitrite-mediated damage in Alzheimer's disease. *The Journal of Neuroscience*. 17 (8), 2653-7.

526) Sordet, O. Larochelle, S. Nicolas, E. Stevens, EV. Zhang, C. Shokat, KM. Fisher, RP. Pommier, Y. (2008). RNA polymerase II is Hyperphosphorylated in Response to Topoisomerase I-DNA Cleavage Complexes and is Associated with Transcription- and BRCA1-Dependent Degradation of Topoisomerase I. *Journal of Molecular Biology*. 381 (3), 540-49.

527) Sordet, O. Nakamura, AJ. Redon, CE. Pommier, Y. (2010). DNA double-strand breaks and ATM activation by transcription-blocking DNA lesions. *Cell Cycle*. 9 (2), 274-8.

528) Spiegel, JO. Van Houten, B. Durrant, JD. (2021). PARP1: Structural insights and pharmacological targets for inhibition. *DNA Repair*. 103 (103125), 1-14.

529) Spivak, G. (2015). Nucleotide excision repair in humans. *DNA Repair*. 36, 13-18.

530) Stampfl, B. Fee, D. (2021). Novel Mutation in CACNA1A Associated with Activity-Induced Dystonia, Cervical Dystonia, and Mild Ataxia. *Case Reports in Neurological Medicine*. 2021. E7797770.

531) Stan, A. Pielarski, KN. Brigadski, T. Wittenmayer, N. Fedorchenko, O. Gohla, A. Lessmann, V. Dresbach, T. Gottmann, K. (2010). Essential cooperation of N-cadherin and neuroligin-1 in the transsynaptic control of vesicle accumulation. *Proceedings of the National Academy of Sciences of the United States of America*. 107 (24), 11116-21.

532) Steinert, JR Chernova, T. Forsythe, ID. (2010). Nitric oxide signaling in brain function, dysfunction, and dementia. *Neuroscientist*. 16 (4), 435-52.

533) Stewart, L. Redinbo, MR. Qiu, X. Hol, WGJ. Champoux, JJ. (1998). A model for the mechanism of human topoisomerase I. *Science*. 279 (5356), 1534-41.

534) Stoica, BA. Loane, DJ. Zhao, Z. Kabadi, SV. Hanscom, M. Byrnes, KR. Faden, AI. (2014). PARP-1 inhibition attenuates neuronal loss, microglia activation and neurological deficits after traumatic brain injury. *Journal of Neurotrauma*. 31 (8), 758-72.

535) Stoll, G. Pietilainen, OPH. Linder, B. Suvisaari, J. Brosi, C. et al. (16). Deletion of TOP3β, a component of FMRP-containing mRNPs, contributes to neurodevelopmental disorders. *Nature Neuroscience*. 2013, 1228-37.

536) Ström, CE. Johansson, F. Uhlen, M. Szigyarto, CAK. Erixon, K. Helleday, T. (2011). Poly (ADP-ribose) polymerase (PARP) is not involved in base excision repair but PARP inhibition traps a single-strand intermediate. *Nucleic Acids Research*. 39 (12), 3166-75.

537) Stott, RT. Kritsky, O. Tsai, LH. (2021). Profiling DNA break sites and transcriptional changes in response to contextual fear learning. *PLOS one*. 16 (7). E0249691.

538) Stuehr, DJ. (2004). Enzymes of the L-Arginine to Nitric Oxide Pathway. *The Journal of Nutrition*. 143 (10), 2748-51.

539) Südhof, TC. (2012). Calcium Control of Neurotransmitter Release. *Cold Spring Harbour Perspectives in Biology*. 4 (1) E011353.

540) Sudhof, TC. Malenka, RC. (2008). Understanding Synapses: Past, Present, and Future. *Neuron*. 60 (3), 469-76.

541) Sugaware, T. Hisatsune, C. Le, TD. Hashikawa, T. Hirono, M. Hattori, M. Nagao, S. Mikoshiba, K. (2013). Type 1 Inositol Trisphosphate Receptor Regulates Cerebellar Circuits by Maintaining the Spine Morphology of Purkinje Cells in Adult Mice. *The Journal of Neuroscience*. 33 (30), 12186-96.

542) Suh, SW. Aoyama, K. Alano, CC. Anderson, CM. Hamby, AM. Swanson, RA. (2007). Zinc inhibits astrocyte glutamate uptake by activation of poly(ADP-ribose) polymerase-1. *Molecular Medicine*. 13 (7-8), 344-9.

543) Sultanov, D. Gerasimova, N. Kudryashova, K. Maluchenko, N. Kotova, E. Langelier, MF. Pascal, J. Kirpichnikov, M. Feofanov, A. Studitsky, V. (2017). Unfolding of core nucleosomes by PARP-1 revealed by spFRET microscopy. *AIMS Genetics*. 4 (1), 21-31.

544) Sun, FH. Zhao, P. Zhang, N. Kong, LL. Wong, CCL. Yun, CH. (2021). HPF1 remodels the active site of PARP1 to enable the serine ADP-ribosylation of histones. *Nature Communications*. 12 (1), 1028.

545) Sun, K. Mikule, K. Wang, Z. Poon, G. Vaidyanathan, A. Smith, G. Zhang, ZY. Hanke, J. Ramaswamy, S. Wang, J. (2018). A comparative pharmacokinetic study of PARP inhibitors demonstrates favorable properties for niraparib efficacy in preclinical tumor models. *Oncotarget*. 98 (9), 37080-96.

546) Sun, Y. Feng, X. Ding, Y. Li, M. Yao, J. Wang, L. Gao, Z. (2019). Phased Treatment Strategies for Cerebral Ischemia Based on Glutamate Receptors. *Frontiers in Cellular Neuroscience*. 13, 1-23.

547) Sykora, P. Wilson, DM. Bohr, VA. (2012). Repair of persistent strand breaks in the mitochondrial genome. *Mechanisms of Ageing and Development*. 133 (4), 169-75.

548) Szabo, C. Ohshima, H. (1997). DNA Damage Induced by Peroxynitrite: Subsequent Biological Effects. *Nitric Oxide*. 1 (5), 373-85.

549) Tajes, M. Ill-Raga, G. Palomer, E. Ramos-Fernandez, E. Guiz, FX. et al. (2013). Nitro-Oxidative Stress after Neuronal Ischemia Induces Protein Nitrotyrosination and Cell Death. *Oxidative Medicine and Cellular Longevity*. 2013 (826143), 1-9.

550) Takashima, H. Boerkoel, CF. John, J. Saifi, GM. Salih, MAM. et al. (2002). Mutation of TDP1, encoding a topoisomerase I-dependent DNA damage repair enzyme, in spinocerebellar ataxia with axonal neuropathy. *Nature Genetics*. 32 (2), 267-72.

551) Takeuchi, T. Ohtsuki, G. Yoshida, T. Fukaya, M. Wainai, T. et al. (2008). Enhancement of Both Long-Term Depression Induction and Optokinetic Response Adaptation in Mice Lacking Delphilin. *PLOS one*. 3 (5), E2297.

552) Tang, S. Wong, HC. Wang, ZM. Huang, Y. Zou, J. Zhuo, Y. Pennati, A. Gadda, G. Delbono, O. Yang, JJ. (2011). Design and application of a class of sensors to monitor Ca2+ dynamics in high Ca2+ concentration cellular compartments. *Proceedings of the National Academy of Sciences of the United States of America*. 108 (39), 16265-70.

553) Tauchi, H. Matsuura, S. Kobayashi, J. Sakamoto, S. Komatsu, K. (2002). Nijmegen breakage syndrome gene, NBS1, and molecular links to factors for genome stability. *Oncogene*. 21, 8967-80.

554) Taylor, RM. Thistlethwaite, A. Caldecott, KW. (2002). Central Role for the XRCC1 BRCT I Domain in Mammalian DNA Single-Strand Break Repair. *Molecular and Cellular Biology*. 22 (8), 2556-63

555) Tebbs, RS. Flannery, ML. Meneses, JJ. Hartmann, A. Tucker, JD. Thompson, LH. Cleaver, JE. Pedersen, RA. (1999). Requirement for the Xrcc1 DNA base excision repair gene during early mouse development. *Developmental Biology*. 208 (2), 513-29.

556) Thakur, S. Sarkar, B. Cholia, RP. Gautam, N. Dhiman, M. Mantha, AK. (2014). APE1/Ref-1 as an emerging therapeutic target for various human diseases: phytochemical modulation of its functions. *Experimental and Molecular Medicine*. 46. E106.

557) Thomas, C. Ji, Y. Wu, C. Datz, H. Boyle, C. et al. (2019). Hit and run versus long-term activation of PARP-1 by its different domains fine-tunes nuclear processes. *Proceedings of the National Academy of Sciences of the United States of America*. 116 (20), 9941-6.

558) Thomas, C. Mackey, MM. Diaz, AA. Cox, DP. (2009). Hydroxyl radical is produced via the Fenton reaction in submitochondrial particles under oxidative stress: implications for diseases associated with iron accumulation. *Redox Report*. 14 (3), 102-8.

559) Thompson, LH. Brookman, KW. Jones, NJ. Allen, SA. Carrano, AV. (1992). Molecular cloning of the human XRCC1 gene, which corrects defective DNA strand break repair and sister chromatid exchange. *Molecular and Cellular Biology*. 10 (12), 6160-72.

560) Tian, YN. Chen, HD. Tian, CQ. Wang, YQ. Miao, ZH. (2020). Polymerase independent repression of FoxO1 transcription by sequence-specific PARP1 binding to FoxO1 promoter. *Cell Death and Disease*. 11 (1), 71.

561) Tikhanovich, I. Cox, J. Weinman, S. (2013). FOXO Transcription Factors in Liver Function and Disease. *The Journal of Gastroenterology and Hepatology*. 28 (1), 125-31.

562) Todorov, B. Kros, L. Shyti, R. Plak, P. Haasdijk, ED. et al. (2012). Purkinje Cell-Specific Ablation of CaV2.1 Channels is Sufficient to Cause Cerebellar Ataxia in Mice. *Cerebellum*. 11 (1), 246-58.

563) Togo, T. Katsuse, O. Iseki, E. (2004). Nitric oxide pathways in Alzheimer's disease and other neurodegenerative dementias. *Neurological Research*. 26 (5), 563-6.

564) Topolnik, L. Camiré, O. (2019). Non-linear calcium signalling and synaptic plasticity in interneurons. *Current Opinion in Neurobiology*. 54, 98-103.

565) Tubbs, A. Nussenzweig, A. (2017). Endogenous DNA Damage as a Source of Genomic Instability in Cancer. *Cell*. 168 (4), 644-56.

566) Tumbale, P. Williams, JS. Schellenberg, MJ. Kunkel, TA. Williams, RS. (2014). Aprataxin resolves adenylated RNA-DNA junctions to maintain genome integrity. *Nature*. 506 (7486), 111-5.

567) Turkmen, S. Guo, G. Garshasbi, M. Hoffmann, K. Alshalah, AJ. Mischung, G. Kuss, A. Humphrey, N. Mundlos, S. Robinson, PN. (2009). CA8 mutations cause a novel syndrome characterized by ataxia and mild mental retardation with predisposition to quadrupedal gait. *PLOS Genetics*. 5 (5), E1000487.

568) Ueda, K. Ogata, N. Kawaichi, M. Inada, S. Hayaishi, O. (1982). ADP-Ribosylation Reactions. *Current Topics in Cellular Regulation*. 21, 175-87.

569) ul Islam, B. Habib, S. Ahmad, P. Allarakha, S. Ali, M Ali, A. (2015). Pathophysiological Role of Peroxynitrite Induced DNA Damage in Human Diseases: A Special Focus on Poly(ADP-ribose) Polymerase (PARP). *Indian Journal of Clinical Biochemistry*. 30, 368-85.

570) Vaisman, A. Woodgate, R. (2017). Translesion DNA polymerases in eukaryotes: what makes them tick? *Critical Reviews in Biochemistry and Molecular Biology*. 52 (3), 274-303.

571) Vakharia, K. Shallwani, H. Beecher, JS. Jowdy, PK. Levy, EI. (2018). 23 - Endovascular Treatment of Acute Stroke and Occlusive Cerebrovascular Disease. In: - *Principles of Neurological Surgery*. 4th ed. 343-54.

572) Valabrega, G. Scotto, G. Tuninetti, V. Pani, A. Scaglione, F. (2021). Differences in PARP Inhibitors for the Treatment of Ovarian Cancer: Mechanisms of Action, Pharmacology, Safety, and Efficacy. *Internation Journal of Molecular Sciences*. 22 (4203), 1-16.

573) Vandecaetsbeek, I. Vanghelue, Raeymaekers, L. Wuytack, F. Vanoevelen, J. (2011). The Ca2+ Pumps of the Endoplasmic Reticulum and Golgi Apparatus. *Cold Spring Harbour Perspectives in Biology*. 3 (5), E004184.

574) Veeranpandiyan, A. Enner, S. Thulasi, V. Ming, X. (2017). A Rare Syndrome of GRID2 Deletion in 2 Siblings. *Child Neurology Open*. 4, 1-3.

575) Verdone, L. La Fortezza, M. Ciccarone, F. Caiafa, P. Zampieri, M. Caserta, M. (2015). Poly(ADP-ribosylation) Affects Histone Acetylation and Transcription. *PLOS one*. 10 (12), 577.

576) Vilenchik, MM. Knudson, AG. (2003). Endogenous DNA double-strand breaks: production, fidelity of repair, and induction of cancer. *Proceedings of the National Academy of Sciences of the United States of America*. 100 (22), 12871-6.

577) Vis, JC. Schipper, E. de Boer-van Huizen RT. Verbeek, MM. de Waal, RMW. Wesseling, P. ten Donkelaar, HJ. Kremer, B. (2005). Expression pattern of apoptosis-related markers in Huntington's disease. *Acta Neuropathologica*. 109, 321-8.

578) Visochek, L. Grigoryan G. Kalal, A. Milshtein-Parush, H. Gazit, N. et al. (2016). A PARP1-ERK2 synergism is required for the induction of LTP. *Scientific Reports*. 6 (24950), 1-16.

579) Vogel, MW. Caston, J. Yuzaki, M. Mariani, J. (2007). The Lurcher mouse: fresh insights from an old mutant. *Brain Research*. 1140, 4-18.

580) Vos, M. Lauwers, E. Verstreken, P. (2010). Synaptic mitochondria in synaptic transmission and organization of vesicle pools in health and disease. *Frontiers in Synaptic Neuroscience*. 2 (139), 1-10.

581) Vriend, LEM. Krawczyk, PM. (2017). Nick-initiated homologous recombination: Protecting the genome, one strand at a time. *DNA Repair*. 50, 1-13.

582) Wallace, SS. (2014). Base excision repair: a critical player in many games. *DNA Repair*. 19, 14-26.

583) Wang, C. Pan, YH. Wang, Y. Blatt, G. Yuan, XB. (2019). Segregated expressions of autism risk genes Cdh11 and Cdh9 in autism-relevant regions of developing cerebellum. *Molecular Brain*. 12 (1), 40.

584) Wang, J. Swanson, RA. (2020). Superoxide and Non-ionotropic Signaling in Neuronal Excitotoxicity. *Frontiers in Neuroscience*. 14 (861), 1-10.

585) Wang, JC. (1971). Interaction between DNA and an Escherichia coli protein omega. *Journal of Molecular Biology*. 55 (3), 523-33.

586) Wang, K. Zhang, H. Ma, D. Bucan, M. Glessner, JT. et al. (2009). Common genetic variants on 5p14.1 associate with autism spectrum disorders. *Nature*. 459 (7246), 528-33.

587) Wang, Q. Liu, Z. Lin, Z. Zhang, R. Lu, Y. Su, W. Li, F. Xu, X. Tu, M. Lou, Y. Zhao, J. Zheng, X. (2019). De Novo Germline Mutations in SEMA5A Associated With Infantile Spasms. *Frontiers in Genetics*. 10 (605), 1-11.

588) Wang, R. Li, C. Qiao, P. Xue, Y. Zheng, X. Chen, H. Zeng, X. Liu, W. Boldogh, I. Ba, X. (2018). OGG1-initiated base excision repair exacerbates oxidative stress-induced parthanatos. *Cell Death & Disease*. 9 (6), 628.

589) Wang, Y. An, R. Umanah, GK. Park, H. Nambiar, K. et al. (2016). A nuclease that mediates cell death induced by DNA damage and poly(ADP-ribose) polymerase-1. *Science*. 354 (6308). E6872.

590) Watson, M. Holman, DM. Maguire-Eisen, M. (2016). Ultraviolet Radiation Exposure and Its Impact on Skin Cancer Risk. *Seminars in Oncology Nursing*. 32 (3), 241-54.

591) Watts, ME. Pocock, R. Claudianos, C. (2018). Brain Energy and Oxygen Metabolism: Emerging Role in Normal Function and Disease. *Frontiers in Molecular Neuroscience*. 11 (286), 1-13.

592) Weber, AR. Krawczyk, C. Robertson, AB. Kusnierczyk, A. Vagbo, CB. Schuermann, D. Klungland, A. Schar, P. (2016). Biochemical reconstitution of TET1–TDG–BER-dependent active DNA demethylation reveals a highly coordinated mechanism. *Nature Communications*. 7 (10806), 1-13.

593) Welty, S. Teng, Y. Liang, Z. Zhao, W. Sanders, L. Greenamyre, JT. Rubio, ME. Thathiah, A. Kodali, R. Wetzel, R. Levine, AS. Lan, L. (2018). RAD52 is required for RNA-templated recombination repair in post-mitotic neurons. *Journal of Biological Chemistry*. 293 (4), 1353-62.

594) Wengert, ER. Patel, MK. (2021). The Role of the Persistent Sodium Current in Epilepsy. *Epilepsy Currents*. 21 (1), 40-7.

595) West, AE. Greenberg, ME. (2011). Neuronal Activity–Regulated Gene Transcription in Synapse Development and Cognitive Function. *Cold Spring Harbour Perspectives in Biology*. 3, 1-22.

596) Whitaker, AM. Freudenthal, BD. (2018). APE1: A skilled nucleic acid surgeon. *DNA Repair*. 71, 93-100.

597) Wiebe, S. (2000). Epidemiology of temporal lobe epilepsy. *The Canadian Journal of Neurological Sciences*. 27, 1-5.

598) Wiederhold, L. Leppard, JB. Kedar, P. Karimi-Busheri, F. Rasouli-Nia, A. et al. (2004). AP endonuclease-independent DNA base excision repair in human cells. *Molecular Cell*. 15 (2), 209-20.

599) Wiel, C. Daher, HL. Gitenay, D. Gras, B. le Calve, B. et al. (2014). Endoplasmic reticulum calcium release through ITPR2 channels leads to mitochondrial calcium accumulation and senescence. *Nature Communications*. 5 (3792), 1-10.

600) Wright, WD. Shah, SS. Heyer, WD. (2018). Homologous recombination and the repair of DNA double-strand breaks. *Journal of Biological Chemistry*. 293 (27), 10524-35.

601) Wu, W. Hill, SE. Nathan, WJ. Paiano, J. Callen, E. et al. (2021). Neuronal enhancers are hotspots for DNA single-strand break repair. *Nature*. 593 (7859), 440-4.

602) Wu, X. Zhang, Y. (2017). TET-mediated active DNA demethylation: mechanism, function and beyond. *Nature Reviews Genetics*. 18, 517-34.

603) Xu, D. Shen, W. Guo, R. Xue, Y. Peng, W. (2013). Top3β is an RNA topoisomerase that works with fragile X syndrome protein to promote synapse formation. *Nature Neuroscience*. 16, 1238-47.

604) Xu, G. Chapman, JR. Brandsma, I. Yuan, J. Mistrik, M. et al. (2015). REV7 counteracts DNA double-strand break resection and affects PARP inhibition. *Nature*. 521 (7553), 541-4.

605) Yamagata, M. Duan, X. Sanes, JR. (2018). Cadherins Interact With Synaptic Organizers to Promote Synaptic Differentiation. *Frontiers in Molecular Neuroscience*. 11 (142), 1-15.

606) Yamamori, T. Yasui, H. Yamazumi, M. Wada, Y. Nakamura, Y. Nakamura, H. Inanami, O. (2012). Ionizing radiation induces mitochondrial reactive oxygen species production accompanied by upregulation of mitochondrial electron transport chain function and mitochondrial content under control of th. *Free Radical Biology and Medicine*. 53 (2), 260-70.

607) Yan, H. Tammaro, M. Liao, S. (2016). Collision of Trapped Topoisomerase 2 with Transcription and Replication: Generation and Repair of DNA Double-Strand Breaks with 5′ Adducts. *Genes*. 7 (7), 32.

608) Yang, AW. Sachs, AJ. Nystuen, AM. (2015). Deletion of Inpp5a causes ataxia and cerebellar degeneration in mice. *Neurogenetics*. 16, 277-85.

609) Yang, D. Shu, T. Zhao, H. Sun, Y. Xu, W. Tu, G. (2020). Knockdown of macrophage migration inhibitory factor (MIF), a novel target to protect neurons from parthanatos induced by simulated post-spinal cord injury oxidative stress. *Biochemical and Biophysical Research Communication*. 523 (3), 719-25.

610) Yang, JL. Sykora, P. Wilson III, DM. Mattson, MP. Bohr, VA. (2011). The Excitatory Neurotransmitter Glutamate Stimulates DNA Repair to Increase Neuronal Resiliency. *Mechanisms of Ageing and Development*. 132 (8-9), 405-11.

611) Yang, SW. Burgin Jr, AB. Huizenga, BN. Robertson, CA. Yao, KC. Nash, HA. (1996). A eukaryotic enzyme that can disjoin dead-end covalent complexes between DNA and type I topoisomerases. *Proceedings of the National Academy of Sciences of the United States of Americ*. 93 (21), 11534-9.

612) Yap, EL. Greenberg, ME. (2018). Activity-Regulated Transcription: Bridging the Gap between Neural Activity and Behavior. *Neuron*. 100, 330-48.

613) Yap, SM. Smyth, S. (2019). Ryanodine receptor 2 (RYR2) mutation: A potentially novel neurocardiac calcium channelopathy manifesting as primary generalised epilepsy. *Seizure*. 67, 11-14.

614) Yermilov, V. Rubio, J. Becchi, M. Friesen, MD Pignatelli, B. Ohshima, H. (1995). Formation of 8-nitroguanine by the reaction of guanine with peroxynitrite in vitro. *Carcinogenesis*. 16 (9), 2045-50.

615) Ying, W. Chen, Y. Alano, CC. Swanson, RA. (2002). Tricarboxylic Acid Cycle Substrates Prevent PARP-Mediated Death of Neurons and Astrocytes. *Journal of Cerebral Blood Flow and Metabolism*. 22 (7), 774-9.

616) Ying, W. Garnier, P. Swanson, RA. (2003). NAD+ repletion prevents PARP-1-induced glycolytic blockade and cell death in cultured mouse astrocytes. *Biochemical and Biophysical Research Communication*. 308 (4), 809-13.

617) Yokoyama, H. Mizutani, R. (2014). Structural Biology of DNA (6-4) Photoproducts Formed by Ultraviolet Radiation and Interactions with Their Binding Proteins. *International Journal of Molecular Sciences*. 15 (11), 20321-38.

618) Yoon, G. Caldecott, KW. (2018). Chapter 7 - Nonsyndromic cerebellar ataxias associated with disorders of DNA single-strand break repair. *Handbook of Clinical Neurology*. 155. 105-15.

619) Yoshida, T. Fukaya, M. Uchigashima, M. Miura, E. Kamiya, H. Kano, M. Watanabe, M. (2006). Localization of Diacylglycerol Lipase-␣around Postsynaptic Spine Suggests Close Proximity between Production Site ofan Endocannabinoid, 2-Arachidonoyl-glycerol, and Presynaptic Cannabinoid CB1 Receptor. *The Journal of Neuroscience*. 26 (18), 4740-51.

620) Yu, SL. Lee, SK. (2017). Ultraviolet radiation: DNA damage, repair, and human disorders. *Molecular and Cellular Toxicology*. 13, 21-28.

621) Yu, SW. Wang, H. Poitras, MF. Coombs, C. Bowers, WJ. Federoff, HJ. Poirier, GG. Dawson, TM. Dawson, VL. (2002). Mediation of poly(ADP-ribose) polymerase-1-dependent cell death by apoptosis-inducing factor. *Science*. 297 (5579), 259-63.

622) Yu, Y. Chen, S. Mo, X. Gong, J. Li, C. Yang, X. (2018). Accessory and Central α-helices of Complexin Selectively Activate Ca2+ Triggering of Synaptic Exocytosis. *Frontiers in Molecular Neuroscience*. 11 (61), 1-8.

623) Yuste, JE. Tarragon, E. Campuzano, CM. Ros-Bernal, F. (2015). Implications of glial nitric oxide in neurodegenerative diseases. *Frontiers in Cellular Neuroscience*. 9 (322), 1-13.

624) Zagnoli-Vieira, G. Bruni, F. Thompson, K. He, L. Walker, S. de Brouwer, APM. Taylor, R. Niyazov, D. Caldecott, KW. (2018). Confirming TDP2 mutation in spinocerebellar ataxia autosomal recessive 23 (SCAR23). *Neurology Genetics*. 4 (4). E262.

625) Zambonin, JL. Bellomo, A. Ben-Pazi, H. Everman, DB. Frazer, LM. et al. (2017). Spinocerebellar ataxia type 29 due to mutations in ITPR1: a case series and review of this emerging congenital ataxia. *Orphanet Journal of Rare Diseases*. 12 (1), 121.

626) Zandarashvili, L. Langelier, MF. Velagapudi, UK. Hancock, MA. Steffen, JD. et al. (2020). Structural basis for allosteric PARP-1 retention on DNA breaks. *Science*. 368 (6486), 6367.

627) Zanjani, H. McFarland, R. Cavelier, P. Blokhin, A. Gautheron, V. Levenes, C. Bambrick, LL. Mariani, J. Vogel, MW. (2009). Death and survival of heterozygous Lurcher Purkinje cells in vitro. *Developmental Neurobiology*. 69 (8), 505-17.

628) Zdzienicka, MZ. van der Schans, GP. Natarajan, AT. Thompson, LH. Neuteboom, I. Simons, JW. (1992). A Chinese hamster ovary cell mutant (EM-C11) with sensitivity to simple alkylating agents and a very high level of sister chromatid exchanges. *Mutagenesis*. 7 (4), 265-9.

629) Zhang, H. Zhu, L. Wang, F. Wang, R. Hong, Y. et al. (2019). Novel KCNJ10 Compound Heterozygous Mutations Causing EAST/SeSAME-Like Syndrome Compromise Potassium Channel Function. *Frontiers in Genetics*. 10 (912). 1-9.

630) Zhang, S. Williamson, NA. Duvick, L. Lee, A. Orr, HT. Korlin-Downs, A. Yang, P. Mok, YF. Jans, DA. Bogoyevitch, MA. (2020). The ataxin-1 interactome reveals direct connection with multiple disrupted nuclear transport pathways. *Nature Communications*. 11 (1), 3343.

631) Zhang, T. Kraus, WL. (2010). SIRT1-dependent Regulation of Chromatin and Transcription: Linking NAD+ Metabolism and Signaling to the Control of Cellular Functions. *Biochimica et Biophysica Acta*. 1804 (8), 1666-75.

632) Zheng, F. Liu, G. Dang, T. Chen, Q. An, Y. Wu, M. Kong, X. Qiu, Z. Wu, BL. (2021). GABA Signaling Pathway-associated Gene PLCL1 Rare Variants May be Associated with Autism Spectrum Disorders. *Neuroscience Bulletin*. 37, 1240-5.

633) Zhou, L. Zhu, DY. (2009). Neuronal nitric oxide synthase: structure, subcellular localization, regulation, and clinical implications. *Nitric Oxide*. 20 (4), 223-30.

634) Zhou, T. Lee, JW. Tatavarthi, H. Lupski, JR. Valerie, K. Poirk, LF. (2005). Deficiency in 3′-phosphoglycolate processing in human cells with a hereditary mutation in tyrosyl-DNA phosphodiesterase (TDP1). *Nucleic Acids Research*. 33 (1), 289-97.

635) Zhou, T. Prather, ER. Garrison, DE. Zuo, L. (2018). Interplay between ROS and Antioxidants during Ischemia-Reperfusion Injuries in Cardiac and Skeletal Muscle. *International Journal of Molecular Sciences*. 19 (2), 417.

636) Zhou, W. Doetsch, PW. (1993). Effects of abasic sites and DNA single-strand breaks on prokaryotic RNA polymerases. *Proceedings of the National Academy of Sciences of the United States of America*. 90 (14), 6601-5.

637) Zhou, Y. Danbolt, NC. (2014). Glutamate as a neurotransmitter in the healthy brain. *Journal of Neural Transmission*. 121 (8), 799-817.

638) Zhou, Y. Feng, X. Koh, DW. (2011). Activation of cell death mediated by apoptosis-inducing factor due to the absence of poly(ADP-ribose) glycohydrolase. *Biochemistry*. 50 (14), 2850-9.

639) Zhou, Y. Liu, L. Tao, S. Yao, Y. Wang, Y. Wei, Q. Shao, A. Deng, Y. (2021). Parthanatos and its associated components: Promising therapeutic targets for cancer. *Pharmacological Research*. 163, 105299.

640) Zhou, Y. Wang, S. Li, Y. Yu, S. Zhao, Y. (2017). SIRT1/PGC-1α Signaling Promotes Mitochondrial Functional Recovery and Reduces Apoptosis after Intracerebral Hemorrhage in Rats. *Frontiers in Molecular Neuroscience*. 10 (443), 1-14.

641) Zhu, G. Yoshida, S. Migita, K. Yamada, J. Mori, F. et al. (2012). Dysfunction of extrasynaptic GABAergic transmission in phospholipase C-related, but catalytically inactive protein 1 knockout mice is associated with an epilepsy phenotype. *The Journal of Pharmacology and Experimental Therapeutics*. 340 (3), 520-8.

642) Zhu, JK. (2009). Active DNA Demethylation Mediated by DNA Glycosylases. *Annual Review of Genetics*. 43, 143-66.

643) Zorova, LD. Popkov, VA. Plotnikov, EY. Silachev, DN. Pevzner, IB. et al. (2011). Mitochondrial membrane potential. *Analytical Biochemistry*. 552, 50-59.

644) Zu, Y. Shannon, RJ. Hirst, J. (2003). Reversible, electrochemical interconversion of NADH and NAD+ by the catalytic (Ilambda) subcomplex of mitochondrial NADH:ubiquinone oxidoreductase (complex I). *Journal of the American Chemical Society*. 125 (20), 6020-1.